ANALYSIS OF DISTRIBUTED RESISTANCE-CAPACITANCE NETWORKS

by

Gregory Roy Haack

B.E., University of Queensland, 1964
M.Eng. Sc. University of Queensland, 1967

Submitted in fulfillment of the requirements for the Degree of Doctor of Philosophy in Electrical Engineering, University of Adelaide, July 1974.

CONTENTS

SUMMARY

The problem of analyzing multiport distributed resistance-capacitance networks is considered. In particular, the problem of obtaining the admittance matrix elements and its poles and zeros is investigated.

The potential in the resistive layer of the DRC network satisfies the two-dimensional Helmholtz equation, which may be transformed to a system of coupled first-order differential equations or to an integral equation.

The basic solution technique is to reduce the differential or integral equation to a matrix equation. Approximate solutions of the differential equations are obtained by the Rayleigh-Ritz variational method. The integral equation is solved by point matching, which is equivalent to the method of moments.

Numerical results for a number of examples are presented, and the different methods are compared. In addition, some numerical results obtained by one-dimensional analysis and two-dimensional analysis are compared.

This thesis contains no material which has been accepted for the award of any other degree or diploma in any University, and, to the best of my belief, the thesis contains no material previously published or written by another person, except when due reference is made in the text of the thesis.

ACKNOWLEDGEMENT

I wish to extend my sincere thanks to Dr. B. R. Davis and Mr. D. C. Pawsey for their assistance and guidance in this work.

This work was supported in part by the Australian Government by a Commonwealth Public Service Postgraduate Scholarship, and by the Electrical Engineering Department of the University of Adelaide.

Chapter 1

INTRODUCTION

The central problem considered in this dissertation is that of analysing thin-film distributed resistance-capacitance (DRC) networks.

A cross-section of a portion of a thin film DRC network is shown in Fig. 1.1, Fig. 1.2 shows a top view of a typical DRC network. As shown in the diagrams, the DRC network consists of resistive, insulating and conducting layers placed on top of one another. Electrical connections are made to the device by means of conducting strips placed on the boundary of the resistive layer.

The study of distributed networks has been prompted by the trend in electronic equipment toward smaller and smaller physical structures. Distributed RC networks can be combined with lumped passive elements and active elements to produce a wide range of filter characteristics (70). Such realizations usually require fewer components than comparable realizations using lumped elements. The most common DRC network for these applications is the two-port DRC line. Although the uniform RC line with a simple rectangular shape is easy to analyse, there are definite advantages to be gained by geometrically tapering the RC line; it has been shown that tapering is useful for obtaining sharper cutoff low pass filters, and for narrowing the rejection band of "notch" filters (5).

In the following Chapters we will consider numerical methods for analysing DRC networks of arbitrary shape. Chapters 2-6 are concerned with two-port networks which can be represented

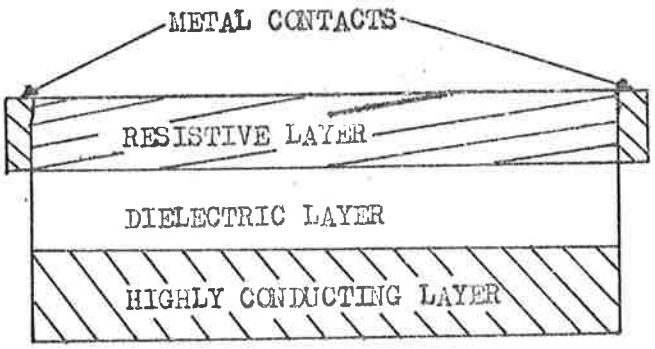

Figure 1.1. Cross-section of a portion of a DRC network.

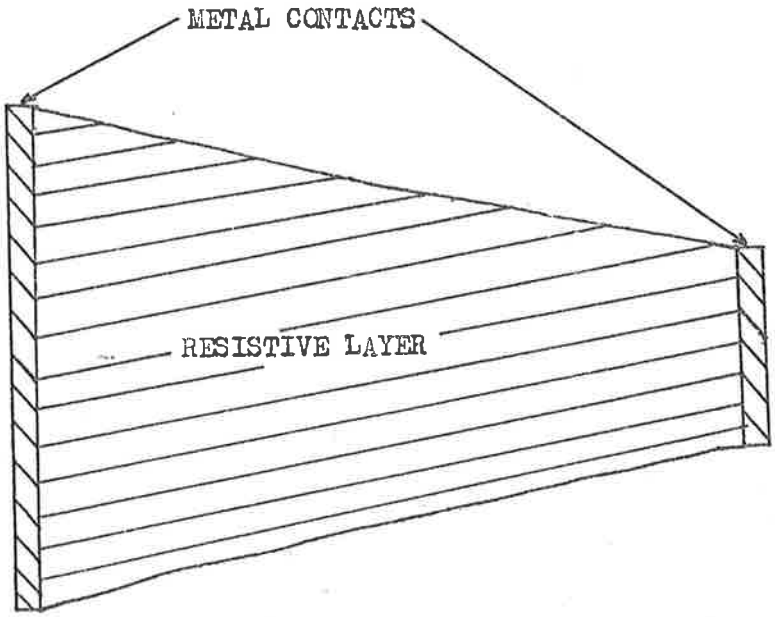

Figure 1.2. Top view of a typical DRC network.

by a one-dimensional model i.e. the network can be represented by a non-uniform line having a prescribed series resistance and shunt capacitance per unit length. The techniques used to analyse such networks can obviously be applied to DRC networks where the variation in resistance and capacitance per unit length is due to variations in the composition of the resistive and dielectric layers, instead of variations in the width of a line whose resistive and dielectric layers are of uniform composition.

Chapters 7-10 are concerned with the two-dimensional analysis of multi-port distributed RC network. The importance of this work is that it provides a means of assessing the errors due to the assumption of a one-dimensional model. In addition, it provides a means of investigating phenomena which do not occur in one dimensional structures; for example, transmission zeros can occur in tapered structures, but these are not predicted by the one-dimensional model (17), (58), (69), (71).

In Chapter 2 the properties of the admittance parameters of DRC lines supporting one-dimensional current flow are discussed. Some important results derived from the theory of Sturm equations (1) are presented.

In Chapter 3 the problem of obtaining the poles and zeros of the two-port parameters of nonuniform RC lines is considered. The poles and zeros are proportional to the stationary values of a suitably chosen functional, and the Rayleigh-Ritz method is used to obtain approximate solutions. Some problems associated with the practical application of the method are considered. In particular, methods of reducing the effects of rounding errors by using orthogonal polynomials are considered. Although it has been

suggested previously, (12), that it is advantageous to use orthogonal polynomials for problems such as least-squares curve fitting, the use of these methods for solving eigenvalue problems of the type considered here does not appear to have been considered previously. Finally, numerical results are presented for a number of examples.

In Chapter 4 an alternative method of obtaining poles and zeros is presented. The variational method of Chapter 3 gives a solution which approximately satisfies the second-order differential equation (Sturm equation) which determines the potential along the transmission line. In Chapter 4 the Method of Moments (14) is used to obtain approximate solutions of a pair of first-order equations which are equivalent to the Sturm equation. One problem considered here is that of detecting or avoiding "extraneous" solutions; this problem does not appear to have been considered previously. By slightly modifying the basic technique presented in (14) it is found that the extraneous solutions are eliminated, and the accuracy of the numerical results is improved. Finally, the rate of convergence of the Moment method solutions is investigated and compared with other methods.

In Chapter 5 the results obtained by the Rayleigh-Ritz Variational method of Chapter 3 are compared with the Moment method of Chapter 4. In particular, some inequalities which are believed to be new, are derived to show the relationship between the two methods.

In Chapter 6 a brief discussion of other numerical methods for obtaining poles and zeros is presented.

A brief discussion of numerical methods for two-dimensional analysis of DRC networks is presented in Chapter 7.

The Variational method for obtaining poles and zeros of DRC networks by solving the two-dimensional Helmholtz equation is considered in detail in Chapter 8. A number of functionals whose stationary values are proportional to an admittance matrix element or its poles or zeros are presented. Although the functionals which are used to obtain the poles and the zero frequency values of the diagonal elements of the admittance matrix have been presented previously, (25), the other functionals presented here are believed to be new. Application of the Rayleigh-Ritz method to the problem of obtaining stationary values of the functionals is considered in detail. Several methods of obtaining suitable expansion functions to approximate the unknown potential functions are discussed, and some numerical results are presented. In particular, the numerical results show that finite zeros of transmission occur. In addition, the results obtained from the two-dimensional analysis are compared with those obtained by a one-dimensional analysis.

In Chapter 9 the Variational method is used to obtain the poles and zeros of DRC networks by approximately solving a system of first-order partial differential equations which are equivalent to the second-order differential equation, (Helmholtz equation) considered in Chapter 8. A number of new functionals whose stationary values are proportional to the value of an admittance matrix element or its poles or zeros are derived. The Rayleigh-Ritz method is then used to obtain the stationary values of these functionals. One of the difficulties associated with this method

is that of detecting extraneous solutions, and this aspect is considered in detail. The numerical results obtained by this method are also compared with those obtained by the Variational method of Chapter 8.

In Chapter 10 an alternative method of solving two-dimensional problems is considered. The partial differential equation is transformed to an integral equation which is then solved by point matching. In most previous applications of the Integral equation method, it was necessary to approximate the boundary by straight line segments. In this Chapter we also consider methods for solving problems with circular boundaries without the need for such approximations. Some numerical solutions are presented, and methods of minimizing the effects of rounding errors by using orthogonal polynomials are discussed.

A discussion of some problems which can be solved by the methods used for DRC networks is given in Chapter 11. The methods used in previous Chapters are shown to be directly applicable to other problems such as analysis of lossless transmission line networks. In addition, the results of some further work on transient analysis of transmission lines and the applications of equivalent network theory are discussed.

Finally, in Chapter 12 the methods studied in previous Chapters are reviewed, and their relative advantages are assessed with the objective of determining which is the best method for solving a given problem.

PART I

ONE DIMENSIONAL ANALYSIS

Chapter 2

DISTRIBUTED RESISTANCE - CAPACITANCE NETWORKS SUPPORTING ONE-DIMENSIONAL CURRENT FLOW

2.1 Introduction

A cross section of a portion of a thin-film DRC network is shown in Fig. 1.1. Fig. 1.2 shows a top view of a typical DRC network. As shown in the diagrams the DRC network consists of resistive, insulating and conducting layers. Electrical connections are made to the device by means of conducting strips placed on the boundary of the resistive layer.

If the layers of resistive and dielectric materials are homogeneous and of constant thickness the potential ϕ in the resistive layer can be shown to satisfy the partial differential equation, (1) pp. 241-243,

$$\frac{\partial^2 \phi}{\partial x^2} + \frac{\partial^2 \phi}{\partial y^2} = sRC\phi \qquad (2.1)$$

where

R is the sheet resistance of the resistive layer,

C is the capacitance per unit area coupling the resistive layer to the ground plane,

and

s is the complex frequency variable.

It is assumed that the resistive layer is sufficiently thin that variations of ϕ in the direction normal to the ground plane can be ignored. On each of the conducting strips the boundary condition is that the potential be constant, and on the remaining segments of the boundary of the resistive region the boundary condition is that there is no current flow out of the resistive region. This is equivalent to the condition,

$$\underline{n} \cdot \nabla\phi = 0 \qquad (2.2)$$

on the insulating parts of the boundary; $\underline{n}$ is the unit length outward-pointing normal to the boundary.

In the following discussion we will be primarily concerned with the problem of calculating the admittance parameters of two-port DRC networks (only two conducting strips on the boundary of the resistive layer). The pole-zero approach will be emphasized in the analysis because it provides a direct connection between lumped and distributed-parameter systems, and it also facilitates evaluation of the admittance parameters at any desired frequency.

2.2 Properties of Admittance Parameters of Non-uniform RC Lines

If the physical boundaries of the distributed circuit match the coordinate lines of an orthogonal coordinate system, the partial differential equation (2.1) may be solved by the method of separation of variables. Only four such coordinate systems exist for planar two dimensional networks. These are the rectangular, polar, parabolic, and elliptic coordinate systems ((1), Chapter 7). For distributed networks of other shapes, the variables cannot be separated, and hence one dimensional current flow is not possible. However, in some cases, one dimensional current flow can be approximated to an acceptable degree of accuracy. (69).

Consider the two-port tapered DRC network shown in Fig. 2.1. An orthogonal coordinate system (x,z) is chosen so that a fixed value of x represents an equipotential, and z represents the distance along an equipotential line from a reference axis such as the centre line of the element. A circuit model of an elemental section of the network may be constructed as shown in Fig. 2.2. As the length of the section approaches zero, the voltage and current in the resistive layer can be shown to satisfy the differential equations,

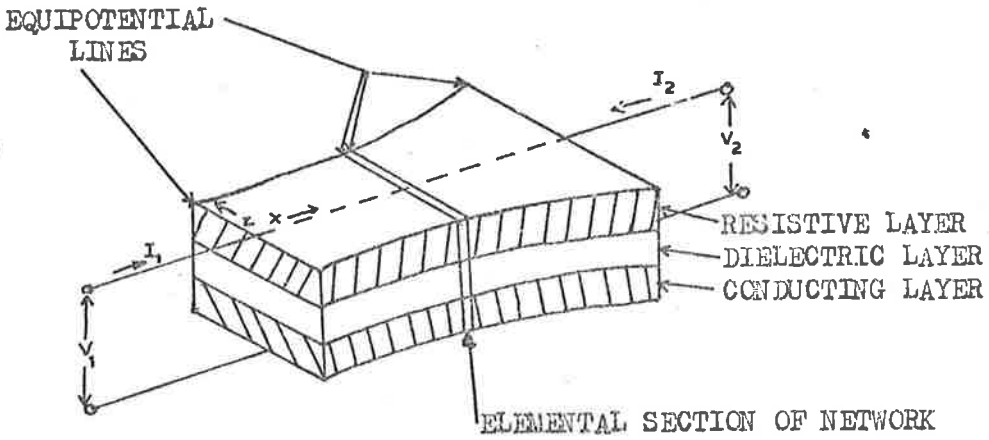

Figure 2.1. Two-port tapered distributed RC network.

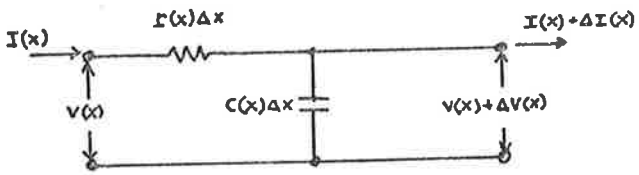

Figure 2.2. Circuit model of elemental section of distributed RC network.

$$\frac{\partial V(x,s)}{\partial x} = -r(x)\, I(x,s) \qquad (2.3a)$$

$$\frac{\partial I(x,s)}{\partial x} = -s\, C(x)\, V(x,s) \qquad (2.3b)$$

where

s is the complex frequency variable

$$r(x) = \rho / w(x).h_1 \qquad (2.3c)$$

$$c(x) = \epsilon\, w(x)/h_2 \qquad (2.3d)$$

ρ and h_1 are the resistivity and thickness of the resistive sheet.

ϵ and h_2 are the permittivity and thickness of the dielectric sheet

and

w(x) is the length of the equipotential line at x.

i.e. r(x) and c(x) are the series resistance and shunt capacitance respectively per unit length of the section.

From equations (2.3a) and (2.3b) the second order differential equation obtained for V(x,s) is

$$\frac{d}{dx}\left[w(x)\frac{dV}{dx}\right] + \lambda\, w(x)\, V = 0 \qquad (2.4)$$

where

$$\lambda = -s\, r_o\, c_o$$

and

$$r_o = r(o)$$

$$c_o = c(o)$$

It is noted that (2.4) is a Sturm Equation, and the known properties of solutions of these equations can be used to deduce a number of interesting conclusions about the behaviour of distributed RC networks.

It is known from the theory of differential equations that a second-order differential equation has two linearly independent

solutions. Thus the solution of the voltage equation (2.4) can be written as

$$V(s,x) = a\,V_I(s,x) + b\,V_{II}(s,x)$$

where a and b are determined by the network boundary conditions, and V_I and V_{II} are the linearly independent solutions.

The "basic set" solutions ((2), p. 531) defined by

$$V_I = 1, \quad \frac{dV_I}{dx} = V_I' = 0 \text{ at } x = 0 \tag{2.5a}$$

$$V_{II} = 0, \quad \frac{dV_{II}}{dx} = V_{II}' = 1 \text{ at } x = 0 \tag{2.5b}$$

are particularly convenient for calculation of the two-port admittance parameters.

The short-circuit admittance parameters are given in terms of the basic set solutions by the following simple relations ((1), p. 33)

$$y_{11} = \frac{1}{r(o)} \cdot \frac{V_I(s,d)}{V_{II}(s,d)} \tag{2.6a}$$

$$y_{12} = y_{21} = -\frac{1}{r(o)} \cdot \frac{1}{V_{II}(s,d)} \tag{2.6b}$$

$$y_{22} = \frac{1}{r(d)} \cdot \frac{V_{II}'(s,d)}{V_{II}(s,d)} \tag{2.6c}$$

where d is the network length (Fig. 2.2).

A number of interesting conclusions can be drawn about the behaviour of distributed RC networks with w(x) and w'(x) continuous and bounded in the interval $0 \leq x \leq d$. These results follow from the theory of Sturm equations.

1. $V_I(s,x)$, $V_{II}(s,x)$ and $V_{II}(s,x)$ are analytic functions of s and x over the interval $0 \leq x \leq d$. Hence the poles of (y_{ij}) are determined only by the zeros of $V_{II}(s,d)$.

2. The zeros of $V_I(s,d)$ and $V'_{II}(s,d)$ do not coincide with the zeros of $V_{II}(s,d)$. Hence the zeros of $y_{11}(s,d)$ and $y'_{22}(s,d)$ are determined only by the zeros of $V_I(s,d)$ and $V'_{II}(s,d)$ respectively, since there is no cancellation of common factors in numerator and denominator.

3. The poles and zeros of y_{11} and y_{22} lie on the negative real axis, and are simple, and have no accumulation point in the finite plane. The poles and zeros are infinite in number with an accumulation point at $-\infty$.

4. The poles and zeros of y_{11} and y_{22} interlace on the negative real axis.

5. The first zero of y_{11} or y_{22} occurs closer to the origin than the first pole.

2.3 Obtaining Poles and Zeros of Admittance Matrix Parameters

In the preceding section, we saw how the two-port admittance matrix parameters of a tapered distributed RC network may be written as simple relations containing ratios of the basic set solutions. By using the Factor Theorem of Weirstrass ((1), Appendix B), and the series expansions for the basic set solutions ((2), p. 531), it can be shown that the functions $V_I(s,d)$ $V_{II}(s,d)$ and $V'_{II}(s,d)$ can be expressed as infinite products. For $V_I(s,d)$, the infinite-product expansion is

$$V_I(s,d) = V_I(o,d) \prod_{k=1}^{\infty} \left(1 - \frac{s}{s_k}\right) \qquad (2.7)$$

where

$$0 > s_1 > s_2 > s_3 \cdots \quad \text{and} \quad \lim s_n = -\infty$$

Similar infinite-product expansions are obtained for $V_{II}(s,d)$ and $V'_{II}(s,d)$.

The poles and zeros of the short-circuit admittance

parameters (y_{ij}) coincide with the zeros of V_I (s,d), V_{II} (s,d), and V'_{II} (s,d). Thus we need to determine the values of $\lambda = -sr_o c_o$ such that V (s,x) satisfies the differential equation (2.4), and also satisfies certain homogeneous boundary conditions.

The boundary conditions which must be imposed on V (s,x) to determine the poles and zeros of the admittance matrix parameters are as follows:

1. Poles of the admittance matrix

$$V(s,o) = 0 \qquad (2.8a)$$

$$V(s,d) = 0 \qquad (2.8b)$$

2. Zeros of y_{11}

$$V'(s,o) = 0 \qquad (2.9a)$$

$$V(s,d) = 0 \qquad (2.9b)$$

3. Zeros of y_{22}

$$V'(s,d) = 0 \qquad (2.10a)$$

$$V(s,o) = 0 \qquad (2.10b)$$

For some special classes of tapered DRC networks the basic set solutions are known in closed form. These include the uniform, exponential, square law, trigonometric and Bessel tapers ((1), p. 30). The poles and zeros of the admittance matrix parameters are the zeros of transcendental functions, and in most cases, closed form solutions for the zeros are not known. Various methods for computing the poles and zeros will be presented in the following Chapters.

Chapter 3

OBTAINING POLES AND ZEROS OF NON-UNIFORM RC LINES BY THE RAYLEIGH-RITZ METHOD

3.1 Introduction

In this Chapter we will consider the Rayleigh-Ritz method for obtaining approximate values of the poles and zeros of the admittance matrix parameters for non-uniform RC lines. The theoretical basis of this method is given in (3) Chapter 6, and (4) Chapter 6 and 7, and only the essential results are given here.

With the Rayleigh-Ritz method, the potential function along the transmission line is usually approximated by a linear combination of polynomials with undetermined coefficients. These coefficients are determined from the condition that a suitably chosen functional should be stationary with respect to small variations in each of the coefficients. In practice when the necessary computations are carried out on a finite-precision computer, the results will be subject to rounding errors. In the following section, we will show that for high-order polynomials it is sometimes extremely difficult to obtain accurate solutions because of the effects of rounding errors. However, it is also shown that this problem can be solved by using orthogonal polynomials.

Although it has been shown previously that it is advantageous to use orthogonal polynomials for problems such as the calculation of least-squares polynomial approximations, (12), the application of these methods to eigenvalue problems of the type considered here does not appear to have been discussed in the literature.

The Rayleigh principle ((3) Chapter 6) asserts that any particular solution $V_j(x)$ of equation (2.4) which is consistent with

the boundary conditions (2.8), (2.9) or (2.10) renders the value of the "Rayleigh quotient".

$$R(V_j) = \frac{\int_o^d w(x) \left|\frac{dV_j}{dx}\right|^2 dx}{\int_o^d w(x) \; V_j^2 \; dx} \tag{3.1}$$

stationary; these stationary values are equal to the corresponding eigenvalues λ_j.

The simplest use we can make of the Rayleigh principle is to approximate the lowest eigenvalue λ_1 of the corresponding boundary value problem; since $w(x)$ is assumed >0 for $0 \leq x \leq d$, it follows that $\lambda_j \geq 0$. If we choose any continuous function $u(x)$ satisfying the boundary conditions, then ((3), Chapter 6)

$$R(u) \geq \lambda_1 \tag{3.2}$$

The Ritz generalization of Rayleigh's method rests in a more general choice of the minimizing function $u(x)$ ((3) chapter 6). Suppose that $v_j(x)$ denotes any polynomial (or function) satisfying all required boundary conditions. Let us now choose our minimizing function to be a linear combination of $v_j(x)$'s of the form

$$u(x) = c_1 v_1(x) + c_2 v_2(x) + - - + c_k v_k(x) \tag{3.3}$$

Where the c_j's are coefficients as yet undetermined.

Suppose now that we introduce the above minimizing function into the Rayleigh Quotient $R(u)$. We find that both numerator and denominator become homogeneous and quadratic forms in the undetermined coefficients c_j. From Rayleigh's principle we know that $R(u)$ is a minimum for the smallest eigenvalue λ_1, and becomes stationary for the functions $u(x) = V_j(x)$ corresponding to the larger eigenvalues λ_j $(j > 1)$. The necessary conditions that

R(u) be stationary are

$$\frac{\partial R(u)}{\partial c_i} = 0 \tag{3.4}$$

for $i = 1,2,3 - - k$

Now after performing the differentiation of the Rayleigh Quotient, we obtain the homogeneous system of linear equations

$$\left[A - k^2 B\right]\left[C\right] = 0 \tag{3.5}$$

where

$$a_{ij} = a_{ji} = \int_o^d w(x) \frac{dv_i}{dx} \frac{dv_j}{dx} dx \tag{3.6}$$

$$b_{ij} = b_{ji} = \int_o^d w(x) v_i v_j dx \tag{3.7}$$

for $i,j = 1,2,3 - - - k$

$$k^2 = R(u) \tag{3.8}$$

and

$$\left[C\right] = \begin{bmatrix} c_1 \\ c_2 \\ \vdots \\ c_k \end{bmatrix} \tag{3.9}$$

The eigenvalues k_j^2 of the homogeneous system (3.5) can be shown to be always greater than, or equal to the exact eigenvalues λ_j, and are all positive and real. By increasing the number of terms in (3.3) the errors in the approximate solutions can be made arbitrarily small.

In addition, we note that it is not necessary to constrain the expansion functions $v_i(x)$ in (3.3) to satisfy boundary conditions of the form $\frac{dv}{dx} = 0$ at $x = 0$ or $x = d$, since these are "natural" boundary conditions for minimization of the Rayleigh quotient R(u), (4) p. 152. However it is necessary for the $v_i(x)$

to satisfy "prescribed" boundary conditions of the form $V(x) = 0$ at $x = 0$ or $x = d$; this restriction on the expansion functions $v_i(x)$ can also be removed if an "extended" Rayleigh quotient (14), Chapter 7, is used instead of (3.1). When the extended Rayleigh quotient is used it is not necessarily correct to assume that the approximate eigenvalues are upper bounds on the exact eigenvalues.

3.2 Numerical Results

We consider the problem of calculating the poles and zeros of the admittance matrix parameters for a distributed RC network with a linear taper. In this case we have

$$w(x) = w_o (1 + \alpha x) \tag{3.10}$$

for

$$0 \leq x \leq d$$

where $w(x)$ is the length of the equipotential line at x.

We define a taper factor τ as the ratio of the network width at Port 1 to the width at Port 2.

$$\tau = w(o)/w(d) \tag{3.11}$$

Thus

$$\alpha = (\frac{1}{\tau} - 1)/d \tag{3.12}$$

The poles and zeros of the admittance matrix parameters are the zeros of functions containing products of Bessel functions of the first and second kind of order zero and one (5).

Define an auxilliary parameter k by

$$k^2 = - s r_o c_o d^2 \tag{3.13}$$

The poles of the admittance matrix are the solutions of

$$J_o (\frac{k\tau}{\tau-1}) \cdot Y_o (\frac{k}{\tau-1}) - J_o (\frac{k}{\tau-1}) \cdot Y_o (\frac{k\tau}{\tau-1}) = 0 \tag{3.14}$$

The zeros of y_{11} are the solutions of

$$J_1\left(\frac{k\tau}{\tau-1}\right)\cdot Y_0\left(\frac{k}{\tau-1}\right) - J_0\left(\frac{k}{\tau-1}\right)\cdot Y_1\left(\frac{k\tau}{\tau-1}\right) = 0 \qquad (3.15)$$

The zeros of y_{22} are the solutions of

$$J_0\left(\frac{k\tau}{\tau-1}\right)\cdot Y_1\left(\frac{k}{\tau-1}\right) - J_1\left(\frac{k}{\tau-1}\right)\cdot Y_0\left(\frac{k\tau}{\tau-1}\right) = 0 \qquad (3.16)$$

It is easily shown that the zeros of the impedance matrix parameter z_{11} are equal to the zeros of y_{22}, and the zeros of z_{22} are equal to the zeros of y_{11}. In addition, the poles of the impedance matrix are the solutions of (5),

$$J_1\left(\frac{k\tau}{\tau-1}\right)\cdot Y_1\left(\frac{k}{\tau-1}\right) - J_1\left(\frac{k}{\tau-1}\right)\cdot Y_1\left(\frac{k\tau}{\tau-1}\right) = 0 \qquad (3.17)$$

The first four solutions k_i $(i = 1,2,3,4)$ of (3.14) and (3.17) are tabulated for various values of τ between 1 and 4 in ((6), p. 74 and p. 75)*. Also in (7) the first ten solutions $k_i/(1-\tau)$ $(i = 1,2 - - 10)$ of (3.14) and (3.17) are tabulated for various values of τ between 0.05 and 0.95. We note that the solutions k_i of (3.14) and (3.17) are unchanged if τ is replaced by $1/\tau$. Also (3.17) has a solution $k = 0$.

Asymptotic expansions for the zeros of (3.14), (3.16) and (3.17) are given in (8) p. 374 for $\tau \geq 1$. The asymptotic expansion for the zeros of (3.16) with $\tau \geq 1$ can also be used to obtain approximations for the zeros of (3.15) with $\tau \leq 1$. These asymptotic formulae are most accurate for τ approximately equal to unity, and for $k_i/(\tau-1) >> 1$.

A computer program which can be used to calculate accurate values of the zeros of (3.14) - (3.17) for $0.1 \leq \tau \leq 10$ was developed. Approximate values of the zeros are obtained from the

* In the limit $\tau = 1$, (3.14) to (3.16) are still valid, and the asymptotic solutions in (8) p.374 are exact.

asymptotic expansions, or from empirical formula based on the numerical results given in (9). These approximate zeros are then refined using the secant modification of Newton's method in which the derivatives of the function are replaced by difference quotients. Values of the Bessel functions $J_o(x)$, $Y_o(x)$, $J_1(x)$ and $Y_1(x)$ are calculated using the polynomial approximations in (8) p. 369 - 370.

Table 3.1 shows the first 20 poles and zeros of the impedance and admittance matrix parameters for a taper factor $\gamma = 0.1$. (The numerical values shown are $k_i^2 = -s_i r_o c_o d^2$ where the s_i are the poles and zeros). The results are believed to be accurate to at least 7 significant figures. This conclusion is based on comparison of these results with those given in (7), and the fact that the polynomial approximations for the Bessel functions are accurate to at least 7 decimals.

We now consider application of the Rayleigh-Ritz method to the problem of calculating the poles and zeros of the immittance matrix parameters for a linearly tapered distributed RC network.

A convenient form of the minimizing function u(x) (equation (3.3)) is

$$u(x) = v(x) \sum_{j=0}^{k} c_j x^j \qquad (3.18)$$

where $v(x)$ is a polynomial satisfying the "prescribed" boundary conditions of the problem, and which has no zeros in the interval $0 \leq x \leq d$.

For calculation of poles of the admittance matrix we choose

$$v(x) = x\,(1-x/d) \qquad (3.19a)$$

TABLE 3.1. Exact eigenvalues corresponding to the first 20 poles and zeros of the immittance matrix parameters for a linearly tapered distributed RC line.

τ = 0.1 = network width at port 1/width at port 2

The poles and zeros, s_i, are related to the eigenvalues k_i^2 by equation (3.13).

N	POLES ADMITTANCE MATRIX	POLES IMPEDANCE MATRIX	ZEROS Y11 Z22	ZEROS Y22 Z11
1	8.89557362	12.58012664	4.85448790	0.98490701
2	38.09138441	43.52716112	26.55534506	20.07898068
3	87.22959042	93.57739449	67.01051331	59.27239275
4	156.19448471	163.06709480	126.76360512	118.33356857
5	244.94342422	252.14182854	206.03919601	197.19490623
6	353.45703888	360.86991882	304.93795013	295.82851028
7	481.72539520	489.28616714	423.50908661	414.22083664
8	629.74296570	637.40956879	561.77857971	552.36463928
9	797.50643158	805.25119781	719.76105499	710.25569153
10	985.01377869	992.81772614	897.46520233	887.89146423
11	1192.26364136	1200.11337280	1094.89640808	1085.27032471
12	1419.25509644	1427.14102173	1312.05822754	1302.39118958
13	1665.98760986	1673.90252686	1548.95294189	1539.25334167
14	1932.46075439	1940.39918518	1805.58213806	1795.85630798
15	2218.67419434	2226.63192749	2081.94699097	2072.19967651
16	2524.62765503	2532.60159302	2378.04830933	2368.28314209
17	2850.32098389	2858.30844116	2693.88671875	2684.10656738
18	3195.75405884	3203.75305176	3029.46258545	3019.66979980
19	3560.92675781	3568.93569946	3384.77609253	3374.97274780
20	3945.83905029	3953.85638428	3759.82803345	3750.01528931

For the zeros of y_{11}

$$v(x) = (1-x/d) \tag{3.19b}$$

For the zeros of y_{22}

$$v(x) = x \tag{3.19c}$$

And for the poles of the impedance matrix

$$v(x) = 1 \tag{3.19d}$$

The next step is the calculation of the matrices A and B in the homogeneous system (3.5). With u(x) defined by (3.18) Equations (3.6) and (3.7) become

$$a_{ij} = a_{ji} = \int_o^d w(x) \frac{d}{dx}\left[v(x)x^{i-1}\right].\frac{d}{dx}\left[v(x)x^{j-1}\right] dx \tag{3.20}$$

$$b_{ij} = b_{ji} = \int_o^d w(x) \left[v(x)\right]^2 x^{i+j-2} dx \tag{3.21}$$

for

$$i,j = 1,2,3 \text{ --- } (k+1)$$

with w(x) and v(x) defined by (3.10) and (3.19).

It is seen that the a_{ij} and b_{ij} are linear combinations of integrals of the type

$$I_m = \int_o^d w(x)\, x^m\, dx \tag{3.22}$$

for

$$m = 0,1,2 \text{ --- } 2(k+1)$$

where 1 is the degree of v(x)

For a linearly tapered DRC network, $w(x) = w_o(1 + \alpha x)$, and the integrals in (3.22) can be easily evaluated. For other types of taper functions w(x) such as exponential, and squared tapers (9),

analytic expressions for the integrals (3.22) are readily obtained. However, for other taper functions, it may be necessary to resort to approximate numerical integration techniques (3), Chapter 8.

The final part of the calculation is the solution of $[A - k^2 B][C] = 0$. This was done by a library program (10) which starts by decomposing B into the form $L L^t$ where L is a lower triangular matrix. Matrix A is then premultiplied by L^{-1} and postmultiplied by $(L^t)^{-1}$ to give

$$\left[L^{-1} A (L^t)^{-1} - k^2 I\right]\left[L^t C\right] = 0 \qquad (3.23)$$

This is the usual form of the eigenvalue problem, and we note that the symmetry of the problem has been preserved. The new matrix $L^{-1} A (L^t)^{-1}$ can now be tridiagonalized by the Householder algorithm, and the eigenvalues found by Sturm sequence and bisection (11), Chapter 5.

The output from this procedure consists of a set of eigenvalues k_i^2, and the corresponding eigenvectors $\left[c_{ji}\right]$, where c_{ji} is the jth coefficient for the ith eigenfunction defined by (3.18).

Thus the ith eigenfunction is

$$u_i(x) = v(x) \sum_{j=1}^{k+1} c_{ji}\ x^{j-1} \qquad (3.24)$$

The procedure described above was used to compute approximate values for the poles and zeros of the immittance matrix parameters for a linearly tapered DRC network with $\tau=1$ and $\tau=0.1$. An attempt was made to obtain solutions with polynomials u(x) of degree 5, 10, 15 and 20, using two computers with different word

lengths; the computers used were an IBM 7090 with a word length of 36 bits, and a CDC 6400 with a word length of 60 bits. When the program was run on the IBM 7090, it either failed for u(x) of degree ≥ 15 because it was determined that a negative diagonal element occurred during the decomposition of B into LL^t, or a negative eigenvalue was found. Both of these conditions result from rounding errors during the calculations. For u(x) of degree 10, it was found that the lowest eigenvalues obtained using the program on the IBM 7090 agreed with those obtained using the CDC 6400 program to 7 significant figures, but the largest eigenvalues agreed only in the first 1 or 2 significant figures.

The reason for the difficulties encountered above is that the off-diagonal elements of the B matrix are not significantly smaller than the diagonal elements for the larger row or column numbers. In fact, for a taper factor $\tau=1$, and $v(x)=1$, the B matrix is identical to the principal minor of order k+1 of the infinite Hilbert matrix (12). It has been observed frequently that systems of linear equations involving minors of this matrix are very difficult to solve accurately. Thus we conclude that solution of the eigenvalue problem with a minimizing function of the form (3.18) is likely to be inaccurate.

We now consider some possible methods of reducing the problems of numerical inaccuracy experienced with the method described above. Firstly we note that the elements in each row of the lower triangular matrix L^{-1} (or each column of $(L^t)^{-1}$) are the coefficients of a system of polynomials which are orthogonal with respect to the weight function $w(x).[v(x)]^2$ on the interval $0 \leq x \leq d$.

Let $$T = L^{-1} \tag{3.25}$$

and

$$P_{i-1}(x) = \sum_{j=1}^{i} t_{ij}\, x^{j-1} \tag{3.26}$$

Then

$$\int_0^d w(x)\,[v(x)]^2\, P_{i-1}(x)\, P_{j-1}(x)\, dx = 1 \text{ for } i=j \tag{3.27}$$
$$= 0 \text{ for } i \neq j$$

This follows since, by definition,

$$B = L\, L^t \tag{3.28}$$

$$\therefore \quad T B T^t = I = \text{Unit matrix} \tag{3.29}$$

and the left hand side of (3.27) is the (i,j)th element of the matrix product (3.29).

It is now clear that the (i,j)th element of the matrix

$$D = L^{-1} A (L^t)^{-1} = T A T^t \tag{3.30}$$

in Equation (3.23) is given by

$$d_{ij} = d_{ji} = \int_0^d w(x) \cdot \frac{d}{dx}\left[v(x) P_{i-1}(x)\right] \cdot \frac{d}{dx}\left[v(x) P_{j-1}(x)\right] dx \tag{3.31}$$

If the minimizing function u(x) in Equation (3.18) is replaced by

$$u(x) = v(x) \sum_{j=0}^{k} c_j\, P_j(x) \tag{3.32}$$

Then Equation (3.23) becomes

$$\left[D - k^2 I\right]\left[C\right] = 0 \tag{3.33}$$

Thus both choices of the minimizing function u(x) (3.18) or (3.32) lead to the same matrix eigenvalue problem.

The problems we are now faced with are the determination of the orthogonal polynomials $P_j(x)$ satisfying (3.27), and accurate evaluation of the integrals in (3.31).

It can be shown that any set of polynomials which are orthogonal with respect to some weight function w(x) over an interval $a \leq x \leq b$ satisfy a three-term recurrence relation (12), (13)

$$P_r(x) = (x-\alpha_r) P_{r-1}(x) - \beta_r P_{r-2}(x) \text{ for } r \geq 2 \tag{3.34a}$$

with

$$P_1(x) = (x-\alpha_1) P_0(x) \tag{3.34b}$$

and

$$P_0(x) = 1 \tag{3.34c}$$

For certain classes of weight function w(x), the coefficients α_r, β_r are known (8), Chapter 22. In other cases, these coefficients may be computed as follows (12), (13). We define the scalar product of two functions $f_1(x)$ and $f_2(x)$ by

$$\langle f_1, f_2 \rangle = \int_a^b w(x) f_1(x) f_2(x) \, dx \tag{3.35}$$

Then

$$\alpha_r = \langle x P_{r-1}(x), P_{r-1}(x) \rangle / \langle P_{r-1}(x), P_{r-1}(x) \rangle \tag{3.36}$$

for $r \geq 1$

and

$$\beta_r = \langle x P_{r-1}(x), P_{r-2}(x) \rangle / \langle P_{r-2}(x), P_{r-2}(x) \rangle \tag{3.37}$$

for $r \geq 2$

We note that the highest coefficient of each polynomial is unity, so that they are not orthonormal in general. The orthonormalization is achieved by dividing each of the polynomials in (3.34) by

$$\gamma_r = \langle P_r(x), P_r(x) \rangle^{\frac{1}{2}} \tag{3.38}$$

For purposes of numerical work it is necessary to replace integrals of the type (3.35) by appropriate rules for numerical integration. That is, we introduce a fixed set of abscissae $x_1, x_2 - - - x_m$, and assume that

$$\langle f_1, f_2 \rangle = \int_a^b W(x)\, f_1(x)\, f_2(x)\, dx \approx \sum_{i=1}^{m} w_i\, f_1(x_i)\, f_2(x_i) \tag{3.39}$$

is sufficiently accurate for the functions in question. For certain classes of weight functions $W(x)$, the values of the weights w_i and abscissae x_i which render the numerical integration formula (3.39) exact for polynomials f_1 and f_2 up to a certain degree have been tabulated (3) Chapter 7, Appendix 4. For the case when $w(x)$, $f_1(x)$ and $f_2(x)$ are polynomials, the Gaussian quadrature formula, (3) Appendix 4, yields a numerical integration rule which is exact when the integrand in (3.39) is any polynomial of degree less than 2m.

We now return to the problem of determining the coefficients α_r, β_r and γ_r for the case of a linearly tapered DRC network with $W(x) = w(x).\,[v(x)]^2$ where $w(x)$ and $v(x)$ are given by Equations (3.10) and (3.19) respectively. We use Gaussian integration to evaluate the integrals on the right hand of equations (3.36) and (3.37), and the recurrence relation (3.34a) is used to generate the

values of the orthogonal polynomials as required at the abscissae $x_1, x_2 - - - x_m$. The integrals in (3.31) can also be evaluated using Gaussian integration once the values of $\frac{d}{dx}\left[v(x)\, P_r(x)\right]$ for r=0, 1, -- k, have been determined.

From (3.34) we obtain

$$v(x)\, P_0(x) = v(x) \tag{3.40a}$$

$$v(x)\, P_1(x) = v(x)\, (x-\alpha_1)\, P_0(x) \tag{3.40b}$$

and

$$v(x)\, P_r(x) = v(x)\left[(x-\alpha_r)\, P_{r-1}(x) - \beta_r P_{r-2}(x)\right] \text{ for } r \geq 2 \tag{3.40c}$$

Thus the values of $\frac{d}{dx}\left[v(x)\, P_r(x)\right]$ at $x = x_1, x_2 --- x_m$ can be found using the following relations*

$$g_0(x) = \frac{d}{dx}\left[v(x)\, P_0(x)\right] = v'(x) \tag{3.41a}$$

$$g_1(x) = \frac{d}{dx}\left[v(x)\, P_1(x)\right] = v(x) + (x-\alpha_1)\, g_0(x) \tag{3.41b}$$

$$g_r(x) = \frac{d}{dx}\left[v(x)\, P_r(x)\right] = (x-\alpha_r)\, g_{r-1}(x) + v(x)\, P_{r-1}(x) - \beta\, g_{r-2}(x) \quad \text{for } r \geq 2 \tag{3.41c}$$

The method outlined above was used to calculate the poles and zeros of the immittance matrix parameters for linearly tapered DRC networks with taper factors τ equal to 0.1 and 1.0. The program was run on both the IBM 7090 and CDC 6400 computers. It was found that for k = 5, 10, 15, 20 (Equation (3.32)) the eigenvalues obtained using the two computers, (one with 36 bit words and the other with 60 bit words), agreed to at least 6 significant figures. Tables 32-36 show the approximate eigenvalues obtained for distributed RC lines with taper factor τ equal to 1.0 and 0.1.

* As discussed in (12), and verified by the results obtained here, roundoff errors in the computation do not accumulate excessively when the recurrence relations (3.34), (3.35), (3.40) and (3.41) are used.

TABLE 3.2. Approximate eigenvalues corresponding to the poles of the admittance matrix for a uniform RC line. NP is the degree of the polynomial used to approximate the potential function. The poles, s_i, are related to the eigenvalues, k_i^2, by equation (3.13).

N / NP	5	10	15	20	EXACT
1	9.869749	9.869604	9.869604	9.869604	9.869604
2	39.50155	39.47841	39.47841	39.47841	39.47841
3	102.1302	88.82644	88.82644	88.82644	88.82643
4	200.4984	157.9569	157.9136	157.9136	157.9136
5		247.0427	246.7401	246.7401	246.7401
6		376.4744	355.3062	355.3057	355.3057
7		531.6718	483.8120	483.6106	483.6106
8		1298.090	632.4449	631.6551	631.6546
9		1852.589	825.8688	799.4410	799.4379
10			1039.418	987.3940	986.9604
11			1630.858	1195.545	1194.222
12			2067.941	1451.099	1421.223
13			5996.024	1723.096	1667.963
14			7677.497	2303.771	1934.442
15				2749.649	2220.660
16				4762.078	2526.618
17				5728.540	2852.315
18				18153.30	3197.751
19				21934.68	3562.927
20					3947.841

TABLE 3.3. Approximate eigenvalues corresponding to the zeros of the admittance matrix elements $y_{11} = y_{22}$ for a uniform RC line.

NP is the degree of the polynomial used to approximate the potential function.

The zeros, s_i, are related to the eigenvalues, k_i^2, by equation (3.13).

N / NP	5	10	15	20	EXACT
1	2.467401	2.467401	2.467401	2.467401	2.467401
2	22.21385	22.20661	22.20661	22.20661	22.20661
3	63.02767	61.68503	61.68502	61.68502	61.68502
4	148.2050	120.9046	120.9026	120.9026	120.9026
5	545.7527	200.0428	199.8594	199.8594	199.8594
6		302.5545	298.5558	298.5555	298.5555
7		451.8311	417.0108	416.9907	416.9907
8		742.4795	555.7070	555.1652	555.1652
9		1563.910	719.4639	713.0808	713.0789
10		6011.918	930.7517	890.7922	890.7317
11			1254.004	1089.081	1088.1238
12			1843.956	1313.523	1305.255
13			3127.797	1585.402	1542.125
14			6811.562	1956.095	1798.735
15			26729.07	2522.980	2075.084
16				3472.600	2371.172
17				5234.998	2686.999
18				9058.351	3145.936
19				20000.01	3377.872
20				79111.91	3752.917

TABLE 3.4. Approximate eigenvalues corresponding to the poles of the admittance matrix for a linearly tapered RC line.

τ = 0.1 = network width at port 1/width at port 2

The poles, s_i, are related to the eigenvalues, k_i^2, by equation (3.13).

NP is the degree of the polynomial used to approximate the potential function.

N/NP	5	10	15	20	EXACT
1	8.905809	8.895589	8.895573	8.895573	8.895573
2	38.12073	38.09143	38.09138	38.09138	38.09138
3	91.60245	87.22962	87.22959	87.22959	87.22959
4	201.7800	156.2063	156.1944	156.1944	156.1944
5		245.3986	244.9434	244.9434	244.9434
6		365.0764	353.4580	353.4570	353.4570
7		531.9913	481.8123	481.7254	481.7254
8		1089.6852	630.7700	629.7431	629.7429
9		1854.019	813.7700	797.5114	797.5064
10			1039.551	985.2309	985.0138
11			1516.524	1193.876	1192.263
12			2068.745	1438.731	1419.255
13			5142.097	1723.147	1665.987
14			7679.079	2215.945	1932.460
15				2750.220	2218.674
16				4378.051	2524.627
17				5729.565	2850.320
18				15979.16	3195.754
19				21936.38	3560.926
20					3945.839

TABLE 3.5. Approximate eigenvalues corresponding to the zeros of the admittance matrix element y_{11} for a linearly tapered RC line.

The zeros, s_i, are related to the eigenvalues, k_i^2, by equation (3.13).

τ and NP are as in TABLE 3.4.

N/NP	5	10	15	20	EXACT
1	4.854510	4.854488	4.854488	4.854488	4.854487
2	26.56305	26.55534	26.55534	26.55534	26.55534
3	67.36751	67.01052	67.01051	67.01051	67.01051
4	165.6900	126.7638	126.7636	126.7636	126.7636
5	403.0070	206.2692	206.0392	206.0392	206.0392
6		306.5022	304.9382	304.9379	304.9379
7		466.6106	423.5138	423.5091	423.5090
8		676.3830	562.4187	561.7786	561.7785
9		1716.533	722.5191	719.7632	719.7610
10		4521.535	945.1306	897.4821	897.4652
11			1201.358	1096.012	1094.896
12			1925.024	1315.889	1312.058
13			2725.284	1599.438	1548.952
14			7331.931	1908.852	1805.582
15			21333.12	2538.217	2081.947
16				3216.986	2378.048
17				5470.335	2693.886
18				7892.402	3029.462
19				21223.57	3384.776
20				65931.30	3759.828

TABLE 3.6. Approximate eigenvalues corresponding to the zeros of the admittance matrix element y_{22} for a linearly tapered RC line.
The zeros, s_i, are related to the eigenvalues, k_i^2, by equation (3.13).
Υ and NP are as in TABLE 3.4.

N \ NP	5	10	15	20	EXACT
1	0.987317	0.984910	0.984907	0.984907	0.984907
2	20.09811	20.07901	20.07898	20.07898	20.07898
3	60.15842	59.27245	59.27239	59.27239	59.27239
4	125.2519	118.3345	118.3335	118.3335	118.3335
5	640.3668	197.2177	197.1949	197.1949	197.1949
6		300.0832	295.8285	295.8285	295.8285
7		428.6888	414.2392	414.2208	414.2208
8		771.5219	552.4891	552.3646	552.3646
9		1219.237	717.2805	710.2559	710.2556
10		6693.059	907.0734	887.9524	887.8914
11			1273.773	1085.553	1085.270
12			1656.542	1311.577	1302.391
13			3299.329	1561.604	1539.253
14			5458.203	1972.429	1795.856
15			28905.62	2379.161	2072.199
16				3574.251	2368.283
17				4629.479	2684.106
18				9521.190	3019.669
19				16625.08	3374.972
20				84109.34	3750.015

The eigenvalues k_i^2 are related to the poles and zeros of the admittance matrix parameters by (3.13).

We therefore conclude that this method is numerically superior to the one previously described, which uses a minimizing function u(x) of the form given in (3.18).

Some additional numerical experiments were carried out using a minimizing function

$$u(x) = v(x) \sum_{j=0}^{k} o_j T_j^*(x) \tag{3.42}$$

where $T_j^*(x)$ is the Chebyshev polynomial of degree j, shifted to the interval $0 \leq x \leq d$.

In this case, the elements of the A and B matrices become

$$a_{ij} = a_{ji} = \int_o^d w(x) \cdot \frac{d}{dx}\left[v(x)\, T_{i-1}^*(x)\right] \cdot \frac{d}{dx}\left[v(x)\, T_{j-1}^*(x)\right] dx \tag{3.43}$$

$$b_{ij} = b_{ji} = \int_o^d w(x) \cdot \left[v(x)\right]^2 T_{i-1}^*(x) \cdot T_{j-1}^*(x)\, dx \tag{3.44}$$

The Chebyshev polynomials satisfy a three-term recurrence relation of the form (3.34) and the coefficients α_r, β_r are known (8), Chapter 22. Gaussian quadrature can then be used to evaluate the integrals in (3.43) and (3.44) since $T_r^*(x)$ and $\frac{d}{dx}\left[v(x)\, T_r(x)\right]$ are easily obtained at $x = x_1, x_2, \cdots x_m$, using recurrence relations of the form (3.34) and (3.41) respectively.

It was found that the eigenvalues obtained using Chebyshev polynomials differed from those obtained using the orthogonal

polynomials $P_r(x)$ in only the last one or two decimals. Thus we conclude that both of these methods give essentially the same numerical accuracy.

Finally, the eigenvalue problem was solved with

$$u(x) = v(x) \sum_{j=0}^{k} c_j L_j(x) \tag{3.45}$$

where

$L_j(x)$ are the Lagrangian interpolation polynomials

corresponding to equally spaced points in the interval $0 \leq x \leq d$ (3), Chapter 2. It was found that for the larger values of k, the accuracy of the lowest eigenvalues decreased markedly, while the largest eigenvalues were in close agreement with those obtained by the two methods described above.

3.3 Conclusion

Although we have only considered the class of non-uniform transmission lines for which

$$r(x) = r_o/w(x) \tag{3.46}$$

and

$$c(x) = c_o w(x) \tag{3.47}$$

the method can easily be adapted to solve problems for which

$$r(x) = r_o/f(x) \tag{3.48}$$

$$c(x) = c_o g(x) \tag{3.49}$$

In this case the Rayleigh Quotient (3.1) is replaced by (1), p. 59,

$$R(u) = \frac{\int_0^d f(x) \left|\frac{du}{dx}\right|^2 dx}{\int_0^d g(x)\, u^2 \, dx} \qquad (3.50)$$

and the solution is obtained in the manner previously described.

In order to minimize the effects of rounding errors it is better to choose the minimizing function u(x) of the form (3.32) instead of the form (3.18); if the form (3.18) is chosen, an ill-conditioned system of equations is likely to result. The $P_j(x)$ in (3.32) may be any system of orthogonal polynomials, but it is generally most convenient to use polynomials orthogonal with respect to w(x) in the interval $0 \leq x \leq d$. The integrals should be evaluated by a numerical integration formula of the type (3.39) where the values of the orthogonal polynomials at the abscissae x_i are obtained by means of a recurrence relation; this method was found to give better numerical accuracy than other methods.

Chapter 4

OBTAINING POLES AND ZEROS OF THE ADMITTANCE MATRIX BY SOLUTION OF FIRST-ORDER DIFFERENTIAL EQUATIONS

4.1 Introduction

We now wish to consider a direct method for obtaining approximate eigenvalues of the boundary value problem defined in Chapter 2, which uses the pair of first-order differential equations (2.3a) and (2.3b). The first-order equations (2.3a), (2.3b) are equivalent to the second-order differential equation (2.4), and the eigenvalues are proportional to either the poles or zeros of the admittance matrix parameters, depending on which of the boundary conditions (2.8) - (2.10) are satisfied by the eigenfunctions. As before, we consider only two-port distributed RC lines supporting one-dimensional current flow.

The numerical technique used here is known as the Method of Moments, which is described in some detail in (14), Chapter 7. Although the method as described in (14) is directly applicable to analysis of lossless transmission lines, it is easily modified to solve distributed RC transmission line problems. One interesting feature of the present method is that under certain conditions the approximate eigenvalues are smaller in magnitude than the exact eigenvalues; with the method described in Chapter 3, the approximate eigenvalues are always larger than the exact eigenvalues. This sometimes introduces difficulties in the practical application of the method, since the approximate eigenvalues corresponding to the larger eigenvalues may be comparable with the smaller (dominant) eigenvalues. This problem does not appear to have been considered previously in the literature, and some techniques for detecting

these "extraneous" solutions are described in this Chapter. In addition, by modifying the triangle functions which are used to approximate the unknown voltage and current in the transmission line it is shown that the accuracy of the solutions may be improved, and the "extraneous" solutions mentioned above are avoided.

In (14), Chapter 7 it is shown that when similar series expansions are used for the unknown voltage and current functions, the solutions to the first-order equations converge faster than those to the second-order equation. It is shown here that if the transmission line is divided into a number of incremental sections of length h, and piecewise linear approximations are used for the voltage and current functions, then the asymptotic error in the eigenvalues is generally of order h^4. For the second-order differential equation the asymptotic error is generally of order h^2.

4.2 Solution of First-Order Differential Equations by the Method of Moments

The first-order equations (2.3a), (2.3b) may be written in the form

$$\begin{bmatrix} 0 & \frac{d}{dx} \\ \frac{d}{dx} & 0 \end{bmatrix} \begin{bmatrix} V \\ I \end{bmatrix} = \begin{bmatrix} sc(x) & 0 \\ 0 & -r(x) \end{bmatrix} \begin{bmatrix} V \\ I \end{bmatrix} \qquad (4.1)$$

where

$c(x)$ and $r(x)$ are the capacitance and resistance respectively per unit length of the transmission line, and $V(x)$ and $I(x)$ are the voltage and current in the resistive layer at x.

The poles and zeros s_i of the admittance parameters are the values of s such that (4.1) has a non-trivial solution when $V(x)$ satisfies the boundary conditions (2.8) - (2.10). These boundary conditions may be put into the form:-

1. Poles of the admittance matrix

$$V(0) = 0 \tag{4.2a}$$

$$V(d) = 0 \tag{4.2b}$$

2. Zeros of y_{11}

$$I(0) = 0 \tag{4.3a}$$

$$V(d) = 0 \tag{4.3b}$$

3. Zeros of y_{22}

$$V(0) = 0 \tag{4.4a}$$

$$I(d) = 0 \tag{4.4b}$$

where

d is the length of the transmission line, and $0 \leq x \leq d$

Next, we choose two sets of basis functions, $\phi_1, \phi_2,$ ---, and $\psi_1, \psi_2,$ ---, and approximate V(x) and I(x) as follows:

$$V(x) = \sum_{j=1}^{k} c_j \phi_j (x) \tag{4.5a}$$

$$I(x) = \sum_{j=1}^{l} d_j \psi_j (x) \tag{4.5b}$$

where

c_j and d_j are coefficients to be determined. The number of basis functions, k and l respectively, need not be equal.

The unknown coefficients c_j and d_j and the approximate eigenvalues are obtained by the method of moments as described in (14), Chapter 7. The matrix eigenvalue problem to be solved is

$$\left[A - \lambda B \right] \left[C \right] = 0 \tag{4.6}$$

where

$$A = \left[L^{\psi\phi}\right]^t \left[M^{\psi}\right]^{-1} \left[L^{\psi\phi}\right] \tag{4.7a}$$

$$B = M^{\phi} \tag{4.7b}$$

$$\lambda = -s \tag{4.7c}$$

and

$$I^{\psi\phi}_{ij} = \int_0^d \psi_i \frac{d\phi_j}{dx}\, dx \tag{4.8a}$$

$$m^{\psi}_{ij} = \int_0^d r(x)\, \psi_i(x).\psi_j(x)\, dx \tag{4.8b}$$

$$m^{\phi}_{ij} = \int_0^d c(x)\, \phi_i(x).\phi_j(x)\, dx \tag{4.8c}$$

The coefficients d are obtained from c by using

$$\left[d\right] = -\left[M^{\psi}\right]^{-1} \left[L^{\psi\phi}\right]\left[c\right] \tag{4.9}$$

In the above it is assumed that the $\phi_j(x)$ are such that the V(x) satisfies the boundary conditions (4.2) - (4.4). However, it is not necessary to constrain I(x) to satisfy the boundary conditions (4.3) - (4.4), since these are "natural" boundary conditions which must be satisfied by the exact solution of our problem. In addition, the boundary conditions on V(x) could be made "natural" by modifying (4.8a); this is discussed in (14) pp. 147 - 148.

Techniques for solving the matrix eigenvalue problem (4.6) have already been discussed in Chapter 3, and will not be considered further here.

4.3 Numerical Results

We now consider the choice of the expansion functions ϕ_j and ψ_j.

Piecewise linear approximations to V(x) and I(x) may be obtained by choosing triangle functions for $\phi_j(x)$ and $\psi_j(x)$ as discussed in (14), Chapter 7.

Suppose we choose N points, $0 = x_1 < x_2 < x_3 \cdots x_{N-1} < x_N = d$, and denote the distance between successive points by

$$h_j = x_{j+1} - x_j \tag{4.10}$$

for

$$j = 1, 2 \cdots (N-1)$$

We now define the triangle function $T_j(x)$ as follows

$$T_j(x) = 1 - \frac{(x-x_j)}{h_j} \quad \text{for} \quad x_j \leq x \leq x_{j+1}$$

$$= \frac{(x-x_{j-1})}{h_{j-1}} \quad \text{for} \quad x_{j-1} \leq x \leq x_j \tag{4.11a}$$

$$= 0 \quad \text{elsewhere}$$

$$\text{for} \quad j = 2, 3, 4 \cdots (N-1)$$

$$T_1(x) = 1 - \frac{x}{h_1} \quad \text{for } 0 \leq x \leq x_2 \tag{4.11b}$$

$$= 0 \quad \text{elsewhere}$$

$$T_N(x) = \frac{(x - x_{N-1})}{h_{N-1}} \quad \text{for} \quad x_{N-1} \leq x \leq d \qquad (4.11c)$$

$$= 0 \qquad \text{elsewhere}$$

The piecewise linear approximations to V(x) and I(x) are

$$V(x) = \sum_{j=1}^{N} c_j T_j(x) \qquad (4.12a)$$

$$I(x) = \sum_{j=1}^{N} d_j T_j(x) \qquad (4.12b)$$

Since

$$T_j(x) = 1 \quad \text{for } x = x_j$$

and

$$T_i(x) = 0 \quad \text{for } x = x_j \quad \text{and } i \neq j$$

the coefficients c_j and d_j are interpreted as the values of V(x) and I(x) respectively at $x = x_j$.

With $\phi_k(x)$ and $\psi_k(x)$ replaced by $T_k(x)$, the integrals in (4.8) may be easily evaluated.

Using (4.8a) it can be shown that

$$L^{\phi\phi} = \frac{1}{2} \begin{bmatrix} -1 & 1 & & & & & & \\ -1 & 0 & 1 & & & & & \\ 0 & -1 & 0 & 1 & & & & \\ & & \ddots & \ddots & \ddots & & & \\ & & & \ddots & \ddots & \ddots & & \\ & & & & \ddots & \ddots & \ddots & \\ & & & & & -1 & 0 & 1 \\ & & & & & & -1 & 1 \end{bmatrix} \qquad (4.13)$$

where the number of rows and columns is N

Although exact analytical solutions for the integrals (4.8b) and (4.8c) can be found for various c(x) and r(x), sufficiently accurate approximate solutions can usually be obtained by assuming that c(x) and r(x) varying linearly in each interval $x_k \leq x \leq x_{k+1}$ for k=1, 2- - (n-1).

Assuming a linear variation of c(x) in each interval, the integrals in (4.8c) are given by

$$m^{\phi}_{11} = \frac{h_1}{12} \left(3\, C(x_1) + C(x_2)\right)$$

$$m^{\phi}_{kk} = \frac{h_{k-1}}{12} \left(C\,(x_{k-1}) + 3\, C(x_k)\right) + \frac{h_k}{12} \left(3\, C(x_k) + C(x_{k+1})\right)$$

$$\text{for} \quad k = 2,3, \text{---} (N-1) \qquad (4.14)$$

$$m^{\phi}_{k,k+1} = m_{k+1,k} = \frac{h_k}{12} \left(C(x_k) + C(x_{k+1})\right)$$

$$m^{\phi}_{NN} = \frac{h_{N-1}}{12} \left(C(x_{N-1}) + 3\, C(x_N)\right)$$

for k = 1, 2, 3-- (N-1)

and $m^{\phi}_{ij} = 0$ otherwise

Similarly, assuming a linear variation of r(x) in each interval, the integrals m^{ψ}_{ij} in (4.8b) are given by a set of equations identical to those in (4.14), but with $c(x_k)$ replaced by $r(x_k)$.

We note that $M^{\emptyset}$ and $M^{\emptyset\emptyset}$ are symmetric, tridiagonal positive definite matrices.

As yet, we have not considered the problem of choosing the approximations to V(x) and I(x) such that they satisfy the homogeneous boundary conditions (4.2) - (4.4).

When the basis function $\emptyset_j(x)$ and $\emptyset_k(x)$ are triangle functions as defined above, boundary conditions of the type V(0) = 0 or I(0) = 0 are satisfied simply by setting the coefficient c_1 or d_1 to zero, while boundary conditions of the type V(d) = 0 or I(d) = 0 are satisfied by setting c_N or d_N to zero. This means that we simply delete the rows and columns corresponding to these zero coefficients from the matrices $\left[L^{\emptyset\emptyset}\right]$, $\left[M^{\emptyset}\right]$ and $\left[M^{\emptyset\emptyset}\right]$

Having formed these matrices, we can then obtain the A and B matrices using equations (4.7a) and (4.7b). We note that although B is a tridiagonal matrix, A has no zero elements in general, because $\left[M^{\emptyset\emptyset}\right]^{-1}$ is a full matrix, even though $\left[M^{\emptyset\emptyset}\right]$ is tridiagonal.

Table 4.1 shows the approximate eigenvalues $\lambda_i = - s_i\, r(o)\, c(o)\, d^2$ obtained for a uniform distributed RC line with boundary conditions V(o) = V(d) = 0 i.e. the corresponding s_i are the poles of the admittance matrix. These results we obtained with all h_i, i = 1, 2 -- equal to the values of H given in the table, and with r(o) = c(o) = d = 1.

Firstly, we note that the approximate eigenvalues are all less than the exact eigenvalues. This was also found to be true for the zeros of the admittance matrix parameters y_{11} and y_{22}. In addition, it was found that the approximate eigenvalues

TABLE 4.1. Approximate eigenvalues corresponding to the poles of the admittance matrix for a uniform RC line.
The poles, s_i, are related to the eigenvalues, λ_i, by $\lambda_i = -s_i r(0)c(0)d^2$

H = 1/(No. of segments into which the line is divided)
The voltage and current in the resistive layer are approximated by triangle functions $T_j(x)$.

N	H = 0.25	0.125	0.0625	0.03125	EXACT
1	9.82475	9.86694	9.86943	9.86955	9.869604
2	36.0000	39.2990	39.4677	39.4777	39.47841
3	43.0732	86.5005	88.7026	88.8188	88.82643
4		144.000	157.196	157.871	157.9136
5		187.958	243.893	246.576	246.7401
6		172.292	346.402	354.810	355.3057
7		72.8416	459.965	482.343	483.6106
8			576.000	628.784	631.6546
9			680.329	793.509	799.4379
10			751.835	975.57	986.9604
11			763.453	1173.59	1194.222
12			689.171	1385.60	1421.223
13			520.811	1608.91	1667.963
14			291.366	1839.86	1934.442
15			84.4155	2073.63	2220.660
16				2304.00	2526.618
17				2521.11	2852.315
18				2721.31	3197.751
19				2887.11	3562.927
20				3007.34	3947.841

TABLE 4.2. Approximate eigenvalues corresponding to the poles of the admittance matrix for a uniform RC line.
s_i, λ_i, and H are as in TABLE 4.1, but the voltage and current in the resistive layer are approximated by triangle functions $T_j(x)$, and $T_j^*(x)$ respectively, as in Fig. 4.1.

N	H = 0.25	0.125	0.0625	0.03125	EXACT
1	9.891088	9.870807	9.869675	9.869608	9.869604
2	40.76470	39.55503	39.48294	39.47869	39.47841
3	98.10891	89.68572	88.87787	88.82955	88.82643
4		162.5293	158.2018	157.9311	157.9136
5		262.3656	247.8333	246.8068	246.7401
6		389.4754	358.5391	355.5049	355.3057
7		517.4557	491.6325	484.1123	483.6106
8			649.0547	632.7706	631.6546
9			833.2017	801.6952	799.4379
10			1046.157	991.1950	986.9604
11			1287.783	1201.693	1194.222
12			1552.093	1433.750	1421.223
13			1822.146	1688.073	1667.963
14			2066.098	1965.534	1934.442
15			2240.283	2267.159	2220.660
16				2594.105	2526.618
17				2947.603	2852.315
18				3328.849	3197.751
19				3738.833	3562.927
20				4178.073	3947.841

obtained for various types of tapered distributed RC lines were less than the exact eigenvalues. There does not appear to be a formal proof that this method always gives eigenvalues less than the exact eigenvalues, although all numerical results obtained are in agreement with this conjecture.

In comparison, the Rayleigh-Ritz method for solution of the second-order differential equation for V(x), always gives eigenvalues which are greater than the exact eigenvalues. Thus by using both the Rayleigh-Ritz method and the method described above, to solve the same eigenvalue problem, we would expect to obtain rigorous upper and lower bounds on the exact eigenvalues.

A further examination of the approximate eigenvalues given in Table 4.1 shows that for the smaller values of H, the eigenvalues are not arranged in order of increasing magnitude i.e. the eigenvalues near the bottom of the table are less than those immediately above them. The reason for arranging the eigenvalues in this manner is as follows. Upon inspection of eigenfunctions corresponding to some of the smaller eigenvalues, it was found that they had a greater number of nodes (zero-crossings) than the eigenfunctions corresponding to larger eigenvalues. It is known from the theory of Sturm-Liouville equations that the eigenvalues increase as the number of nodes in the exact eigenfunctions increases (2), pp 721 - 723. Therefore, instead of arranging the approximate eigenvalues in order of increasing magnitude, we should arrange them according to the number of nodes in the approximate eigenfunctions. However if this method of ordering the eigenvalues is used, ambiguities may arise because some of the eigenfunctions corresponding to the smaller

eigenvalues have the same number of nodes. An alternative method of ordering the approximate eigenvalues which avoids these ambiguities was used. The Rayleigh Quotient,

$$R(u) = \frac{\int_o^d w(x) \left(\frac{dv}{dx}\right)^2 dx}{\int_o^d w(x) \; u^2 \; dx} \qquad (4.15)$$

where

$$r(x) = r(o)/w(x)$$

$$c(x) = c(o).w(x)$$

and

u(x) is an eigenfunction

was computed for each approximate eigenfunction. The approximate eigenvalues are then ordered such that the corresponding Rayleigh Quotients are monotonically increasing.

Finally, we note that the approximate eigenvalues in Table 4.1 converge to the exact eigenvalues as the interval length H decreases. In all cases the lowest order eigenvalues are most accurate, and the error increases to about 10% at the mid-point of each column. (Note that there are actually 31 eigenvalues corresponding to H = 0.03125, but only the first 20 eigenvalues are given in the table). Below the mid-point of each column in the table, the error between the approximate and exact eigenvalues increases markedly, and the successive approximate eigenvalues begin to decrease at some point, whereas the exact eigenvalues are monotonically increasing.

If the method just described is used to obtain approximations to the poles and zeros of the two-port admittance matrix parameters,

and these are then used to calculate the frequency response of the distributed RC network, it is evident that better accuracy will be obtained if we discard all of the "higher-order" extraneous eigenvalues i.e. if we adopt the procedure of ordering the eigenvalues according to the magnitude of the Rayleigh Quotient, then we discard those eigenvalues which are decreasing while the Rayleigh Quotient is increasing. In practice, this means that approximately one third of the total number of eigenvalues calculated would have to be discarded.

We now describe a modification of the preceding method which was found to give more accurate eigenvalues, does not give "extraneous" higher-order eigenvalues, and which is just as easy to program on a computer.

The modified procedure uses piecewise linear approximations to V(x) and I(x), and the approximation to V(x) is identical to that given by (4.12), with triangle functions defined by equations (4.10) - (4.11). For I(x) we use a different set of triangle functions. For convenience we suppose that the triangle function $T_i(x)$ used to approximate V(x) are centred on N equally spaced points, $0 = x_1 < x_2 < x_3 < \cdots < x_{N-1} \quad x_N = d$, and denote the distance between successive points by $h = \frac{d}{(N-1)}$. The piecewise linear approximation to I(x) is

$$I(x) = \sum_{j=1}^{N+1} d_j \, T_j^*(x) \qquad (4.16)$$

where the modified triangle functions $T_j^*(x)$ are as shown in Fig. 4.1. We note that the $T_j^*(x)$ are centred on a number of equally spaced points which are midway between the centre points

for the $T_j(x)$, and in addition, at $x = 0$ and $x = d$, the spacing between triangles is $h/2$ instead of h.

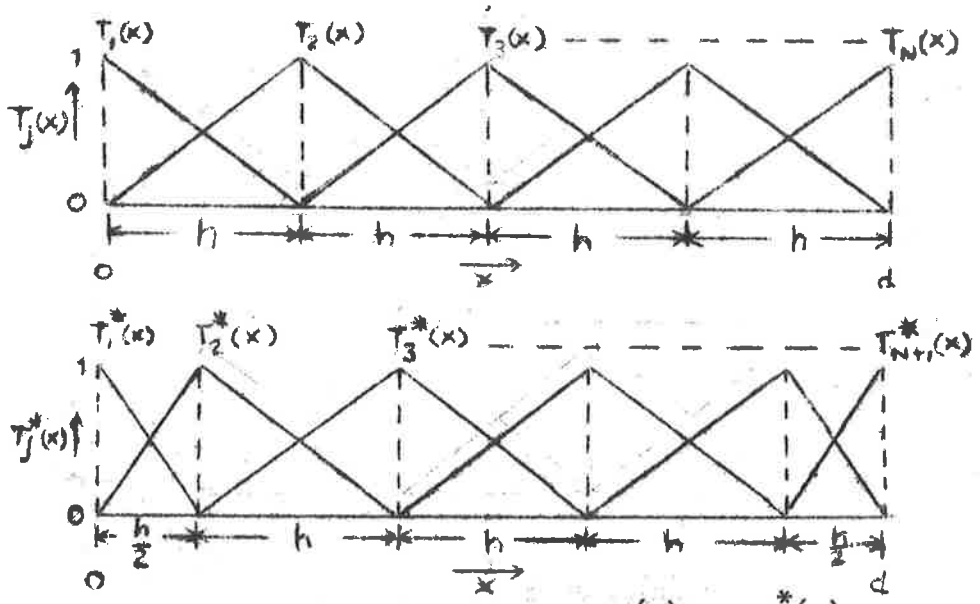

Fig. 4.1 Triangle Functions $T_j(x)$ and $T_j^*(x)$

The integrals $I_{ij}^{\phi\phi}$ in (4.8a) with $\phi_i(x) = T_i^*(x)$ and $\phi_j(x) = T_j(x)$ are readily evaluated, and we obtain

$$I^{\phi\phi} = \frac{1}{8}\begin{bmatrix} -2 & 2 & & & & & & \\ -5 & 4 & 1 & & & & & \\ -1 & -5 & 5 & 1 & & & & \\ & -1 & -5 & 5 & 1 & & & \\ & & \ddots & \ddots & \ddots & \ddots & & \\ & & & \ddots & \ddots & \ddots & \ddots & \\ & & & & -1 & -5 & 5 & 1 \\ & & & & & -1 & -4 & 5 \\ & & & & & & -2 & 2 \end{bmatrix} \qquad (4.17)$$

where the number of rows is (N+1) and the number of columns is N.

The integrals $m^{\emptyset}_{ij}$ in (4.8b) may be evaluated using a set of equations similar to (4.14), with c(x) replaced by r(x). As previously mentioned the equations (4.14) are exact only if c(x) or r(x) vary linearly with x. In the computer program which was written, equations (4.14) were not used to evaluate $m^{\emptyset}_{ij}$ and $m^{\emptyset}_{ij}$. These integrals were evaluated using an automatic numerical integration routine which is based on the method described in (15). The advantage of this is that the integrals can be accurately evaluated for arbitrary r(x) and c(x).

Boundary conditions of the type given in (4.2) - (4.4) are satisfied by setting the coefficients c_1 or d_1 and c_N or d_{N+1} to zero in equations (4.5a) and (4.5b). This is equivalent to deleting the corresponding rows and columns of the matrices $\left[L^{\emptyset\emptyset}\right]$, $\left[M^{\emptyset}\right]$, and $\left[M^{\emptyset}\right]$. Then the A and B matrices may be formed and the eigenvalues are computed as previously discussed.

Some numerical results obtained using the method just described are shown in Tables 4.2 - 4.9. The Tables show the approximate eigenvalues $\lambda_i = -s_i\, r_o c_o d^2$ obtained with h = 0.25, 0.125, 0.0625, and 0.03125, where s_i are the poles or zeros of the admittance matrix parameters for three different distributed RC networks. Tables 4.2 and 4.3 give the eigenvalues for a uniform RC line; Tables 4.4- 4.6 give the eigenvalues for a distributed RC network with a linear taper, and a taper factor of 0.1, and Tables 4.7 - 4.9 give the eigenvalues for a distributed RC network with an exponential taper, and a taper factor of 0.1. In the latter case, the exact eigenvalues were obtained using equation (16) of (9) for the poles, while the zeros were obtained

TABLE 4.3. Approximate eigenvalues corresponding to the zeros of the admittance matrix elements $y_{11} = y_{22}$ for a uniform RC line.

s_i, λ_i, H, and the approximations to the voltage and current in the resistive layer are as in TABLE 4.2.

N	H= 0.25	0.125	0.0625	0.03125	EXACT
1	2.467701	2.467418	2.467402	2.467401	2.467401
2	22.42143	22.21946	22.20738	22.20665	22.20660
3	65.59141	61.95834	61.70171	61.68605	61.68502
4	129.3639	122.9081	121.0280	120.9103	120.9026
5		208.3004	200.4238	199.8944	199.8594
6		321.9457	300.4234	298.6718	298.5555
7		455.5366	422.0183	417.3073	416.9907
8		560.0707	566.7898	559.9111	555.1652
9			736.9008	714.6565	713.0781
10			934.7082	893.7987	890.7317
11			1161.560	1093.695	1088.123
12			1415.157	1314.828	1305.255
13			1685.077	1557.819	1542.125
14			1947.513	1823.448	1798.735
15			2163.538	2112.649	2075.084
16			2287.617	2426.507	2371.172
17				2766.211	2686.999
18				3132.983	3145.936
19				3527.939	3377.872
20				3951.879	3752.917

TABLE 4.4. Approximate eigenvalues corresponding to the poles of the admittance matrix for a linearly tapered RC line.

Taper factor, $\tau = 0.1 =$ (width of line at port 1)/(width at port 2)

s_i, λ_i, H, and the approximations to the voltage and current in the resistive layer are as in TABLE 4.2.

N	H= 0.25	0.125	0.0625	0.03125	EXACT
1	9.166074	8.957653	8.907216	8.897402	8.895573
2	40.09537	38.40583	38.14069	38.09857	38.09138
3	95.92762	88.61445	87.38480	87.24833	87.22959
4		161.6077	156.6774	156.2406	156.1944
5		261.1370	246.3594	245.0572	244.9434
6		386.5710	357.1771	353.7280	353.4570
7		512.5960	490.4186	482.3314	481.7254
8			647.9773	631.0050	629.7429
9			832.1584	799.9618	797.5064
10			1044.890	989.5100	985.0138
11			1285.815	1200.0726	1192.263
12			1548.739	1432.206	1419.255
13			1816.797	1686.620	1665.987
14			2059.010	1964.179	1932.460
15			2233.889	2265.905	2218.674
16				2592.946	2524.627
17				2946.518	2850.320
18				3327.800	3195.754
19				3737.757	3560.926
20				4176.874	3945.839

TABLE 4.5. Approximate eigenvalues corresponding to the zeros of the admittance matrix element y_{11} for a linearly tapered RC line.

τ, s_i, λ_i, H, and the approximations to the voltage and current in the resistive layer are as in TABLE 4.4.

N	H = 0.25	0.125	0.0625	0.03125	EXACT
1	4.857061	4.854901	4.854547	4.854496	4.854487
2	26.72479	26.56603	26.55611	26.55541	26.55534
3	70.36937	67.25632	67.02567	67.01148	67.01051
4	131.3946	128.6333	126.8815	126.7709	126.7636
5		214.0067	206.5798	206.0727	206.0392
6		327.0071	306.7456	305.0509	304.9379
7		458.7866	428.4022	423.8187	423.5090
8		557.8932	573.1308	562.5113	561.7785
9			743.0718	721.3155	719.7610
10			940.5427	900.4936	897.4652
11			1166.841	1100.406	1094.896
12			1419.613	1321.537	1312.058
13			1688.364	1564.505	1548.952
14			1949.113	1830.088	1805.582
15			2162.344	2119.218	2081.947
16			2280.609	2432.971	2378.048
17				2772.534	2693.886
18				3139.117	3029.462
19				3533.829	3384.776
20				3957.464	3759.828

TABLE 4.6. Approximate eigenvalues corresponding to the zeros or the admittance matrix element y_{22} for a linearly tapered RC line.

τ, s_i, λ_i, H, and the approximations to the voltage and current in the resistive layer are as in TABLE 4.4.

N	H = 0.25	0.125	0.0625	0.03125	EXACT
1	1.036632	0.9976405	0.9873677	0.9852989	0.9849070
2	20.81635	20.22275	20.10437	20.08287	20.07898
3	64.08126	59.92643	59.35938	59.28407	59.27239
4	126.6718	121.0933	118.6060	118.3628	118.3335
5		206.6705	198.0229	197.2672	197.1949
6		319.7013	298.1233	296.0044	295.8285
7		451.1202	419.8833	414.6270	414.2208
8		556.0315	564.8556	553.2397	552.3646
9			735.1416	712.0132	710.2556
10			932.9785	891.2019	887.8914
11			1159.513	1091.163	1085.270
12			1412.186	1312.378	1302.391
13			1680.404	1555.469	1539.253
14			1940.704	1821.212	1795.856
15			2155.666	2110.539	2072.199
16			2283.007	2424.525	2368.283
17				2764.352	2684.106
18				3131.223	3019.669
19				3526.233	3374.972
20				3950.154	3750.015

TABLE 4.7. Approximate eigenvalues corresponding to the poles of the admittance matrix for an exponentially tapered RC line.
τ, s_i, λ_i, H, and the approximations to the voltage and current in the resistive layer are as in TABLE 4.4.

N	H = 0.25	0.125	0.0625	0.03125	EXACT
1	11.31495	11.21069	11.19705	11.19532	11.19507
2	41.91339	40.91840	40.81497	40.80506	40.80389
3	95.05331	90.99382	90.21372	90.15680	90.15191
4		163.4532	159.5334	159.2591	159.2391
5		262.0231	249.1398	248.1349	248.0655
6		386.2081	359.7777	356.8316	356.6312
7		509.8301	492.7255	485.4352	484.9360
8			649.8705	634.0860	632.9801
9			833.5321	802.9974	800.7634
10			1045.694	992.4762	988.2859
11			1286.113	1202.943	1195.547
12			1548.735	1434.953	1422.548
13			1816.681	1689.211	1669.288
14			2058.415	1966.581	1935.767
15			2230.839	2268.083	2221.986
16				2594.866	2527.944
17				2948.149	2853.641
18				3329.118	3199.077
19				3738.750	3564.252
20				4177.549	3949.167

TABLE 4.8. Approximate eigenvalues corresponding to the zeros of the admittance matrix element y_{11} for an exponentially tapered RC line.
τ, s_i, λ_i, H, and the approximations to the voltage and current in the resistive layer are as in TABLE 4.4.

N	H = 0.25	0.125	0.0625	0.03125	EXACT
1	5.656680	5.641721	5.639533	5.639235	5.639193
2	25.84061	25.75834	25.74411	25.74218	25.74191
3	67.13958	65.48066	65.29310	65.27830	65.27692
4	126.6009	126.0972	124.6227	124.5194	124.5118
5		210.4688	203.9840	203.5090	203.4760
6		321.9298	303.8929	302.2858	302.1758
7		452.4101	425.3059	420.9152	420.6132
8		554.9278	569.7532	559.5061	558.7891
9			739.3320	718.2297	716.7037
10			936.3252	897.3382	894.3572
11			1162.020	1097.185	1091.749
12			1414.117	1318.249	1308.881
13			1682.306	1561.145	1545.752
14			1943.042	1826.646	1802.362
15			2157.738	2115.681	2078.711
16			2281.272	2429.324	2374.799
17				2768.756	2690.626
18				3135.189	3026.193
19				3529.728	3381.499
20				3953.166	3756.544

TABLE 4.9. Approximate eigenvalues corresponding to the zeros of the admittance matrix element y_{22} for an exponentially tapered RC line.

τ, s_i, λ_i, H, and the approximations to the voltage and current in the resistive layer are as in TABLE 4.4.

N	H = 0.25	0.125	0.0625	0.03125	EXACT
1	0.8652050	0.8586579	0.8577600	0.8576426	0.8576258
2	21.50543	21.24247	21.21766	21.21517	21.21487
3	64.09272	61.00713	60.72497	60.70456	60.70282
4	122.7866	121.9162	120.0577	119.9320	119.9229
5		206.9738	199.4561	198.9178	198.8808
6		319.3461	299.4488	297.6965	297.5773
7		449.7270	421.0134	416.3228	416.0129
8		550.1308	565.7033	554.9367	554.1875
9			735.6312	713.6811	712.1013
10			933.0695	892.8203	889.7543
11			1159.238	1092.711	1087.146
12			1411.676	1313.833	1304.277
13			1679.831	1556.806	1541.148
14			1939.958	1822.405	1797.758
15			2153.604	2111.562	2074.107
16			2276.139	2425.353	2370.195
17				2764.961	2686.022
18				3131.594	3021.589
19				3526.357	3376.894
20				3950.033	3751.939

by numerically solving equation (15) of (9), which, incidentally, is incorrect, and should read

$$\tanh \theta = -\frac{\theta}{\eta} \qquad (4.18)$$

instead of

$$\tanh \theta = -\eta\,\theta$$

In the tables, only the first 20 eigenvalues are shown for $h = 0.03125$, although the number of eigenvalues actually calculated is 31 in the case of the poles, and 32 in the case of the zeros.

On examination of the tables, we see that with the exception of one of the larger eigenvalues in some of the tables, the approximate eigenvalues are greater than the exact eigenvalues. Comparing Tables 4.1 and 4.2, we see that the approximate eigenvalues in the latter are more accurate. In particular, we note that the higher order approximate eigenvalues in Table 4.2 are generally within 10% of the exact eigenvalues, whereas the accuracy of the corresponding eigenvalues in Table 4.1 is much worse.

Comparing the results in Tables 3.2 - 3.6 with those in Tables 4.2 - 4.6, we see that the smaller eigenvalues are less accurate in the latter, whereas the larger eigenvalues are much more accurate.

The outstanding feature of the method using the modified triangle functions is the greatly improved accuracy of the larger eigenvalues, in comparison with the previous methods discussed.

4.4 Extrapolation procedures

One advantage of the methods using triangle functions to obtain approximations to the eigenvalues is that extrapolation can be used to obtain more accurate eigenvalues, and to estimate the accuracy of the solutions. In the polynomial approximation method, increasing the highest order of polynomial improves the accuracy of the eigenvalues, but in an irregular and unpredictable manner.

In the approximation methods using triangle functions, we assume that the error in each eigenvalue is an analytic function of the interval h between N equispaced points on the interval $0 \leq x \leq d$. Suppose that f_1 is the approximate eigenvalue obtained with $h = h_1$, and f_o is the exact eigenvalue, and we assume that the error is given by

$$f_1 = f_o + A_1 h_1^p \tag{4.19}$$

Similarly, if f_2 and f_3 are the approximate eigenvalues obtained with $h = h_2$ and $h = h_3$ respectively, we assume

$$f_2 = f_o + A_1 h_2^p \tag{4.20}$$

$$f_3 = f_o + A_1 h_3^p \tag{4.21}$$

The constants f_o, A_1, and p are readily calculated if $h_1 : h_2 : h_3 = 1 : c : c^2$. It is easily verified that

$$p = \ln \frac{f_1 - f_2}{f_3 - f_2} \Big/ \ln c \tag{4.22}$$

and

$$f_o = f_1 - \frac{f_1 - f_2}{1 - c^p} \tag{4.23}$$

The procedure just described is known as Aitkin's δ^2 extrapolation (16). In general, the value of f_o given by (4.28) will not be equal to the exact eigenvalue because we have ignored terms of the form $A_2 h^q$, $A_3 h^r$ --- in equations (4.19) - (4.21). However, for h sufficiently small, the value f_o given by (4.23) is a better approximation to the exact eigenvalue than f_1, f_2 or f_3, and we are then able to estimate the error in the approximate solutions.

Application of the Aitkin's δ^2 process to the approximate eigenvalues given in Tables 4.1, 4.2 and 4.3 for the uniform distributed RC line indicate that for h sufficiently small, the value of p given by (4.22) approaches 4 i.e. the asymptotic error in any approximate eigenvalue as $h \to 0$ is of order h^4. The results obtained using Tables 4.4-4.6 (linearly tapered distributed RC line with taper factor = 0.1) indicate that the asymptotic value of p for the lowest eigenvalue is about 3 or slightly less, and that the asymptotic value of p increases with the number of the eigenvalue to a maximum of about 4.

For other similar methods of solution such as the finite-difference method (25), which gives about the same accuracy as the variational method of solving the second-order differential equation with triangle functions (41), the rate of convergence is somewhat slower. A typical value of p in (4.23) for the two methods just mentioned is 2 or less. However for these two methods the A and B matrices (4.6) are tridiagonal or diagonal, which reduces the computer storage requirements, and in addition, special techniques are available for computing the eigenvalues (72); with the Moment method described in this Chapter the A

and $\mathbf{B}$ matrices are full matrices, and these special techniques cannot be used.

4.5 Conclusion

The Method of Moments has been used to obtain eigenvalues of the first-order system (4.1). Some numerical results were obtained by using piecewise linear approximation for the unknown voltage and current functions. When the triangle functions for $V(x)$ and $I(x)$ were chosen to be the same, the approximate eigenvalues were found to be less than the exact solutions i.e. lower bounds. However when the triangle functions for $V(x)$ and $I(x)$ were chosen as shown in Fig. 4.1 the approximate eigenvalues were greater than the exact solutions. In general, the second type of piecewise linear approximation gives more accurate solutions than the first type. In addition, the second method does not appear to give "extraneous" solutions.

An advantage of the Moment method discussed here is that it appears to give smaller errors and more rapid convergence than other methods when the same expansion functions are used. The basic reason for this is that we are approximating the voltage function and its derivative with the same order of accuracy, whereas with other methods the differentiation of the voltage function increases the errors. This aspect is discussed in more detail in the next Chapter.

Chapter 5

COMPARISON OF RAYLEIGH-RITZ AND MOMENT METHOD SOLUTIONS OF EIGENVALUE PROBLEMS

5.1 Introduction

In Chapter 3, the Rayleigh-Ritz method for obtaining eigenvalues of the second-order differential equation (2.4) was presented. The eigenvalues are the stationary values of the functional (3.1). In practice the stationary values of the functional (3.1) can only be found approximately, and if the expansion functions satisfy the "prescribed" boundary conditions $v(x) = 0$ at $x = 0$ and/or $x = d$, the approximate eigenvalues are greater than the exact eigenvalues.

In Chapter 4, the Moment method for obtaining eigenvalues of the first-order differential equations (4.1) was presented; these first-order equations are equivalent to the second-order equation (2.4). It has been suggested that this method provides a lower bound to the eigenvalues (14), p 142. However, from the results presented in Chapter 4, it is clear that this is not necessarily so. It appears that for certain types of expansion functions, the approximate solutions are lower bounds.

We now propose to investigate in more detail the relationship between the two methods mentioned above, in an attempt to determine why the Moment method sometimes gives lower bounds. In addition, it will be shown that the two methods give identical results for some types of expansion functions.

5.2 Variational Interpretation of the Moment Method

From (14), Chapter 7, it is obvious that the voltage and current functions $V(x)$ and $I(x)$ obtained from the Moment method satisfy

$$\int_o^d V \frac{dI}{dx} dx = -s \int_o^d c(x) V^2 \, dx \tag{5.1a}$$

$$\int_o^d I \frac{dV}{dx} dx = -\int_o^d r(x) I^2 \, dx \tag{5.1b}$$

when $V(x)$ and $I(x)$ satisfy the appropriate homogeneous boundary conditions.

By using integration by parts it is also obvious that

$$-\int_o^d V \frac{dI}{dx} \, dx = \int_o^d I \frac{dV}{dx} \, dx \tag{5.2}$$

is satisfied under these boundary conditions, and from (5.1a), (5.2) we see that the eigenvalues and eigenvectors satisfy

$$-s = \frac{\int_o^d V \frac{dI}{dx} \, dx}{\int_o^d c(x) V^2 \, dx} = \frac{-\int_o^d I \frac{dV}{dx} \, dx}{\int_o^d c(x) V^2 \, dx} \tag{5.3}$$

In order to compare this result with the Rayleigh Quotient used in Chapter 3, we will need to use the inequality (38), p. 16

$$\left[-\int_o^d I \frac{dV}{dx} \, dx\right]^2 \leq \left[\int_o^d r(x) I^2 \, dx\right] \left[\int_o^d \frac{1}{r(x)} \left|\frac{dV}{dx}\right|^2 dx\right] \tag{5.4}$$

From (5.1b) we see that this is equivalent to

$$-\int_o^d I \frac{dV}{dx}\, dx \leq \int_o^d \frac{1}{r(x)} \left| \frac{dV}{dx} \right|^2 dx \qquad (5.5)$$

Thus from (5.3) and (5.5) it is seen that the eigenvalues and eigenvectors satisfy

$$-s \leq \frac{\int_o^d \frac{1}{r(x)} \left| \frac{dV}{dx} \right|^2 dx}{\int_o^d c\,(x)\, V^2\, dx} \qquad (5.6)$$

The expression on the right side of (5.6) becomes identical to the Rayleigh Quotient (3.1) if we substitute

$$r(x) = r(o)/w(x) \qquad (5.7a)$$

$$c(x) = c(o).w(x) \qquad (5.7b)$$

into (5.6), and then multiply by r(o).c(o).

From (5.3) and (5.6) we can immediately deduce the following. If V(x) is any continuous function satisfying the boundary conditions of the eigenvalue problem, and I(x) is chosen to satisfy (5.1b), then (5.3) may be used to approximate the smallest eigenvalue $\lambda_1 = -s_1$. The approximate solution given by the right hand side of (5.6) will always be greater than or equal to that given by (5.3). Since the Rayleigh Quotient is an upper bound on λ_1, it follows that (5.3) gives either a more accurate upper bound than (5.6), or else it is a lower bound. Clearly

if I(x) is chosen to satisfy

$$I(x) = -\frac{1}{r(x)}\frac{dV}{dx} \qquad (5.8)$$

then (5.5) becomes an equality, and the expressions on the right of (5.3) and (5.6) are identical. Note that if (5.8) is satisfied then (5.1b) is also true, but the converse does not necessarily apply, i.e. (5.1b) is a necessary condition for (5.8) to be satisfied, but it is not sufficient.

In general, the approximate eigenfunctions and eigenvalues obtained by the methods of Chapters 3 and 4 will be different even though the voltage function V(x) is approximated with the same expansion functions. Therefore, it is not possible to state on the basis of the relations (5.3), (5.5) that the Moment method will always give eigenvalues which are less than those obtained by the Rayleigh-Ritz method. In practice, it usually happens that this is so, provided that (5.8) is not satisfied.

When piecewise linear approximations are used for both V(x) and I(x), it is generally impossible to satisfy (5.8), and the approximate eigenvalues are likely to be lower bounds as found in Chapter 4. However this will depend on the type of approximation used for I(x). When the modified triangle functions in Chapter 4 were used to approximate I(x) the eigenvalues were generally upper bounds. Intuitively the reason for the improved accuracy found with these modified triangle functions is that the errors in (5.8) are reduced, but are not zero. Since the eigenvalues obtained when (5.8) is satisfied are upper bounds, and the method which uses identical triangle functions for both

V(x) and I(x) appears to give lower bounds, we would therefore expect the solutions obtained with the modified triangle functions to lie somewhere between these upper and lower bounds, and would therefore be more accurate. These expectations are supported by the numerical results obtained in Chapter 4.

When polynomials are used to approximate both V(x) and I(x), (5.8) is exactly or almost exactly satisfied, and the Moment method and Rayleigh-Ritz solutions are equal or almost equal. For example, if r(x) and c(x) are independent of x, i.e. a uniform RC line, the two methods give identical eigenvalues.

5.3 Conclusion

We have considered the relationship between the solutions obtained by the Rayleigh-Ritz method and Moment method. From the inequality (5.5) we generally expect the Moment method to give smaller eigenvalues which are either lower bounds, or are more accurate than those obtained by the Rayleigh-Ritz method.

Chapter 6

ALTERNATIVE METHODS FOR ANALYZING NON-UNIFORM RC DISTRIBUTED NETWORKS

6.1 Introduction

In previous Chapters we have considered in some detail the Moment method and the Rayleigh-Ritz method for obtaining poles and zeros of the admittance parameters for non-uniform RC lines. In this Chapter we will briefly consider some alternative methods.

As discussed previously in Chapter 2, and in (1), Chapter 2, the admittance matrix elements can be expressed as ratios of the basic set solutions, and the zeros of these basic set solutions are either poles or zeros of the admittance matrix elements. The basic set solutions may be expanded as infinite power series in the complex frequency variable s, or as infinite product expansions.

Once the coefficients of the power series expansion have been determined, the zeros may be found approximately by truncating the series to a finite number of terms, and then using a polynomial root extraction program on a computer. Some numerical techniques for obtaining the coefficients in the power series expansion are given in (1), Chapter 2, Section 5, and will not be considered further here.

In the following we will consider only direct methods for estimating the poles and zeros; with these methods it is not necessary to compute the coefficients in the power series expansions.

Several of the methods to be discussed give both upper and lower bounds on the exact solutions, which is a desirable feature.

6.2 Numerical Methods

One of the simplest methods which can be used to obtain approximate solutions of the differential equation (2.4) is the finite-difference method, which is also known as Lagrange's method, (1) pp 52 - 59, (3) pp 299-319. In this method a number of points are chosen on the line, and the potential at each point is expanded in the form of a truncated Taylor series. The derivatives of the potential function at each mesh point can then be estimated from the values of the potential function at the mesh points. When these approximations are substituted into the differential equation a matrix eigenvalue problem is obtained, and this may be solved for the eigenvalues and the unknown potential values at the mesh points. This method is equivalent to dividing the line into a number of incremental lengths which are then modelled in the form of a T-network, (1) p 54. The accuracy of the results is improved by increasing the number of mesh points, and extrapolation procedures can also be used to improve the accuracy and to estimate the errors in the solutions.

Another method which was developed by Schwarz is based on the Rayleigh Principle (1) p 60. This is an iterative procedure by which more accurate solutions are generated from an initial approximation. At each step of the iteration both upper and lower bounds on the desired eigenvalue are obtained, so that the iteration can be stopped when the desired accuracy is achieved.

One possible disadvantage of this method is that it does not appear to be easy to program on a computer for arbitrary taper functions.

Another method for obtaining upper and lower bounds on the eigenvalues is based on the Enclosure theorem which is due to

Collatz (1), p 64. However, this method also suffers from the problem that it is not easy to program for arbitrary tapers; in general it would be necessary to prepare a separate computer program for each type of taper.

In addition to the above methods, there are a number of numerical techniques which exploit the capability of computers to solve initial value problems. The possibility of using these techniques to solve eigenvalue problems was first presented by Fox (73), and subsequently several variations were presented (74). The use of these methods avoids some of the difficulties associated with the methods previously discussed. For example, with the Rayleigh-Ritz and Moment Methods it is necessary to solve a high degree determinantal equation in order to obtain the higher order eigenvalues, and to reduce the error for the low order eigenvalues. The solution of this equation may then entail such an accumulation of round-off errors that accurate eigenvalues cannot be obtained.

6.3 Conclusion

In addition to the methods discussed in this Chapter there are many others.

In (87) it is shown that both upper and lower bounds on the eigenvalues can be obtained from the Rayleigh-Ritz solution with piecewise linear approximations to the eigenfunctions.

In (88) a method which involves a change of dependent variables is used. This transforms the boundary value problem to an initial value problem, and the eigenvalues are obtained by Newton's method.

Finally, in (89), the non-uniform transmission line is replaced by a cascade of uniform lines. This method is claimed

to give much better accuracy at high frequencies.

Clearly there are many methods which may be used to solve non-uniform transmission line problems. Since the various methods all have some associated problems, the method chosen will be determined by personal preference in most cases.

PART II

TWO DIMENSIONAL ANALYSIS

Chapter 7

BOUNDARY EFFECTS IN DISTRIBUTED RC STRUCTURES

7.1 Introduction

Up to this point, we have been concerned with the network properties of distributed RC circuits with one-dimensional variation in per-unit-length series impedance and shunt conductance. We have placed particular emphasis on the analysis of distributed RC networks since these structures have applications in micro-electronics.

In practice it is advantageous to use tapered RC networks instead of uniform RC networks in certain applications. In particular, sharper rates of cut-off are achieved for low pass filters, and better selectivity is obtained with notch networks (5), (17).

So far, we have not considered in detail the physical realization of tapered distributed RC networks. If we consider the class of tapered distributed RC networks which support only one-dimensional current flow, we find that electrical taper and geometrical shape are generally different. Furthermore, one dimensional current flow is only possible if the physical boundaries of the distributed circuit match the co-ordinate lines of one of four orthogonal co-ordinate systems (1), Chapter 7. These are the cartesian, polar, parabolic, and elliptic co-ordinate systems. The cartesian and polar co-ordinate geometries represent the uniform RC line and linearly tapered RC lines respectively. The parabolic and elliptic co-ordinate geometries represent more complicated electrical taper functions which approximate the

square-root and linear electrical tapers respectively for small taper ratios (1), Chapter 7.

Various other procedures can be used to determine the geometric shape of a distributed RC network which approximates a given electrical taper. One such method uses a conformal transformation of the cartesian co-ordinate system, and an alternative graphical construction procedure is based on the use of curvilinear squares (1), Chapter 7. Both of these methods yield geometric shapes which only approximate one-dimensional current flow, and are most accurate for small taper ratios.

In this Chapter we will briefly consider some methods for two-dimensional analysis of distributed RC networks. Firstly, we will consider the problem of obtaining the zero frequency admittance matrix parameters for a multi-terminal network. Then we will present solutions which may be used to evaluate admittance matrix parameters at any desired frequency. These solutions are in the form of a partial fraction expansion which is obtained by expanding the unknown potential functions in terms of solutions of Laplace's equation and a set of eigenvalues and eigenfunctions which satisfy the Helmholtz equation in two dimensions.

In Chapters 8 and 9 we will consider in more detail variational methods for obtaining approximate values of the admittance matrix parameters and the poles and zeros, and in Chapter 10 we consider a method which is based on the solution of an integral equation.

7.2 Two-Dimensional Analysis of Distributed RC Lines

As discussed above, there is a very limited range of geometrical shapes for distributed RC networks which can be analysed exactly by assuming one-dimensional current flow. In addition, experimental results given in the literature indicate that the assumption of a one-dimensional model for the distributed RC network may result in considerable errors. For example, experimental studies have shown that the frequency of the notch produced by a circuit containing an exponentially tapered RC network may be in error by 10 per cent or more when compared with the theoretical predictions (17), (18). In view of the inadequacies of the one-dimensional model for many types of tapered distributed RC lines and also with the objective of investigating whether it is possible to obtain better electrical performance from distributed networks which do not support one-dimensional current flow, we now wish to consider methods for two-dimensional analysis of distributed RC networks.

The first requirement to be considered when attempting a two-dimensional analysis of a distributed RC network is that the potential, ϕ between the resistive layer and the ground plane must satisfy the Helmholtz equation, (1) Chapter 7

$$\nabla^2 \phi = sRC \phi \qquad (7.1)$$

where

R is the resistance per square of the resistive layer

C is the capacitance per unit area coupling the resistive layer to the ground plane

s is the complex frequency variable

and

∇^2 is the two-dimensional Laplacian operator

In addition, the potential in the resistive layer must satisfy certain boundary conditions. The boundary of the resistive region is made up of metal contacts and insulating segments. On each of the metal contacts, the boundary condition is that the potential be constant. On each of the insulating parts of the boundary, the boundary condition is that no current flows out of the resistive region. This is equivalent to the condition,

$$\hat{n} \cdot \nabla \phi = 0 \tag{7.2}$$

on insulating parts of the boundary; $\hat{n}$ is the unit- length outward-pointing normal to the boundary.

Having found the potential function ϕ satisfying (7.1), and the boundary conditions of any particular problem, we are then able to compute any desired set of network parameters. A convenient set of network parameters for many applications is the admittance matrix which relates the potential between the metal contacts and ground to the current entering the metal contacts. If there are N metal contacts on the boundary of the resistive layer, the relation between the N voltages and currents may be written in matrix form as,

$$I] = [Y]\, V] \tag{7.3}$$

where

$I]$ and $V]$ are column vectors of length N,

$[Y]$ is the N X N admittance matrix

I_j is the current entering the jth metal contact

V_j is the potential between the jth metal contact and ground.

If the potential, ϕ, within the resistive layer, or the normal derivative of ϕ on each metal contact is known when the jth metal contact is at a potential of 1 volt and all other metal contacts are at zero potential, the elements in the jth column of the admittance matrix may be computed using the relation

$$y_{ij} = \frac{1}{R} \oint_{C_i} \frac{\partial \phi}{\partial n} \, dl \qquad (7.4)$$

where

C_i is the boundary segment containing the ith metal contact

dl is the elemental distance along the boundary.

By choosing $j = 1, 2 - - - N$, and computing the y_{ij} for each j, the complete admittance matrix in (7.3) is obtained.

7.3 Distributed Resistance Calculations

Before considering in detail methods for solution of (7.1) we wish to discuss the solution of a simpler problem. If the complex frequency variable s in (7.1) is set to zero, the Helmholtz equation reduces to Laplace's equation,

$$\nabla^2 \phi = 0 \qquad (7.5)$$

Analytical solutions for the resistance between two terminals placed arbitrarily on the perimeter of resistive films having a restricted set of geometries have been obtained by various techniques. The usual method for solving such problems involves the determination of some conformal transformation which maps the given geometry into a rectangle such that the conducting terminals

become two opposite edges of the rectangle. The resistance between these two terminals can then be easily determined. An example of this approach is the work of Moulton (19), and Wyndrum (20) which provides the resistance between two terminals placed arbitrarily on the perimeter of a rectangular structure.

The Schwartz-Christoffel transformation was also used by Anderson (21) to calculate the capacitance per unit length between coaxial cylinders of rectangular cross-section. This is analogous to the problem of calculating the resistance between a pair of terminals placed on opposite edges of an "L" shaped resistive film; having solved this problem, one can then easily solve the dual problem of a distributed resistor consisting of a right-angle bend. Numerous other examples of analytical solutions for two terminal distributed resistance networks may be found in the literature. A comprehensive list of these results is given in the work of Hall (22).

Computer implementation of resistance calculations using the known analytical solution techniques is feasible. However, any such computer program of reasonable sophistication can only handle resistors of a restricted set of predetermined geometries, and not resistors of general shape. Furthermore, it cannot handle multi-terminal distributed resistive networks, with the exception of three-terminal resistive networks with a plane of symmetry as considered in (20).

Because of the limitations of analytical solution techniques, greater emphasis has been placed on numerical techniques for analysing multi-terminal distributed resistance networks in recent years. Although the results obtained by these numerical techniques

are not exact in general, there is much greater flexibility in the types of networks which can be analysed. In addition, some numerical techniques provide two approximate solutions which are upper and lower bounds on the exact solution, and this allows the user to decide whether the approximate solutions are sufficiently accurate.

We now wish to discuss some of the numerical techniques which are applicable to multi-terminal distributed resistance networks of arbitrary geometries.

7.3.1 Finite Difference Method

The finite difference technique is perhaps the most popular numerical method for solution of Laplace's equation. In this method the partial differential equation is approximated by a system of linear algebraic equations. This is done by superimposing a regular grid over the region of interest, and assigning an unknown potential to each intersection of the grid. Approximations to $\partial^2\phi/\partial x^2$ and $\partial^2\phi/\partial y^2$ at each grid point are obtained in terms of differences between the potentials at adjacent grid points (24). At grid points on or near the boundary, the difference equations must be modified to account for the boundary conditions. Various techniques have been developed for satisfying boundary conditions when the boundaries do not coincide with the grid points. In practice, however, this is one of the major drawbacks of the method, and it is no mean feat to program the logic for boundaries of arbitrary shape(24).

In this method an initial guess at the potential is made with a fairly coarse mesh. An iterative procedure is then used

to reduce the error in each finite difference equation to a sufficiently small value; iterative methods are generally more practical than direct methods for solving the simultaneous equations since the coefficient matrix is very sparse, with only five non-zero elements per row in most cases. Once the potential values have been computed, the normal derivatives along the terminals of the distributed resistance network can be found using finite difference approximations, and then (7.4) is used to obtain the admittance matrix elements. A further limitation of this method is that for a multi-terminal structure one would have to repeat the whole iteration scheme each time a different potential configuration is specified.

In spite of the difficulties associated with this method, it does permit solutions of any desired accuracy (limited only by round-off errors in the calculations) by using successively smaller mesh intervals. An excellent review of this method is given by Green (23), and various aspects are described in (24) and (25). A comparison of this method with one other method (to be discussed later) is also given in (26).

7.3.2 Integral Equation Method

In addition to the finite difference method, another method which reformulates the partial differential equation (7.5) as an integral equation has been used by various authors to obtain numerical solutions of Laplace's equation in two dimensions. The integral equation method is based on the fact that the potential at a point on or inside the boundary of the region depends on the weighted integrals of the charge density (for TEM field problems),

and the potential on the entire boundary. This relationship is expressed mathematically by

$$\sigma(x,y').\phi(x',y') = \int_{\Gamma}\left[G_0(r).\psi(x,y) - G_1(r).\phi(x,y)\right] ds \qquad (7.6)$$

where

$\sigma(x',y')$ is a constant depending on the position of the point (x',y')

$\psi(x,y)$ is the normal derivative of the potential function $\phi(x,y)$ on the boundary

r is the distance between the points (x',y') and (x,y)

and the integral on the right is evaluated over Γ the boundary of the resistive region.

The weighting function $G_0(r)$ is a Green's function for two-dimensional space, and the weighting function $G_1(r)$ is the normal derivative of $G_0(r)$.

The relation (7.6) is derived from (7.5) by using Green's boundary value formula in (27), (28), (29).

The Green's function $G_0(r)$ satisfies Laplace's equation inside the boundary, except at $x=x'$, $y=y'$. At this point $G_0(r)$ has a singularity, and behaves as $k \log r$ as $r \to 0$. The simplest example of a function which satisfies these conditions is the free-space Green's function

$$G_0(r) = -\log r = -\log\sqrt{(x-x')^2 + (y-y')^2} \qquad (7.7)$$

By choosing a Green's function which satisfies certain boundary conditions it is possible to obtain an explicit solution for the potential in terms of the specified boundary conditions of the problem. This subject is treated in some detail in (4), pp 243-259. However this approach has several disadvantages. If the natural log function is not used for the Green's function, a suitable one must be found for each problem. Often this can be as difficult as the original problem itself. In addition, this Green's function will usually be expressed as an infinite series, and therefore techniques must be found for efficiently computing it and its derivative. Some examples using a Green's function which satisfies homogeneous boundary conditions on a rectangular boundary are given in (30).

Approximate solutions satisfying the integral equation (7.6) can be obtained as described in (29) - (31). This problem will also be considered in detail in Chapter 10.

7.3.3 Integral Equation Method Based on Cauchy's Integral Equation

We now consider an alternative method of reformulating the partial differential equation (7.5) as an integral equation (32). From the theory of complex variables it is well known that if a function $\psi(z)$ is defined on the boundary C of a region R, and is analytic in R and on C, then at point Z' in the region R, the function is given by Cauchy's integral formula,

$$\psi(z') = \frac{1}{2\pi i}\oint_C \frac{\psi(z)}{z-z'}\,dz \qquad (7.8)$$

Now it is also known that the real and imaginary parts of a complex function (subject to restrictions given above), both satisfy Laplace's equation in the region R. We may therefore consider the real and imaginary parts of the complex function $\psi(z)$ to be the potential function V(x,y) and the stream function U(x,y) (integral of the current density), respectively.

For the type of physical problems under consideration, part of the boundary consists of metallized segments, and the rest of insulated segments. On each metallized segment, the real part V of ψ is constant and given, whereas on each insulated segment the imaginary part U of ψ is constant and unknown. Additional unknowns are the function U(z) on metallized segments, and the function V(z) on insulated segments.

For purposes of numerical computations it is necessary to approximate the integral equation (7.9) by a set of simultaneous equations which may be solved for the unknown potential and stream functions on the boundary. One such method is described in detail in (32).

7.3.4 Variational Method

In addition to the methods previously discussed for solving Laplace's equation, there is another method commonly known as the Variational Method. This method is based on the following principle:

The functional $F(\phi)$ given by

$$F(\phi) = \iint_R |\nabla\phi|^2 \, da - 2\oint_{C_1} (\phi - g)\frac{\partial\phi}{\partial n} \, ds \qquad (7.9)$$

has for its stationary conditions (Euler equation) (7.5) and the natural boundary conditions

$$\phi = g(s) \text{ on } C_1 \text{ and } \frac{\partial \phi}{\partial n} = 0 \text{ on } C_2 \qquad (7.10)$$

where

$C = C_1 \cup C_2$ is the boundary of a region R.

The set of admissible trial functions for $F(\phi)$ is the class of continuous scalar functions ϕ with bounded, piecewise continuous, first derivatives such that $\iint_R |\nabla \phi|^2 \, da$ exists.

The proof of the statement that $F(\phi)$ given by (7.10) is stationary when (7.5) and (7.11) are satisfied is quite straightforward as shown in (33).

Methods for solving the stationary problem will be discussed in more detail in Chapter 8. In addition, it will be shown that if g(s) is suitably chosen, then $F(\phi)$ given by (7.10) is proportional to the zero frequency value of an admittance matrix element y_{ij}. Furthermore, it is shown in Chapter 8, that other functionals can be constructed such that the stationary value is proportional to an off-diagonal element y_{jk}.

7.3.5 Reduction to First-Order Partial Differential Equations

An interesting variant to the above methods is proposed by Harrington (14), pp 162-166. Equation (7.5) can be reduced to the following system of coupled first-order differential equations:

$$-\nabla\phi = R\tilde{J} \tag{7.11a}$$

$$-\nabla.\tilde{J} = 0 \tag{7.11b}$$

ϕ is the potential in the resistive layer

R is the sheet resistance in ohms/square

$\tilde{J}$ is the current density vector in the resistive layer (amperes per unit width).

In cartesian co-ordinates, the system of equations (7.11) becomes

$$-\frac{\partial\phi}{\partial x} = RJ_x \tag{7.12a}$$

$$-\frac{\partial\phi}{\partial y} = RJ_y \tag{7.12b}$$

$$\frac{\partial J_x}{\partial x} + \frac{\partial J_y}{\partial y} = 0 \tag{7.12c}$$

Although the method of solution described in (14) pp 162 - 166, is concerned with eigenvalue problems, it can be easily adapted to obtain approximate solutions of Laplace's equation. Alternatively, as shown in Chapter 9, approximate solutions of the first-order system (7.12) may be obtained by the variational method. It is shown there that it is possible to construct functionals whose stationary conditions are (7.12), subject to certain boundary conditions, and the stationary value of the functional is proportional to an admittance matrix element y_{kj}.

7.4 Frequency Domain Analysis of Distributed RC Lines

In this section we will consider techniques for frequency domain analysis of distributed RC networks. As in the one-dimensional case, we will concentrate primarily on the problem of obtaining poles and zeros of the admittance matrix parameters. The pole-zero approach provides a direct connection between lumped and distributed-parameter systems, and also simplifies the calculation of the various network transfer functions at any desired frequency.

As discussed in Section 7.1, the admittance matrix parameters may be obtained by calculating the current entering each metal contact when the potential V between the jth metal contact and ground is prescribed for j=1, 2, ..., N. For example, if V_j is unity and $V_k = 0$, for $k \neq j$ then the current entering the kth metal contact is y_{kj} where $[Y]$ is the NXN admittance matrix.

The potential ϕ in the resistive layer satisfies the Helmholtz equation (7.1), which we will write in the form

$$\nabla^2 \phi + \lambda \phi = 0 \tag{7.13}$$

subject to the boundary conditions

$$\begin{aligned} \hat{n} \cdot \nabla \phi &= 0 && \text{on insulating boundary segments} \\ \phi &= V_j && \text{on } C_j, \text{ where } V_j \text{ is the potential on the jth metal contact} \\ \text{and} \quad \phi &= 0 && \text{on all other metal contacts} \\ \lambda &= -sRC \end{aligned} \tag{7.14}$$

where

s is the complex frequency variable, and R and C are as previously defined.

In the following, the surface of the resistive region will be denoted by R, and the boundary of the resistive region by C.

The boundary value problem with the homogeneous differential equation (7.13) and non-homogeneous boundary conditions (7.14) is essentially equivalent to a problem with a non-homogeneous differential equation with homogeneous boundary conditions as discussed in (4) Chapter 5.

If there exists a twice differentiable function F_j which satisfies the same boundary conditions as ϕ,

$$\begin{aligned} \hat{n} \cdot \nabla F_j &= 0 && \text{on insulating boundaries} \\ F_j &= V_j && \text{on the jth metal contact} \\ \text{and} \quad F_j &= 0 && \text{on all other metal contacts} \end{aligned} \tag{7.15}$$

Then we let

$$\psi = \phi - F_j \tag{7.16}$$

We then have

$$\begin{aligned} n \cdot \nabla \psi &= 0 && \text{on insulating boundaries} \\ \psi &= 0 && \text{on the metal contacts} \end{aligned} \tag{7.17}$$

From (7.16) we obtain

$$\nabla^2 \psi + \lambda \psi = \nabla^2 \phi + \lambda \phi - \nabla^2 F_j - \lambda F_j \tag{7.18}$$

If we define

$$\nabla^2 F_j + \lambda F_j = f_j \tag{7.19}$$

then from (7.13), (7.18), (7.19) we obtain

$$\nabla^2 \psi + \lambda \psi = -f_j \tag{7.20}$$

Thus ψ satisfies a non-homogeneous differential equation (7.20) and homogeneous boundary conditions (7.17).

The non-homogeneous problem may be solved in terms of the eigenfunctions of the homogeneous problem, (4), p 223.

$$\nabla^2 \psi_i + \lambda_i \psi_i = 0 \tag{7.21}$$

$$\begin{aligned} \hat{n} \cdot \nabla \psi_i &= 0 \quad \text{on insulating boundary} \\ \psi_i &= 0 \quad \text{on the metal contacts} \end{aligned} \tag{7.22}$$

The eigenvalues λ_i may be shown to be positive and real, and the eigenfunctions ψ_i are also real.

The coefficients in a "best" approximation to ψ by a linear combination $c_i \psi_i$ in the least-mean-square sense are,

$$c_i = \iint_R \psi \cdot \psi_i \, da \tag{7.23}$$

The ψ_i are orthogonal, and are assumed to be normalized so that

$$\iint_R \psi_i \psi_j \, da = \delta_{ij} \tag{7.24}$$

The c_i are obtained from the coefficients,

$$\gamma_i = \iint_R f_j \psi_i \, da \tag{7.25}$$

As shown in (4), p. 223 we obtain

$$c_i = \gamma_i/(\lambda_i - \lambda) \tag{7.26}$$

The approximate solution of our original problem is then given by

$$\phi(x,y) = F_j(x,y) + \sum_i \frac{\gamma_i \psi_i(x,y)}{(\lambda_i - \lambda)} \tag{7.27}$$

By using an argument similar to that in (4) pp 158 -161, it may be shown that the eigenfunctions ψ_i form a complete set with respect to continuous functions $\psi(x,y)$ which satisfy homogeneous boundary conditions of the form (7.17), and which have piecewise continuous first derivatives. In addition to proving that the eigenfunction expansion converges in the mean, it is also possible to establish uniform convergence at any point in R or on C.

Once the potential function has been found in the form (7.27), the admittance matrix element y_{ij} can then be computed by using (7.4).

The result is

$$y_{ij} = \frac{1}{R} \oint_{C_i} \frac{\partial F_j}{\partial n} \, dl + \sum_l \frac{\gamma_l}{(\lambda_l - \lambda)} \oint_{C_i} \frac{\partial \psi_l}{\partial n} \, dl \qquad (7.28)$$

This equation can be put into an alternative form which shows the symmetry of the admittance matrix. By using the Green's formula

$$\oint_C v \frac{\partial u}{\partial n} \, dl = \iint_R \nabla u \cdot \nabla v \, da + \iint_R v \nabla^2 u \, da \qquad (7.29)$$

and by defining a function F_i which satisfies the boundary conditions

$$\begin{aligned} \hat{n} \cdot \nabla F_i &= 0 && \text{on insulating boundaries} \\ F_i &= V_i && \text{on the ith metal contact} \\ &= 0 && \text{on all other metal contacts} \end{aligned} \qquad (7.30)$$

We can put (7.28) into the form

$$y_{ij} = \frac{1}{R} \iint_R \nabla F_i \cdot \nabla F_j \, da + \sum_l \frac{-\lambda \lambda_l \left[\iint_R F_i \psi_l da \right] \left[\iint_R F_j \psi_l \, da \right]}{(\lambda_l - \lambda)} \qquad (7.31)$$

where

F_i and F_j are assumed to satisfy Laplace's equation.

Clearly it follows from (7.31) that

$$y_{ij} = y_{ji} \qquad (7.32)$$

as one would expect from consideration of reciprocity.

In addition, we note that (7.31) has the form of a partial fraction expansion of the Foster canonical form for an RC driving point admittance. The complex frequency variable s is related to λ by (7.14). Since the eigenvalues λ_i are positive and real, it follows that the poles are all negative and real. In addition, since the residues of the partial fraction expansion (7.31) are all positive for diagonal elements of the admittance matrix, the zeros of these elements must be on the negative real axis, and the poles and zeros alternate on the negative real axis. For an off-diagonal element of the admittance matrix the residues are not necessarily positive, and the zeros may be anywhere in the complex frequency plane.

7.5 Conclusion

In the preceding sections some methods for obtaining approximate values of the admittance parameters for distributed resistance networks were presented. The numerical results obtained by several of these methods will be presented in the following Chapters.

A method for obtaining the admittance parameters of distributed RC networks was also discussed. The solutions obtained by this method are in the form of a partial fraction expansion which is obtained from the eigenvalues and eigenfunctions corresponding to the poles of the admittance matrix. This method also requires the zero frequency admittance parameters of the network to be computed.

In the following Chapters we will concentrate primarily on direct methods for obtaining the poles and zeros of the admittance parameters, i.e. methods which do not require calculation of the eigenfunctions.

The eigenfunction expansion method has been included here for completeness since it is the classical method given in textbooks for solving boundary value problems of this type.

The author is indebted to one of the Reviewers who suggested that some comment on the work of Weinstein should be included. A good source of information is the book by S.H. Gould, "Variational Methods for Eigenvalue Problems", University of Toronto Press, Second Edition 1966, which is devoted entirely to the Rayleigh-Ritz method for upper bounds, and the Weinstein method for obtaining lower bounds on the eigenvalues.

Chapter 8

VARIATIONAL METHODS FOR OBTAINING ADMITTANCE MATRIX PARAMETERS OF DISTRIBUTED RC NETWORKS

8.1 Introduction

In this Chapter we will consider variational methods for obtaining the poles and zeros of the admittance parameters, and/or the value of any desired admittance parameter at a given frequency. The required solutions are proportional to the stationary values of a suitably chosen functional. These stationary values are found (approximately in general), by using the Rayleigh-Ritz method.

Silvester, (62), has considered an analogous problem to that of analyzing distributed RC networks. The problem considered by Silvester is analysis of planar microwave networks, but the technique is directly applicable to distributed RC networks, since the transformation from one type of network to the other is equivalent to the lc - rc transformation for lumped networks. The solution for the admittance matrix in (62) is in the form of a partial fraction expansion involving potential functions satisfying Laplace's equation and a set of eigenvalues and eigenfunctions satisfying the Helmholtz equation in the two-dimensional region. In practice the infinite partial fraction expansion must be truncated to a finite number of terms, so that each admittance matrix term may be expressed as a rational function in the complex frequency variable. If desired, the zeros may be obtained by computing the roots of the numerator

polynomial; the poles are proportional to the eigenvalues.

A possible disadvantage of the above method is that the time required to compute the eigenvectors of a matrix is much greater than that required to compute the eigenvalues. In addition, on a finite precision computer, the accuracy of the eigenvalues is generally better than that of the corresponding eigenvectors, which means that the zeros of the rational function may be subject to rounding errors.

In the following sections we will consider direct methods for computing the poles and zeros of the admittance matrix; it is not necessary to compute any eigenvectors with these methods. Although variational methods have been used previously to obtain the poles of the admittance matrix, (62), these methods do not appear to have been used to obtain the zeros.

In addition, the use of variational methods for obtaining numerical values of the admittance parameters at a given frequency does not appear to have been considered previously.

After presenting the theoretical basis of these techniques, methods for obtaining numerical solutions will be discussed, and some numerical results are presented.

8.2 Variational Expressions for the Admittance Matrix Elements and the Poles and Zeros

We assert that the functionals

$$F_1(u,v) = \frac{\iint_R \nabla u \cdot \nabla v \, da}{\iint_R u \cdot v \, da} \qquad (8.1)$$

$$F_2(u,v) = \iint_R \nabla u \cdot \nabla v \, da - \lambda \iint_R u.v \, da \qquad (8.2)$$

are variational expressions whose stationary values are proportional to the poles or zeros, and the value of an admittance matrix element respectively, provided that the functions u and v are constrained to satisfy certain Dirichlet boundary conditions; the parameter λ in (8.2) is proportional to the complex frequency variable.

In addition, the functionals

$$F_3(u,v) = \frac{\iint_R \nabla u . \nabla v \, da - \oint_{C_2+C_j+C_k} \left[(u-g_u) \frac{\partial v}{\partial n} + (v-g_v) \frac{\partial u}{\partial n} \right] dl}{\iint_R u \cdot v \, da} \qquad (8.3)$$

$$F_4(u,v) = \iint_R \nabla u . \nabla v \, da - \oint_{C_2+C_j+C_k} \left[(u-g_u) \frac{\partial v}{\partial n} + (v-g_v) \frac{\partial u}{\partial n} \right] dl - \lambda \iint_R u \cdot v \, da \qquad (8.4)$$

are also variational expressions whose stationary values are proportional to the poles or zeros, and the value of an admittance matrix element respectively; in this case u and v are not constrained to satisfy any boundary conditions, although appropriate values of g_u and g_v must be specified on the boundary segments $C_2 + C_j + C_k$.

The area integrals in (8.1)-(8.4) are evaluated over the two-dimensional region R. The boundary of R is denoted by C, which is divided into a number of sectors, C_1, C_2, C_j and C_k,

such that

$$C = C_1 + C_2 + C_j + C_k \tag{8.5}$$

The functionals presented above were derived from consideration of the differential equation and the boundary conditions which must be satisfied by the potential function u(x,y) which is appropriate to the problem being considered. The potential function v(x,y) satisfies the adjoint equation, and boundary conditions adjoint to those satisfied by u(x,y), Appendix A, (42) p 148 - 149. By taking the scalar product of the adjoint field v(x,y) and the differential equation satisfied by u(x,y), and rearranging the resulting equation we obtain a functional which is either proportional to a pole or zero of an admittance matrix element, or is proportional to the value of an admittance matrix element at a given frequency. The functionals (8.3), (8.4) were obtained by using an "extended" differential operator which operates on functions u(x,y) or v(x,y) which need not satisfy any boundary conditions, but which is identical with the original operator when the boundary conditions are satisfied (14) p 161.

In Appendix B it is shown that if u and v are constrained to satisfy the boundary conditions

$$\begin{aligned} u &= 0 \quad \text{on } C_2 + C_k \\ u &= U_j = \text{constant on } C_j \end{aligned} \tag{8.6}$$

$$v = 0 \quad \text{on } C_2 + C_j$$
$$v = V_k = \text{constant on } C_k \tag{8.7}$$

then the necessary conditions for $F_1(u,v)$ to be stationary are

$$\nabla^2 u_i + \lambda_i u_i = 0 \quad \text{in R} \tag{8.8a}$$

$$\frac{\partial u_i}{\partial n} = 0 \quad \text{on } C_1 \tag{8.8b}$$

$$\oint_{C_k} \frac{\partial u_i}{\partial n} dl = 0 \quad \text{if } V_k \neq 0 \tag{8.8c}$$

and

$$\nabla^2 v_i + \lambda_i v_i = 0 \quad \text{in R} \tag{8.9a}$$

$$\frac{\partial v_i}{\partial n} = 0 \quad \text{on } C_1 \tag{8.9b}$$

$$\oint_{C_j} \frac{\partial v_i}{\partial n} dl = 0 \quad \text{if } U_j \neq 0 \tag{8.9c}$$

where

$$\lambda_i = F_1(u_i, v_i) \tag{8.10}$$

Now the boundary of the distributed resistance capacitance network consists of metal contacts and insulated

segments. On the insulated boundary segments which will be denoted by C_1, the potential function u_i or v_i satisfies (8.8b) or (8.9b) respectively. On each of the metal contacts the potential function is a constant. The boundary segments corresponding to metal contacts will be denoted by $C_2 + C_j + C_k$, where C_j and C_k are the jth and kth metal contacts respectively, and C_2 denotes all of the remaining metal contacts. In the special case where $j = k$ the boundary segments corresponding to metal contacts will be denoted by $C_2 + C_j$ and in (8.6), (8.7) $C_2 + C_k$ and $C_2 + C_j$ are replaced by C_2.

The poles of the admittance matrix of the distributed RC network are the frequencies of the free modes which can exist in the two dimensional region with zero potential on each of the metal contacts, and zero normal derivative on each of the insulating boundary segments. Assuming that these modes are of the form

$$\phi_i(x,y)\, e^{s_i t} \tag{8.11}$$

then we recall that the function $\phi_i(x,y)$ must satisfy the Helmholtz equation

$$\nabla^2 \phi_i(x,y) = s_i RC\, \phi_i(x,y) \tag{8.12}$$

where

R is the resistance in ohms per square of the resistive layer, and C is the capacitance per unit area between the resistive layer and the ground plane of the distributed RC network .

It therefore follows that the poles of the admittance matrix, s_i, are related to the eigenvalues, λ_i, of the eigenvalue problem given by (8.6) - (8.10) with $U_j = 0$ and $V_k = 0$ by

$$s_i = -\lambda_i/RC \tag{8.13}$$

Note that u_i and v_i are identical for this problem, since they satisfy the same differential equation and boundary conditions i.e. we have a self-adjoint problem, Appendix A.

The zeros of the admittance matrix term y_{kj} may be obtained by noting that if the potential function u(x,y) satisfies the boundary conditions (8.6) and (8.8b), and also satisfies the Helmholtz equation (8.8a), then

$$y_{kj} = \frac{1}{U_j R} \oint_{C_k} \frac{\partial u}{\partial n} \, dl \tag{8.14}$$

It therefore follows that the zeros of y_{kj}, s_i, are related to the eigenvalues λ_i, of the eigenvalue problem (8.6) - (8.10) by (8.13).

Similarly, it can be shown that since

$$y_{jk} = \frac{1}{V_k R} \oint_{C_j} \frac{\partial v}{\partial n} \, dl \tag{8.15}$$

then the zeros of y_{jk} are equal to those of y_{kj}. This is what we would expect from consideration of reciprocity.

By similar reasoning to Appendix B, we can also show that the necessary conditions for $F_2(u,v)$ to be stationary, with u and v constrained to satisfy (8.6), (8.7), are

$$\nabla^2 u + \lambda u = 0 \quad \text{in } R \tag{8.16a}$$

$$\frac{\partial u}{\partial n} = 0 \quad \text{on } C_1 \tag{8.16b}$$

and

$$\nabla^2 v + \lambda v = 0 \quad \text{in } R \tag{8.17a}$$

$$\frac{\partial v}{\partial n} = 0 \quad \text{on } C_1 \tag{8.17b}$$

In this case, U_j and V_k are fixed constants, so that in Appendix B $\mu = 0$ on C_k and $\eta = 0$ on C_j.

By using the Green's formula

$$\oint_C v \frac{\partial u}{\partial n}\, dl = \iint_R \nabla v \cdot \nabla u \, da + \iint_R v \cdot \nabla^2 u \, da \tag{8.18}$$

together with the boundary conditions (8.6), (8.7), (8.16b) and (8.17b), and (8.16a), (8.17a), it follows that

$$F_2^o(u,v) = V_k \oint_{C_j} \frac{\partial u}{\partial n}\, dl \tag{8.19a}$$

$$= U_j \oint_{C_k} \frac{\partial v}{\partial n} \, dl \qquad (8.19b)$$

where $F_2^o(u,v)$ is the stationary value of $F_2(u,v)$ for a given value of λ.

It then follows from (8.14), (8.15) that

$$y_{jk} = y_{kj} = \frac{F_2^o(u,v)}{RV_k U_j} \qquad (8.20)$$

where λ and the complex frequency variable s are related by

$$s = -\lambda/RC \qquad (8.21)$$

Note the admittance matrix elements satisfy reciprocity as expected.

Next we consider the functionals $F_3(u,v)$ and $F_4(u,v)$.

In Appendix C it is shown that if

$$\begin{aligned} g_u &= 0 \quad \text{on } C_2 + C_k \\ &= U_j = \text{constant on } C_j \end{aligned} \qquad (8.22)$$

$$\begin{aligned} g_v &= 0 \quad \text{on } C_2 + C_j \\ &= V_k = \text{constant on } C_k \end{aligned} \qquad (8.23)$$

Then the necessary conditions for $F_3(u,v)$ are (8.6) - (8.10). In the special case $j = k$ the boundary segments corresponding to metal contacts will be denoted by $C_2 + C_j$, and in (8.22), (8.23), $C_2 + C_k$ and $C_2 + C_j$ are replaced by C_2.

We note that if functional $F_1(u,v)$ is used, then the functions u and v must be constrained to satisfy the "prescribed" boundary conditions (8.6), (8.7), and the remaining boundary conditions (8.8b), (8.8c), (8.9b), (8.9c) are "natural" conditions for the functional to be stationary i.e. it is not necessary to constrain u and v to satisfy the "natural" boundary conditions since these must be satisfied at a stationary point of the functional. For the functional $F_3(u,v)$ the natural boundary conditions are (8.6), (8.7), (8.8b) and (8.9b), and the prescribed boundary conditions are (8.8c), (8.9c).

By similar reasoning to that in Appendix C we can show that the necessary conditions for $F_4(u,v)$ to be stationary are (8.6), (8.7) and (8.16), (8.17). In addition, it is easily shown that the stationary value of $F_4(u,v)$ for a given λ is related to the admittance matrix terms y_{jk} and y_{kj} by

$$y_{jk} = y_{kj} = \frac{\overset{\circ}{F}_4(u,v)}{RV_k U_j} \tag{8.24}$$

Thus we have shown that the poles and zeros of an admittance matrix element are proportional to the stationary values of functional $F_1(u,v)$ or $F_3(u,v)$, where the functions u and v are constrained to satisfy prescribed boundary conditions as discussed above. In addition, it was shown that the value of an admittance matrix element at a given frequency is proportional to $F_2(u,v)$ or $F_4(u,v)$, provided that u and v satisfy the prescribed boundary conditions.

8.3 Solution of the Stationary Problem by the Rayleigh-Ritz Method

The Rayleigh-Ritz method for obtaining approximations to the stationary values of the functionals presented previously is based on the assumption that the unknown functions u and v may be approximated by a class of functions containing n linearly independent parameters. For our purposes it is convenient to choose the approximation in the form of a linear combination of n linearly independent functions with undetermined coefficients. In addition to satisfying any prescribed boundary conditions, the only restriction on the approximations is that they must be continuous, with bounded, piecewise-continuous first derivatives in R, and on C, such that the required integrals in (8.1) - (8.4) exist.

The approximations to the unknown functions u and v may be written in the form

$$u = \sum_{i=1}^{n} c_i f_i (x,y) \tag{8.25}$$

$$v = \sum_{i=1}^{n} d_i g_i (x,y) \tag{8.26}$$

Then the conditions for the functional F(u,v) to be stationary are

$$\frac{\partial F}{\partial c_i} = 0 \qquad \text{for } i = 1,2 \text{ -- } n \tag{8.27}$$

and

$$\frac{\partial F}{\partial d_i} = 0 \qquad \text{for } i = 1,2 \text{ -- } n \tag{8.28}$$

After substituting the approximations (8.25), (8.26) for u and v into (8.3) and (8.4) and imposing the stationary conditions (8.27), (8.28), we obtain

$$\left[A - \lambda B\right] d\Big] = - d_u \Big] V_k \tag{8.29}$$

$$\left[A^t - \lambda B^t\right] c\Big] = - d_v \Big] U_j \tag{8.30}$$

where

$$a_{ij} = \iint_R \nabla f_i \cdot \nabla g_j \, da - \oint_{C_2 + C_j + C_k} \left[f_i \frac{\partial g_j}{\partial n} + g_j \frac{\partial f_i}{\partial n} \right] dl$$

$$b_{ij} = \iint_R f_i \, g_j \, da$$

$$d_{u_i} = \oint_{C_k} \frac{\partial f_i}{\partial n} \, dl \tag{8.31}$$

$$d_{v_i} = \oint_{C_j} \frac{\partial g_i}{\partial n} \, dl$$

For the functional $F_3(u,v)$ to be stationary it was previously shown that it is necessary to constrain the u and v functions to satisfy (8.8c) and (8.9c) respectively. These conditions are equivalent to

$$\left[c\right]^t \left[d_u\right] = 0 \tag{8.32}$$

and

$$\left[d \right]^t \left[d_v \right] = 0 \tag{8.33}$$

From this it follows that the coefficients c_i and d_i are not all independent, and one of each set of coefficients, the nth say, may be expressed as a linear combination of the remaining coefficients as follows,

$$c_n = - \frac{1}{d_{u_n}} \sum_{i=1}^{n-1} d_{u_i} \; c_i \tag{8.34}$$

$$d_n = - \frac{1}{d_{v_n}} \sum_{i=1}^{n-1} d_{v_i} \; d_i \tag{8.35}$$

If the expressions on the right of (8.34), (8.35) are substituted into (8.25), (8.26) and the stationary conditions (8.27) (8.28) for i = 1, 2 -- (n-1) are applied to (8.3), it can be shown that the conditions for $F_3(u,v)$ to be stationary subject to the constraints (8.8c), (8.8d), are

$$\left[S \right]^t \left[A - \lambda B \right] \left[T \right] d \Big]_{n-1} = 0 \tag{8.36}$$

and

$$\left[T \right]^t \left[A^t - \lambda B^t \right] \left[S \right] c \Big]_{n-1} = 0 \tag{8.37}$$

where A and B are defined by (8.31), and

$$d\Big]_{n-1} = \begin{bmatrix} d_1 \\ d_2 \\ \cdot \\ \cdot \\ d_{n-1} \end{bmatrix} \tag{8.38}$$

$$c\Big]_{n-1} = \begin{bmatrix} c_1 \\ c_2 \\ \cdot \\ \cdot \\ c_{n-1} \end{bmatrix} \tag{8.39}$$

$$[S] = \begin{bmatrix} 1 & & \bigcirc \\ & 1 & \\ & & \ddots \\ \bigcirc & & 1 \\ -\frac{d_{u_1}}{d_{u_n}} & -\frac{d_{u_2}}{d_{u_n}} & \cdots\cdots -\frac{d_{u_{n-1}}}{d_{u_n}} \end{bmatrix} \tag{8.40}$$

$$[T] = \begin{bmatrix} 1 & & \bigcirc \\ & 1 & \\ & & \ddots \\ \bigcirc & & 1 \\ -\frac{d_{v_1}}{d_{v_n}} & -\frac{d_{v_2}}{d_{v_n}} & \cdots\cdots -\frac{d_{v_{n-1}}}{d_{v_n}} \end{bmatrix} \tag{8.41}$$

Clearly (8.36) may be converted to the usual matrix eigenvalue problem of the form

$$\left[A' - \lambda I \right] x \Big] = 0 \tag{8.42}$$

by premultiplying (8.36) by $\left[S\right]^{t}\left[B\right]\left[T\right]^{-1}$ In the special case where $\left[A\right]$ and $\left[B\right]$ are symmetric and $\left[S\right] = \left[T\right]$, other methods for obtaining an equation of the form (8.42) with A' symmetric are available (53), (55).

Now considering the functional $F_4(u,v)$, we note its stationary value obtained from (8.29), (8.30) is

$$\begin{aligned} F_4^{o}(u,v) &= V_k \oint_{C_k} \frac{\partial u}{\partial n}\, dl \\ &= U_j \oint_{C_j} \frac{\partial v}{\partial n}\, dl \end{aligned} \tag{8.43}$$

where

u and v approximately satisfy (8.6), (8.7) and (8.16), (8.17).

This follows since (8.29) is equivalent to

$$\iint_R (\nabla u.\nabla v - \lambda u.v)\, da - \oint_{C_2 + C_j + C_k} (u \frac{\partial v}{\partial n} + v \frac{\partial u}{\partial n})\, dl + V_k \oint_{C_k} \frac{\partial u}{\partial n}\, dl = 0$$

and (8.30) is equivalent to

$$\iint_R (\nabla u \cdot \nabla v - \lambda u \cdot v) - \oint_{C_2 + C_j + C_k} \left(u \frac{\partial v}{\partial n} + v \frac{\partial u}{\partial n}\right) dl$$

$$+ U_j \oint_{C_j} \frac{\partial v}{\partial n} dl = 0$$

and when these expressions are substituted into (8.4) we obtain (8.43). Thus we choose as our approximate solution,

$$y_{kj} = y_{jk} = \frac{1}{RU_j} \left[c\right]^t \left[d_u\right] = \frac{1}{RV_k} \left[d\right]^t \left[d_v\right] \qquad (8.44)$$

where $\left[c\right]$ and $\left[d\right]$ satisfy (8.29), (8.30).

We now consider the functions $F_1(u,v)$ and $F_2(u,v)$. Since the functions u and v are required to satisfy the boundary conditions (8.6), (8.7) it is convenient to choose the expansion functions $f_i(x,y)$ and $g_i(x,y)$ in (8.25), (8.26) as follows

$$f_i(x,y) = g_i(x,y) = 0 \quad \text{on } C_2 + C_j + C_k \qquad (8.45)$$

$$\text{for } i = 1, 2 \cdots n-1$$

$$\begin{aligned} f_n(x,y) &= 0 \quad \text{on } C_2 + C_k \\ f_n(x,y) &= 1 \quad \text{on } C_j \end{aligned} \qquad (8.46)$$

$$\begin{aligned} g_n(x,y) &= 0 \quad \text{on } C_2 + C_j \\ g_n(x,y) &= 1 \quad \text{on } C_k \end{aligned} \qquad (8.47)$$

For the functional $F_1(u,v)$, application of the stationary

conditions (8.27), (8.28) gives

$$\left[A - \lambda B\right] d\right] = 0 \tag{8.48}$$

$$\left[A^t - \lambda B^t\right] c\right] = 0 \tag{8.49}$$

where

$$a_{ij} = \iint_R \nabla f_i \cdot \nabla g_j \, da$$

$$b_{ij} = \iint_R f_i \cdot g_j \, da \tag{8.50}$$

The matrix equation (8.48) may be transformed to the form (8.42) by premultiplying the left side by $\left[B\right]^{-1}$, or when $\left[A\right]$ and $\left[B\right]$ are symmetrical the methods described in (53), (55) may be used.

For the functional $F_2(u,v)$, $u(x,y)$ is fixed on C_j and $v(x,y)$ is fixed on C_k. Let $u(x,y) = U_j$ on C_j and $v(x,y) = V_k$ on C_k. These constraints are then satisfied by choosing

$$c_n = U_j$$

$$d_n = V_k \tag{8.51}$$

Then by applying the stationary conditions (8.27), (8.28) for $i = 1, 2 -- (n-1)$ and substituting U_j and V_k for c_n and d_n respectively, we obtain two systems of linear equations which may be solved for the unknown coefficients $d_1 - - - d_{n-1}$ and $c_1 - - - c_{n-1}$. The equations are

$$\underline{n}\left[A - \lambda B\right]\underline{n} \quad d\right]_{(n-1)} = - d_u\Big]_{(n-1)} V_k \tag{8.52}$$

$$\underline{\underline{n}}\left[A^t - \lambda B^t\right]\underline{\underline{n}}\ c\Big]_{(n-1)} = -\,d_v\Big]_{(n-1)}\ U_j \qquad (8.53)$$

where $\underline{\underline{n}}\left[A\right]\underline{\underline{n}}$ denotes the matrix obtained by deleting the nth row and column of $\left[A\right]$, $d\Big]_{(n-1)}$ and $c\Big]_{(n-1)}$ are given by (8.38), (8.39), and $d_u\Big]_{(n-1)}$ and $d_v\Big]_{(n-1)}$ are obtained by deleting the nth element from the nth column of $\left[A - \lambda B\right]$ and $\left[A^t - \lambda B^t\right]$ respectively.

Once (8.52) and (8.53) have been solved for the unknown coefficients the admittance matrix element $y_{jk} = y_{kj}$ may be computed as follows.

Since our approximation to the stationary value of $F_2(u,v)$ is

$$F_2^o(u,v) = \left[c^t\right]\left[A - \lambda B\right] d\Big] = \left[d^t\right]\left[A^t - \lambda B^t\right] c\Big] \qquad (8.54)$$

where $c\Big]$ and $d\Big]$ satisfy (8.52), (8.53), $y_{jk} = y_{kj}$ may then be obtained from $F_2^o(u,v)$ as in (8.20). In addition, because of (8.52), (8.53) it is easily shown that (8.54) is equivalent to

$$F_2(u,v) = c_{n\cdot n}\left[A - \lambda B\right] d\Big] = d_{n\cdot n}\left[A^t - \lambda B^t\right] c\Big] \qquad (8.55)$$

where $_n\left[A - \lambda B\right]$ denotes the nth row of $\left[A - \lambda B\right]$.

8.4 Functional Approximations for Variational Solutions

In the preceding sections we have considered the theoretical basis of variational methods for obtaining approximate solutions for the admittance matrix elements and the poles and zeros. We now wish to consider in more detail the problem of choosing suitable expansion functions for use in the approximations to the potential functions $u(x,y)$ and $v(x,y)$, (8.25), (8.26). In addition, we will also consider the problem of evaluating the area integrals over a two-dimensional region R, and the contour integrals over the boundary C as required for the Rayleigh-Ritz solutions.

When the functionals $F_1(u,v)$ and $F_2(u,v)$ are used, the expansion functions $f_i(x,y)$ and $g_i(x,y)$ are required to satisfy the boundary conditions (8.45) - (8.47). When the functionals $F_3(u,v)$ and $F_4(u,v)$ are used, the expansion functions are not required to satisfy any boundary conditions. However the exact solutions of the boundary value problem are required to satisfy boundary conditions of the form given in (8.6), (8.7) and (8.8), (8.9) or (8.16), (8.17) as well as the Helmholtz equation, and we should therefore attempt to choose a set of expansion functions which will satisfy these requirements as closely as possible.

As previously mentioned, the functions $u(x,y)$ and $v(x,y)$ must be continuous with piecewise continuous derivatives in R, in order to ensure the existence of the integrals occurring in the functionals (8.1) - (8.4). In addition, we note that when the approximations to $u(x,y)$ and $v(x,y)$ are constrained to satisfy the Dirichlet boundary conditions (8.6), (8.7), it is not necessary to evaluate any contour integrals. However, it is often extremely

difficult to obtain expansion functions satisfying these conditions, and it is then more practical to use the functionals (8.3), (8.4).

One of the simplest types of approximation which is commonly used is a polynomial in the two coordinates x and y, (10), (53), i.e.

$$u(x,y) = \sum_{i=1}^{n} c_i \, x^p \, y^q \tag{8.56}$$

which is defined over the entire region R.

If the order of the polynomial is N, then it contains all p,q combinations such that $0 \leq p + q \leq N$, and the total number of terms, n, is

$$n = \frac{1}{2} (N+1) (N+2) \tag{8.57}$$

A simple linear ordering scheme is obtained by taking

$$i = (p+1) (p+q+1) + p+1 \tag{8.58}$$

thus giving an expanded version of (8.56) that is

$$u(x,y) = c_1 + c_2 y + c_3 x + c_4 y^2 + c_5 xy + c_6 x^2 - - \tag{8.59}$$

Comparing (8.25) and (8.59) we make the identification

$$f_i(x,y) = x^p \, y^q \tag{8.60}$$

where

i, p and q are related by (8.58).

Similarly, if v(x,y) is approximated by a polynomial, i.e.

$$v(x,y) = \sum_{i=1}^{n} d_i \, x^p \, y^q \tag{8.61}$$

we make the identification,

$$g_i(x,y) = x^p y^q \tag{8.62}$$

The problem of evaluating the surface integrals over R and the contour integrals on C in (8.31) when $f_i(x,y)$ and $g_i(x,y)$ are of the form (8.60), (8.62) has been considered in (10), (53), and (56). All of the surface integrals involve terms of the form

$$\iint_R x^m y^n \, dy \, dx \tag{8.63}$$

If the boundary is represented by piecewise polynomials, the resulting integrals can be easily evaluated on a computer. For simplicity, it is common to approximate a curved boundary in a piecewise-linear (polygonal) fashion. In this case both the contour integrals and surface integrals are linear combinations of terms of the form

$$\int_{x_a}^{x_b} x^m (\alpha + \beta x)^n \, dx \tag{8.64}$$

Since the integrand is a polynomial in x only, these integrals are easily evaluated by using integration by parts (56), or by Gaussian quadrature (3), (10), (53).

For reasons of convenience it is often preferable to choose $f_i(x,y)$ and $g_i(x,y)$ such that the coefficients c_i and d_i are the values of the potential functions $u(x_j,y_j)$ and $v(x_j,y_j)$ at n particular node points specified by the coordinates (x_j,y_j). In this case, instead of (8.60), (8.62) we choose $f_i(x,y)$ and

$g_i(x,y)$ to be complete polynomials of order N such that

$$f_j(x_j,y_j) = g_j(x_j,y_j) = 1$$
$$f_k(x_j,y_j) = g_k(x_j,y_j) = 0 \qquad \text{for } k \neq j \tag{8.65}$$

In the finite-element method described by Silvester (54), (55), the region R is subdivided into a number of triangular subregions. The node points (x_j,y_j) are chosen so that there are (N+1) equally spaced points on each triangle side, and the remaining points are regularly spaced in the triangle interior. Silvester, (54), has computed a set of universal element matrices which simplify the numerical evaluation of the surface integrals in (8.31) for triangles of any shape and size for polynomials of order 1 to 4. The contour integrals in (8.31) may be evaluated by the method described in (56).

Since the potential function is required to be continuous in R it is necessary to place constraints on the potential function in each triangle. These constraints are satisfied by ensuring that all points which have the same coordinates (i.e. points on an edge common to two triangles), are assigned the same potential value (c_j or d_j).

One advantage of the finite-element type of approximation over the polynomial approximation given previously is that it is sometimes easier to obtain a potential function which satisfies Dirichlet boundary conditions of the form (8.6), (8.7).

In addition, better accuracy is sometimes obtained by using a piecewise polynomial approximation to the potential instead

of a single polynomial over the entire region R. The finite-element method is one example of a piecewise polynomial approximation. An example using a piecewise polynomial approximation with polygonal subregions is given in (10), and in (56) the possibility of using "triangular" elements with one curved side is discussed.

In addition to the polynomial approximations discussed above, it is sometimes more convenient to use other types of expansion functions, for example, Thomas (57) has used expansions involving the polar coordinates (r,θ) of the form

$$u(r,\theta) \text{ or } v(r,\theta) = b_o + \sum_{m=1}^{N} \sum_{n=1}^{N} b_{m,n} r^m \cos n\theta \qquad (8.66)$$

In this case the integrals (8.31) can be transformed into integrals involving the variable θ only, if the boundary is expressed as a radial function of angle $R(\theta)$. The integrals may be evaluated exactly if $R(\theta)$ is expressed in the form of a Fourier series, but in general it is necessary to use approximate numerical integration techniques.

The potential functions could also be expanded as products of trigonometric functions in the coordinates (x,y) (55). However, these functions are most suitable for rectangular regions, and will not be considered here.

We now wish to consider the problem of obtaining polynomial or piecewise-polynomial approximation to $u(x,y)$ and $v(x,y)$ which satisfy the Dirichlet boundary conditions (8.6), (8.7). We note that it is not necessary to constrain the approximate solutions to satisfy the Neumann boundary conditions (8.8b), (8.9b), since these

are natural conditions for the functions (8.1) - (8.4) to be stationary. An important advantage of using functions which satisfy the Dirichlet boundary conditions is that for self adjoint problems, i.e. $u(x,y) = v(x,y)$, the approximate eigenvalues are always greater than the exact eigenvalues i.e. they are upper bounds. In addition, the approximate values of the diagonal elements of the admittance matrix for $s = 0$ are upper bounds on the true values, and lower bounds can be obtained by solving the dual problem as discussed in (35).

A polynomial approximation which satisfies homogeneous Dirichlet boundary conditions of the form (8.45) can be obtained by choosing(53)

$$f_i(x,y) = g_i(x,y) = x^p y^q g(x,y) \qquad (8.67)$$

for $i = 1,2 -- (n-1)$

where

$g(x,y)$ is a polynomial such that

$$g(x,y) = 0 \qquad \text{on } C_2 + C_j + C_k \qquad (8.68)$$

and

$g(x,y)$ does not vanish inside R.

For some problems a suitable $g(x,y)$ can be found by inspection (53). For example, if the boundary condition is $g(x,y) = 0$ for $x = 0$ and $x = 1$, we choose $g(x,y) = x(x-1)$. *For more complicated boundary shapes it is necessary to use other methods. Bulley (53) used a numerical technique to find a $g(x,y)$ polynomial whose integrated squared amplitude along the boundary is a minimum. This led to an algebraic eigenvalue problem whose solution yielded a set of functions having nodal lines corresponding closely with the boundary segments $C_2 + C_j + C_k$. The eigenfunction having no nodal

* The following description of Bulley's method (53) in this paragraph is extracted from (33).

lines well within the boundary was selected for $g(x,y)$. The method worked well, but suffers from the disadvantage that more work must probably be done in discovering the $g(x,y)$ polynomial than in the remaining computation. Also, human intervention is required to inspect the eigenfunctions and reject those having internal nodal contours.

Next we consider methods for obtaining functions $f_n(x,y)$ and $g_n(x,y)$ which satisfy the Dirichlet boundary conditions (8.46), (8.47). Suppose that each of the boundary segments corresponding to metal contacts is defined by

$$y = w_i(x) \qquad (8.69)$$

$$\text{for } i = 1,2 -- N_p$$

where

N_p is the number of metal contacts.

Then, provided that $w_j(x)-w_i(x)$ is non-zero inside R for $i \neq j$, then a suitable $f_n(x,y)$ is

$$f_n(x,y) = \prod_{\substack{i=1 \\ i\neq j}}^{N_p} \frac{y - w_i(x)}{w_j(x) - w_i(x)} \qquad (8.70)$$

Similarly,

$$g_n(x,y) = \prod_{\substack{i=1 \\ i\neq k}}^{N_p} \frac{y - w_i(x)}{w_k(x) - w_i(x)} \qquad (8.71)$$

Note that $f_n(x,y)$ and $g_n(x,y)$ defined by (8.70) and (8.71) are not polynomials in general, even when the $w_i(x)$ are polynomials, so that the previous methods for integrating polynomials over

two-dimensional regions are no longer directly applicable.

If the above method does not provide a suitable $f_n(x,y)$, the coefficients of a least-squares polynomial approximation may be found by minimizing

$$\oint_{C_2 + C_j + C_k} (f_n(x,y) - g_u)^2 \, dl \qquad (8.72)$$

where

g_u satisfies the boundary conditions (8.46). This leads to a system of equations of the form

$$\left[G \right] cg \Big] = b \Big] \qquad (8.73)$$

where

$$G_{ij} = \oint_{C_2 + C_j + C_k} x^{p+r} \, y^{q+s} \, dl$$

$$b_i = \oint_{C_2 + C_j + C_k} g_u \, x^p \, y^q \, dl$$

and the cg_i are the coefficients of the polynomial $f_n(x,y)$.

A similar method may be used to find a $g_n(x,y)$ which gives a least-squares approximation to g_v which satisfies (8.47).

Finally, we consider the constraints which must be imposed on finite-element solutions in order to satisfy homogeneous and inhomogeneous boundary conditions of the form (8.45) - (8.47). Because of (8.65), the coefficients in the expansions (8.25), (8.26) are equal to the value of the potential function $u(x,y)$ or $v(x,y)$ at a number of node points. If triangular elements are used, there are generally (N+1) node points on each triangle side, and the

potential along each side is a polynomial function of the distance along that side. Therefore, if the boundary segments $C_2 + C_j + C_k$ can be accurately represented by triangle sides, then polynomials $u(x,y)$ and $v(x,y)$ satisfying the required boundary conditions (8.45) - (8.47) are obtained by constraining the node potentials c_i and d_i to be equal to the specified values on these boundary segments.

8.5 Numerical Results

8.5.1 Solution of Laplace's Equation

We now present the results of calculations to determine the zero frequency admittance parameters of a number of two port distributed resistance networks.

The type of network considered is shown in Fig. 8.1

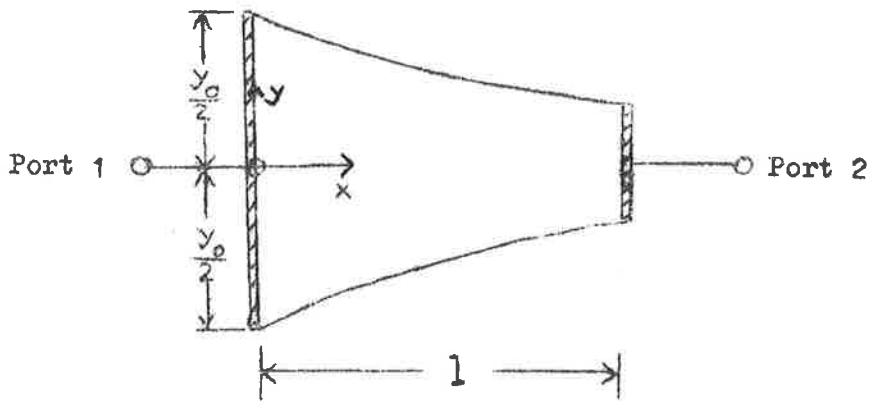

Figure 8.1. Two port tapered resistance network.

The input and output ports are the conducting strips at x=0 and x=1 respectively and the width of the resistance layer is specified by a taper function w(x) for $0 \leq x \leq 1$. The taper ratio is defined as the ratio w(o)/w(1). Since the structure is assumed to be symmetrical about the x axis it is only necessary to consider the portion in the first quadrant, which is bounded by the curve

$$y = \frac{y_o}{2} \frac{w(x)}{w(o)} \qquad \text{for} \quad 0 \leq x \leq 1 \tag{8.74}$$

and the input/output ports at x=0 and x=1. The first step in obtaining a solution is the choice of suitable expansion functions $f_i(x,y)$ and $g_i(x,y)$ to be used in the approximations (8.25), (8.26). For the problem of Fig. 8.1, polynomial functions satisfying the required Dirichlet boundary conditions are

$$f_n(x,y) = 1 - \frac{x}{1}$$

$$g_n(x,y) = \frac{x}{1} \tag{8.75}$$

$$f_i(x,y) = g_i(x,y) = g(x,y)\, x^p\, y^q$$

$$\text{for } i=1,\ 2 \text{ -- } (n-1)$$

where

$$g(x,y) = \frac{x}{1}\left(1 - \frac{x}{1}\right)$$

The next step in the solution is the evaluation of the integrals a_{ij}, (8.50) which are linear combinations of terms of the form

$$\int_{x=0}^{x=1} \int_{y=0}^{y = \frac{y_o}{2}\frac{w(x)}{w(o)}} \nabla x^p\, y^q \cdot \nabla x^r\, y^s \, dy\, dx \tag{8.76}$$

The final steps are the solution of equations (8.52), (8.53) for the coefficients d_j or c_j, and the zero frequency admittance parameters are then obtained by using (8.55).

Numerical solutions were obtained for two different taper functions.

These were the linear taper defined by

$$w(x) = (1 + \alpha x) \tag{8.77}$$

and the exponential taper defined by

$$w(x) = e^{-\alpha x} \tag{8.78}$$

where α is determined from the taper ratio τ, and the length l.

When these expressions are substituted into (8.76) the integral becomes a function of the single variable x. The required integrals may then be generated recursively using integration by parts to express the integrals involving higher powers of x and w(x) in terms of the integrals involving lower powers of x and w(x). Alternatively, when w(x) is a polynomial, as in (8.77), Gaussian quadrature may be used to evaluate the integrals. In connection with the recursive method for generating the integrals it should be realized that the integrals for the higher powers of x and y can sometimes suffer from loss of accuracy due to an accumulation of rounding errors.

Since the expansion functions (8.75) satisfy the Dirichlet boundary conditions, the values obtained for y_{11} and y_{22} are upper bounds on the exact values. In addition, it is only necessary to compute one of the admittance parameters, since for a two port resistance network of the form of Fig. 8.1

$$y_{11} = y_{22} = -y_{12} = -y_{21} \tag{8.79}$$

Lower bounds on the exact solutions can also be obtained by solving the dual problem to that in Fig. 8.1. The dual problem is obtained by interchanging the conducting and insulating boundaries. Because of symmetry about the x axis, we need only consider the portion of the network in the upper half plane, so that the input and output ports are on the curve defined by (8.74), and the vertical boundaries of x=0 and x=1 become insulating boundaries. A lower bound on y_{11} or y_{22} for the original problem is the reciprocal of y_{11} or y_{22} obtained for the dual problem if the resistance of the resistive sheet is one ohm/square in both cases (35). The method of solution proceeds as before, except that $f_n(x,y)$ and $g_n(x,y)$ in (8.75) are replaced by

$$f_n(x,y) = 1 - \frac{y}{\frac{y_o}{2}\frac{w(x)}{w(o)}}$$

$$g_n(x,y) = \frac{y}{\frac{y_o}{2}\frac{w(x)}{w(o)}} \tag{8.80}$$

$$g(x,y) = y\left[1 - \frac{y}{\frac{y_o}{2}\frac{w(x)}{w(o)}}\right]$$

Numerical results were obtained for linearly and exponentially tapered resistance network having various widths y_o and taper ratios τ. Upper and lower bounds on y_{ij} $i,j = 1, 2$ were obtained by using $u(x,y)$ and $v(x,y)$ functions of the form given previously, where terms containing $x^p y^q$ were chosen to have $0 \leq p + q \leq 7$.

Tables 8.1 and 8.2 show the average of the computed upper and lower bounds, together with the maximum percentage errors which were obtained by taking the ratio of the difference between the upper and lower bounds to the mean value. The numerical results are normalized to a sheet resistance of one ohm/square, and the length l is assumed to be unity. We note that the accuracy of the numerical values in the tables decreases as y_o increased with τ constant. Also for y_o/l constant, the error increases as τ deviates further from the value unity.

These results may be compared with the admittance parameters obtained by assuming a one-dimensional model of the tapered network. The one-dimensional results are obtained by integrating the resistance per unit length r(x) from x= 0 to x=1, where r(x) is inversely proportional to the width w(x), (5)

$$r(x) = R/w(x) \tag{8.81}$$

where

R is the sheet resistance in ohms/square.

After performing the integration

$$y_{11} = \frac{1}{\int_0^1 r(x)\,dx} \tag{8.82}$$

we obtain for the linear taper

$$y_{11} = \frac{y_o}{R}\,\frac{\alpha}{\log_e(1+\alpha l)} = \frac{y_o}{Rl}\,\frac{\tau-1}{\tau \log_e \tau} \tag{8.83}$$

and for the exponential taper

$$y_{11} = \frac{y_o}{R} \quad \frac{\alpha}{e^{\alpha \cdot 1} - 1} \qquad (8.84)$$

$$\frac{y_o}{Rl} \quad \frac{\log_e \tau}{\tau - 1}$$

Values of $y_{11}/(y_o/Rl)$ for these two tapers are given in Tables 8.3 and 8.4 for the same values of τ as in Tables 8.1 and 8.2.

Comparison of the numerical results obtained from the one and two dimensional analyses shows that they are in close agreement for networks with taper ratios near unity, and for networks whose maximum width is less than or equal to the length. For other shapes there are considerable differences between the two sets of results.

τ \ y_o/l	0.1	0.4	1.0	2.5	10.0
0.1	.37028 ± .47%	1.06625 ± 5.3%	1.89397 ± 17%		
0.4	.163412 ± .004%	.639016 ± .05%	1.47945 ± .44%	3.21489 ± 2.9%	
1.0	0.1	0.4	1.0	2.5	10.0
2.5		.260765 ± .0095%	.639016 ± .05%	1.47945 ± .44%	4.80967 ± 5.4%
10.0			.37028 ± .47%	.17978 ± 2.5%	1.8397 ± 17%

y_{11}

Table 8.1 Zero Frequency Admittance Parameters for Linearly Tapered Resistance Networks (Two Dimensional Analysis)

τ \ y_o/l	0.1	0.4	1.0	2.5	10.0
0.1	.24820 ±.016%	.8374 ± .27%	1.6709 ± 2.7%		
0.4	.152466 ±.003%	.59781 ±.022%	1.4028 ± .15%	3.132 ± 1.2%	
1.0	0.1	0.4	1.0	2.5	10.0
2.5		.243356 ±.006%	.59781 ±.022%	1.4029 ± .17%	4.737 ± 3%
10.0			.24820 ±.016%	.5698 ±.1%	1.6709 ±2.7%

y_{11}

Table 8.2 Zero Frequency Admittance Parameters for Exponentially Tapered Resistance Networks (Two Dimensional Analysis)

τ	0.1	0.4	1.0	2.5	10.0
$y_{11}/(y_o/R_1)$	3.90865	1.63703	1.0	0.65481	0.39086

Table 8.3 Zero Frequency Admittance Parameters for Linearly Tapered Resistance Networks (One Dimensional Analysis)

τ	0.1	0.4	1.0	2.5	10.0
$y_{11}/(y_o/R_1)$	2.55842	1.52715	1.0	.61086	.25584

Table 8.4 Zero Frequency Admittance Parameter for Exponentially Tapered Resistance Networks (One Dimensional Analysis)

It can be shown that the results obtained from a one-dimensional analysis (8.83), (8.84) are always greater than those which would be obtained from an exact two-dimensional analysis with $\Upsilon \neq 1$. This follows since (8.83), (8.84) can be obtained by assuming that the potential function in the two-dimensional region has the form given in (5), and then calculating $\frac{1}{R}\iint_R (\nabla\phi)^2$ da. Since this surface integral is a minimum for the potential function ϕ which satisfies Laplace's equation and the boundary conditions of the two-dimensional problem, it follows that the one-dimensional admittance parameters must be greater than or equal to the exact values.

In addition to the numerical results given above, the zero frequency admittance parameters of the linearly tapered resistance network shown in Fig. 8.2 were obtained by using the finite element method.

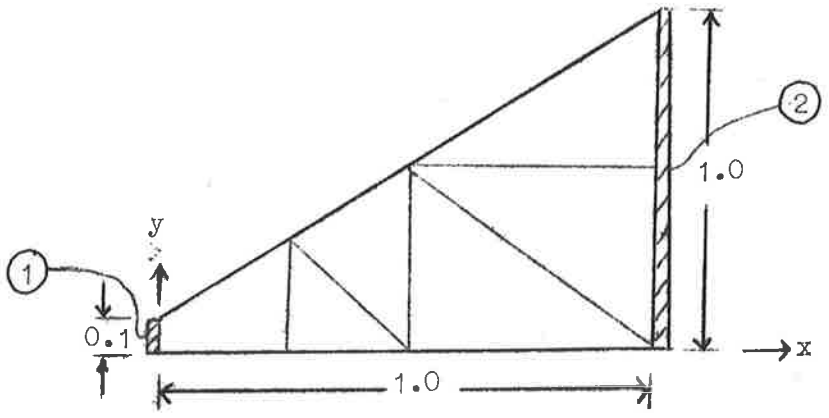

Figure 8.2. Linearly tapered distributed resistance network solved by the finite-element method.

The resistive sheet was divided into seven triangular elements as shown, and the admittance matrix element y_{11} was computed with polynomials of order 2, 3, and 4 in each element. The computer program used was a modified version of the one described in (55) and (61). The main modifications required were

(1) the substitution of a subroutine for solving simultaneous equations in place of the package of subroutines for computing eigenvalues and eigenvectors,

and

(2) the incorporation of constraints to ensure that the potential is constant on the triangle sides which coincide with input and output ports.

The original program allows the user to constrain the potential function to be zero on specified triangle sides. This facility, together with the second modification described above allows the user to compute diagonal or off-diagonal admittance elements of a multiport network by specifying the triangle vertices which lie on the input port or output port, as well as those vertices on the ports at zero potential.

In addition to the problem in Fig. 8.2 the dual problem, which is obtained by interchanging the insulating and conducting boundaries of the original problem, was also solved. The triangular elements and polynomial orders were identical with those used to solve the original problem.

If it is assumed that the resistance of the sheet is one ohm/square for both problems, the reciprocal of the value of y_{11} or y_{22} obtained for the dual problem is a lower bound on y_{11} or y_{22} for the original problem. Since the approximate solution for y_{11} of

the original problem is an upper bound on the exact value, we can take the mean of the upper and lower bounds as our solution, and the maximum possible error is one half of the difference between the upper and lower bounds. The values obtained for y_{11} or y_{22} with polynomials of order 2, 3 and 4 in each element are shown in Table 8.5

Polynomial Order	Lower Bound	Upper Bound	Mean Value	Error
2	.322846	.335921	.329383	2%
3	.326585	.331095	.328840	1.4%
4	.327518	.329755	.328636	.34%

Table 8.5 Numerical Values of the Zero Frequency Admittance Matrix Elements y_{11} or y_{22} For the Resistance Network of Fig. 8.2

8.5.2 Eigenvalue problems

We now present the results of some calculations to determine the poles and zeros of the admittance matrix parameters of some two port distributed resistance - capacitance networks. The first problem considered is shown in Fig. 8.2. Two different forms of polynomial approximations were used for the potential functions $u(x,y)$ and $v(x,y)$. One form of approximation used was an nth order polynomial defined over the entire region R; the approximation for $u(x,y)$ is given by (8.25), (8.75) and the approximation for $v(x,y)$ is given by (8.26), (8.75). The second method of solution used was the finite element method, i.e. the region R was divided into a number of triangular subregions, and the potentials in each sub-region were approximated by nth order polynomials defined by the values of potential functions $u(x,y)$ or $v(x,y)$ at a number of regularly spaced node points.

With both types of approximations, the polynomial coefficients or node potential values were constrained to satisfy the appropriate Dirichlet boundary conditions on the metal contacts.

The computer program in which the potential functions is approximated by an nth order polynomial defined over the entire region R is a modified version of the program EHPOL (53). This program can be used in its original form to compute the poles of the admittance matrix since $u(x,y) = v(x,y)$ satisfies homogeneous Dirichlet boundary conditions on $C_2 + C_j + C_k$, and only the first (n-1) expansion functions in (8.75) are used in (8.25), (8.26). When the zeros of an admittance matrix element are computed it is necessary to include the terms $f_n(x,y)$ and $g_n(x,y)$, (8.75) in (8.25), (8.26), and additional programming is required to evaluate

the integrals in (8.50) which contain these terms. Since the $f_n(x,y)$ and $g_n(x,y)$ are polynomials, all of the required integrals are obtained as a linear combination of integrals of the form $\iint_R x^p y^q \, da$ so that very little extra computation is involved. Finally the eigenvalues of (8.48) or (8.49) are computed. When the zeros of a diagonal element, y_{jk} with j=k are to be found, [A] and [B] are both symmetric matrices and the eigenvalue-eigenvector subroutines in EHPOL are used. For the zeros of off-diagonal elements of the admittance matrix, [A] and [B] are asymmetrical, and the QR method (11) for general real matrices is then used to find the eigenvalues of (B^{-1}) (A).

The second computer program, in which the region R is divided into triangular sub-regions, with an nth order polynomial approximation to the potential in each triangle, is a modified version of the finite element program described in (55), (61).

This program can be used in its original form to compute the poles of the admittance matrix, since $u(x,y) = v(x,y)$ satisfies homogeneous Dirichlet boundary conditions on $C_2 + C_j + C_k$. Since the expansion functions $f_i(x,y)$, $g_i(x,y)$ are piecewise polynomials satisfying (8.65), these constraints are satisfied simply by setting the coefficients c_i, d_i corresponding to node points on $C_2 + C_j + C_k$ to zero. When the zeros of an admittance matrix term $y_{jk} = y_{kj}$ are to be computed, the coefficients c_i corresponding to node points on C_j are constrained to be equal, and those corresponding to node points on C_k are zero; the coefficients d_i corresponding to node points on C_k are constrained to be equal, and those corresponding to node points on C_j are set to zero. Since the existing program contains all of the programming necessary to

compute the integrals (8.50), the modifications required to compute the zeros of y_{jk} are fairly trivial. When the zeros of a diagonal element y_{jj} are required, the matrices $[A]$ and $[B]$ in (8.48), (8.49) are symmetrical, and the eigenvalues are computed by using the package of subroutines in (61). When the zeros of an off-diagonal element are required, $[A]$ and $[B]$ are asymmetrical in general, and the QR method, (11), for general real matrices is then used to find the eigenvalues of $[B]^{-1}[A]$.

We now present the results obtained for the poles and zeros of the admittance matrix elements for the network of Fig. 8.2.

The results in Tables 8.6 - 8.9 show the eigenvalues obtained by using the modified version of the program EHPOL, with the potential functions over the entire region R approximated by polynomials of order 5 to 8. The poles and zeros (s_i) are obtained from the eigenvalues λ_i by using the relation $\lambda_i = -s_i RC$, where R and C are the resistance in ohms/square of the resistive layer, and the capacitance per unit area between the resistive layer and the ground plane respectively.

The corresponding eigenvalues obtained by using the modified finite-element program (61) are shown in Tables 8.10 - 8.13. The resistive sheet was divided into seven triangular sub-regions as shown in Fig. 8.2, and polynomials of order 2 to 4 were used in each triangle.

The results obtained for the poles and zeros of the diagonal elements y_{11} and y_{22} will be considered first.

Since the potential functions were constrained to satisfy the appropriate Dirichlet boundary conditions, the eigenvalues obtained are greater than or equal to the exact values. It is seen

TABLE 8.6 APPROXIMATE EIGENVALUES CORRESPONDING TO THE POLES OF THE ADMITTANCE MATRIX FOR A LINEARLY TAPERED RC LINE - FROM PROGRAM EHPOL.
THE DIMENSIONS OF THE LINE ARE GIVEN IN FIG. 8.2.
DEG = DEGREE OF POLYNOMIAL USED TO APPROXIMATE THE POTENTIAL IN THE RESISTIVE LAYER
THE POLES, S_i, ARE RELATED TO THE EIGENVALUES, λ_i, BY EQUATION (8.13)

N	DEG 5	6	7	8
1	8.12861	8.04002	7.98374	7.94715
2	31.4263	31.1101	30.8885	30.7894
3	46.1805	45.1892	44.9650	44.8767
4	83.5809	68.7177	68.1606	67.3885
5	114.731	96.6163	92.4965	91.4197
6	160.021	124.022	113.275	112.514
7	189.460	159.179	127.685	125.264
8	220.178	208.315	169.744	158.973
9	331.031	271.937	203.484	176.381
10	476.592	323.413	248.338	208.310
11		366.301	267.784	234.281
12		377.591	340.290	267.325
13		523.459	430.973	308.286
14		728.930	505.262	372.228
15		984.932	562.072	412.068
16			583.209	426.445
17			732.397	521.277
18			783.727	652.373
19			1072.90	752.750
20			1407.61	802.156
21			1823.40	886.472
22				1003.25

TABLE 8.7 APPROXIMATE EIGENVALUES CORRESPONDING TO THE ZEROS OF THE ADMITTANCE MATRIX ELEMENT Y11 FOR A LINEARLY TAPERED RC LINE - FROM PROGRAM EHPOL. THE DIMENSIONS OF THE LINE ARE GIVEN IN FIG. 8.2.
DEG = DEGREE OF POLYNOMIAL USED TO APPROXIMATE THE POTENTIAL IN THE RESISTIVE LAYER
THE ZEROS, S_i, ARE RELATED TO THE EIGENVALUES, λ_i, BY EQUATION (8.13)

N	DEG 5	6	7	8
1	4.233907	4.232570	4.232248	4.232135
2	22.4235	22.2594	22.2403	22.2351
3	41.4555	41.1460	40.8533	40.8485
4	62.7522	59.0088	58.3502	58.2480
5	111.548	81.2114	80.4002	78.6539
6	154.649	121.859	112.084	110.8974
7	170.481	124.849	118.442	115.981
8	210.193	202.058	141.267	139.649
9	330.773	268.649	201.640	176.030
10	403.213	302.354	206.562	195.033
11	476.680	342.775	248.644	224.856
12		377.354	325.647	234.473
13		523.400	429.446	307.254
14		723.937	490.190	312.978
15		736.260	534.369	372.959
16		984.951	562.925	424.994
17			732.144	483.563
18			783.641	651.909
19			1072.30	743.823
20			1240.77	801.988
21			1407.74	812.838
22			1823.40	1002.109

TABLE 8.8 APPROXIMATE EIGENVALUES CORRESPONDING TO THE ZEROS OF THE ADMITTANCE MATRIX ELEMENT Y22 FOR A LINEARLY TAPERED RC LINE - FROM PROGRAM EHPOL. THE DIMENSIONS OF THE LINE ARE GIVEN IN FIG. 8.2.
DEG = DEGREE OF POLYNOMIAL USED TO APPROXIMATE THE POTENTIAL IN THE RESISTIVE LAYER
THE ZEROS, S_i, ARE RELATED TO THE EIGENVALUES, λ_i, BY EQUATION (8.13)

N	DEG	5	6	7	8
1		0.873907	0.85682	0.845716	0.838447
2		17.0822	16.8661	16.75508	16.6814
3		43.4349	42.9803	42.79535	42.7892
4		53.7772	49.7216	49.22508	48.9116
5		113.212	87.6061	86.11484	84.9741
6		115.654	113.018	97.27345	96.4706
7		164.703	124.244	119.3887	117.258
8		210.803	197.058	151.8447	148.037
9		331.031	213.598	199.7081	159.997
10		476.572	281.303	206.1948	193.334
11		640.639	340.898	248.4939	232.744
12			377.236	309.2218	239.178
13			523.418	357.9057	307.186
14			728.899	442.3242	330.375
15			984.931	522.6257	372.425
16			1162.44	562.5322	424.481
17				732.1293	453.972
18				783.0812	560.569
19				1072.889	663.807
20				1407.618	771.009
21				1823.399	802.528
22				1947.645	1312.35

TABLE 8.9 APPROXIMATE EIGENVALUES CORRESPONDING TO THE ZEROS OF THE ADMITTANCE MATRIX ELEMENT Y12 FOR A LINEARLY TAPERED RC LINE - FROM PROGRAM EMPOL. THE DIMENSIONS OF THE LINE ARE GIVEN IN FIG. 8.2.
DEG = DEGREE OF POLYNOMIAL USED TO APPROXIMATE THE POTENTIAL IN THE RESISTIVE LAYER
THE ZEROS, S_i, ARE RELATED TO THE EIGENVALUES, λ_i, BY EQUATION (8.13)

N	DEG	4	
		REAL	IMAGINARY
1		-25.0155	21.6342
2		-25.0155	-21.6342
3		12.0620	51.1533
4		12.0620	-51.1533
5		53.0249	
6		115.919	
7		194.874	

N	DEG	5		6	
		REAL	IMAGINARY	REAL	IMAGINARY
1		43.3456		43.1570	
2		-45.0630		-56.7424	27.8279
3		-21.6834	50.4164	-56.7424	-27.8279
4		-21.6834	-50.4164	87.9467	
5		27.3290	73.5417	-9.6275	90.3006
6		27.3290	-73.5417	-9.6275	-90.3006
7		114.281		44.9131	92.3616
8		163.074		44.9131	-92.3616
9		208.169		123.930	
10		331.029		204.861	
11		476.563		276.549	
12				336.742	
13				377.266	
14				523.524	
15				728.839	
16				984.929	

TABLE 8.10 APPROXIMATE EIGENVALUES CORRESPONDING TO THE POLES OF THE ADMITTANCE MATRIX FOR A LINEARLY TAPERED RC LINE - FROM FINITE ELEMENT PROGRAM.
NFIT = DEGREE OF POLYNOMIAL USED TO APPROXIMATE THE POTENTIAL IN EACH TRIANGULAR REGION (FIG. 8.2)
THE POLES, S_i, ARE RELATED TO THE EIGENVALUES, λ_i, BY

EQUATION (8.13)

N	NFIT 2	3	4
1	7.99576	7.89298	7.87061
2	32.1244	30.7247	30.6013
3	50.7615	45.3918	44.7769
4	76.2957	68.7360	67.2224
5	114.049	92.9073	90.9687
6	152.571	122.088	112.390
7	196.023	139.587	126.487
8	256.461	173.862	156.672
9	285.699	188.586	175.649
10	353.138	236.401	202.707
11	466.977	278.357	235.584
12	599.135	294.211	255.065
13	631.302	343.706	278.714
14	905.759	428.061	324.203
15	1216.30	439.912	342.299
16	3174.21	506.295	379.507
17		572.559	391.289
18		630.481	432.147
19		716.552	453.167
20		775.523	542.565

TABLE 8.11 APPROXIMATE EIGENVALUES CORRESPONDING TO THE ZEROS OF THE ADMITTANCE MATRIX ELEMENT Y11 FOR A LINEARLY TAPERED RC LINE - FROM FINITE ELEMENT PROGRAM.
NFIT = DEGREE OF POLYNOMIAL USED TO APPROXIMATE THE POTENTIAL IN EACH TRIANGULAR REGION (FIG. 8.2)
THE ZEROS, S_i, ARE RELATED TO THE EIGENVALUES, λ_i, BY

EQUATION (8.13)

N	NFIT 2	3	4
1	4.24071	4.23213	4.23205
2	22.7458	22.2558	22.2313
3	45.5731	41.2930	40.8699
4	64.7819	59.0619	58.2653
5	94.3366	81.0506	78.8017
6	146.912	115.415	111.116
7	165.548	127.047	116.956
8	223.577	157.513	137.941
9	265.978	183.482	173.917
10	341.608	210.189	189.521
11	378.273	258.991	220.054
12	494.307	280.121	241.186
13	601.284	343.250	277.150
14	780.539	371.889	298.294
15	1040.26	432.946	331.300
16	1270.97	492.014	365.469
17	3207.31	508.944	382.666
18		605.194	425.667
19		695.194	434.599
20		765.190	495.969

TABLE 8.12 APPROXIMATE EIGENVALUES CORRESPONDING TO THE ZEROS OF THE ADMITTANCE MATRIX ELEMENT Y22 FOR A LINEARLY TAPERED RC LINE - FROM FINITE ELEMENT PROGRAM.
NFIT = DEGREE OF POLYNOMIAL USED TO APPROXIMATE THE POTENTIAL IN EACH TRIANGULAR REGION (FIG. 8.2)
THE ZEROS, S_i, ARE RELATED TO THE EIGENVALUES, λ_i, BY

EQUATION (8.13)

N	NFIT 2	3	4
1	0.843511	0.827508	0.823089
2	16.8767	16.5913	16.5335
3	49.9712	43.2464	42.8317
4	51.6778	49.1388	48.5226
5	113.259	86.7539	85.4801
6	121.314	98.7780	95.0693
7	183.157	131.012	119.869
8	228.133	162.707	147.133
9	271.634	176.934	157.513
10	287.534	216.767	187.777
11	360.889	255.839	225.008
12	467.314	294.164	239.020
13	607.647	342.605	261.867
14	631.374	407.579	302.893
15	905.769	436.093	324.215
16	1217.10	471.691	356.137
17	3174.29	550.678	391.287
18		613.398	417.315
19		688.249	450.129
20		720.559	504.636

TABLE 8.13 APPROXIMATE EIGENVALUES CORRESPONDING TO THE ZEROS OF THE ADMITTANCE MATRIX ELEMENT Y12 FOR A LINEARLY TAPERED RC LINE - FROM FINITE ELEMENT PROGRAM. NFIT = DEGREE OF POLYNOMIAL USED TO APPROXIMATE THE POTENTIAL IN EACH TRIANGULAR REGION (FIG. 8.2) THE ZEROS, S_i, ARE RELATED TO THE EIGENVALUES, λ_i, BY EQUATION (8.13)

N	NFIT 2		3	
	REAL	IMAGINARY	REAL	IMAGINARY
1	50.1701		43.5020	
2	-51.1525	65.4668	85.8418	
3	-51.1525	-65.4668	127.458	
4	118.047		-146.836	
5	171.079		-26.1047	156.536
6	-24.6380	195.080	-26.1047	-156.536
7	-24.6380	-195.080	187.809	7.25718
8	-131.644	161.026	187.809	-7.25718
9	-131.644	-161.026	290.542	
10	272.202		-314.306	39.4208
11	319.339		-314.306	-39.4208
12	441.554		337.621	
13	649.071		385.982	
14	765.182	345.998	-39.6328	400.987
15	765.182	-345.998	-39.6328	-400.987
16	853.152		263.263	313.590
17	2872.45		263.263	-313.590
18			476.106	12.7057
19			476.106	-12.7057
20			703.502	44.3550
21			703.502	-44.3550

N	NFIT 4	
	REAL	IMAGINARY
1	42.9855	
2	84.2393	
3	114.840	
4	147.056	
5	168.797	
6	-196.164	108.795
7	-196.164	-108.795
8	232.445	11.3714
9	232.445	-11.3714
10	31.9759	274.936
11	31.9759	-274.936
12	287.952	
13	323.708	
14	391.796	
15	420.461	
16	435.354	63.4992
17	435.354	-63.4992
18	-274.647	338.560
19	-274.647	-338.560
20	-480.118	222.549
21	-480.118	-222.549

from the tables that the eigenvalues decrease as the polynomial order increases. The smaller eigenvalues are generally more accurate than the larger ones, since the eigenfunctions corresponding to the larger eigenvalues are required to be orthogonal to each of the eigenfunctions corresponding to the smaller eigenvalues, and the smallest eigenvalue is the minimum value of the functional $F_1(u,v)$. A comparison between the results obtained with the two different types of polynomial approximations may be made with the same order of matrix eigenvalue problem in both cases. For example, the number of eigenvalues obtained by using program EHPOL with a polynomial of degree 6 is one less than the number of eigenvalues obtained by using the finite element method with polynomials of degree 2 in each of the seven triangular regions. A direct comparison of these two sets of results shows that most of the eigenvalues obtained by the former method are less than those obtained by the latter method. Since the approximate eigenvalues are greater than or equal to the exact eigenvalues, this observation tends to support the view that better accuracy is usually obtained if the potential is approximated by a high order polynomial over the entire region instead of lower order polynomials in several subregions. However, a disadvantage of the former method is that for polynomials of high order it is more difficult to obtain accurate numerical solutions of the eigenvalue problem $[A - \lambda B]\ c] = 0$ because of the accumulation of rounding errors during the computation. The results in Tables 8.6 - 8.9 were obtained by using single precision arithmetic on a CDC 6400 computer, which gives an accuracy of about 14 significant

figures for each arithmetic operation. An attempt was then made to solve the same eigenvalue problems with polynomials of order seven or greater, on an IBM 7090 computer, which performs single precision arithmetic operations with an accuracy of about 8 significant figures. This attempt failed because it was found that a negative diagonal element occurred during the Choleski decomposition (10), (53), of the [B] matrix into upper and lower triangular factors. Since the [B] matrix is known to be positive definite for this class of problems, a negative diagonal element can only occur as a result of rounding errors during the computation. A similar problem was encountered previously when using polynomial approximations to solve one-dimensional eigenvalue problems. Thus the finite element method is generally preferable to the polynomial approximation method since it is less susceptible to loss of numerical accuracy due to rounding errors.

We now consider the eigenvalues obtained for the zeros of the admittance matrix element y_{12} (Tables 8.9 and 8.13). In contrast with the previous results where the eigenvalues are all positive and real, we find that negative and complex eigenvalues are also obtained. However, as the polynomial order increases it is seen that the positive real eigenvalues tend to decrease in magnitude, and each one appears to be approaching a different limiting value. The negative and complex eigenvalues appear to be increasing in modulus as the polynomial order increases, and they do not appear to be approaching any limiting value. This type of behaviour has been observed in connection with the solution of a somewhat simpler eigenvalue problem (14), p148-150, i.e. when the potential functions are not constrained to satisfy

all of the boundary conditions it is possible to obtain extraneous eigenvalues whose eigenfunctions do not approximately satisfy the boundary conditions of the problem. A comparison of the results obtained by using the two different types of polynomial approximations shows that the smaller positive real eigenvalues are in close agreement, whereas the negative and complex eigenvalues are quite different. It is therefore concluded that only the small positive real eigenvalues obtained for y_{12} are accurate, while the negative and complex eigenvalues are extraneous and should be ignored. It should also be realized that if it is desired to compute the admittance parameters at low frequencies, then it is only necessary to consider the smaller eigenvalues, (poles and zeros), in the product form expansion. In any case it is seen that the larger poles and zeros are approximately equal and their effects would tend to cancel one another at low frequencies.

The poles and zeros obtained by a one-dimensional analysis of the linearly tapered network Fig. 8.2 differ considerably from those obtained from the two-dimensional analysis. The one-dimensional results are given in Chapter 3, Tables 3.4 - 3.6. The smallest poles and zeros differ by about 10 percent, while there are larger differences between the larger poles and zeros. The eigenvalues obtained from the one-dimensional analysis are all greater than those corresponding eigenvalues obtained by the two-dimensional analysis. In addition, the zeros of the off-diagonal elements y_{12} obtained by the one-dimensional analysis are all at infinity, while the two-dimensional analysis yields some zeros on the negative real axis of the complex frequency plane. However, these finite zeros have only a small effect on the input/

output characteristics of the network at low frequencies since they are very nearly coincident with poles of the admittance matrix. There will still be considerable differences between the admittance parameters obtained by one and two dimensional analyses, because of the differences between the zero frequency parameters and the smaller poles and zeros.

We now wish to calculate the poles and zeros of the admittance matrix of a rectangular structure "a" units long and "b" units wide, with the input/output ports occupying the two ends of width "b". The admittance matrix of this structure is easily shown to be (1), pp 243-245 and pp.7-9.

$$[Y] = \frac{b\gamma}{r} \begin{bmatrix} \coth \gamma a & -\operatorname{csch} \gamma a \\ -\operatorname{csch} \gamma a & \coth \gamma a \end{bmatrix} \tag{8.85}$$

where

$\gamma = \sqrt{src}$, and r and c are the resistance and capacitance per unit area respectively. It is assumed, as is usual in transmission line theory that no lateral variations in voltage can occur. It is easily verified that the poles of $[Y]$ are given by

$$s = p_n = -\frac{n^2\pi^2}{a^2 rc} \tag{8.86}$$

for $n = 1,2 \ldots$

and the zeros of $y_{11} = y_{22}$ are

$$s = z_n = -\frac{(2n-1)^2\pi^2}{a^2 rc} \tag{8.87}$$

for $n = 1,2 - -$

while $y_{12} = y_{21}$ has no finite zeros.

However, if one obtains the poles and zeros by solving the appropriate boundary value problems, the eigenvalues and eigenfunctions corresponding to the poles are found to be

$$\lambda_{n,m} = \frac{1}{rc} \left(\frac{n^2\pi^2}{a^2} + \frac{m^2\pi^2}{b^2} \right)$$

and

(8.88)

$$\psi_{n,m}(x,y) = \sin \left(\frac{n\pi}{a} \cdot x\right) \cos \left(\frac{m\pi}{b} y\right)$$

for $n = 1, 2 - - -$

$m = 0, 1 - - -$

Clearly the poles (8.86) correspond to the eigenvalues and eigenfunctions of (8.88) with m=0, i.e. the poles given by (8.86) correspond only to the eigenfunctions with no lateral (y) variation.

The eigenvalues and eigenfunctions corresponding to the zeros of $y_{11} = y_{22}$ are

$$\lambda_{n,0} = \frac{1}{rc} \frac{(2n-1)^2\pi^2}{4\,a^2}$$

(8.89)

and

$$\psi_{n,0}(x,y) = \cos \frac{(2n-1)\pi}{2\,a} \cdot x$$

for $n = 1, 2 - - -$

$$\lambda_{n,m} = \frac{1}{rc}\left[\frac{n^2\pi^2}{a^2} + \frac{m^2\pi^2}{b^2}\right] \qquad (8.90)$$

and

$$\psi_{n,m}(x,y) = \sin\frac{n\pi}{a}\cdot x \quad \cos\frac{m\pi}{b}\, y$$

for $n = 1, 2, 3 - - -$

and $m = 1, 2, 3 - - -$

The eigenvalues and eigenfunctions corresponding to the zeros of $y_{12} = y_{21}$ are also given by (8.90). Clearly the zeros (8.87) correspond to the eigenvalues and eigenfunctions of (8.89) i.e. the eigenvalues and eigenfunctions given by (8.87) correspond only to the eigenfunctions with no lateral (y) variation.

We note that the zeros of y_{ij} given by (8.90) exactly cancel the poles corresponding to $m > 0$ in (8.88), so that the remaining poles and zeros of the admittance parameters are given by (8.86), (8.87).

The eigenvalues corresponding to the poles and zeros of a rectangular RC structure with length a=1 and width b=1/9 are given in Tables (8.14) - (8.16). These values were obtained from (8.88) - (8.90) where the rc product is assumed to be unity. Approximate solutions were also obtained by using polynomials of order 4 to 6 to approximate the potential functions u(x,y) and v(x,y) over the entire rectangle i.e. the modified version of the program EHPOL was used. The numerical results are shown in Tables 8.17 - 8.19. In addition, solutions were also obtained by using the finite element program with the rectangle divided into 6 identical right angled triangles. The numerical results obtained with polynomials of order 2 to 4 are shown in Tables 8.20 - 8.22.

TABLE 8.14 EXACT EIGENVALUES CORRESPONDING TO THE POLES OF THE ADMITTANCE MATRIX FOR A UNIFORM RC LINE.
LENGTH OF LINE = 1, WIDTH = 1/9 .
M AND N ARE MODE NUMBERS.
THE POLES, S_i, ARE RELATED TO THE EIGENVALUES, λ_i, BY

EQUATION (8.13).

M	N 0	1	2
1	9.86960	809.307	3207.62
2	39.4784	838.916	3237.23
3	88.8264	888.264	3286.57
4	157.913	957.351	3355.66
5	246.740	1046.17	3444.49
6	355.305	1154.74	
7	483.610		
8	631.654		
9	799.437		
10	986.960		

TABLE 8.15 EXACT EIGENVALUES CORRESPONDING TO THE ZEROS OF THE ADMITTANCE MATRIX ELEMENT Y11 FOR A UNIFORM RC LINE.
LENGTH OF LINE = 1, WIDTH = 1/9 .
M AND N ARE MODE NUMBERS.
THE ZEROS, S_i, ARE RELATED TO THE EIGENVALUES, λ_i, BY

EQUATION (8.13).

M	N 0	1	2
1	2.46740	809.307	3207.62
2	22.2066	838.916	3237.23
3	61.6850	888.264	3286.57
4	120.902	957.351	3355.66
5	199.859	1046.17	3444.49
6	298.555	1154.74	
7	416.990		
8	555.165		
9	713.078		

TABLE 8.16 EXACT EIGENVALUES CORRESPONDING TO THE ZEROS OF THE ADMITTANCE MATRIX ELEMENT Y12 FOR A UNIFORM RC LINE.
LENGTH OF LINE = 1, WIDTH = 1/9 .
M AND N ARE MODE NUMBERS.
THE ZEROS, S_i, ARE RELATED TO THE EIGENVALUES, λ_i, BY

EQUATION (8.13).

M	N 1	2
1	809.307	3207.62
2	838.916	3237.23
3	888.264	3286.57
4	927.351	3355.66
5	1046.17	3444.49
6	1154.74	
7		
8		

TABLE 8.17 APPROXIMATE EIGENVALUES CORRESPONDING TO THE POLES OF THE ADMITTANCE MATRIX FOR A UNIFORM RC LINE - FROM PROGRAM EMPOL.
LENGTH OF LINE = 1, WIDTH = 1/9 .
DEG = DEGREE OF POLYNOMIAL USED TO APPROXIMATE THE POTENTIAL IN THE RESISTIVE LAYER.
THE POLES, S_i, ARE RELATED TO THE EIGENVALUES, λ_i, BY EQUATION (8.13).

N	DEG , 4	5	6
1	9.86974	9.86974	9.86960
2	42.0002	39.5024	39.5024
3	102.141	102.141	89.4577
4	982.000	201.121	201.049
5	1014.00	809.835	394.995
6	4870.00	1013.99	809.835
7		1074.04	840.532
8		4870.00	1074.01
9		4900.74	1155.96
10		13787.3	3231.30
11			4887.13
12			4908.53
13			13772.8
14			13805.3
15			30776.1
16			
17			

TABLE 8.18 APPROXIMATE EIGENVALUES CORRESPONDING TO THE ZEROS OF THE ADMITTANCE MATRIX ELEMENT, Y11, FOR A UNIFORM RC LINE - FROM PROGRAM EMPOL.
LENGTH OF LINE = 1, WIDTH = 1/9 .
DEG = DEGREE OF POLYNOMIAL USED TO APPROXIMATE THE POTENTIAL IN THE RESISTIVE LAYER.
THE ZEROS, S_i, ARE RELATED TO THE EIGENVALUES, λ_i, BY EQUATION (8.13).

N	DEG 4	5	6
1	2.46740	2.46740	2.46740
2	22.3217	22.2139	22.2068
3	69.4050	63.0396	61.8627
4	265.875	148.308	128.863
5	982.000	548.590	280.414
6	1014.00	809.835	809.834
7	4870.00	1014.00	840.457
8		1074.01	1073.95
9		4870.00	1139.60
10		4900.69	1205.47
11		13787.2	3231.36
12			4887.45
13			4908.74
14			13770.4
15			13804.0
16			30780.5

TABLE 8.19 APPROXIMATE EIGENVALUES CORRESPONDING TO THE ZEROS OF THE ADMITTANCE MATRIX ELEMENT, Y12, FOR A UNIFORM RC LINE - FROM PROGRAM EMPOL.
LENGTH OF LINE = 1, WIDTH = 1/9 .
DEG = DEGREE OF POLYNOMIAL USED TO APPROXIMATE THE POTENTIAL IN THE RESISTIVE LAYER.
THE ZEROS, S_i, ARE RELATED TO THE EIGENVALUES, λ_i, BY EQUATION (8.13).

N	DEG	4		5	
		REAL	IMAGINARY	REAL	IMAGINARY
1		-35.3709	23.0155	-59.7274	
2		-35.3709	-23.0155	-37.2101	52.3331
3		11.3753	52.1782	-37.2101	-52.3331
4		11.3553	-52.1782	32.1996	75.6736
5		982.000		32.1996	-75.6736
6		1014.00		809.835	
7		4870.00		1014.00	
8				1074.04	
9				4870.00	
10				4900.75	
11				13787.3	

N	DEG	6	
		REAL	IMAGINARY
1		-73.3509	31.5768
2		-73.3509	-31.5768
3		-29.6907	84.2963
4		-29.6907	-84.2963
5		60.1119	98.0467
6		60.1119	-98.0467
7		809.834	
8		840.488	
9		1074.00	
10		1154.34	
11		3231.22	
12		4884.98	
13		4907.80	
14		13765.8	
15		13801.9	
16		30765.0	

TABLE 8.20 APPROXIMATE EIGENVALUES CORRESPONDING TO THE POLES OF THE ADMITTANCE MATRIX FOR A UNIFORM RC LINE - FROM FINITE ELEMENT PROGRAM.
LENGTH OF LINE = 1, WIDTH = 1/9 .
NFIT = DEGREE OF POLYNOMIAL USED TO APPROXIMATE THE POTENTIAL IN EACH TRIANGULAR REGION.
THE POLES, S_i, ARE RELATED TO THE EIGENVALUES, λ_i, BY EQUATION (8.13).

N	NFIT 2	3	4
1	9.88454	9.86977	9.86946
2	40.3143	39.5045	39.4787
3	90.0000	89.8905	88.8277
4	204.577	162.343	158.236
5	388.234	266.464	249.038
6	956.007	378.000	375.178
7	1006.13	736.234	521.451
8	1333.58	814.099	729.653
9	1501.09	857.723	809.836
10	1646.01	918.268	840.498
11	4929.80	1059.94	897.677
12	5201.45	1151.14	919.172
13	5341.48	1247.75	9738.30
14	5727.03	1732.69	1085.95
15	5748.62	1982.23	1204.62

TABLE 8.21 APPROXIMATE EIGENVALUES CORRESPONDING TO THE ZEROS OF THE ADMITTANCE MATRIX ELEMENT, Y11, FOR A UNIFORM RC LINE - FROM FINITE ELEMENT PROGRAM.
LENGTH OF LINE = 1, WIDTH = 1/9 .
NFIT = DEGREE OF POLYNOMIAL USED TO APPROXIMATE THE POTENTIAL IN EACH TRIANGULAR REGION.
THE ZEROS, S_i, ARE RELATED TO THE EIGENVALUES, λ_i, BY EQUATION (8.13).

N	NFIT 2	3	4
1	2.46753	2.46739	2.46714
2	22.3662	22.2095	22.2066
3	64.5146	61.8255	61.6890
4	144.294	122.612	120.997
5	285.345	209.752	200.781
6	490.637	331.869	303.567
7	957.549	589.312	438.698
8	1006.27	814.070	617.994
9	1341.53	857.635	809.835
10	1525.02	918.257	840.489
11	1725.66	929.026	849.162
12	4946.82	1060.24	897.677
13	5215.51	1235.04	973.822
14	5357.15	1405.67	1085.95
15	5729.64	1754.97	1204.62
16	5786.03	2006.00	1417.38

TABLE 8.22 APPROXIMATE EIGENVALUES CORRESPONDING TO THE ZEROS OF THE ADMITTANCE MATRIX ELEMENT, Y12, FOR A UNIFORM RC LINE - FROM FINITE ELEMENT PROGRAM.
LENGTH OF LINE = 1, WIDTH = 1/9 .
NFIT = DEGREE OF POLYNOMIAL USED TO APPROXIMATE THE POTENTIAL IN EACH TRIANGULAR REGION.
THE ZEROS, S_i, ARE RELATED TO THE EIGENVALUES, λ_i, BY EQUATION (8.13).

N	NFIT = 2		NFIT = 3	
	REAL	IMAGINARY	REAL	IMAGINARY
1	5.56091	.	5.55203	
2	51.7846		50.1360	
3	-56.1149	108.356	142.795	
4	-56.1149	-108.356	-178.263	
5	170.049		25.7959	247.953
6	428.557		25.7959	-247.953
7	878.829		300.754	
8	995.043		645.958	
9	1286.13	95.3304	816.728	
10	1286.13	-95.3304	856.899	
11	1619.43		918.278	
12	4188.93		1080.46	
13	5071.64		1208.87	33.9042
14	5306.69		1208.87	-33.9042
15	5564.35		1776.24	94.3069
16	5763.62		1776.24	-94.3069

N	NFIT = 4	
	REAL	IMAGINARY
1	5.55108	
2	49.9604	
3	139.070	
4	276.818	
5	-211.706	161.978
6	-211.706	-161.978
7	195.705	411.225
8	195.705	-411.225
9	483.799	
10	791.705	
11	810.308	
12	841.564	
13	897.703	
14	973.187	
15	1084.56	
16	1204.63	

Considering the results obtained from program EHPOL first, we see that the eigenvalues obtained for the zeros of y_{12} are all positive and real, except for some extraneous complex and negative real eigenvalues. The positive real eigenvalues are seen to be exactly (except for rounding errors) equal to a subset of the eigenvalues obtained for the poles of Y and the zeros of y_{11}. The complex and negative eigenvalues are extraneous because they do not converge to a definite limit, as the polynomial degree increases, and they do not approximately satisfy the boundary conditions. It is interesting to note that the number of extraneous eigenvalues is exactly equal to the order of polynomial used. This was also found to be true for the linearly tapered RC network (Fig. 8.2) considered previously. In addition, the poles and zeros which do not cancel one another, approximate the solutions (8.86), (8.87). The remaining poles and zeros which are common to each y_{ij} approximate the solutions given by (8.90).

Now considering the results obtained from the finite element program, we note that we do not get exact cancellation of the eigenvalues corresponding to laterally varying eigenfunctions. This is particularly noticeable for low order polynomial approximations; when higher order polynomials are used the poles and zeros corresponding to laterally varying eigenfunctions are almost exactly equal. This effect is believed to be due to the choice of triangular elements which are not positioned symmetrically with respect to the mid-point of the rectangle; all of the eigenfunctions have either even or odd symmetry about this point. In addition, we find that the eigenvalues obtained for the zeros of y_{12} include some extraneous eigenvalues which are positive and

real, and which appear to converge to some limiting value; as with previous solutions we also obtain some extraneous complex eigenvalues. The extraneous positive real eigenvalues can only be positively isolated by examination of their eigenfunctions.

Apart from the extraneous eigenvalues obtained with the two types of polynomial approximations, the remaining eigenvalues approximate the smaller eigenvalues (8.88) - (8.90) quite accurately. Thus we expect that the accuracy of the admittance parameters obtained from the product form expansion would be adequate at low frequencies.

Finally, we note that Silvester (62) has used the finite element method to analyse a rectangular structure having the same dimensions as that just considered. The network considered by Silvester was a lossless TEM mode transmission line, whereas we have considered a distributed RC line. The results obtained for one problem are directly applicable to the other problem, since the methods for transforming r-c admittance functions into l-c admittance functions can be used. For example, if an admittance function of a lossless l-c network is in the form of a partial fraction expansion

$$y_{ij} = \frac{1}{pL_o} + \sum_{k=1}^{\infty} \frac{p}{p^2+\omega_k^2} \frac{1}{L_k} \qquad (8.91)$$

then if each inductance L is replaced by a resistance R, the partial fraction expansion becomes

$$y_{ij} = \frac{1}{R_o} + \sum_{k=1}^{\infty} \frac{p}{p+\omega_k^2} \frac{1}{R_k} \qquad (8.92)$$

Thus the lc network has a pole of y_{ij} at p=0 whereas the rc network as a transfer admittance $\frac{1}{R_o}$ between ports i and j at p=0. The lc network has imaginary finite poles at $p = \pm j\omega_k$ whereas the rc network has real poles at $p = -\omega_k^2$. The numerical values of $L_0, L_1, L_2 - - -, \omega_1^2, \omega_2^2 - - -$ for the distributed lc network will coincide with $R_0, R_1, R_2 - - -, \omega_1^2, \omega_2^2 - - -$ for the distributed rc network respectively if the inductance and capacitance of the former per unit area is equal to the resistance and capacitance of the latter.

The partial fraction expansions for the admittance matrix of a lossless planar-TEM mode network given by Silvester (62) are essentially equivalent to that given in Chapter 7 for distributed RC structures. Both expansions involve the eigenfunctions corresponding to poles of the network, and zero frequency potential functions satisfying Laplace's equation and boundary conditions of the form $\phi = 1$ on one port and $\phi = 0$ on the remaining ports.

For the rectangular structure just considered, Silvester calculated the admittance matrix elements y_{11} and y_{12} at frequencies up to the third pole. The finite element method was used to compute the poles and the residues of the partial fraction expansions, with the rectangle subdivided as previously discussed into 6 triangles, and with second order polynomials in each triangle. For frequencies up to the third pole it was claimed, (62), that y_{11} and y_{12} were accurate to four significant figures when compared with the exact solution obtained from a one-dimensional analysis. It was further claimed that for

frequencies beyond the third pole, inclusion of laterally varying eigenfunctions in the partial fraction expansion precludes detailed agreement with the one dimensional solution.

This latter statement is considered to be incorrect. From the analysis and results given here it is evident that the laterally varying eigenfunctions have no effect at all on the admittance matrix, since they correspond to poles and zeros which exactly cancel one another. This is equivalent to having residues which are exactly zero in the partial fraction expansions. The difference between the theoretical and numerical results observed by Silvester (62) is believed to be due to errors in the eigenvalues and eigenfunctions corresponding to poles greater than the third pole. These errors are primarily due to the approximation of the potential functions by polynomials, and in principle the errors can be made arbitrarily small by using higher order polynomials.

8.6 Conclusion

In this Chapter we have presented the theoretical basis of variational methods for obtaining the poles and zeros and numerical values of the admittance matrix elements for a multiport distributed RC network.

Some numerical results were presented, with the potential functions approximated by polynomials or piecewise polynomials defined either by coefficients or the potential values at a set of node points. The examples chosen were such that polynomial approximations could be found to satisfy the appropriate Dirichlet boundary conditions on the input/output ports. However, there are

no particular difficulties in solving problems where polynomials cannot be found to satisfy these boundary conditions. The main problem encountered with the methods used here is the isolation of extraneous eigenvalues when the zeros of off-diagonal elements of $[Y]$ are computed. The only satisfactory method of detecting these extraneous solutions seems to involve inspection of the corresponding eigenfunctions. Alternatively, it may be convenient with some problems to restrict the approximating functions to satisfy all of the boundary conditions which the exact solution must satisfy.

One aspect which has not been considered in detail is the relationship between the zeros of the admittance parameters which are obtained from partial fraction expansion as in Chapter 7, and those which are obtained by the direct methods presented in this Chapter. It is this author's conjecture that at least in the case where the approximate potential functions satisfy the appropriate Dirichlet boundary conditions, and where these approximations are linear combinations of the same set of basis functions, then both methods should give identical results. A theoretical justification of this conjecture is not known. Some numerical computations which were performed suggest that this conjecture is correct, but it is difficult to obtain accurate solutions for the zeros from the partial fraction expansions. The main difficulties with the partial fraction expansion are in obtaining accurate eigenfunctions, and in the numerical solution of the polynomial whose roots are the zeros of the admittance matrix element. The direct methods for obtaining the poles and zeros by solving a matrix eigenvalue problem appear to be less subject to problems of numerical accuracy.

Chapter 9

VARIATIONAL SOLUTIONS OF FIRST-ORDER DIFFERENTIAL EQUATIONS USING TRIANGLE FUNCTIONS

9.1 Introduction

The admittance parameters of a multiport distributed resistance capacitance network are obtained by solving the second order partial differential equation

$$\nabla^2 \phi = sRC\,\phi \tag{9.1}$$

where

R is the resistance per square of the resistance layer

C is the capacitance per unit area between the resistive layer and the ground plane

s is the complex frequency variable

and

∇^2 is the two-dimensional Laplacian operator.

In addition to satisfying (9.1) the potential in the resistive layer, $\phi(x,y)$, is also required to satisfy certain boundary conditions as previously discussed.

The second-order differential equation (9.1) is equivalent to the set of coupled first-order differential equations (14) p. 162, (1) p. 242,

$$\begin{aligned} -\nabla\phi &= R.\tilde{J} \\ \nabla.\tilde{J} &= -sC\phi \end{aligned} \tag{9.2}$$

where

$\tilde{J}$ is the current density vector in the resistive layer (amperes per unit width).

In cartesian coordinates, the system of equations (9.2) is

$$-\frac{\partial \phi}{\partial x} = RJ_x \tag{9.3}$$

$$-\frac{\partial \phi}{\partial y} = RJ_y \tag{9.4}$$

$$\frac{\partial J_x}{\partial x} + \frac{\partial J_y}{\partial y} = -sC\phi \tag{9.5}$$

Thus instead of attempting to solve the second-order differential equation (9.1) we may attempt to solve the first-order system of differential equations (9.3) to (9.5).

One method of obtaining approximate solutions of the first-order system (9.3)-(9.5) is the method of Moments, (14), pp 126 - 128, and pp 162 - 166. In this reference, application of the method of Moments to obtain approximate solutions for the eigenvalues and eigenfunctions corresponding to TE or TM modes in waveguides of arbitrary cross-section is discussed, and some numerical results are given. With appropriate modifications this method could also be used to obtain approximate solutions for the poles and zeros of the admittance matrix elements for a distributed RC network.

In the following, we will consider variational methods for obtaining approximate solutions of the first-order equations (9.3) - (9.5). In particular, it will be shown that the poles or zeros of an admittance matrix element are proportional to the stationary values of a suitably chosen functional. Alternatively, one may

obtain the value of an admittance matrix element at a given frequency as the stationary value of a suitable functional. The differential equations (9.3) - (9.5) together with certain boundary conditions, are shown to be necessary conditions for these functionals to be stationary.

Although variational methods have been used previously for solving partial differential equations, application of these methods to the first-order equations (9.3) - (9.5) does not appear to have been considered previously. In addition the functionals presented here do not appear to have been presented elsewhere. In the following we will show how the Rayleigh-Ritz method may be used to obtain approximate solutions of the stationary problems, and in addition, it will be shown that the variational method is equivalent to the Moment method. Finally, some numerical results are given.

One undoubted advantage of the present method is that the derivatives (J_x and J_y) of the potential $\phi(x,y)$ are approximated with the same accuracy as the potential; with the variation methods discussed in Chapter 8, the derivatives J_x and J_y are generally less accurate than the potential $\phi(x,y)$.

9.2 Variational Solution of First-Order Differential Equations

In the following, it is more convenient to use the equations (9.3) - (9.5) in either of the following forms

$$-\frac{\partial \phi}{\partial x} = ku \qquad (9.6a)$$

$$-\frac{\partial \phi}{\partial y} = kv \qquad (9.6b)$$

$$\frac{\partial u}{\partial x} + \frac{\partial v}{\partial y} = k\phi \qquad (9.6c)$$

where

$$k^2 = -sCR$$

$$u = \frac{RJ_x}{k}$$

$$v = \frac{RJ_y}{k}$$

or

$$-\frac{\partial \phi}{\partial x} = u \qquad (9.7a)$$

$$-\frac{\partial \phi}{\partial y} = v \qquad (9.7b)$$

$$\frac{\partial u}{\partial x} + \frac{\partial v}{\partial y} = k^2\phi \qquad (9.7c)$$

where

$$k^2 = -sCR$$

$$u = RJ_x$$

$$v = RJ_y$$

The first form, (9.6), is used for solving eigenvalue problems i.e. poles and zeros of the admittance parameters, and the second (9.7), is used to obtain a variational expression for the admittance matrix term y_{kj} at a given frequency.

Now let

$$L = \begin{bmatrix} 0 & \frac{\partial}{\partial x} & \frac{\partial}{\partial y} \\ -\frac{\partial}{\partial x} & 0 & 0 \\ -\frac{\partial}{\partial y} & 0 & 0 \end{bmatrix} \qquad (9.8a)$$

$$M = \begin{bmatrix} k^2 & 0 & 0 \\ 0 & 1 & 0 \\ 0 & 0 & 1 \end{bmatrix} \tag{9.8b}$$

and

$$\mathbf{f} = \begin{bmatrix} \phi \\ u \\ v \end{bmatrix} \tag{9.8c}$$

Then (9.6) and (9.7) may be written in the standard operator forms

$$Lf = kf \tag{9.9}$$

and

$$Lf = Mf \tag{9.10}$$

respectively.

We will now indicate briefly the procedure for obtaining the functionals whose stationary values are proportional to the value of an admittance matrix element, or whose stationary values are proportional to the poles or zeros.

First, we will need an inner product for the function space f, which is chosen as (14), p. 163

$$\langle f_1, f_2 \rangle = \iint_R f_1 \cdot f_2 \, da$$

$$= \iint_R (\phi_1 \phi_2 + u_1 u_2 + v_1 v_2) \, da \tag{9.11}$$

Next, we will need the adjoint operator L^a, and the function space f^a on which it operates. These are found as described in Appendix A, and in (42), pp. 148 – 149. As shown in (14), p. 163 we obtain

$$\langle f^a, Lf \rangle = \langle L^a f^a, f \rangle + \oint_C \left[n_x(\phi^a u - u^a \phi) + n_y(\phi^a v - v^a \phi) \right] dl \tag{9.12}$$

where

$$L^a = \begin{bmatrix} 0 & \frac{\partial}{\partial x} & \frac{\partial}{\partial y} \\ -\frac{\partial}{\partial x} & 0 & 0 \\ -\frac{\partial}{\partial y} & 0 & 0 \end{bmatrix} \quad ; \quad f^a = \begin{bmatrix} \phi^a \\ u^a \\ v^a \end{bmatrix} \tag{9.13}$$

and n_x and n_y are the x and y components of the unit outward-pointing normal on the boundary C.

The function space f^a is determined by the requirement that the boundary integral in (9.12) must vanish for all functions f and f^a within the domain of the operators L and L^a respectively.

If we wish to compute the admittance matrix element y_{kj} of a distributed RC network, then we require a potential function f which satisfies the differential equation (9.6) or (9.7), and the boundary conditions

$$n_x u + n_y v = 0 \quad \text{on } C_1 \tag{9.14a}$$

$$\phi = G_u \quad \text{on } C_2 + C_j + C_k \tag{9.14b}$$

where

$$G_u = 0 \quad \text{on } C_2 \tag{9.14c}$$

$$= U_j = \text{constant on } C_j \tag{9.14d}$$

$$= 0 \quad \text{on } C_k \tag{9.14 e}$$

where $C = C_1 + C_2 + C_j + C_k$ is the boundary of the resistive layer, C_1 corresponds to the insulating boundary segments, C_j and C_k are the jth and kth metal contacts respectively, and C_2 denotes

all of the remaining metal contacts.

Once a solution satisfying (9.6) or (9.7) and the boundary conditions (9.14) has been found, the admittance matrix element may be computed by using

$$y_{kj} = -\frac{k}{RU_j} \oint_{C_k} (n_x u + n_y v)\, dl \qquad (9.15a)$$

or

$$y_{kj} = \frac{1}{RU_j} \oint_{C_k} (n_x u + n_y v)\, dl \qquad (9.15b)$$

(9.15a) is used if u and v satisfy (9.6), and (9.15b) is used if u and v satisfy (9.7).

If we wish to compute the poles of the admittance matrix, then we require the eigenvalues of the system of equations (9.6) where ϕ, u and v satisfies the boundary conditions (9.14) with $U_j = 0$. The poles s_i are then found from the eigenvalues k_i by using

$$s_i = -k_i^2/CR \qquad (9.16)$$

If we wish to compute the zeros of y_{kj}, then, in addition to boundary conditions (9.14), it follows from (9.15) that u and v must also satisfy

$$\oint_{C_k} (n_x u + n_y v)\ dl = 0 \qquad (9.17)$$

From the requirement that the boundary integral in (9.12) must vanish, we obtain the boundary conditions on the adjoint field f^a as

$$n_x u^a + n_y v^a = 0 \qquad \text{on } C_1 \tag{9.18a}$$

$$\phi^a = G_v \qquad \text{on } C_2 + C_j + C_k \tag{9.18b}$$

where

$$G_v = 0 \qquad \text{on } C_2 \tag{9.18c}$$

$$= V_k = \text{constant on } C_k \tag{9.18d}$$

$$= 0 \qquad \text{on } C_j \tag{9.18e}$$

or

$$G_v = U_j = \text{constant on } C_j \tag{9.18f}$$

$$= 0 \qquad \text{on } C_k \tag{9.18g}$$

from which it follows that

$$V_k \oint_{C_k} (n_x u + n_y v)\, dl = U_j \oint_{C_j} (n_x u^a + n_y v^a)\, dl \tag{9.19a}$$

or

$$U_j \oint_{C_j} (n_x u + n_y v)\, dl = U_j \oint_{C_j} (n_x u^a + n_y v^a)\, dl \tag{9.19b}$$

where (9.19a) applies when the boundary conditions are (9.18d) - (9.18e), and (9.19b) applies when the boundary conditions are (9.18f), (9.18g).

When we wish to compute the poles or zeros of y_{kj}, both sides of (9.19) are zero since $U_j = 0$, or (9.17) must be satisfied.

When we wish to consider an off-diagonal admittance matrix element (i.e. $j \neq k$), the boundary conditions (9.18d), (9.18e), (9.19a) apply, and for a diagonal element y_{jj} the boundary conditions (9.18f), (9.18g), (9.19b) apply. In addition, when we

consider a diagonal element y_{jj} in the following, i.e. $j=k$, V_k is replaced by U_j, and $\oint_{C_k}$ is replaced by $\oint_{C_j}$. If f^a satisfies the boundary conditions (9.18a)-(9.18f) and the adjoint equation

$$L^a f^a = k f^a \tag{9.20}$$

or

$$L^a f^a = M f^a \tag{9.21}$$

it follows that

$$y_{jk} = -\frac{k}{RV_k} \oint_{C_j} (n_x u^a + n_y v^a)\, dl \tag{9.22a}$$

or

$$y_{jk} = -\frac{1}{RV_k} \oint_{C_j} (n_x u^a + n_y v^a)\, dl \tag{9.22b}$$

where

(9.22a) is used if u^a and v^a satisfy (9.20),

and

(9.22b) is used if u^a and v^a satisfy (9.21).

In addition, if f satisfies (9.9) or (9.10) and f^a satisfies (9.20) or (9.21), it follows that

$$\langle f^a, Lf \rangle = \langle L^a f^a, f \rangle \tag{9.23}$$

which is equivalent to the condition previously stated, that the boundary integral in (9.12) is required to be zero. In addition, from (9.15), (9.19) and (9.22) it follows that

$$y_{kj} = y_{jk} \tag{9.24}$$

which is the reciprocity relation, i.e. the reciprocity relation follows naturally as a result of the requirement that f satisfies (9.9) or (9.10) and the boundary conditions (9.14), while the adjoint field f^a satisfies the adjoint equations (9.20) or (9.21), and the adjoint boundary conditions (9.18).

The basic technique for obtaining a functional whose stationary values are equal to the eigenvalues is the following. We take the scalar product of the adjoint field f^a with both sides of the differential equation (9.9), and then after dividing both sides of the resulting equation by $\langle f^a, f \rangle$, we take the expression on the left side of the equation as the desired functional.

We can now show that the functional

$$J_1(f, f^a) = \frac{\langle f^a, Lf \rangle}{\langle f^a, f \rangle} = \frac{\langle L^a f^a, f \rangle}{\langle f^a, f \rangle} \tag{9.25}$$

is a variational expression which has for its stationary conditions the differential equations (9.9) and (9.20), if the functions f and f^a are constrained to satisfy the boundary conditions (9.14), (9.18), and both sides of (9.19) are constrained to be zero. The stationary values of the functional J_1 are equal to the eigenvalues k_i, and these are related to the poles and zeros by (9.16). The proof of the preceding statements is quite direct. Let η be an arbitrary function, and α an arbitrary parameter, and substitute

$$f = f_1 + \alpha \eta \qquad \text{and} \qquad f^a = f_1^a \tag{9.26}$$

into (9.25), where f_1 and f_1^a are such that J_1 is stationary,

and $f_1 + \alpha\eta$ satisfies the boundary conditions of our problem. Next, differentiate (9.25) with respect to α. Then by hypothesis the derivative vanishes when $\alpha = 0$, and we therefore get (9.20) as a stationary condition. Similarly by repeating this procedure with

$$f = f_1$$
$$\text{and} \qquad f^a = f_1^a + \alpha\eta \tag{9.27}$$

we obtain (9.9) as a stationary condition. Similarly, if we wish to obtain a functional whose stationary value is proportional to an admittance matrix element y_{kj}, we proceed as follows. We take the scalar product of the adjoint field f^a, with both sides of the differential equation (9.10), and then transfer the term on the right side to the left side. The resulting expression on the left side can be shown to have a stationary value which is zero. To obtain the required functional, we add a boundary integral which is proportional to y_{kj} to the expression obtained in the previous step. The boundary integral is obtained by rearranging (9.12) such that the integral proportional to y_{kj} is on the same side of the equation as the inner product $\langle f^a, Lf \rangle$.

Thus we obtain the functional

$$J_2(f,f^a) = \langle f^a, Lf \rangle - \langle f^a, Mf \rangle - \oint_{C_k} \phi^a \, (n_x u + n_y v) \, dl \tag{9.28}$$
$$= \langle L^a f^a, f \rangle - \langle f^a, Mf \rangle - \oint_{C_j} \phi \, (n_x u^a + n_y v^a) \, dl$$

which has for its stationary conditions the differential equations (9.10), (9.21), provided that f and f^a are constrained to satisfy the boundary conditions (9.14), (9.18). In addition, it then follows that the stationary value of J_2 is related to the admittance matrix elements by

$$y_{jk} = y_{kj} = \frac{1}{RU_j V_k} \; J_2^o (f, f^a) \tag{9.29a}$$

or

$$y_{jj} = \frac{1}{RU_j^2} \; J_2^o (f, f^a) \tag{9.29b}$$

where

$J_2^o(f,f^a)$ is the stationary value of $J_2(f,f^a)$ for a given value of k, and (9.29a) is used for $j \neq k$.

The stationary conditions for the functional J_2 are derived in the same manner as those for J_1.

Next we wish to derive functionals such that the trial functions f and f^a need not satisfy all of the boundary conditions of our problem, and yet we are assured that the stationary value of the functional is furnished only by the solutions which satisfy the required differential equations and boundary conditions. This simplifies the problem of obtaining approximate numerical solutions, since it is often as difficult to find trial functions that satisfy the boundary conditions as it is to find the solution itself.

These functionals are formed by defining an extended operator L^e, and an extended adjoint operator L^{ae}, such that

$$\langle f^a, L^e f \rangle = \langle L^{ae} f^a, f \rangle \tag{9.30}$$

or an equivalent condition is satisfied for functions which need not satisfy the boundary conditions of our problem, and the operators L^e and L^{ae} are identical to the original operators L and L^a when the boundary conditions of our problem are satisfied; we have previously shown that the solutions of the boundary value problem must satisfy (9.23) which is identical to (9.30) when the boundary conditions are satisfied.

When the functions ϕ and ϕ^a satisfy the Dirichlet boundary conditions of our problem (9.14b) - (9.14e), and (9.18b) - (9.18g), we define the extended functionals as follows for eigenvalue problems:-

$$\langle f^a, L^e f \rangle = \langle f^a, Lf \rangle - \oint_C \phi^a \, (n_x u + n_y v) \, dl \qquad (9.31)$$

$$\langle L^{ae} f^a, f \rangle = \langle L^a f^a, f \rangle - \oint_C \phi \, (n_x u^a + n_y v^a) \, dl \qquad (9.32)$$

(9.31) was obtained by rearranging (9.12) so that the inner product containing Lf was on the same side of the equation as the boundary integrals containing $n_x u + n_y v$, and the resulting expression was identified with $\langle f^a, L^e, f \rangle$. Similarly, (9.32) was identified with the expression on the other side of the rearranged equation. We note that the boundary integrals in (9.31), contain only those components of f which have not been constrained to satisfy the appropriate boundary conditions, and similarly in (9.32) the boundary integral contains only those components of f^a which do not satisfy the required boundary conditions. When $(n_x u + n_y v)$ and $(n_x u^a + n_y v^a)$ satisfy the required boundary conditions $L^e = L$, and

$L^{ae} = L^{a}$ as required.

When we wish to compute the value of the admittance matrix element instead of the poles or zeros, we use the following definitions of L^{e} and L^{ae} in place of (9.31), (9.32),

$$\langle f^{a}, L^{e} f \rangle = \langle f^{a}, Lf \rangle - \oint_{C_1} \phi^{a} \, (n_x u + n_y v) \, dl \tag{9.33}$$

$$\langle L^{ae} f^{a}, f \rangle = \langle L^{a} f^{a}, f \rangle - \oint_{C_1} \phi \, (n_x u^{a} + n_y v^{a}) \, dl \tag{9.34}$$

Then, instead of (9.30), it follows from (9.12) that the solutions satisfy the equivalent condition

$$\begin{aligned} &\langle f^{a}, L^{e} f \rangle - \oint_{C_k} \phi^{a} \, (n_x u + n_y v) \, dl \\ &= \langle L^{ae} f^{a}, f \rangle - \oint_{C_j} \phi \, (n_x u^{a} + n_y v^{a}) \, dl \end{aligned} \tag{9.35}$$

We note that (9.35) is actually equivalent to (9.30), since it follows from (9.19) that the two boundary integrals in (9.35) are equal for the exact solution of the boundary value problem.

Finally, if none of the functions ϕ, u, v or ϕ^{a}, u^{a}, v^{a} are constrained to satisfy the boundary conditions of our problem, for eigenvalue problems, we define

$$\langle f^a, L^e f \rangle = \langle f^a, Lf \rangle - \oint_{C_1} \phi^a \, (n_x u + n_y v) \, dl$$

$$+ \oint_{C_2 + C_j + C_k} \left[(\phi - G_u) \, (n_x u^a + n_y v^a) - G_v (n_x u + n_y v) \right] dl \qquad (9.36)$$

and

$$\langle L^{ae} f^a, f \rangle = \langle L^a f^a, f \rangle - \oint_{C_1} \phi \, (n_x u^a + n_y v^a) \, dl$$

$$- \oint_{C_2 + C_j + C_k} \left[(\phi^a - G_v) \, (n_x u + n_y v) - G_u (n_x u^a + n_y v^a) \right] dl \qquad (9.37)$$

where

G_u and G_v are defined in (9.14) and (9.18). (9.36) and (9.37) were obtained by rearranging (9.12) and subtracting

$$\oint_{C_2 + C_j + C_k} \left[G_u \, (n_x u^a + n_y v^a) + G_v \, (n_x u + n_y v) \right] dl$$

from both sides of the resulting equation. It should be noted that if ϕ and ϕ^a satisfy the Dirichlet boundary conditions of our problem, then (9.36) and (9.37) are identical to (9.31) and (9.32) respectively.

Similarly, if we wish to compute the value of an admittance matrix element with no constraints of the potential functions, we define

$$\langle f^a, L^e f \rangle = \langle f^a, Lf \rangle - \oint_{C_1} \phi^a (n_x u + n_y v) \, dl$$

$$+ \oint_{C_2 + C_j + C_k} (\phi - G_u) (n_x u^a + n_y v^a) \, dl \tag{9.38}$$

and

$$\langle L^{ae} f^a, f \rangle = \langle L^a f^a, f \rangle - \oint_{C_1} \phi (n_x u + n_y v) \, dl$$

$$+ \oint_{C_2 + C_j + C_k} (\phi^a - G_v) (n_x u + n_y v) \, dl \tag{9.39}$$

We note that (9.38) and (9.39) are identical to (9.33) and (9.34) respectively if ϕ and ϕ^a satisfy the required Dirichlet boundary conditions.

In addition, from (9.12) it follows that (9.36), (9.37) satisfy (9.30), while (9.38) and (9.39) satisfy

$$\langle f^a, L^e f \rangle - \oint_{C_2 + C_j + C_k} G_v (n_x u + n_y v) \, dl$$

$$= \langle L^{ae} f^a, f \rangle - \oint_{C_2 + C_j + C_k} G_u (n_x u^a + n_y v^a) \, dl \tag{9.40}$$

We now consider the functionals

$$J_3(f,f^a) = \frac{\langle f^a, L^e f\rangle}{\langle f^a, f\rangle} = \frac{\langle L^{ae} f^a, f\rangle}{\langle f^a, f\rangle} \qquad (9.41)$$

where

L^e and L^{ae} are defined by (9.31), (9.32)

and

f and f^a are constrained to satisfy the Dirichlet boundary conditions (9.14b) - (9.14e) and (9.18b) - (9.18g) respectively.

It may be shown that the conditions for J_3 to be stationary are (9.9), (9.20), and the boundary conditions (9.14a), (9.18a). In addition, the stationary values of J_3 are equal to the eigenvalues k_i, and the eigenfunctions are such that both sides of (9.19) are zero.

Similarly for the functional

$$J_4(f,f^a) = \langle f^a, L^e f\rangle - \langle f^a, Mf\rangle - \oint_{C_k} \phi^a (n_x u + n_y v)\, dl \qquad (9.42)$$

$$= \langle L^{ae} f^a, f\rangle - \langle f^a, Mf\rangle - \oint_{C_j} \phi (n_x u^a + n_y v^a)\, dl$$

where

L^e and L^{ae} are defined by (9.33), (9.34),

and

f and f^a are constrained to satisfy the same boundary conditions as for J_3, it can be shown that the stationary conditions are (9.10), (9.21) and the boundary conditions (9.14a), (9.18a). In addition, the stationary value of J_4 is related to the admittance matrix elements $y_{jk} = y_{kj}$ by (9.29), where J_2 is replaced by J_4.

Finally we consider the functionals

$$J_5(f,f^a) = \frac{\langle f^a, L^e f\rangle}{\langle f^a, f\rangle} = \frac{\langle L^{ae} f^a, f\rangle}{\langle f^a, f\rangle} \tag{9.43}$$

where

L^e and L^{ae} are defined by (9.36), (9.37) and

$$J_6(f,f^a) = \langle f^a, L^e f\rangle - \langle f^a, Mf\rangle - \oint_{C_2+C_j+C_k} G_v\,(n_x u + n_y v)\;dl \tag{9.44}$$

$$= \langle L^{ae} f^a, f\rangle - \langle f^a, Mf\rangle - \oint_{C_2+C_j+C_k} G_u\,(n_x u^a + n_y v^a)\;dl$$

where

L^e and L^{ae} are defined by (9.38), (9.39). No boundary constraints are imposed on f or f^a in (9.43), (9.44).

In Appendix D it is shown that the stationary conditions for J_5 are (9.9), (9.20) and the boundary conditions (9.14a) - (9.14e), and (9.18a) - (9.18g). Similarly, the stationary conditions for J_6 are (9.10), (9.21) and the boundary conditions (9.14a) - (9.14e) and (9.18a) - (9.18g). The stationary values of J_5 are also equal to the eigenvalues k_i, provided that the solutions are constrained to satisfy

$$\oint_{C_2+C_j+C_k} G_v(n_x u + n_y v)\;dl = 0 \tag{9.45}$$

and

$$\oint_{C_2 + C_j + C_k} G_u \, (n_x u^a + n_y v^a) \, dl = 0 \tag{9.46}$$

Similarly, it can be shown that the stationary value of J_6 is related to the admittance matrix elements $y_{jk} = y_{kj}$ by (9.29), where J_2 is replaced by J_6.

We now consider application of the Rayleigh-Ritz method to the problem of obtaining the stationary values of the functionals presented previously. Approximate solutions are obtained by assuming that f and f^a may be expanded as

$$f(x,y) = \begin{bmatrix} \sum a_i \phi_i(x,y) \\ \sum b_i u_i(x,y) \\ \sum c_i v_i(x,y) \end{bmatrix} = \begin{bmatrix} \phi(x,y) \\ u(x,y) \\ v(x,y) \end{bmatrix} \tag{9.47}$$

$$f^a(x,y) = \begin{bmatrix} \sum \alpha_i \phi_i^a(x,y) \\ \sum \beta_i u_i^a(x,y) \\ \sum \gamma_i v_i^a(x,y) \end{bmatrix} = \begin{bmatrix} \phi^a(x,y) \\ u^a(x,y) \\ v^a(x,y) \end{bmatrix} \tag{9.48}$$

where $\phi_i(x,y)$, $u_i(x,y)$, $v_i(x,y)$, $\phi_i^a(x,y)$, $u_i^a(x,y)$ and $v_i^a(x,y)$ are arbitrary functions of x and y which may or may not be constrained to satisfy boundary conditions. The unknown coefficients are determined by applying the Rayleigh-Ritz stationary conditions

$$\frac{\partial J}{\partial a_i} = \frac{\partial J}{\partial b_i} = \frac{\partial J}{\partial c_i} = 0 \tag{9.49}$$

and

$$\frac{\partial J}{\partial \alpha_i} = \frac{\partial J}{\partial \beta_i} = \frac{\partial J}{\partial \gamma_i} = 0 \tag{9.50}$$

First we consider the functional $J_5(f,f^a)$ (9.43) where f and f^a are not required to satisfy any boundary conditions.

From the stationary conditions (9.49) we obtain

$$\begin{bmatrix} 0 & {}_1\phi u^a & {}_1\phi v^a \\ {}_1u\phi^a & 0 & 0 \\ {}_1v\phi^a & 0 & 0 \end{bmatrix} \begin{bmatrix} \alpha \\ \beta \\ \gamma \end{bmatrix} - k \begin{bmatrix} {}_m\phi\phi^a & 0 & 0 \\ 0 & {}_m uu^a & 0 \\ 0 & 0 & {}_m vv^a \end{bmatrix} \begin{bmatrix} \alpha \\ \beta \\ \gamma \end{bmatrix} = \begin{bmatrix} 0 \\ g^{vu} \\ g^{vv} \end{bmatrix} \tag{9.51}$$

where k is identified with $J_5(f,f^a)$,

and

$${}_1\phi u^a_{ij} = \iint_R \phi_i \frac{\partial u_j^a}{\partial x}\, da - \oint_{C_1} \phi_i n_x u_j^a\, dl \tag{9.52a}$$

$${}_1\phi v^a_{ij} = \iint_R \phi_i \frac{\partial v_j}{\partial y}\, da - \oint_{C_1} \phi_i n_y v_j^a\, dl \tag{9.52b}$$

$${}_1u\phi^a_{ij} = -\iint_R u_i \frac{\partial \phi_j^a}{\partial x}\, da + \oint_{C_2+C_j+C_k} \phi_j^a n_x u_i\, dl \tag{9.52c}$$

$$l_{ij}^{v\phi^a} = -\iint_R v_i \frac{\partial \phi_j^a}{\partial y}\, da + \oint_{C_2 + C_j + C_k} \phi_j^a n_y v_i\, dl \qquad (9.52d)$$

$$m_{ij}^{gg^a} = \iint_R g_i g_j^a\, da \qquad (9.52e)$$

where

$$g_i = \phi_i,\ u_i \text{ or } v_i$$

and

$$g_j^a = \phi_j^a,\ u_j^a \text{ or } v_j^a$$

if G_v satisfies the boundary conditions (9.18d), (9.18e) then

$$g_i^{vu} = V_k \oint_{C_k} n_x u_i dl \qquad (9.52f)$$

$$g_i^{uv} = V_k \oint_{C_k} n_y v_i dl \qquad (9.52g)$$

and if G_v satisfies the boundary conditions (9.18f), (9.18g) then

$$g_i^{vu} = U_j \oint_{C_j} n_x u_i\, dl \qquad (9.52h)$$

$$g_i^{uv} = U_j \oint_{C_j} n_y v_i\, dl \qquad (9.52i)$$

From the last row of (9.51) we obtain

$$\left[\gamma\right] = \frac{1}{k}\left[{}_{m}v^{a}\right]^{-1}\left\{\left[{}_{1}v\phi^{a}\right]\left[\alpha\right] - \left[g^{vv^{a}}\right]\left[\delta\right]\right\} \qquad (9.53)$$

where

$$\delta = V_k \text{ or } U_j$$

Similarly from the second last row of (9.51) we obtain

$$\left[\beta\right] = \frac{1}{k}\left[{}_{m}u^{a}\right]^{-1}\left\{\left[{}_{1}u\phi^{a}\right]\left[\alpha\right] - \left[g^{vu^{a}}\right]\left[\delta\right]\right\} \qquad (9.54)$$

After substituting these two results into the first row of (9.51) we obtain

$$\left\{\left[{}_{1}\phi u^{a}\right]\left[{}_{m}u^{a}\right]^{-1}\left[{}_{1}u\phi^{a}\right] + \left[{}_{1}\phi v^{a}\right]\left[{}_{m}v^{a}\right]^{-1}\left[{}_{1}v\phi^{a}\right] - k^{2}\left[{}_{m}\phi\phi^{a}\right]\right\}\left[\alpha\right]$$

$$-\left\{\left[{}_{1}\phi u^{a}\right]\left[{}_{m}u^{a}\right]^{-1}\left[g^{vu}\right] + \left[{}_{1}\phi v^{a}\right]\left[{}_{m}v^{a}\right]^{-1}\left[g^{vv}\right]\right\}\left[\delta\right] = 0 \qquad (9.55)$$

which may be rearranged to give

$$k^{2}\left[M\right]\left[\alpha\right] = \left[A\right]\left[\alpha\right] + \left[B\right]\left[\delta\right] \qquad (9.56)$$

where

$$M = \left[{}_{m}\phi\phi^{a}\right]$$

$$A = \left[{}_{1}\phi u^{a}\right]\left[{}_{m}u^{a}\right]^{-1}\left[{}_{1}u\phi^{a}\right] + \left[{}_{1}\phi v^{a}\right]\left[{}_{m}v^{a}\right]^{-1}\left[{}_{1}v\phi^{a}\right]$$

$$B = \left[{}_1\phi u^a \right] \left[m^{uu^a} \right]^{-1} \left[g^{vu} \right] + \left[{}_1\phi v^a \right] \left[m^{vv^a} \right]^{-1} \left[g^{vv} \right]$$

and

$$\delta = V_k \text{ or } U_j.$$

Since f and f^a (9.45), (9.46) are not constrained to satisfy any boundary conditions, the expansion functions ϕ_i, u_i, v_i, ϕ_i^a, u_i^a, v_i^a belong to the same function space and hence:

$$\phi_i = \phi_i^a, \; u_i = u_i^a \text{ and } v_i = v_i^a$$

Thus from equations (9.53) - (9.56) it is seen that M and A are symmetrical matrices.

To obtain the poles of the admittance matrix, we impose the constraint $\delta = 0$ in (9.56) which becomes

$$\left\{ \left[A \right] - k^2 \left[M \right] \right\} \alpha \Big] = 0 \qquad (9.57)$$

The approximate poles are then obtained from the eigenvalues k_i^2 by using (9.16).

To obtain the zeros of the admittance matrix term y_{kj} or y_{jk} we have to impose the constraint (9.45) or (9.46) on the solutions of (9.56).

If we define

$$g_i^{uu^a} = \oint_{C_j} n_x u_i^a \, dl \qquad (9.58a)$$

$$g^{uv^a} = \oint_{C_j} n_x v_i^a \, dl \qquad (9.58b)$$

then (9.46) may be written in the form

$$\left[g^{uu^a}\right]^t \left[\beta\right] + \left[g^{uv^a}\right]^t \left[\gamma\right] = 0 \qquad (9.59)$$

By using (9.53) and (9.54) this may be transformed to the form

$$\left[c\right]^t \left[\alpha\right] = 0 \qquad (9.60)$$

Methods for obtaining the eigenvalues of a system of the form (9.56) subject to the constraint (9.60) are presented in (52) and (63), and will not be considered further here.

We now consider the functional J_6, (9.44). From the stationary conditions (9.49) we obtain a system of equations which are identical to (9.51), except that the second matrix in this equation becomes

$$\left[\begin{array}{c|c|c} k^2 m^{\phi\phi} & 0 & 0 \\ \hline 0 & m^{uu} & 0 \\ \hline 0 & 0 & m^{vv} \end{array}\right] \qquad (9.61)$$

By using the procedure outlined previously, the equation may be transformed to the form (9.56), which may be solved for the unknown coefficients $\alpha]$ for any given k^2. The approximate value of J_6 may then be obtained by solving (9.53) and (9.54) for $\gamma]$ and $\beta]$, and then using

$$J_6 = U_j \left\{ \left[g^{uu^a}\right]^t \left[\beta\right] + \left[g^{uv^a}\right]^t \left[\gamma\right] \right\} \qquad (9.62)$$

where g^{uu^a} and g^{uv^a} are defined by (9.58).

We now consider the functional J_3, (9.41), where f and f^a

are constrained to satisfy only the Dirichlet boundary conditions in (9.14), (9.18). From the stationary conditions (9.49) we obtain

$$\left[\begin{array}{c|cc} 0 & {}_1\phi u^a & {}_1\phi v^a \\ \hline {}_1u\phi^a & 0 & 0 \\ \hline {}_1v\phi^a & 0 & 0 \end{array}\right]\left[\begin{array}{c}\alpha\\ \hline \beta \\ \hline \gamma\end{array}\right] = k\left[\begin{array}{c|cc} {}_m\phi\phi^a & 0 & 0 \\ \hline 0 & {}_muu^a & 0 \\ \hline 0 & 0 & {}_mvv^a \end{array}\right]\left[\begin{array}{c}\alpha\\ \hline \beta \\ \hline \gamma\end{array}\right] \tag{9.63}$$

where

k is identified with the stationary values of J_3, ${}_m\phi\phi^a$, ${}_muu^a$ and ${}_mvv^a$ are given by (9.52), and

$$\begin{aligned}
{}_1\phi u_{ij}^a &= \iint_R \phi_i \frac{\partial u_j^a}{\partial x}\, da - \oint_C \phi_i n_x u_j^a\, dl \\
{}_1\phi v_{ij}^a &= \iint_R \phi_i \frac{\partial v_j^a}{\partial y}\, da - \oint_C \phi_i n_y v_j^a\, dl \\
{}_1u\phi_{ij}^a &= -\iint_R u_i \frac{\partial \phi_j^a}{\partial x}\, da \\
{}_1v\phi_{ij}^a &= -\iint_R v_i \frac{\partial \phi_j^a}{\partial y}\, da
\end{aligned} \tag{9.64}$$

From the last two rows of (9.63) we can obtain $\beta]$ and $\gamma]$ in terms of $\alpha]$, and then after substituting these expressions into

the first row of (9.63) we obtain an equation of the form

$$\left\{\left[A\right] - k^2\left[M\right]\right\}\left[\alpha\right] = 0 \qquad (9.65)$$

which may be solved for the eigenvalues k_i which approximate the poles or zeros of the admittance matrix elements.

Similarly, when we apply the stationary conditions (9.49) to the functional J_4, we obtain a matrix equation which is identical to (9.63), except that the matrix on the right side is replaced by the matrix in (9.61). However, the potential functions $\phi(x,y)$ and $\phi^a(x,y)$ are required to be fixed constants on the boundary segments C_j and C_k respectively. Thus if the $\phi_i(x,y)$ and $\phi_i^a(x,y)$ in (9.47), (9.48) are such that

$$\phi_i(x,y) = \phi_i^a(x,y) = 0 \quad \text{on } C_2 + C_j + C_k \qquad (9.66a)$$

$$\text{for } i = 1, 2 \text{ --- } (n-1)$$

$$\begin{aligned} \phi_n(x,y) &= 1 \quad \text{on } C_j \\ &= 0 \quad \text{on } C_2 + C_k \end{aligned} \qquad (9.66b)$$

and

$$\begin{aligned} \phi_n^a(x,y) &= 1 \quad \text{on } C_k \\ &= 0 \quad \text{on } C_2 + C_j \end{aligned} \qquad (9.66c)$$

Then the boundary conditions imply that a_n and α_n are fixed constants equal to U_j and V_k respectively, and the stationary conditions $\frac{\partial J}{\partial a_n} = \frac{\partial J}{\partial \alpha_n} = 0$ cannot be applied. This is equivalent to deleting the nth row of (9.65). If the nth column of the matrix on the left side of (9.65) is multiplied by $-V_k$ and moved to the right side of the equation we can solve for the coefficients α_1,

$\alpha_2 \text{ --- } \alpha_{n-1}$ for any given k^2. Finally, our approximation to the stationary value of J_4 is obtained by taking the scalar product of the nth row of the matrix on the left side of (9.65) with the vector of coefficients α_j, and then multiplying the result by $a_n = U_j$. The approximate value of the admittance matrix element $y_{kj} = y_{jk}$ is then obtained by substituting this value of J_4 into (9.29).

9.3 Comparison of Variational Solutions of First-Order and Second-Order Differential Equations

We now wish to consider the relationship between the functionals derived in Section 9.2, and those which were used in Chapter 8. In particular we will consider self adjoint problems for which $\phi = \phi^a$, $u = u^a$, and $v = v^a$, and ϕ is assumed to satisfy the Dirichlet boundary conditions in (9.14), (9.18).

By using Gauss' Theorem and the rule for differentiating a product we can then put (9.41) into the form

$$J_3(f,f^a) = \frac{-2\iint_R \left(u\frac{\partial\phi}{\partial x} + v\frac{\partial\phi}{\partial y}\right) da}{\iint_R (\phi^2 + u^2 + v^2)\ da} \tag{9.67}$$

where the stationary values of J_3 are identified with the eigenvalues $k = k_1, k_2, k_3$ --- in (9.9), (9.20).

In Chapter 8, we used the functional

$$F_1(\phi,\phi^a) = \frac{\iint_R |\nabla\phi|^2\ da}{\iint_R \phi^2\ da} \tag{9.68}$$

where the stationary values of F_1 are identified with the square of the eigenvalues, i.e. $k^2 = k_1^2, k_2^2, k_3^2 \text{ ---}$.

For self adjoint problems the eigenvalues are all positive and real, and the approximate eigenvalues obtained from (9.68) are always greater than or equal to the exact eigenvalues.

Let $\hat{k}_i$ and $\hat{\phi}_i$ be an approximate eigenvalue and eigenfunction obtained from (9.68). Then we have

$$\hat{k}_i^2 = \frac{\iint_R |\nabla \hat{\phi}_i|^2 \, da}{\iint_R \hat{\phi}_i^2 \, da} \tag{9.69}$$

Let $\hat{\hat{k}}_i$, $\hat{\hat{\phi}}_i$, $\hat{\hat{u}}_i$ and $\hat{\hat{v}}_i$ be the corresponding eigenvalue and eigenfunction obtained from (9.67). Then we have

$$\hat{\hat{k}}_i = \frac{-2\iint_R (\hat{\hat{u}}_i \frac{\partial \hat{\hat{\phi}}_i}{\partial x} + \hat{\hat{v}}_i \frac{\partial \hat{\hat{\phi}}_i}{\partial y}) \, da}{\iint_R (\hat{\hat{\phi}}_i^2 + \hat{\hat{u}}_i^2 + \hat{\hat{v}}_i^2) \, da} \tag{9.70}$$

From (9.63) we obtain

$$-\iint_R \hat{\hat{u}}_i \frac{\partial \phi_i}{\partial x} \, da = \hat{\hat{k}}_i \iint_R \hat{u}_i^2 \, da \tag{9.71a}$$

and

$$-\iint_R \hat{\hat{v}}_i \frac{\partial \phi_i}{\partial y} \, da = \hat{\hat{k}}_i \iint_R \hat{\hat{v}}_i^2 \, da \tag{9.71b}$$

Then from (9.70), (9.71) it follows that

$$\hat{\hat{k}}_i = \frac{-\iint_R \left(\hat{\hat{u}}_i \frac{\partial \phi_i}{\partial x} + \hat{\hat{v}}_i \frac{\partial \phi_i}{\partial x}\right) da}{\iint_R \hat{\hat{\phi}}_i^2 \, da} \tag{9.72}$$

From Schwartz inequality (38), p. 16

$$\left[\iint_R \left(\hat{\hat{u}}_i \frac{\partial \hat{\hat{\phi}}_i}{\partial x} + \hat{\hat{v}}_i \frac{\partial \hat{\hat{\phi}}_i}{\partial y}\right) da\right]^2 \leq \left[\iint_R \left(\hat{\hat{u}}_i^2 + \hat{\hat{v}}_i^2\right) da\right] \left[\iint_R \left|\nabla \hat{\hat{\phi}}_i\right|^2 da\right] \tag{9.73}$$

From (9.71a) and (9.71b) this is equivalent to

$$-\iint_R \left(\hat{\hat{u}}_i \frac{\partial \hat{\hat{\phi}}_i}{\partial x} + \hat{\hat{v}}_i \frac{\partial \hat{\hat{\phi}}_i}{\partial y}\right) da \leq \frac{1}{\hat{\hat{k}}_i} \iint_R \left|\nabla \hat{\hat{\phi}}_i\right|^2 da \tag{9.74}$$

Then from (9.72) and (9.74) we obtain

$$\hat{\hat{k}}_i^2 \leq \frac{-\iint_R \left|\nabla \hat{\hat{\phi}}_i\right|^2 da}{\iint_R \hat{\hat{\phi}}_i^2 \, da} \tag{9.75}$$

As previously mentioned the approximate eigenvalues $\hat{k}_i^2$ are greater than or equal to the exact eigenvalues. Since the approximate eigenfunctions $\hat{\phi}_i$ and $\hat{\hat{\phi}}_i$ are generally different we cannot conclude from (9.69) and (9.75) that $\hat{\hat{k}}_i^2 \leq \hat{k}_i^2$; which would mean that $\hat{\hat{k}}_i^2$ could be taken either as a lower bound on the exact eigenvalue k_i^2, or as a more accurate solution than $\hat{k}_i^2$.

For certain classes of problems (14) p. 142-146, 165, it was found that the approximate eigenvalues $\hat{\hat{k}}_i^2$ were lower bounds on the exact eigenvalues. However, as will be shown later, this is not necessarily true for other eigenvalue problems.

Although it is not possible to deduce from (9.69), (9.75) that the variation method for solution of the first order differential equations will always give more accurate eigenvalues than those obtained from a variational solution of the second order differential equation, the form of these relations tends to support this view; it must be emphasized that the solutions obtained by the former method will depend on the number and form of the expansion functions used to approximate u and v as well as ϕ, whereas in the latter method the expansion functions used to approximate the derivatives of the potential function cannot be arbitrarily chosen. If the expansion functions used for $u(x,y)$, $v(x,y)$ and $\phi(x,y)$ are such that it is possible to satisfy $ku(x,y) = -\frac{\partial \phi}{\partial x}$ and $kv(x,y) = -\frac{\partial \phi}{\partial y}$ everywhere inside R, then both methods will give the same numerical results.

A comparison of the zero frequency admittance parameters may be made in a similar manner to that for the eigenvalues. As before we consider only self adjoint problems, i.e. $f = f^a$, and the potential function ϕ is assumed to satisfy the Dirichlet boundary conditions in (9.14), (9.18).

From Chapter 8, the approximate value of the admittance matrix element y_{jj} obtained from the functional $F_2(\phi,\phi^a)$, (8.1) is

$$\hat{y}_{jj} = \frac{1}{RU_j^2} \iint_R |\nabla \hat{\phi}|^2 \, da \qquad (9.76)$$

The approximate solution obtained from the functional $J_4(f,f^a)$, (9.42) can be shown to satisfy

$$\hat{\hat{y}}_{jj} = -\frac{1}{RU_j^2}\iint_R \left(\hat{\hat{u}}\frac{\partial\hat{\hat{\phi}}}{\partial x} + \hat{\hat{v}}\frac{\partial\hat{\hat{\phi}}}{\partial y}\right) da \qquad (9.77a)$$

where

$$-\iint_R \hat{\hat{u}}\,\frac{\partial\hat{\hat{\phi}}}{\partial x}\,da = \iint_R \hat{\hat{u}}^2\,da \qquad (9.77b)$$

$$-\iint_R \hat{\hat{v}}\frac{\partial\phi}{\partial y}\,da = \iint_R \hat{\hat{v}}^2\,da \qquad (9.77c)$$

and hence

$$\hat{\hat{y}}_{jj} \leq \frac{1}{RU_j^2}\iint_R \left|\nabla\hat{\hat{\phi}}\right|^2 da \qquad (9.77d)$$

As previously discussed the approximate $\hat{y}_{jj}$ given by (9.76) is an upper bound on the exact y_{jj}. In addition, from the form of (9.77d), we would expect the approximation $\hat{\hat{y}}_{jj}$ to be less than $\hat{y}_{jj}$ so that it is either a lower bound on or a more accurate approximation than $\hat{y}_{jj}$. This is not necessarily so however, since the value of $\hat{\hat{y}}_{jj}$ depends on the form of the expansion functions used for $\hat{\hat{u}}$ and $\hat{\hat{v}}$ as well as those used for $\hat{\hat{\phi}}$. The value of $\hat{y}_{jj}$ depends only on the expansion functions used for $\hat{\phi}$; if we wish to compare $\hat{y}_{jj}$ and $\hat{\hat{y}}_{jj}$ the expansion functions for $\hat{\phi}$ and $\hat{\hat{\phi}}$ will usually be identical. For the problems to be considered later it was found that $\hat{\hat{y}}_{jj}$ was

less than $\hat{y}_j$, but $\hat{\hat{y}}_{jj}$ was still an upper bound on the exact solution y_{jj}.

9.4 Area Integrals for Pyramid Functions in Rectangular and Triangular Regions

We now consider the evaluation of the matrix elements required for a variational solution of the first-order differential equations.

For simplicity it will be assumed that the region is subdivided into a number of rectangular and triangular subregions by a system of grid lines parallel to the x and y coordinates. The grid lines need not be equally spaced in either the x or y directions, but it is assumed that the boundary is approximated by linear segments, and each boundary segment either coincides with a grid line or lies on the diagonal of a rectangle enclosed by adjacent pairs of grid lines.

A potential function $\phi(x,y)$ which is defined by the value of the potential α_i at each mesh point may be expressed as follows:

$$\phi(x,y) = \sum_{i=1}^{n} \alpha_i \phi_i(x,y) \tag{9.78}$$

where

$$\phi_i(x_i,y_i) = 1$$

$$\phi_i(x_l,y_l) = 0 \qquad \text{for } l \neq i$$

and

(x_l,y_l) are the coordinates of the lth mesh point.

One of the simplest interpolation functions which gives a continuous $\phi(x,y)$ with piecewise continuous first derivatives is

defined as follows. Suppose that the mesh points at the four corners of a rectangular element are numbered i, j, k, l as shown in Fig. 9.1.

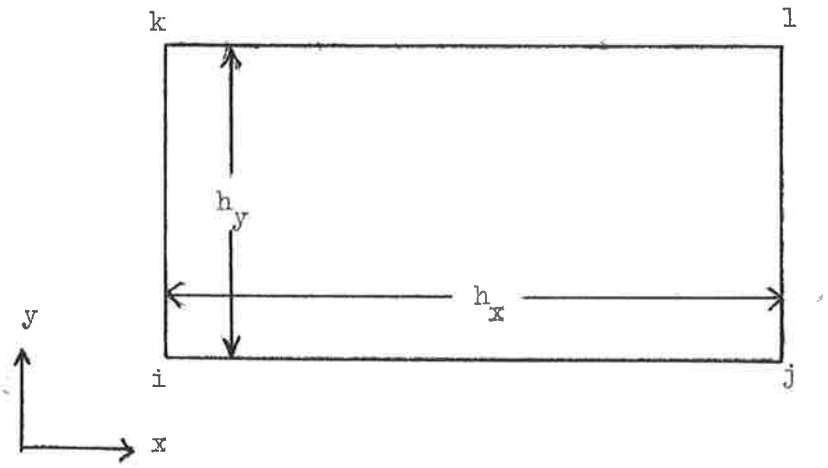

Figure 9.1. Rectangular element with a mesh point at each corner.

Then, inside the rectangle, a set of functions satisfying the requirements given above, is

$$\phi_i(x,y) = \frac{(x-x_j)\,(y-y_k)}{(x_i-x_j)\,(y_i-y_k)} \tag{9.79a}$$

$$\phi_j(x,y) = \frac{(x-x_i)\,(y-y_l)}{(x_j-x_i)\,(y_j-y_l)} \tag{9.79b}$$

$$\phi_k(x,y) = \frac{(x-x_l)\,(y-y_i)}{(x_k-x_l)\,(y_k-y_i)} \tag{9.79c}$$

$$\phi_l(x,y) = \frac{(x-x_k)\,(y-y_j)}{(x_l-x_k)\,(y_l-y_j)} \tag{9.79d}$$

Similarly, if the mesh points at the corners of a triangular element are numbered i, j, k as shown in Fig. 9.2.

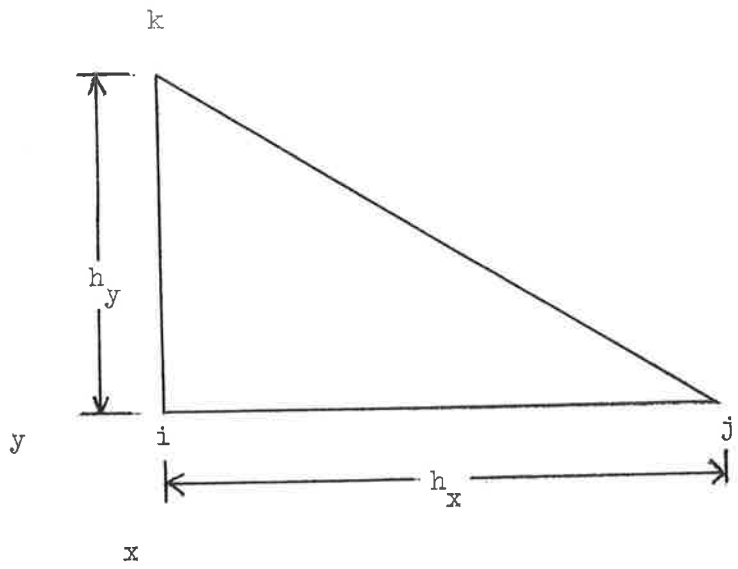

Figure 9.2. Triangular element with a mesh point at each vertex

A set of functions satisfying the above requirements within the triangle is

$$\phi_i(x,y) = 1 - \frac{x-x_i}{x_j-x_i} - \frac{y-y_i}{y_k-y_i} \qquad (9.80a)$$

$$\phi_j(x,y) = \frac{x-x_i}{x_j-x_i} \qquad (9.80b)$$

$$\phi_k(x,y) = \frac{y-y_i}{y_k-y_i} \qquad (9.80c)$$

A similar expansion to (9.78) can be used for the functions $u(x,y)$ and $v(x,y)$. Let β_i and γ_i be the values of $u(x,y)$ and $v(x,y)$ respectively at each mesh point. Then the approximations may be written as

$$u(x,y) = \sum_i \beta_i u_i(x,y) \qquad (9.81)$$

$$v(x,y) = \sum_i \gamma_i v_i(x,y) \qquad (9.82)$$

where

$u_i(x,y)$ and $v_i(x,y)$ are identical with $\phi_i(x,y)$ defined above.

We have assumed that the boundary of the two dimensional region is polygonal and each boundary segment coincides with a side of a rectangular or triangular element. In addition, the potential function $\phi(x,y)$ varies linearly along each side of an element and is defined by the potential values at each mesh point. Thus it is easy to obtain a potential function $\phi(x,y)$ which satisfies Dirichlet

boundary conditions of the form (9.14); we simply constrain the α_i to be zero at mesh points on boundary segments where $\phi(x,y)$ is required to be zero, and on boundary segments where $\phi(x,y)$ is required to be constant, we choose the α_i to be equal. Consequently the matrix elements required for a variational solution are linear combinations surface integrals of the form

$$1_{ij}^{u\phi} = -\iint_R u_i \frac{\partial \phi_j}{\partial x}\, da \tag{9.83}$$

$$1_{ij}^{v\phi} = -\iint_R v_i \frac{\partial \phi_j}{\partial y}\, da \tag{9.84}$$

$$m_{ij}^{gg} = \iint_R g_i\, g_j\, da \tag{9.85}$$

where

$$g_i = \phi_i(x,y),\ u_i(x,y) \quad \text{or} \quad v_i(x,y).$$

The contributions to each of these integrals from a rectangular element can be easily evaluated, and if the mesh points i, j, k, l in Fig. 9.1 are replaced by 1, 2, 3, 4 respectively they may be written in matrix form as

$$\left[1^{u\phi}\right] = \frac{h_y}{12} \begin{bmatrix} 2 & -2 & 1 & -1 \\ 2 & -2 & 1 & -1 \\ 1 & -1 & 2 & -2 \\ 1 & -1 & 2 & -2 \end{bmatrix} \tag{9.86}$$

$$\left[{}_1{}^{v\phi}\right] = \frac{h_x}{12}\begin{bmatrix} 2 & 1 & -2 & -1 \\ 1 & 2 & -1 & -2 \\ 2 & 1 & -2 & -1 \\ 1 & 2 & -1 & -2 \end{bmatrix} \tag{9.87}$$

$$\left[{}_m{}^{\phi\phi}\right] = \frac{h_x h_y}{36}\begin{bmatrix} 4 & 2 & 2 & 1 \\ 2 & 4 & 1 & 2 \\ 2 & 1 & 4 & 2 \\ 1 & 2 & 2 & 4 \end{bmatrix} \tag{9.88}$$

Similarly if the mesh points i, j, k in Fig. 9.2 are replaced by 1, 2, 3 respectively, the elemental matrices for a triangular element are

$$\left[{}_1{}^{u\phi}\right] = \frac{h_y}{6}\begin{bmatrix} 1 & -1 & 0 \\ 1 & -1 & 0 \\ 1 & -1 & 0 \end{bmatrix} \tag{9.89}$$

$$\left[{}_1{}^{v\phi}\right] = \frac{h_x}{6}\begin{bmatrix} 1 & 0 & -1 \\ 1 & 0 & -1 \\ 1 & 0 & -1 \end{bmatrix} \tag{9.90}$$

$$\left[{}_m{}^{\phi\phi}\right] = \frac{h_x h_y}{18}\begin{bmatrix} 2 & 1 & 1 \\ 1 & 2 & 1 \\ 1 & 1 & 2 \end{bmatrix} \tag{9.91}$$

Once the elemental matrices (9.86) - (9.88) or (9.89) - (9.91) have been evaluated for each rectangular or triangular element, the surface integrals (9.83) - (9.85) can then be evaluated.

The only remaining step in the solution is then the solution of a system of linear equations, or an eigenvalue problem.

9.5 Numerical Results

Some numerical results obtained for a number of different problems by using the variational method described in the preceding sections will now be presented. The two-dimensional regions were divided into rectangular and triangular sub-regions, and the potential functions ϕ, u and v were approximated as described in section 4. For each problem considered, the potential function ϕ was constrained to satisfy the required Dirichlet boundary conditions. The approximations for u and v were not constrained to satisfy any boundary conditions in general, since these boundary conditions are "natural" for each of the functionals used. However, for some problems a comparison was made of the results obtained with u and v constrained to satisfy the Neumann boundary conditions, and with no constraints on u and v.

Examples 1 - 3

Zero Frequency Admittance Parameters for Linearly-Tapered Resistance Networks

The network considered is shown in Fig. 9.3; the two-dimensional region was divided into rectangular and triangular sub-regions as shown therein.

Three different approximations to y_{11} $(=y_{22}=-y_{12}=-y_{21})$ were computed for four different mesh sizes.

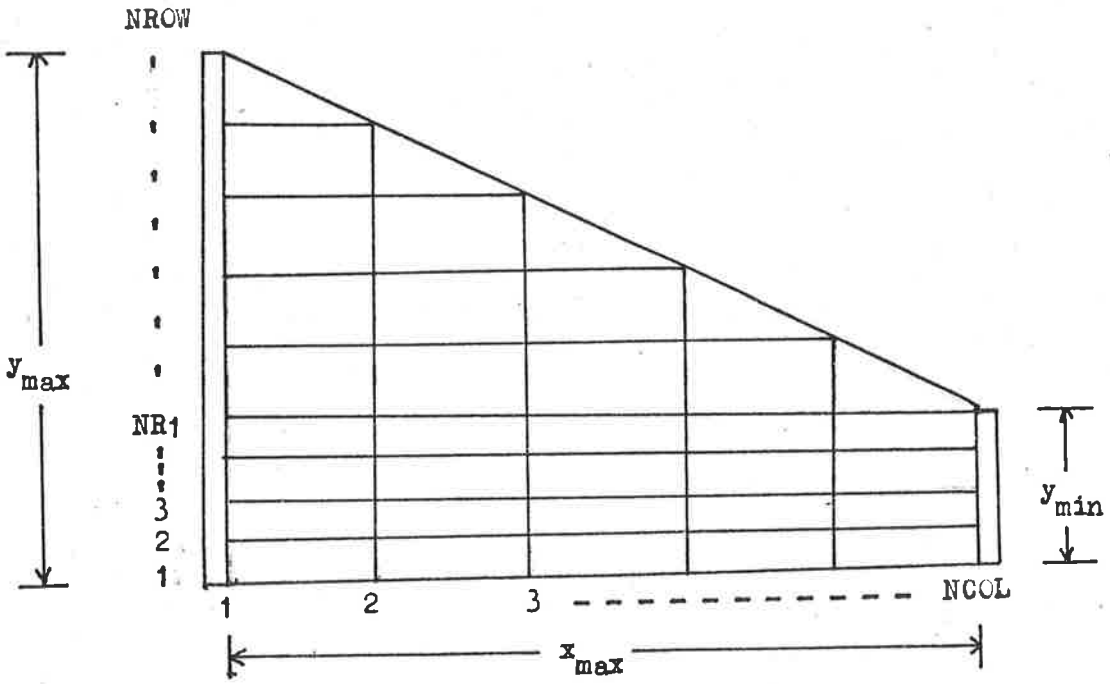

Figure 9.3 Linearly tapered RC line - Subdivision into rectangular and triangular elements.

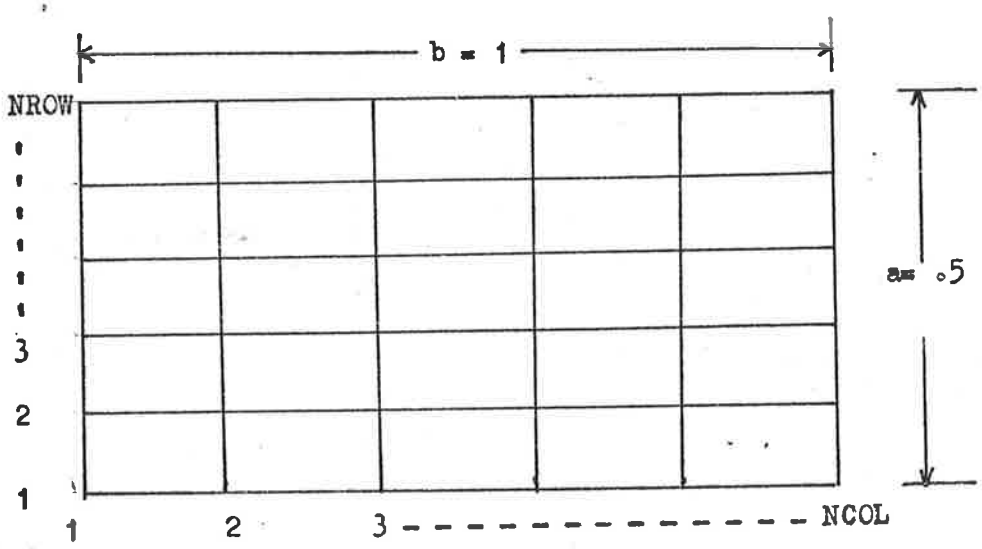

Figure 9.4 Rectangular waveguide - Subdivision into rectangular elements.

The first approximation, $\hat{y}_{11}$, was obtained as the minimum value of the variational expression (9.76). This approximation is an upper bound on the exact solution. The second approximation $\hat{\hat{y}}_{11}$ was obtained by using the potential function ϕ found for $\hat{y}_{11}$ in the variational expression (9.77a), where u and v are related to ϕ by (9.77b), (9.77c). For each of the problems considered $\hat{\hat{y}}_{11}$ was found to be smaller than $\hat{y}_{11}$, but was still greater than the exact value. The third approximation $\hat{\hat{\hat{y}}}_{11}$ was obtained as the stationary value of the functional (9.42). For each of the problems considered, $\hat{\hat{\hat{y}}}_{11}$ was found to be less than $\hat{y}_{11}$ and $\hat{\hat{y}}_{11}$, but greater than the exact values. From the results in Section 9.3 it was conjectured that $\hat{\hat{\hat{y}}}_{11}$ would be less than $\hat{y}_{11}$.

The numerical results and the dimensions of the network for examples 1-3 are shown in Tables 9.1 - 9.3. The number of simultaneous equations solved in each case is shown in the tables as NE. Approximate solutions for examples 1 and 2, with error estimates, were obtained by using polynomial approximations for the potential $\phi(x,y)$. For example 3 an analytical solution is known (32). Comparison of the approximate solutions $\hat{\hat{y}}_{11}$ and $\hat{\hat{\hat{y}}}_{11}$ with the "exact" solutions shows that the error in $\hat{\hat{y}}_{11}$ is about twice as large as the error in $\hat{\hat{\hat{y}}}_{11}$. Thus if the approximations for ϕ, u and v are of the form discussed in Section 9.4, the variational method based on the first-order differential equation is likely to be more accurate than the variational method based on the second-order equation. However the former method generally requires more computation since the coefficient matrix $[A]$ is obtained from the matrix on the left of (9.65) which requires the inverse of the

TABLE 9.1 APPROXIMATE VALUES OF THE DC ADMITTANCE MATRIX ELEMENT, Y11, FOR A LINEARLY TAPERED RC LINE. NCOL, NR1, AND NROW ARE DEFINED IN FIG. 9.3. THE DIMENSIONS ARE - XMAX=1, YMAX=1, AND YMIN=.1 NE = NUMBER OF SIMULTANEOUS EQUATIONS SOLVED. THE EXACT Y11 IS BETWEEN .3275 AND .3297

	NCOL= 4 NR1 = 3 NROW= 6 NE = 9	5 4 8 18	6 4 9 26	7 5 11 40
$\hat{Y}_{11}$	.37177	.35766	.34988	.34502
$\tilde{Y}_{11}$	.36043	.349591	.34351	.33999
$\hat{\hat{Y}}_{11}$	.35707	.346617	.34115	.33809

TABLE 9.2 APPROXIMATE VALUES OF THE DC ADMITTANCE MATRIX ELEMENT, Y11, FOR A LINEARLY TAPERED RC LINE. NCOL, NR1, AND NROW ARE DEFINED IN FIG. 9.3. THE DIMENSIONS ARE - XMAX=1, YMAX=.5, AND YMIN=.2 NE = NUMBER OF SIMULTANEOUS EQUATIONS SOLVED. THE EXACT Y11 IS BETWEEN .3193 AND .3197

	NCOL= 4 NR1 = 3 NROW= 6 NE = 9	5 4 8 18	6 4 9 26
$\hat{Y}_{11}$	.32376	.32202	.32120
$\tilde{Y}_{11}$	.32150	.32060	.32019
$\hat{\hat{Y}}_{11}$	.32116	.32029	.32001

TABLE 9.3 APPROXIMATE VALUES OF THE DC ADMITTANCE MATRIX ELEMENT, Y11, FOR A LINEARLY TAPERED RC LINE. NCOL, NR1, AND NROW ARE DEFINED IN FIG. 9.3. THE DIMENSIONS ARE - XMAX=2, YMAX=3, AND YMIN=1 NE = NUMBER OF SIMULTANEOUS EQUATIONS SOLVED. THE EXACT Y11 IS .776943

	NCOL= 3 NR1 = 2 NROW= 4 NE = 3	5 3 7 15	6 4 9 26
$\hat{Y}_{11}$	.83490	.79719	.79150
$\tilde{Y}_{11}$	.81092	.78820	.78524
$\hat{\hat{Y}}_{11}$	.80537	.78578	.78338

matrices $[m^{uu}]$ and $[m^{vv}]$ as well as a number of matrix products; with the latter variational method, the coefficient matrix $[A]$ is assembled directly from the element matrices for rectangular and triangular subregions.

Example 4

TM and TE Modes in Rectangular Waveguide

The eigenvalues k^2 obtained for the TM modes in a rectangular waveguide with two different mesh sizes are shown in Table 9.4, together with the exact eigenvalues. This problem has also been considered by Harrington (14), p. 166, where the eigenvalues k obtained for the TM_{21} mode are given. The cross-section of the rectangular guide was subdivided into smaller rectangular elements as shown in Fig. 9.4.

The approximate eigenvalues are all found to be lower bounds on the exact solutions for this problem. The approximate eigenvalues obtained by a variational solution of the second-order differential equations are always upper bounds on the exact solutions if the potential function ϕ satisfies the appropriate Dirichlet boundary conditions. In addition, the convergence is significantly faster when the first order equations are used (14) p. 160, p. 166. It should be noted that the exact eigenvalues are arranged in increasing order of magnitude, but the approximate eigenvalues are not. The order of the approximate eigenvalues was obtained from inspection of each eigenfunction to determine which waveguide mode it approximates; we recall that a similar procedure was necessary in the solution of one-dimension eigenvalue problems, Chapter 4.

We now wish to consider the approximate eigenvalues obtained

TABLE 9.4 APPROXIMATE EIGENVALUES CORRESPONDING TO TM MODES IN RECTANGULAR WAVEGUIDE. (B=2A)
THE EXACT EIGENVALUES ARE (M**2+4N**2)*PI**2,
FOR B=1.
M AND N ARE THE MODE NUMBERS.
NCOL AND NROW ARE DEFINED IN FIG. 9.4.

(M,N)	NCOL= 5 NROW= 3	7 4	EXACT
(1,1)	45.825	48.741	49.348
(2,1)	72.0	77.760	78.957
(3,1)	79.073	119.88	128.304
(1,2)		117.86	167.78
(4,1)		146.88	197.39
(2,2)		146.88	197.39
(5,1)		101.87	246.74
(3,2)		189.00	246.74
(4,2)		216.00	315.82
(5,2)		170.99	404.65

TABLE 9.5 EXACT EIGENVALUES CORRESPONDING TO TE MODES IN RECTANGULAR WAVEGUIDE. (B=2A)
THE EXACT EIGENVALUES ARE (M**2+4N**2)*PI**2,
FOR B=1.
M AND N ARE THE MODE NUMBERS
NCOL AND NROW ARE DEFINED IN FIG. 9.4

M \ N	0	1	2	3
0	0.	39.4784	167.78	365.17
1	9.8696	49.348	197.39	394.78
2	39.4784	78.9568	246.74	444.13
3	88.8264	128.304	315.82	
4	157.913	197.392	404.65	
5	246.740	286.218		
6	355.305	394.784		

for TE modes in a rectangular waveguide. The exact eigenvalues, k^2, for this problem are given in Table 9.5 for the first few modes. For TE modes, the exact eigenfunctions satisfy $\frac{d\phi}{dn} = 0$ over the entire boundary. This is equivalent to $n_x u + n_y v = 0$ on the boundary. When the expansions for u and v were constrained to satisfy these boundary conditions, the approximate eigenvalues shown in Table 9.6 were obtained. The first thing we observe is that some of the eigenvalues are simple and the others are of multiplicity two or four. The exact eigenvalues however are generally simple except for a few which are of multiplicity two. A comparison of the approximate and exact eigenvalues indicates that if the multiple eigenvalues are considered to be simple, then the approximate eigenvalues are all less than the exact solutions, i.e. they are lower bounds. It is difficult to determine which modes should be identified with the eigenfunctions corresponding to multiple eigenvalues since the eigenfunctions are not unique. i.e. if $\phi_1(x,y)$ and $\phi_2(x,y)$ are eigenfunctions corresponding to the same eigenvalue, then $a\,\phi_1(x,y) + b\,\phi_2(x,y)$ is also an eigenfunction.

If the expansion functions for u and v are not constrained to satisfy the condition $n_x u + n_y v = 0$ on the boundary C, the approximate eigenvalues shown in Table 9.7 are obtained. We recall that the boundary condition $n_x u + n_y v = 0$ on C is a "natural" condition for stationarity of the functional $J_3(f,f^a)$. Thus, in general, the eigenfunctions obtained by the variational method will approximately satisfy this boundary condition, although we must expect that there will be some "extraneous" eigenfunctions which will not (14) p. 148. The approximate eigenvalues in each line of Table 9.7 are arranged so that the approximate eigenfunction has the

TABLE 9.6 APPROXIMATE EIGENVALUES CORRESPONDING TO TE MODES IN RECTANGULAR WAVEGUIDE. (B=2A)
B=1
NROW AND NCOL ARE DEFINED IN FIG. 9.4.
(U AND V CONSTRAINED TO SATISFY THE NEUMANN BOUNDARY CONDITIONS).

N	NCOL= 5 NROW= 3	7 4
1	0.	0.
2	0.	0.
3	0.	0.
4	0.	0.
5	9.82475	9.8610
6	9.82475	9.8610
7	36.0	38.879
8	36.0	38.879
9	36.0	38.879
10	36.0	38.879
11	43.0731	48.741
12	43.0731	62.990
13	45.8247	62.990
14	72.0	77.759
15	79.0731	81.0
16		81.0

TABLE 9.7 APPROXIMATE EIGENVALUES CORRESPONDING TO TE MODES IN RECTANGULAR WAVEGUIDE. (B=2A)
B=1
NROW AND NCOL ARE DEFINED IN FIG. 9.4.
(U AND V NOT CONSTRAINED TO SATISFY THE NEUMANN BOUNDARY CONDITIONS).

N	NCOL= 5 NROW= 3	EXACT	NCOL= 7 NROW= 4	EXACT
1	0.	0.	0.	0.
2	9.8919	9.8696	9.8732	9.8696
3	32.622	39.4784	38.279	39.4784
4	48.000	39.4784	38.513	39.4784
5	57.892	49.348	48.386	49.348
6	80.622	78.9568	64.80	EXTRANEOUS
7	99.	88.8264	76.792	78.9568
8			79.995	88.8264
9			103.31	EXTRANEOUS
10			118.51	128.304

same form as the mode corresponding to the exact eigenvalue.

Compared with the previous results, we see that there are no multiple eigenvalues in Table 9.7, and at least for the dominant TE modes it is easy to identify the mode corresponding to an approximate eigenfunction. In addition, we obtain some extraneous eigenvalues, but these are easily identified because their eigenfunctions do not approximately satisfy the boundary conditions.

Example 5

TM modes in Right Angled Isosceles Triangle

For this problem an exact analytical solution is known (2), p. 755-756.

Approximate solutions for the first few eigenvalues were obtained by subdividing the triangle into rectangular and triangular sub-regions as shown in Fig. 9.5. The approximate eigenvalues obtained with several different mesh sizes are shown in Table 9.8 together with the exact eigenvalues. The approximate solutions are all less than the exact solutions i.e. lower bounds; this was also found to be so for the TM modes in rectangular waveguide.

Example 6

TM and TE Modes in Ridge Waveguide

The cross-section considered is shown in Fig. 9.6; since the ridge-waveguide is symmetrical we only need to consider one half of the cross-section with the boundary condition $\phi = 0$ on the centre line for those modes with odd symmetry, and $\frac{d\phi}{dn} = 0$ on the centre line for modes with even symmetry.

The approximate eigenvalues obtained for the TM modes with odd symmetry about the centre line are shown in Table 9.9 for two different mesh sizes; the approximation to $\phi(x,y)$ was constrained

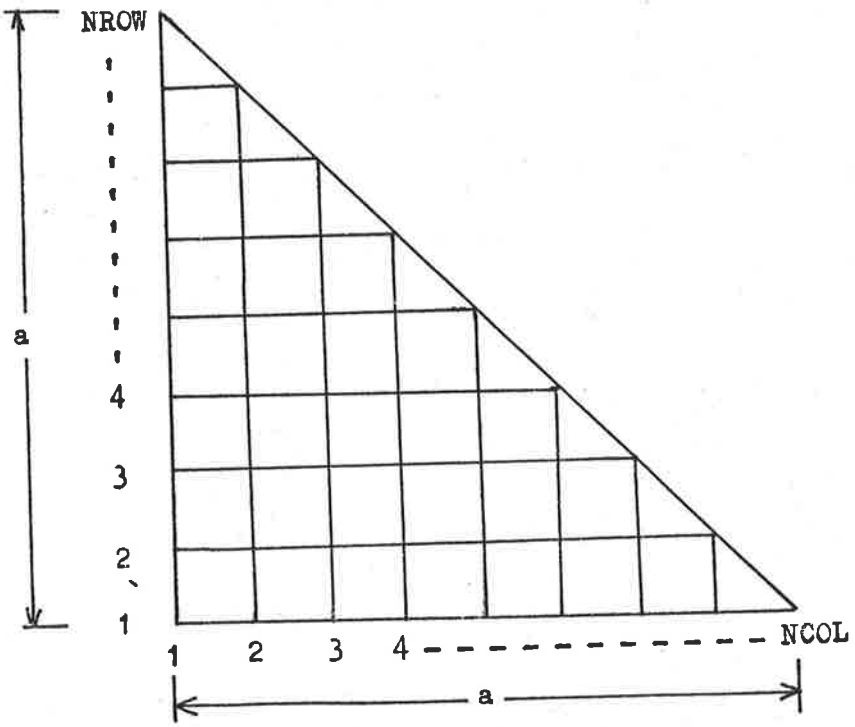

Figure 9.5 Right - angled isosceles triangle - Subdivision into rectangular and triangular elements.

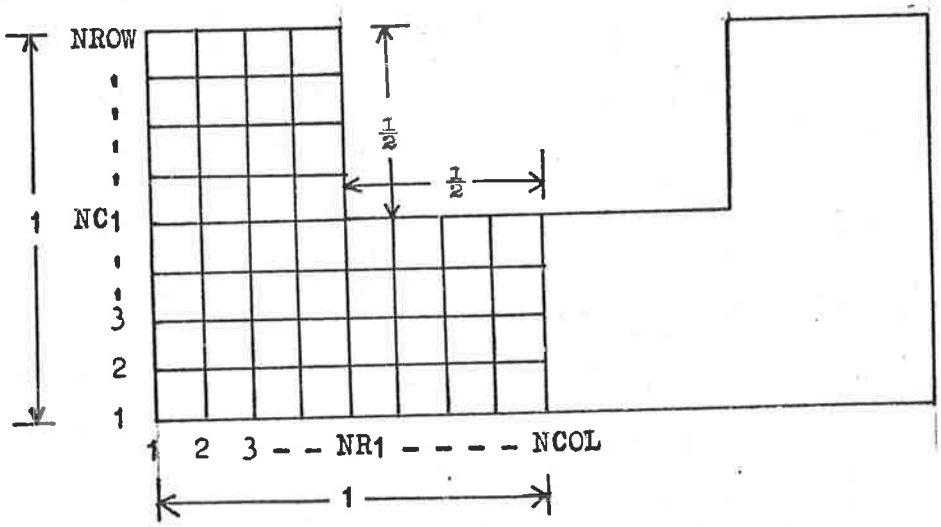

Figure 9.6 Ridge waveguide - Subdivision into rectangular elements.

TABLE 9.8 APPROXIMATE EIGENVALUES CORRESPONDING TO TM MODES IN A RIGHT-ANGLE ISOSCELES TRIANGLE. NROW AND NCOL ARE DEFINED IN FIG. 9.5, WHERE A=1.

N	NCOL= 4 NROW= 4	6 6	8 8	• EXACT
1	41.383	48.096	49.039	49.348
2		81.705	94.820	98.696
3		112.5	124.28	128.304
4			142.74	167.783
5		115.11	176.32	197.392
6		142.65	220.46	246.74

TABLE 9.9 APPROXIMATE EIGENVALUES CORRESPONDING TO TM MODES IN RIDGE WAVEGUIDE WITH ODD SYMMETRY ABOUT THE PLANE OF SYMMETRY. NCOL, NC1, NROW, NR1, AND THE DIMENSIONS ARE AS SHOWN IN FIG. 9.6.

N	NCOL= 5 NC1 = 3 NROW= 5 NR1 = 3	7 4 7 4
1	35.681	37.606
2	52.739	59.443
3	72.000	77.760
4	74.757	93.865
5	76.386	95.171
6		109.16

TABLE 9.10 APPROXIMATE EIGENVALUES CORRESPONDING TO TE MODES IN RIDGE WAVEGUIDE WITH EVEN SYMMETRY ABOUT THE PLANE OF SYMMETRY. NCOL, NC1, NROW, NR1, AND THE DIMENSIONS ARE AS SHOWN IN FIG. 9.6. (U AND V NOT CONSTRAINED TO SATISFY THE NEUMANN BOUNDARY CONDITIONS)

N	NCOL= 3 NC1 = 2 NROW= 3 NR1 = 2	5 3 5 3	7 4 7 4	9 5 9 5
1	0.	0.	0.	0.
2	7.7313	5.8984	5.9162	5.8909
3	16.917	14.164	14.125	14.132
4	37.232	33.767	38.357	39.284
5	38.433	35.964	38.357	39.322
6	53.121	52.048	44.583	45.470
7	60.335	56.458	48.425	50.192
8	76.230	70.981	65.818	75.464

to be zero over the entire boundary. Although the exact eigenvalues are not known for this problem it appears that the approximate eigenvalues are less than the exact solutions since they all increase as the mesh size becomes smaller. Thus the results of all problems solved so far suggest that the approximate eigenvalues obtained for TM modes by variational solutions of the first-order differential equations are almost certainly lower bounds on the exact eigenvalues; for each of the problems considered the approximate potential function was constrained to be zero over the boundary of the region.

The approximate eigenvalues obtained for TE modes in the ridge waveguide with even symmetry about the centre line are shown in Table 9.10. The approximations for $\phi(x,y)$, $u(x,y)$ and $v(x,y)$ were not constrained to satisfy any boundary conditions. The results obtained for this problem by Bulley and Davies (10) are shown in Table 9.11 together with the results obtained from the finite-element program described in (55); the approximate eigenvalues obtained by these two methods are greater than or equal to the exact eigenvalues i.e. upper bounds. Inspection of the approximate eigenvalues obtained by the present method shows that some of the approximate eigenvalues appear to be upper bounds which converge monotonically to the exact eigenvalues as the mesh size decreases.

The remaining approximate eigenvalues appear to be converging to the exact eigenvalues in an oscillatory manner i.e. the successive approximations do not decrease monotonically with the mesh size.

The approximate eigenvalues for TE modes in the ridge waveguide with odd symmetry about the centre line are shown in Table 9.12

TABLE 9.11 APPROXIMATE EIGENVALUES CORRESPONDING TO TE MODES IN RIDGE WAVEGUIDE WITH EVEN SYMMETRY ABOUT THE PLANE OF SYMMETRY.

N	(A) FROM BULLEY REF.(53).	(B) FROM SILVESTER'S FINITE-ELEMENT PROGRAM (6 TRIANGLES WITH 4TH ORDER POLYNOMIALS)
1	0.	0.
2	6.0641	5.95056
3	14.156	14.1382
4	39.479	39.4906
5	39.480	39.4961
6		45.6110
7		50.4358
8		79.0882

TABLE 9.12 APPROXIMATE EIGENVALUES CORRESPONDING TO TE MODES IN RIDGE WAVEGUIDE WITH ODD SYMMETRY ABOUT THE PLANE OF SYMMETRY.
NCOL, NC1, NROW, NR1, AND THE DIMENSIONS ARE AS SHOWN IN FIG. 9.6.
(U AND V NOT CONSTRAINED TO SATISFY THE NEUMANN BOUNDARY CONDITIONS)

	NCOL= 3 NC1 = 2 NROW= 3	5 3 5	7 4 7	9 5 9
N	NR1 = 2	3	4	5
1	1.3047	1.2675	1.2648	1.2642
2	12.775	10.407	10.425	10.409
3	28.895	23.979	23.993	24.125
4	38.067	34.916	39.628	40.565
5	54.566	41.683	43.655	44.762
6	70.163	53.939	58.468	59.978
7		66.514	62.511	65.635
8		79.167	65.905	75.552

TABLE 9.13 APPROXIMATE EIGENVALUES CORRESPONDING TO TE MODES IN RIDGE WAVEGUIDE WITH ODD SYMMETRY ABOUT THE PLANE OF SYMMETRY.

N	(A) FROM BULLEY REF.(53).	(B) FROM SILVESTER'S FINITE-ELEMENT PROGRAM (6 TRIANGLES WITH 4TH ORDER POLYNOMIALS)
1	1.2799	1.27026
2	10.520	10.4517
3	24.249	24.1713
4	40.837	40.8456
5		44.8429
6		61.0171
7		66.3792
8		87.6002

DAVIES AND MUILWICK (90) OBTAINED A VALUE OF 1.2648 FOR THE LOWEST EIGENVALUE BY USING A FINITE-DIFFERENCE PROGRAM

together with the results obtained by Bulley and Davies (10) and Silvester's program (55). Since the approximate potential function $\phi(x,y)$ was constrained to satisfy the Dirichlet boundary condition $\phi(x,y) = 0$ on the centre line the eigenvalues obtained by the latter two methods must be upper bounds on the exact eigenvalues. As with the previous example, some of the approximate eigenvalues obtained by the present method appear to be upper bounds which converge monotonically to the exact solution, while the remaining solutions appear to be converging in an oscillatory manner. The approximations for $u(x,y)$ and $v(x,y)$ were not constrained to satisfy any boundary conditions for these computations.

In addition to the results just presented, an attempt was made to obtain solutions for the TE modes in ridge waveguide with the approximations for $u(x,y)$ and $v(x,y)$ constrained to satisfy the appropriate boundary conditions. It was found that none of the eigenfunctions appeared to satisfy the required Neumann boundary conditions, and the eigenvalues differed significantly from those found previously. An explanation of this behaviour will be presented later.

Example 7

Poles and Zeros of Admittance Parameters for Uniform RC Line

The results obtained for the poles and zeros of the admittance parameters of two distributed RC lines will now be presented. The first example to be considered is a uniform RC line of width 0.5 units and length 1 unit, with the input/output ports on the two narrow edges; the exact solutions for this problem were given in Chapter 8.

The results obtained by variational solution of the first-order differential equations are given in Tables 9.14 and 9.15. The rectangular region was subdivided into smaller rectangles and the approximations for $\phi(x,y)$, $u(x,y)$ and $v(x,y)$ were of the form given in Section 9.4. For both sets of results, $\phi(x,y)$ was constrained to satisfy the appropriate Dirichlet boundary conditions. In addition, the results in Table 9.14 were obtained with no constraints on the approximations $u(x,y)$ and $v(x,y)$ while the results in Table 9.15 were obtained with the Neumann boundary condition, $n_x u + n_y v = 0$, satisfied on the two longer sides of the rectangle. The smaller eigenvalues in Table 9.14, are seen to be approximately equal to the exact eigenvalues, and the errors become smaller as the mesh size decreases. In addition, most of the smaller eigenvalues are less than the exact eigenvalues i.e. lower bounds. The results in Table 9.15 where $n_x u + n_y v$ was constrained to satisfy the Neumann boundary condition, contain a number of smaller eigenvalues which do not converge to any of the eigenvalues obtained from an exact solution; in addition, the eigenfunctions $\phi(x,y)$ corresponding to these extraneous solutions do not approximately satisfy the required Neumann boundary conditions. In both Table 9.14 and Table 9.15 there are a number of poles of $[Y]$ and zeros of y_{11} which exactly cancel one another. The remaining poles and zeros in Table 9.14 are seen to coincide exactly with those in Table 9.15, and in addition, these eigenvalues are seen to correspond to the one-dimensional solutions whose eigenfunctions have no variations with position along co-ordinate lines which are parallel to the input/output ports.

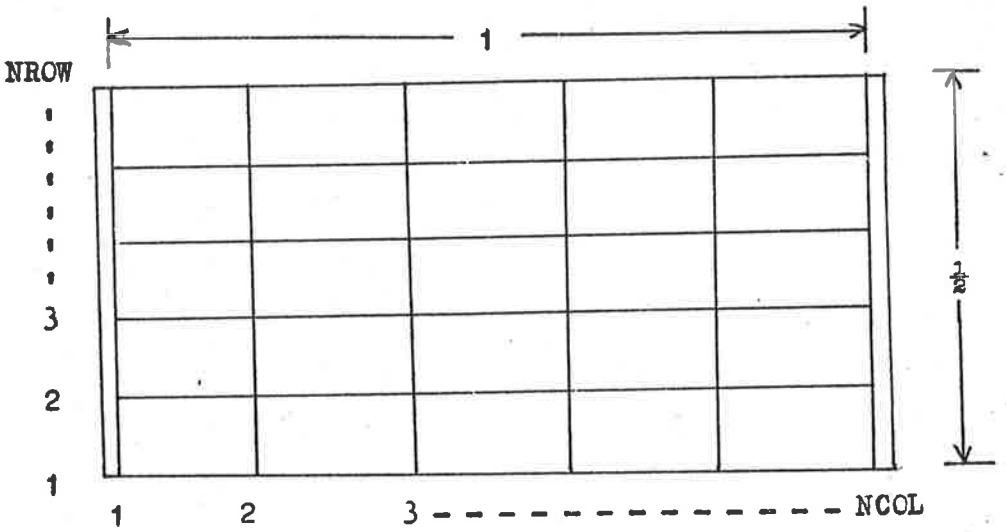

Figure 9.7 Uniform RC line - Subdivision into rectangular elements

TABLE 9.14 APPROXIMATE EIGENVALUES CORRESPONDING TO THE POLES AND ZEROS OF THE ADMITTANCE MATRIX ELEMENT Y11 FOR A UNIFORM RC LINE.
NCOL, NROW, AND THE DIMENSIONS ARE AS SHOWN IN FIG. 9.7.
(U AND V NOT CONSTRAINED TO SATISFY NEUMANN BOUNDARY CONDITIONS)
THE POLES AND ZEROS, S_i, ARE RELATED TO THE EIGENVALUES, k_i^2, BY EQUATION (9.16)

	POLES OF ADMITTANCE MATRIX		ZEROS OF Y11	
N	NCOL= 5 NROW= 3	7 4	5 3	7 4
1	9.82475	9.86109	2.4676	2.4675
2	36.0000	38.8800	21.6151	22.1033
3	43.0731	48.3740	41.4275	48.3740
4	57.8247	62.9909	57.8247	57.0937
5	84.0000	77.3929	84.0	65.7826
6	91.0731	81.0000	91.0731	77.3929
7	153.824	101.503	95.5264	99.2115
8	180.000	108.000	153.824	101.503
9	187.073	119.512	180.0	119.512
10		146.512	187.073	146.512
11		204.261		204.261
12		233.279		216.077
13		252.148		233.279
14		257.390		252.148
15		275.400		257.390
15				275.4

TABLE 9.15 APPROXIMATE EIGENVALUES CORRESPONDING TO THE POLES AND ZEROS OF THE ADMITTANCE MATRIX ELEMENT Y11 FOR A UNIFORM RC LINE.
NCOL, NROW, AND THE DIMENSIONS ARE AS SHOWN IN FIG. 9.7.
(U AND V CONSTRAINED TO SATISFY NEUMANN BOUNDARY CONDITIONS)
THE POLES AND ZEROS, S_i, ARE RELATED TO THE EIGENVALUES, k_i^2, BY EQUATION (9.)

	POLES OF ADMITTANCE MATRIX		ZEROS OF Y11	
N	NCOL= 5 NROW= 3	7 4	5 3	7 4
1	9.82475	9.86108	2.46766	2.46744
2	9.82475	9.86108	9.82475	9.86108
3	36.0	38.88	21.6151	22.1033
4	36.0	38.88	36.0	38.88
5	43.0731	48.7410	41.4275	48.7410
6	43.0731	62.9909	43.0731	57.0937
7	45.8247	62.9909	45.8247	62.9909
8	72.0	77.76	72.0	65.7826
9	79.0731	81.0	79.0731	77.76
10		81.0	95.5264	81.0
11		101.870		99.2115
12		108.0		101.870
13		117.861		108.0
14		119.88		117.861
15				119.88

TABLE 9.16 APPROXIMATE EIGENVALUES CORRESPONDING TO THE POLES OF THE ADMITTANCE MATRIX FOR A LINEARLY TAPERED RC LINE.
NCOL, NR1, NROW, AND THE DIMENSIONS ARE AS SHOWN (U AND V NOT CONSTRAINED TO SATISFY NEUMANN BOUNDARY CONDITIONS)
THE POLES AND ZEROS, S_i, ARE RELATED TO THE EIGENVALUES, k_i^2, BY EQUATION (9.16)

N	NCOL= 4 NR1 = 3 NROW= 6	5 4 8	6 4 9	7 5 11
1	8.39292	8.18886	8.07640	8.01810
2	29.2423	30.6590	30.9835	30.9226
3	40.7034	43.6034	44.5295	44.7211
4	74.4462	50.3457	62.7207	66.0839
5	118.676	67.0780	65.6938	75.4483
6	266.591	89.8142	81.3580	86.7408
7	319.686	105.583	96.0426	102.026
8	2166.48	154.550	104.954	111.763
9	2191.06	213.118	109.018	120.973
10	.	352.199	142.789	122.807

TABLE 9.17 APPROXIMATE EIGENVALUES CORRESPONDING TO THE ZEROS OF THE ADMITTANCE MATRIX ELEMENT Y11 FOR A LINEARLY TAPERED RC LINE.
IN FIG. 9.3.
(U AND V NOT CONSTRAINED TO SATISFY NEUMANN BOUNDARY CONDITIONS)
THE POLES AND ZEROS, S_i, ARE RELATED TO THE EIGENVALUES, k_i^2, BY EQUATION (9.)

N	NCOL= 4 NR1 = 3 NROW= 6	5 4 8	6 4 9	7 5 11
1	.946439	.893344	.870666	.856780
2	17.4620	17.3936	17.0505	16.9423
3	40.5974	40.4427	42.3394	42.6185
4	56.8437	45.6286	48.5355	48.7876
5	81.3860	63.9118	63.7300	74.6852
6	118.639	85.1139	81.1706	82.5053
7	266.606	96.1599	91.1755	90.4539
8	319.791	121.962	104.085	111.558
9	2166.48	155.256	107.192	119.437
10	2191.06	213.144	130.776	122.802

TABLE 9.18 APPROXIMATE EIGENVALUES CORRESPONDING TO THE ZEROS OF THE ADMITTANCE MATRIX ELEMENT Y22 FOR A LINEARLY TAPERED RC LINE.
IN FIG. 9.3.
(U AND V NOT CONSTRAINED TO SATISFY NEUMANN BOUNDARY CONDITIONS)
THE POLES AND ZEROS, S_i, ARE RELATED TO THE EIGENVALUES, k_i^2, BY EQUATION (9.16)

N	NCOL= 4 NR1 = 3 NROW= 6	5 4 8	6 4 9	7 5 11
1	4.26144	4.24441	4.23721	4.23494
2	21.8692	22.1006	22.2128	22.2299
3	40.3738	40.6793	40.8742	40.8550
4	46.8586	46.8266	54.5874	56.8306
5	84.3863	66.7335	65.6549	74.4402
6	125.976	75.4993	75.2706	78.8257
7	266.591	91.5494	94.8336	97.8238
8	319.710	116.594	104.260	110.521
9	2166.51	171.050	107.330	114.616
10	2191.27	216.281	117.714	122.629

TABLE 9.19 APPROXIMATE EIGENVALUES CORRESPONDING TO THE ZEROS OF THE ADMITTANCE MATRIX ELEMENT Y12 FOR A LINEARLY TAPERED RC LINE.
IN FIG. 9.3.
(U AND V NOT CONSTRAINED TO SATISFY NEUMANN BOUNDARY CONDITIONS)
THE POLES AND ZEROS, S_i, ARE RELATED TO THE EIGENVALUES, k_i^2, BY EQUATION (9.)

N	NCOL=4 NR1=3 NROW=6		NCOL=5 NR1=4 NROW=8	
	REAL	IMAGINARY	REAL	IMAGINARY
1	-20.4639		-21.2515	24.3632
2	40.8720		-21.2515	-24.3632
3	17.4594	41.7500	42.2401	
4	17.4594	-41.7500	64.8467	
5	110.098		59.8818	26.1574
6	139.892		59.8818	-26.1574
7	266.537		92.9139	
8	318.084		180.904	
9	2166.39		232.481	
10	2190.45		350.630	

N	NCOL=6 NR1=4 NROW=9		NCOL=7 NR1=5 NROW=11	
	REAL	IMAGINARY	REAL	IMAGINARY
1	-34.4514		42.8299	
2	42.6484		-33.4763	32.2283
3	-.283409	56.4267	-33.4763	-32.2283
4	-.284309	-56.4267	74.6344	
5	65.1968		82.7480	
6	78.2449		55.5649	78.6999
7	97.6711	10.6243	55.5649	-78.6999
8	97.6711	-10.6243	110.687	
9	105.670		116.195	
10	118.596		122.824	

Example 8

Poles and Zeros of Admittance Parameters for Linearly Tapered RC line

The distributed RC network considered is identical with that in Example 1 , and the same subdivision into rectangular and triangular elements is used. The poles and zeros obtained are shown in Tables 9.16 - 9.19; the potential function $\phi(x,y)$ was constrained to satisfy the Dirichlet boundary conditions of the problem, but the approximations for $u(x,y)$ and $v(x,y)$ were not constrained to satisfy any boundary conditions. This problem was also considered previously in Chapter 8, where variational solutions of the second-order differential equation were obtained with polynomial and piecewise polynomial approximations for $\phi(x,y)$. A comparison of the results obtained by the two variational methods shows that the smaller, (i.e. dominant), eigenvalues are generally in close agreement; the main differences are in the complex and negative eigenvalues obtained for the zeros of $y_{12} = y_{21}$.

9.6 Conclusion

The functionals considered in this chapter have for their stationary conditions the first-order partial differential equations (9.2) which are equivalent to the second-order partial differential equation (9.1). Approximate solutions of the stationary problem may be obtained by the Rayleigh-Ritz method which leads to a system of linear equations or a matrix eigenvalue problem. It should be noted that the solutions obtained by the Rayleigh-Ritz method are identical with those obtained by the Moment method described in (14), Chapter 8, section 8.5 - 8.7; although the derivation given in (14) is concerned mainly with

self-adjoint problems, it can also be extended to non self-adjoint problems.

It has been shown how solutions may be obtained if the region is divided into rectangular and triangular subregions, and the potential function in each subregion is approximated by a linear function as discussed in Section 9.4. Clearly this method could be extended to handle curved boundaries, and more accurate solutions could be obtained by using more complicated expansion functions such as polynomials.

The numerical results obtained show that the variation method discussed in this chapter generally gives more accurate solutions than the variation method based on the second-order differential equation; any such comparisons are done with the same expansion functions for the potential functions in both methods. The reason for the improved accuracy with the former method is that the derivatives of the potential function are approximated more accurately. However, a computer program based on the former method is likely to be more complicated, and generally takes more time to execute than the latter method. It should be noted that the two methods are identical if the approximations for $u(x,y)$ and $v(x,y)$ are proportional to $\frac{\partial \phi(x,y)}{\partial x}$ and $\frac{\partial \phi(x,y)}{\partial y}$ respectively. This would be so if $\phi(x,y)$, $u(x,y)$ and $v(x,y)$ were chosen to be polynomials of order n in the two variables x and y over the entire region R.

One difficulty encountered with the present method is the occurrence of extraneous eigenvalues which are comparable in magnitude with the dominant eigenvalues. These extraneous solutions were obtained only when the approximations for $u(x,y)$ and $v(x,y)$ were constrained to satisfy the Neumann boundary conditions, and

the approximation for $\phi(x,y)$ was constrained to satisfy only the Dirichlet boundary conditions of our problem. In addition, it was found that these extraneous solutions $\phi(x,y)$ do not approximately satisfy the Neumann boundary condition $\frac{d\phi}{dn} = 0$.

When solutions were obtained with no constraints on the approximations for $u(x,y)$ and $v(x,y)$ but $\phi(x,y)$ was constrained to satisfy only the Dirichlet boundary conditions, it was found that extraneous solutions still occurred, (i.e. they do not approximately satisfy the Neumann boundary conditions), but the eigenvalues were generally much larger in magnitude than the dominant eigenvalues.

The reason for the difficulties mentioned above is believed to be due to the fact that it is inconsistent to constrain the approximations for $u(x,y)$ and $v(x,y)$ to satisfy Neumann boundary conditions $n_x u + n_y v = 0$, without imposing corresponding constraints on the approximation for $\phi(x,y)$. This follows since the <u>exact</u> solutions for $u(x,y)$ and $v(x,y)$ are proportional to $\frac{\partial\phi}{\partial x}$ and $\frac{\partial\phi}{\partial y}$ respectively. Thus the exact solutions $u(x,y)$ and $v(x,y)$ are dependent on $\phi(x,y)$. In addition, the coefficients of the approximate solutions $u(x,y)$ and $v(x,y)$ are related to those of $\phi(x,y)$ by a pair of equations of the form (9.53), (9.54). These equations show that if the approximate $\phi(x,y)$ is constrained to satisfy boundary conditions of the form $\frac{d\phi}{dn} = 0$, then the corresponding $u(x,y)$ and $v(x,y)$ will approximately satisfy $n_x u + n_y v = 0$ on the same boundary segment. However, if $n_x u + n_y v = 0$ on part of the boundary, there must be certain constraints on the coefficients β and γ. Thus (9.53), (9.54), cannot be satisfied unless corresponding constraints are imposed on the coefficients, α, of $\phi(x,y)$.

It is therefore considered that in the practical application of the Variational method considered here, the boundary condition $n_x u + n_y v = 0$ should be left as a natural condition, and the potential function $\phi(x,y)$ should be constrained to satisfy $\frac{d\phi}{dn} = 0$ on the Neumann boundaries, or this should be also left as a natural condition.

Chapter 10

REFORMULATION OF THE PARTIAL DIFFERENTIAL EQUATION AS AN INTEGRAL EQUATION

10.1 Introduction

In this Chapter we will consider a numerical technique for solving distributed RC networks which is based on the transformation of the partial differential equation

$$\nabla^2 \phi = \gamma^2 \phi \qquad (10.1)$$

where

$$\gamma^2 = p R_s C \qquad (10.2)$$

to an integral equation. ϕ is the potential in the resistive layer, p is the complex frequency variable, R_s is the sheet resistance of the resistive layer, and C is the capacitance per unit area between the resistive layer and the ground plane.

The transformation of (10.1) to an integral equation is accomplished by using Green's boundary value formula as described in (27) and (29). Some numerical techniques for obtaining approximate solutions of the integral equation are described in detail in (29), and the special case with p = 0 in (10.1), (10.2) (i.e. Laplace's equation) is considered in (26), (30), (31) and (65).

Although a method for obtaining approximate values of the admittance matrix elements at any desired frequency is described in detail in (29), numerical results are only given for the zero frequency case, (p = 0). In this Chapter some numerical results

obtained by the method described in (29) are presented for the zero frequency case, and also for frequencies on the $j\omega$ axis in the complex frequency plane.

In addition, we will also consider the application of the method to calculation of the poles and zeros of the admittance parameters. Spielman (90) has used a similar method for calculation of TE or TM modes in waveguides of arbitrary cross-section, but application of the integral equation method to the calculation of poles and zeros of the admittance parameters does not appear to have been considered previously. Some numerical results obtained by this method are presented in this Chapter.

One problem which arises in connection with the practical application of the method described in (29) is that loss of accuracy can occur when the calculations are performed on a finite precision computer. There are essentially two steps at which errors can occur. The first is in the evaluation of the various integrals which are required. If analytical solutions are used, the results may be inaccurate because it is necessary to subtract two quantities which are almost equal. Methods of improving the accuracy of the integration by using quadrature formulae are discussed in this Chapter. The second source of errors is in the solution of the system of linear equations for the coefficients of the polynomial approximations to the unknown functions. It is shown here that these errors can be reduced substantially by using orthogonal polynomials to approximate the unknown functions.

Most of the previous methods for solving the integral equation have been restricted to two-dimensional regions where the boundary is assumed to be polygonal. Although curved boundary

segments can often by approximated by a number of linear segments it is desirable to have a method which can solve such problems directly. In this Chapter we will consider in some detail, methods for solving problems where the boundary includes circles or arcs of circles. Problems containing circular boundaries are often encountered in practice in connection with the solution of Laplace's equation for lossless transmission lines. In addition, other boundary shapes can be approximated by circular arcs and straight lines.

The method of solution to be described is useful for problems where the boundary conditions on the contour C which bounds the two-dimensional region R are of the general form

$$\alpha(l)\phi + \beta(l)\frac{\partial \phi}{\partial n} = \gamma(l) \qquad (10.3)$$

where

α, β and γ are given functions of l, the distance along C from some reference point. The general form (10.3) includes the following special cases:

(a) Dirichlet Boundary conditions, with ϕ specified on C ($\alpha = 1, \beta = 0$)

(b) Neumann Boundary conditions with $\frac{\partial \phi}{\partial n}$ specified on C ($\alpha = 0, \beta = 1$)

(c) Impedance boundary conditions with $\phi/\frac{\partial \phi}{\partial n}$ specified on C ($\alpha = 1, \gamma = 0$).

For distributed RC networks the boundary conditions are "mixed" i.e. over a portion of C we will have ϕ specified, and over the remainder, $\frac{\partial \phi}{\partial n}$ will be specified.

On each of the boundary segments correspond to a metal

contact we have ϕ equal to some constant, and on the remaining boundary segments, $\frac{\partial \phi}{\partial n}$ is zero since no current can flow out of the resistive region on these segments.

If the boundary segments corresponding to the metal contacts are denoted by C_1, C_2, C_3 --- C_N, and the potential has a value V_k on the kth metal contact and is zero on all other metal contacts, the admittance parameters are given by

$$y_{jk} = \frac{1}{V_k R_s} \oint_{C_j} \frac{\partial \phi}{\partial n} \, dl \qquad (10.4)$$

for $j = 1, 2 --- N$.

The poles of the admittance parameters are the frequencies such that y_{jk} goes to infinity, while the zeros of y_{jk} are the frequencies such that y_{jk} is zero.

The method of solution is to transform the partial differential equation (10.1) into an integral equation, i.e. the potential at any point is expressed as a contour integral involving the potential and its normal derivative on the boundary. On the metal contacts, ϕ is known (specified), and $\frac{\partial \phi}{\partial n}$ is to be determined. On insulating boundary segments $\frac{\partial \phi}{\partial n}$ is zero, and ϕ is to be determined.

Approximate solutions for the unknown boundary values of ϕ and $\frac{\partial \phi}{\partial n}$ can be obtained by the general method of Moments (14), which is equivalent to the point matching (collocation) method (29). The integral equation is thus reduced to the matrix form

$$\left[A \right] \left[c \right] = \left[b \right] \qquad (10.5)$$

where

$[A]$ is the coefficient matrix

$b]$ is a vector which depends on the specified potentials on metal contacts

and $c]$ is the vector of coefficients of the series expansions for the boundary values of ϕ and $\frac{\partial \phi}{\partial n}$.

The coefficient matrix $[A]$ depends on the complex frequency variable p, so that it must be calculated for each frequency at which the admittance parameters are to be evaluated. The admittance parameters are then obtained by substituting the solutions of (10.5) into (10.4). Alternatively the poles and zeros of the admittance parameters may be obtained as the frequencies such that y_{jk} defined by (10.4) tends to infinity or zero. If $[A]$ in (10.5) is a square matrix, the poles of y_{jk} are the frequencies such that

$$\det [A] = 0 \tag{10.6}$$

where the expression on the left side of (10.6) denotes the determinant of $[A]$. In general, the poles and zeros are found by evaluating det $[A]$ and/or y_{jk} at a number of different frequencies, and then by using an interpolation or extrapolation formula, the desired poles and zeros may be obtained.

10.2 Integral Equation Formulation

The derivation of the integral equation from the partial differential equation is given in (27) and (29). The result is

$$\sigma(x',y')\,\phi(x',y') = \oint_C \left[G(\gamma r) \frac{\partial \phi(x,y)}{\partial n} - \phi(x,y) \frac{\partial G(\gamma r)}{\partial n} \right] dl \tag{10.7}$$

where

$$r^2 = (x-x')^2 + (y-y')^2 \tag{10.8}$$

$$\begin{aligned} \sigma(x',y') &= 2\pi && \text{for } (x',y') \text{ inside } R \\ &= \theta && \text{for } (x',y') \text{ on } C \\ &= 0 && \text{for } (x',y') \text{ outside } R \end{aligned} \tag{10.9}$$

and

θ is the interior angle at (x',y') subtended by C, equal to π if (x',y') is not a corner point of the boundary. When (x',y') is on the boundary the integral on the right of (10.7) is interpreted as a Cauchy principle value integral, i.e.

$$\int_a^b f(x)dx = \text{Lim}_{d\to 0}\left[\int_a^{c-d} f(x)dx + \int_{c+d}^b f(x)dx\right] \tag{10.10}$$

when $f(x)$ is unbounded in the region of C.

The function $G(\gamma r)$ in (10.7) is a Green's function which is defined as follows:

(a) $$\nabla^2 G - \gamma^2 G = 2\pi\,\delta(r) \tag{10.11}$$

with respect to both pairs of variables (x,y) and (x',y')

(b) at $x = x'$, $y = y'$, G is singular, and

$$G(x,y,x',y') \sim -\log_e \sqrt{(x-x')^2 + (y-y')^2} \tag{10.12}$$

(c) $\delta(r)$ is the Dirac delta function defined by

$$\begin{aligned} \delta(r) &= 0 \quad \text{for } r \neq 0 \\ \iint_R \phi(x,y)\,\delta(r)\,da &= \phi(x',y') \end{aligned} \tag{10.13}$$

for all continuous functions $\phi(x,y)$.

The physical significance of the Green's function is that

$$\frac{R_s}{2\pi} \cdot G(\gamma r) \tag{10.14}$$

is the potential at a point (x',y') which results from a unit point current source at (x,y).

This is verified by (10.7), since the current per unit width entering the resistive layer on the boundary C is $\frac{1}{R_s} \cdot \frac{\partial \phi}{\partial n}$.

By considering the potential due to a pair of point current sources of magnitude $+I_s$ and $-I_s$, and allowing the distance d between these sources to approach zero we obtain

$$\phi(x',y') = (I_s.d) \cos\theta \cdot \frac{R_s}{2\pi} \cdot \frac{\partial G}{\partial r}(\gamma r) \tag{10.15}$$

where the geometry is shown in Fig. 10.1.

Then, since

$$\cos\theta \frac{\partial G}{\partial r} = -\frac{\partial G}{\partial n} \tag{10.16}$$

where $\hat{n}$ is the unit outward pointing normal on the boundary, it follows that the contribution to the potential at (x',y') from the second term on the right of (10.7) is equivalent to that from a double-layer of current sources, one layer on each side of the boundary, such that

$$R_s (I_s.d) = \phi(x,y) \tag{10.17}$$

where $+I_s$ and $-I_s$ are the currents/unit width, and the spacing d between the two current layers is infinitesimal.

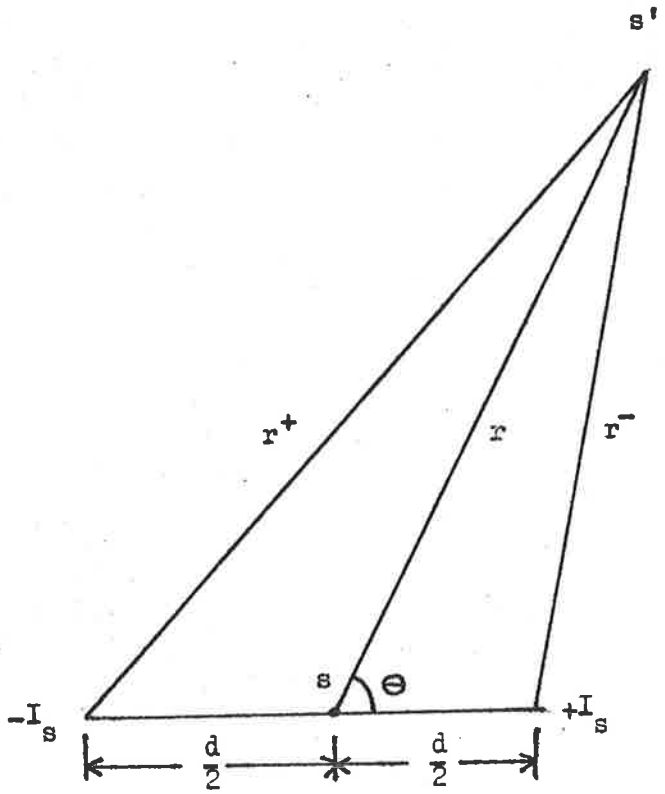

Figure 10.1 Definition of parameters for potential of a pair of point current sources.

We note that the Green's function is not uniquely defined by (10.11), (10.12), and if $G(\gamma r)$ is chosen to satisfy appropriate boundary conditions, an explicit solution may be obtained from (10.7). As previously noted, for distributed RC networks ϕ is given on each boundary segment corresponding to a metal contact, and on the remaining boundary segments $\frac{\partial \phi}{\partial n} = 0$. Therefore, if we choose $G(\gamma r) = 0$ on the metal contacts, and $\frac{\partial G(\gamma r)}{\partial n} = 0$ on the remainder of the boundary, then the right side of (10.7) can be evaluated since there are no unknowns, and we have an explicit solution for the potential at any point.

For many problems it is extremely difficult to find a Green's function which satisfies all of the necessary boundary conditions which allow an explicit solution to be obtained. Another approach is to select a Green's function which does not satisfy all of the boundary conditions, and is thus simpler to find. An example of the latter approach is given in (30).

In the following, we will consider methods for obtaining approximate solutions of (10.7) with

$$G(\gamma r) = K_o(\gamma r) \qquad (10.18)$$

where K_o is the modified Bessel function of the second kind, order zero. The advantage of this approach, which is also used in (29), is that it can be used for two dimensional regions of arbitrary shape; otherwise it would be necessary to find a different Green's function for each problem we wish to solve.

For Laplace's equation we use

$$G(\gamma r) = -\log_e r \qquad (10.19)$$

instead of (10.18).

10.3 Numerical Solution of Integral Equation

An approximate solution to the boundary value problem will be obtained by transforming the integral equation (10.7) - (10.9) to the matrix form (10.5), which may be solved for the coefficients of the series expansions for the boundary values of ϕ and $\frac{\partial \phi}{\partial n}$. The admittance parameters are then obtained by using (10.4).

10.3.1 Linear boundary segments

The usual method for obtaining approximate solutions of the integral equation (10.7) is to assume that the unknown potential or its normal derivative on the kth boundary segment may be approximated as

$$\phi(s) \text{ or } \frac{\partial \phi}{\partial n}(s) = \sum_{j=m_1(k)}^{m_2(k)} c_j f_j(s) \qquad (10.20)$$

where s is the distance along the boundary from some reference point,

$f_j(s)$ is a given function

and the c_j are coefficients to be determined.

If n(k) is the number of expansion functions $f_j(s)$ used on the kth boundary segment then

$$m_2(k) = \sum_{i=1}^{k} n(k) \qquad (10.21a)$$

and

$$m_1(k) = m_2(k) - n(k) + 1 \qquad (10.21b)$$

For simplicity it is common to divide the boundary into N straight line segments, the kth segment being denoted by ΔC_k.

When the approximation (10.20) is substituted into the integral equation (10.7) we obtain

$$\sigma(x',y')\,\phi(x',y') = \sum_{k=1}^{N}\left[\sum_{j=m_1(k)}^{m_2(k)} c_j \oint_{\Delta C_k} f_j(s)K(\gamma r)\,ds\right] \qquad (10.22a)$$

where

r is given by (10.8), and is of the form

$$r^2 = (s-s_p)^2 + p^2 \qquad (10.22b)$$

$$K(\gamma r) = K_o(\gamma r) \quad \text{on conducting boundary segments} \qquad (10.23a)$$

$$K(\gamma r) = -\frac{\partial K_o(\gamma r)}{\partial n} = \frac{\gamma p\, K_1(\gamma r)}{r} \quad \text{on insulating boundary segments} \qquad (10.23b)$$

$K_1(\gamma r)$ is the modified Bessel function of the second kind, order one, and p is the perpendicular distance from (x',y') to the segment ΔC_k as shown in Fig. 10.2.

The sign of p is chosen to be the same as that of the scalar product of the vectors $\tilde{r}$ and $\hat{n}$ in Fig. 10.2.

For Laplace's equation (10.23a) and (10.23b) are replaced by

$$K(\gamma r) = -\log_e r \quad \text{on conducting boundary segments} \qquad (10.24a)$$

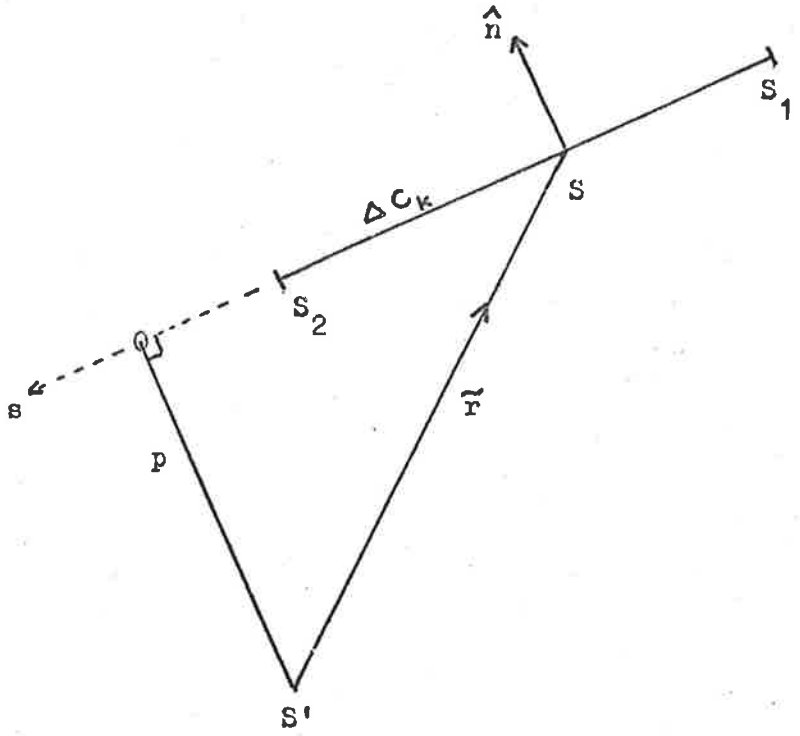

Figure 10.2. Definition of parameters for a typical element ΔC_k

$$K(\gamma r) = \frac{p}{r^2} \qquad \text{on insulating boundary segments} \qquad (10.24b)$$

If M points (x_i, y_i) are chosen on the boundary, then (10.22) becomes

$$\sigma(x_i,y_i)\,\phi(x_i,y_i) = \sum_{j=1}^{N} a_{ij}\, c_j \qquad (10.25)$$

where

$\phi(x_i,y_i)$ on the left of (10.25) is replaced by the expression on the right of (10.20) on the boundary segments where the potential is unknown, and on the remaining segments the known value of $\phi(x_i,y_i)$ is inserted into (10.25). $\sigma(x_i,y_i)$ is defined in (10.9).

The matrix elements a_{ij} are given by

$$a_{ij} = \int_{\Delta C_k} f_j(s)\, K(\gamma r)\, ds \qquad (10.26)$$

Once the matrix elements a_{ij} have been evaluated the system of linear equations (10.25) can be solved for the unknown coefficients c_j provided that $M \geq m_2(N)$.

We now consider the choice of the expansion functions $f_j(s)$ in (10.20). The only restriction on the $f_j(s)$ is that the integrals (10.26) must exist.

One of the simplest types of approximation, but one which is entirely adequate in many cases, is obtained by choosing the $f_j(s)$ to be pulse functions, (14), Chapter 1. This gives a step approximation to the unknown boundary values of $\phi(s)$ and $\frac{\partial \phi(s)}{\partial n}$. Cristal (26), (31) used this method to solve some TEM

transmission line problems with circular and rectangular conductors.

Blue, (29), used piecewise polynomial approximations for $\phi(s)$ and $\frac{\partial \phi(s)}{\partial n}$, which is equivalent to choosing

$$f_j(s) = s^{j - m_2(k)} \tag{10.27}$$

in (10.20).

When either the step approximation or the piecewise polynomial approximation is used, and polynomial approximations are used to approximate the Bessel functions $K_o(\gamma r)$ or $K_1(\gamma r)$ as discussed in (29), then the matrix elements (10.26) are of the form

$$a_{ij} = \int_{s_1}^{s_2} \left[\log_e (s^2 + p^2)\, Q(s) + R(s) \right] ds \tag{10.28}$$

where

$Q(s)$ and $R(s)$ are polynomials in s. These integrals can be evaluated exactly by using integration by parts and a recursion formula to express the integrals involving higher powers of s in terms of integrals with lower powers of s.

When the Bessel function $K_1(\gamma r)$ appears in (10.26) the integrals are of the form (10.28) plus an additional term of the form

$$\int_{s_1}^{s_2} \frac{T(s)}{s^2 + p^2}\, ds \tag{10.29}$$

where $T(s)$ is a polynomial. Analytical solutions for this integral are also easily obtained.

For large arguments the polynomial approximations for the Bessel functions require a large number of terms for convergence, and accuracy is lost on a finite-precision computer due to cancellation. It is then more satisfactory to use the asymptotic expansions for $K_0(x)$ and $K_1(x)$, in which case it is necessary to evaluate the integrals in (10.26) by a numerical integration routine as discussed in (29).

The accuracy of the solutions obtained can be increased by using higher order polynomials on each boundary segment, or the number of boundary segments may be increased while the polynomial order is unchanged. In general the former method is better, up to a point (29). If the order is too high, the matrix of the linear equations becomes ill-conditioned, and accuracy is lost due to the finite word length of the computer. In addition, the effect of errors in the evaluation of the integrals becomes more noticeable for higher order polynomials. Inaccuracies in the evaluation of the integrals can occur because the analytical solutions sometimes require the differences of two quantities which are almost equal; other inaccuracies occur because it is necessary to use numerical integration when analytical solutions are not available. It was found by Blue (29) that the numerical accuracy generally tends to become worse for polynomials of order greater than six or eight on a computer with 8 digit words.

One method of reducing the effect of rounding errors is to replace (10.27) by

$$f_j(s) = T_{j-m_2(k)}(s) \qquad (10.30)$$

where $T_j(s)$ is the Chebychev polynomial of order j shifted to the

interval $s_1 - s_2$ which corresponds to the kth boundary segment; other orthogonal polynomials may also be used instead of the Chebychev polynomials, if desired.

One method of evaluating the integrals (10.28), (10.29) is to expand the Chebychev polynomials in the form $a_o + a_1 s + a_2 s^2 + ---$. The contributions from each term may then be added together. This method is unsatisfactory for numerical purposes because of the loss of significant figures due to subtraction of terms which are almost equal; this problem is most severe for high order polynomials.

A more satisfactory method of evaluating the integrals is by means of a quadrature formula. When polynomial approximations are used for $K_o(\gamma r)$ and $K_1(\gamma r)$, the integral of the polynomial portion of the integrand in (10.28) is obtained in the form

$$\int_a^b p_n(x)\, dx = \sum_{i=1}^{M} w_i\, p_n(x_i) \qquad (10.31)$$

where $p_n(x)$ is a polynomial of order n.

Tables of the weights w_i and abscissae x_i for the Gaussian Quadrature formula are given in (66); an M point Gaussian Quadrature formula is exact for polynomials of order not greater than (2M-1).

The integrals involving the log term in (10.28) can also be evaluated by Guassian Quadrature. For the special case p = 0, Fig. 10.1, these integrals are evaluated by using

$$\int_0^1 p_n(x) \ln\left(\frac{1}{x}\right) dx = \sum_{i=1}^{M} wl_i\, p_n(xl_i) \qquad (10.32)$$

The weights wl_i and the abscissae xl_i are given in (66); the M-point Gaussian Quadrature formula is exact for polynomials of order less than 2M.

For the case $p \neq 0$, Fig. 10.1, the integrals involving the log term in (10.28), are of the form

$$\int_a^b p_n(x) \ln(x^2 + p^2)\, dx \qquad (10.33)$$

An exact evaluation of this integral by Gaussian Quadrature would require calculation of the appropriate weights and abscissae for each value of p and for each set of limits (a,b).

An approximate method which can be used is to subdivide the interval (a,b) into smaller intervals and then apply the Gaussian Quadrature (10.31) to each subinterval. The errors in the integration can be made arbitrarily small by increasing M, and/or by increasing the number of subintervals. A similar method is also suitable for integrals (10.29).

In addition to polynomial trial functions, it is sometimes advantageous to use special trial functions. For example, near corner points on the boundary, the potential may not have a convergent Taylor series expansion; a low-order polynomial is then a poor approximation to the potential or normal derivative. This difficulty may be overcome by using non-polynomial trial functions (29). Near a singular corner the potential may be expanded as

$$\phi(\rho,\theta) = \phi_o + \sum_n f_{\gamma_n}(\rho) \cdot (A_n \sin\gamma_n\theta + B_n \cos\gamma_n\theta) \qquad (10.34)$$

where

$f_\nu(\rho) = I_\nu(\nu\rho)$, the modified Bessel function of the first kind

or

$f_\nu(\rho) = \rho^\nu$ for Laplace's equation

and

(ρ,θ) are the cylindrical coordinates with the origin at the corner.

The ν_n's depend upon the geometry of the corner, and are chosen to satisfy the boundary conditions (26).

In order to improve the approximate potential near a singular corner it is only necessary to use (10.34) for small ρ, in which case $f_{\nu_n}(\rho)$ in (10.34) may be approximated by ρ^{ν_n}, and only the first two or three terms are retained in (10.34).

When these special trial functions are used it is generally necessary to evaluate the integrals required for the matrix elements a_{ij} by numerical integration (26).

The only remaining aspect to be considered in relation to the solution is the selection of the boundary points, (collocation points), (x_i,y_i) at which the integral equation is to be satisfied. This problem was investigated at some length by Blue (29). The results obtained for some test problems suggest that it is generally better to distribute the points on the boundary segments in the same way as the zeros of the Tchebyschev polynomials; the number of points on each boundary segment is chosen to be one greater than the order of the polynomial approximation used on that segment. Other choices of points such as equal spacings along each segment generally give less accurate solutions.

10.3.2 Curved boundary segments

Although it is possible to approximate a curved boundary segment to any desired accuracy by a number of straight line segments, it is sometimes preferable to use special techniques for the more common types of boundary shapes which are likely to be encountered. For example, it is often necessary to obtain the characteristic impedances of transmission lines with conductors of circular cross-section (31); the characteristic impedances are obtained from the static capacitances per unit length between the conductors.

We now wish to consider in detail, methods for solving Laplace's equation in two-dimensional regions where the boundary may consist of circles, arcs of circles, and straight line segments. The geometry and parameters to be used for the circular boundaries are defined in Fig. 10.3.

$$r = \sqrt{R^2+d^2-2dR\cos(\theta-\theta_o)}$$

$$p = R-d\cos(\theta-\theta_o)$$

$$s = R\theta$$

$$\tan\theta_o = \frac{u}{v}$$

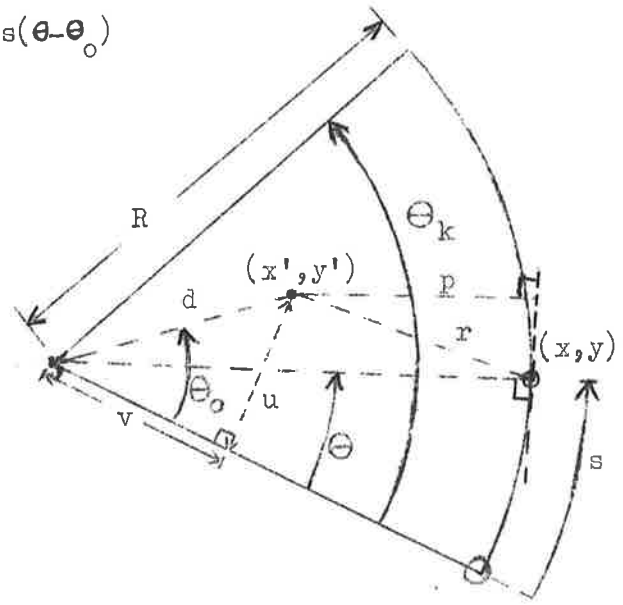

Figure 10.3. Geometry and definition of parameters for circular arcs.

For a circular boundary of the form shown in Fig. 10.3, we replace the expression (10.22b) for r, by

$$r^2 = R^2 + d^2 - 2dR \cos\left(\frac{s}{R} - \theta_o\right) \tag{10.35a}$$

where

$$s = R\theta \tag{10.35b}$$

s, R, d, θ and θ_o are defined in Fig. 10.3, and θ_k is the angle subtended at the centre of the circular arc.

The matrix elements are defined by (10.26). For Laplace's equation, $K(\gamma r)$ in (10.26) is given by (10.24). i.e. (10.26) is of the form

$$a_{ij} = -\int_{s_1}^{s_2} \log_e r \; f_j(s)\, ds \tag{10.36}$$

for circular conductors

and r is given by (10.35).

For problems involving circular conductors with $\theta_k = 2\pi$ it is convenient to expand $-\ln r$ in a Fourier series,

$$-\ln\sqrt{u^2 + v^2 - 2uv\cos\theta} = -\ln u + \sum_{k=1}^{\infty} \frac{1}{k}\left(\frac{v}{u}\right)^k \cos k\theta \qquad \text{for } \frac{v}{u} \leq 1$$

$$= -\ln v + \sum_{k=1}^{\infty} \frac{1}{k}\left(\frac{u}{v}\right)^k \cos k\theta \qquad \text{for } \frac{u}{v} \leq 1 \tag{10.37}$$

Then, because of the orthogonality of the trigonometric functions cos $l\theta$ and sin $m\theta$ over the interval $0 \leq \theta \leq 2\pi$, it follows that if

$$f_j(s) = \cos l\theta \tag{10.38a}$$

then

$$a_{i,j} = 2\pi R \ln v \tag{10.38b}$$

for $l = 0$

$$= \frac{2\pi R}{l}\left(\frac{u}{v}\right)^l \cos l\theta_o \tag{10.38c}$$

for $l \neq 0$

and if

$$f_j(s) = \sin l\theta \tag{10.38d}$$

then

$$a_{i,j} = \frac{2\pi R}{l}\left(\frac{u}{v}\right)^l \sin l\theta_o \tag{10.38e}$$

where

θ_o is defined in Fig. 10.3

and

v = maximum of R and d

u = minimum of R and d.

For distributed RC networks with circular conductors a Fourier series expansion of the Bessel function of the second kind can be written as (8), p. 363

$$Y_0\left(\sqrt{u^2+v^2-2uv\cos\theta}\right) = Y_0(u)\,J_0(v) + 2\sum_{k=1}^{\infty} Y_k(u)\,J_k(v)\cos k\theta \qquad (10.39)$$

The integrals a_{ij} can then be easily evaluated for circular conductors with $\theta_k = 2\pi$ if the trial functions $f_j(s)$ are chosen as (10.38a), (10.38d).

For conductors which consist of circular arcs (i.e. $\theta_k < 2\pi$) there is no particular advantage to be gained by using the Fourier series expansions (10.37). It is then more convenient to choose $f_j(s)$ of the form (10.27), and (10.36) may then be evaluated by using the following approximations.

For the particular case d = R and $\theta_o = 0$, Fig. 10.3, it is easily shown that

$$\log_e r^2 = \ln\left[2d\cos\left(\frac{\theta}{2}-\pi\right)\right]^2 = \ln\left(2d\sin\frac{\theta}{2}\right)^2 \qquad (10.40)$$

For $\frac{\pi}{2} \le \theta \le \frac{3\pi}{2}$ the following polynomial approximation was obtained

$$-\frac{\ln\cos\frac{\alpha}{2}}{2} = .1249990 + .005220931878\,\alpha^2 + .00032260\alpha^4 + .00004091\,\alpha^6 + \epsilon(x) \qquad (10.41)$$

where

$$\alpha = \pi - \theta$$

and

$$|\epsilon(x)| \le 1.3 \times 10^{-6}.$$

This approximation is adequate for most practical purposes.

For $-\frac{\pi}{2} \leq \theta \leq \frac{\pi}{2}$ the following polynomial approximation was obtained

$$\frac{\ln \theta^2 - \ln \left[2 \sin \frac{\theta}{2}\right]^2}{\theta^2} = .083333438 + .00069368258\,\theta^2 + .000011833165\,\theta^4 + \epsilon(x) \qquad (10.42)$$

where

$$\left|\epsilon(x)\right| \leq 1.1 \times 10^{-7}$$

Thus if $\frac{\partial \phi(s)}{\partial n}$ on a circular conducting arc is approximated by a polynomial with $f_j(s)$ of the form (10.27) it is seen that the integral a_{ij}, (10.36), along this boundary segment can be easily evaluated for $d = R$ by using the polynomial approximations (10.41), (10.42); the integral is of the form (10.28).

When the observation point (x_i', y_i') is not on the circular conducting arc (i.e. $d \neq R$) an alternative method is available. The integral (10.36) is a linear combination of integrals of the form

$$\int_{s_1}^{s_2} s^l \left[\ln (R^2 + d^2) + \ln (1 - \alpha \cos \frac{s}{R})\right] ds \qquad (10.43)$$

where

$$\alpha = \frac{2Rd}{R^2 + d^2} < 1 \quad \text{for } R \neq d$$

The first term in (10.43) is readily evaluated, and the second may be evaluated by integrating by parts, as follows

$$\int_{s_1}^{s_2} s^l \ln\left(1-\alpha\cos\frac{s}{R}\right) ds = \frac{s^{l+1}}{l+1} \ln\left(1-\alpha\cos\frac{s}{R}\right)\Bigg|_{s_1}^{s_2} - \frac{\alpha}{l+1}\int_{s_1}^{s_2} \frac{s^{l+1}\sin\frac{s}{R}}{1-\alpha\cos\frac{s}{R}}\, ds \qquad (10.44)$$

The second term on the right of (10.44) may be readily evaluated by using the following polynomial approximations for cos θ and sin θ:-

$$\cos\theta = 1 - .4999888\,\theta^2 + .04158502\,\theta^4 - .0012998\,\theta^6 + \epsilon(\theta) \qquad (10.45)$$

where

$$|\epsilon(\theta)| \leq .00002$$

for $|\theta| \leq \frac{\pi}{2}$

$$\frac{\sin\theta}{\theta} = .9999115 - .166020\,\theta^2 + .00762666\,\theta^4 + \epsilon(\theta) \qquad (10.46)$$

where

$$|\epsilon(\theta)| \leq .00009$$

for $|\theta| \leq \frac{\pi}{2}$

The integrand is then a rational function with the denominator a cubic in s^2, and the required integration can then be done analytically. Since the errors in the approximations (10.45), (10.46) are quite small the integrals should be

sufficiently accurate for all practical purposes.

For Laplace's equation with circular insulating boundary segments and $f_j(s)$ of the form (10.27), the integrals (10.26) are of the form

$$a_{i,j} = \int_{s_1}^{s_2} (s + s_p)^l \cdot \frac{p}{r^2} \, ds \qquad (10.47)$$

where

p and r are defined in Fig. 10.3.

This integral may be put into the form

$$\frac{1}{2} \int_{s_1}^{s_2} (s + s_p)^l \left[1 + \frac{R^2 - d^2}{R^2 + d^2 - 2d\,R \cos \frac{s}{R}} \right] ds \qquad (10.48)$$

When the observation point $(x.', y.')$ lies on the circular arc, (i.e. $R = d$), the integral (10.48) is readily evaluated since the second term vanishes. For $R \neq d$, the second term may be evaluated analytically by using the polynomial approximation (10.45) for $\cos \theta$.

10.4 Numerical Results

Computer programs incorporating the solution techniques discussed in the previous sections were written.

Some numerical values obtained for the conductance matrices of a number of distributed resistance networks are presented below, and these are followed by some results obtained for distributed resistance capacitance networks.

10.4.1 Laplace's equation

The computer program for solution of Laplace's equation generally requires less computer time than that for solving the reduced wave equation (10.1), since the Green's function for the former is simpler, and the latter involves complex arithmetic for solutions at frequencies not on the real axis of the complex frequency plane.

The approximate conductance matrix $[G]$ has the form

$$[G] = \begin{bmatrix} g_{11} & g_{12} & g_{13} & \cdot & \cdot & g_{1n} \\ g_{21} & g_{22} & g_{23} & \cdot & \cdot & g_{2n} \\ \cdot & \cdot & \cdot & & & \cdot \\ \cdot & \cdot & \cdot & & & \cdot \\ g_{n1} & g_{n2} & g_{n3} & \cdot & \cdot & g_{nn} \end{bmatrix} \qquad (10.49)$$

Because of the approximations involved, the $[G]$ matrix obtained will not be exactly symmetrical in general, but except for rounding errors the sum of the elements in any row is zero, as one would expect for the exact solution. The amount of assymmetry in the approximate solution gives an indication of the errors in the solution.

Example 1

The conductance matrix of the two-port resistance network shown in Fig. 10.4 was computed with the unknown potential or its normal derivative on each side approximated by polynomials of order 1 to 11. Curve A in Fig. 10.5 shows the maximum error in the approximate solutions; the maximum error is the greater of

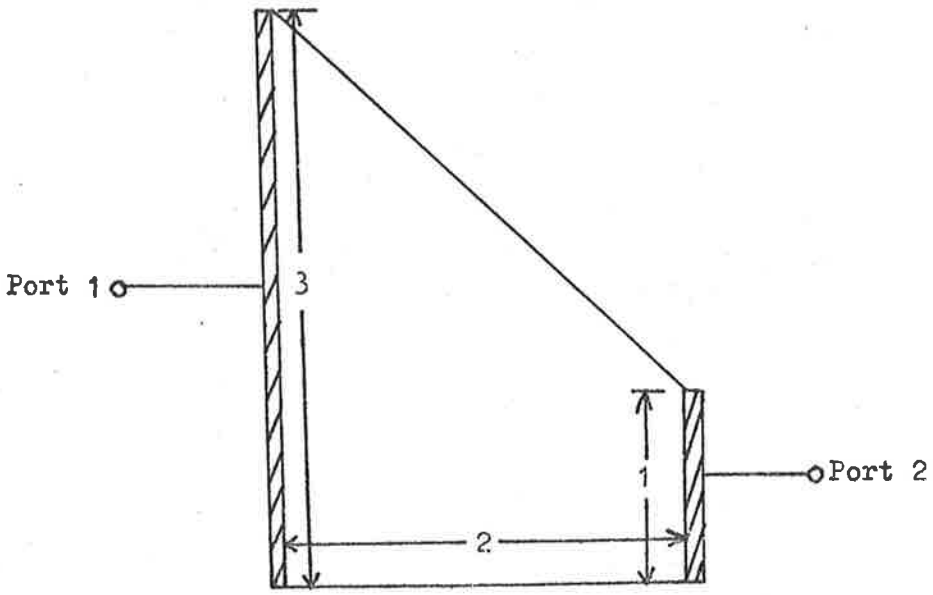

Figure 10.4. Two port resistance network - Example 1.

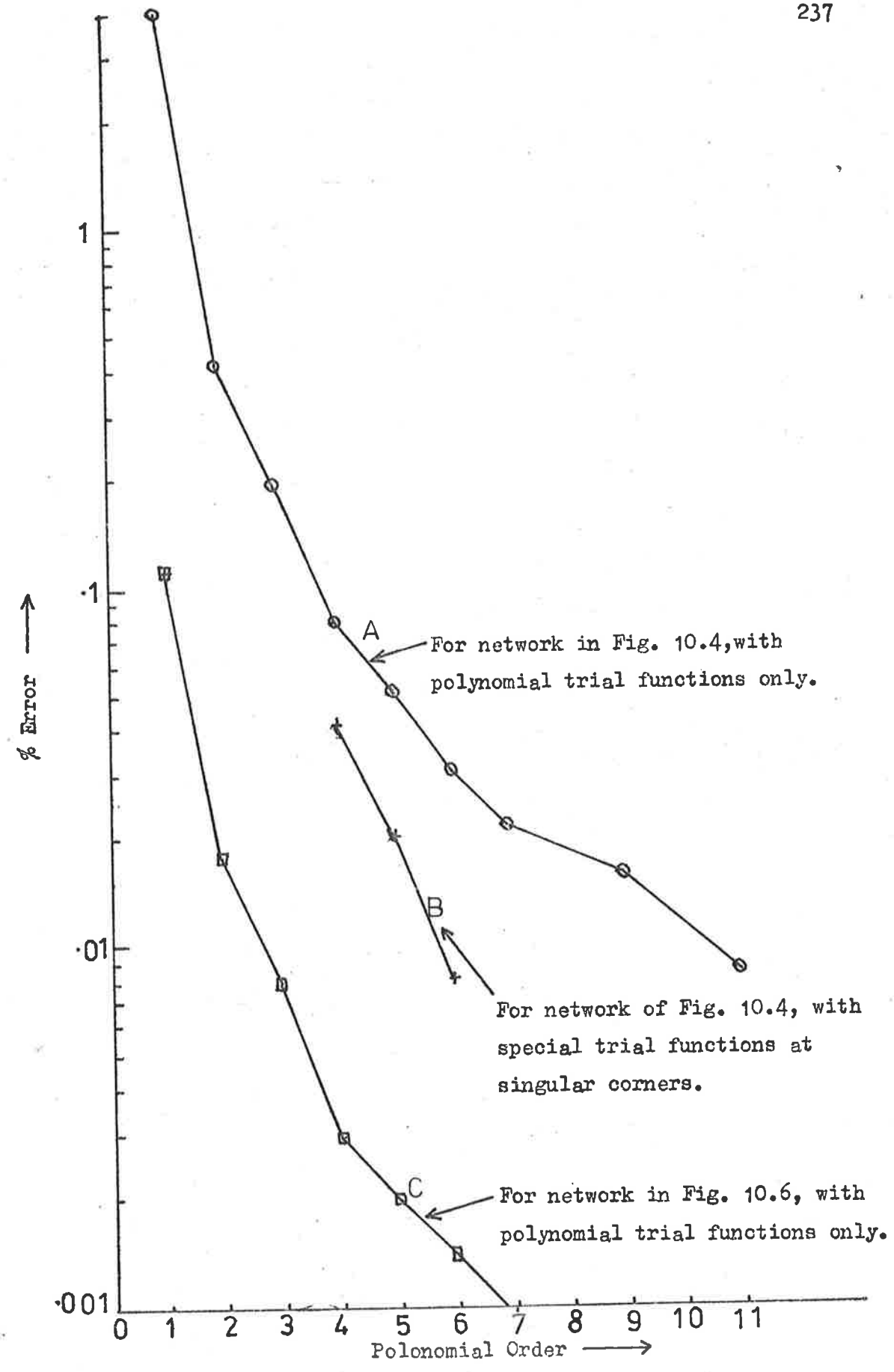

Figure 10.5. Accuracy of approximate conductance matrix elements for distributed resistance networks.

$\left[g_{11} - g_{11}\ (\text{exact})\right] / g_{11}\ (\text{exact})$, and $\left[g_{22} - g_{22}\ (\text{exact})\right] / g_{22}\ (\text{exact})$.

The collocation points on each side were distributed as the zeros of the Chebychev polynomial of order one greater than the order of the polynomial approximation.

This problem was also considered by Blue, but the results obtained, (29) Fig. 7, do not agree with those obtained here. One possible explanation of this discrepancy is that the polynomial orders shown in Blue's Fig. 7 should be increased by one; the two sets of results are then almost identical.

Some additional computations were performed with special trial functions at singular corners as discussed in Section 10.3 and also in (29). Curve B in Fig. 10.5 shows the results obtained; the special (non-polynomial) trial functions were used on the boundary segments extending from the singular corner to a distance of approximately 1/10 of the length of each side adjacent to the corner.

The most significant feature of the results is the marked improvement in the accuracy; for example, it is seen that the accuracy with sixth order polynomials and the special trial functions at singular corners is as good as that obtained with eleventh order polynomials only. A possible disadvantage of using these special trial functions is that it is generally necessary to use numerical integration. In addition, it is necessary to ensure that the length of the boundary segment where the special trial function is used is not excessive, as the resulting accuracy of the solution is then likely to be worse than that obtained with polynomial trial functions only (29).

Example 2

The conductance matrix of the two-port network shown in Fig. 10.6 was computed with the unknown potential or its normal derivative on each side approximated by polynomials of order 1 to 7. Curve C in Fig. 10.5 shows the maximum error in the approximate solutions. A comparison of these results with those for Example 1 shows that the errors for Example 2 are considerably smaller for the same order polynomial.

Example 3

The conductance matrix of the two-port network shown in Fig. 10.7 was computed with the unknown potential or its normal derivative on each side approximated by polynomials of order 3 to 11.

The exact solution for this problem has not been computed, however upper and lower bounds on the exact solution were obtained previously, Chapter 8, by the Variational method; the results obtained previously were,

$$.32751 \leq g_{11} = g_{22} \leq .32975$$

or

$$g_{11} = g_{22} = .32865$$

with an error not greater than $\pm$ .35%.

The results obtained by solving the integral equation are

$$N = 3$$

$$[G] = \begin{bmatrix} .330960 & -.330960 \\ -.332505 & .332505 \end{bmatrix}$$

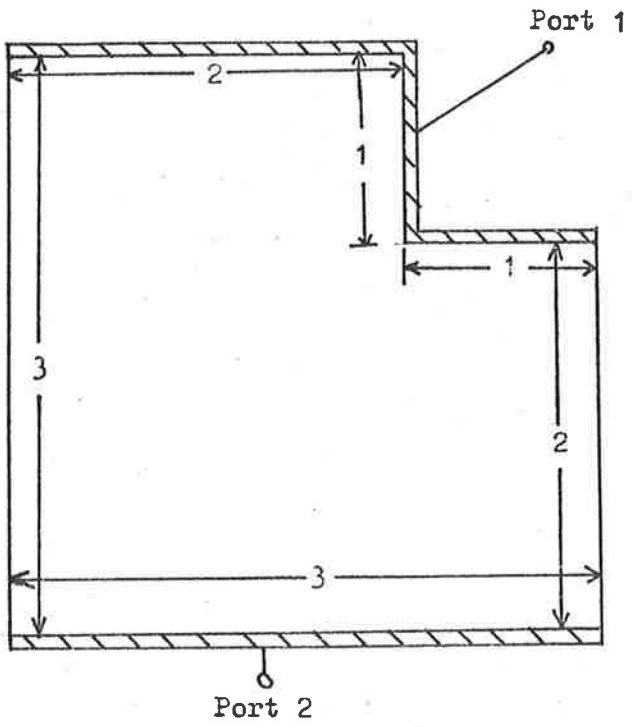

Figure 10.6. Two port resistance network - Example 2.

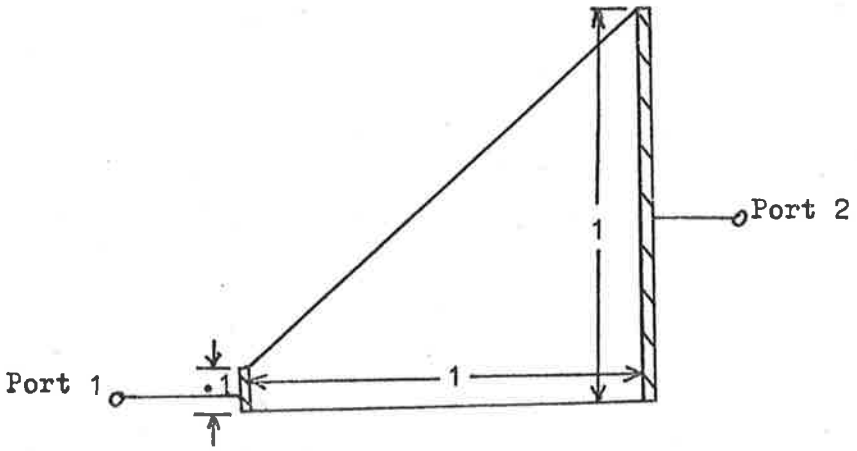

Figure 10.7. Two port resistance network - Example 3.

$$N = 7$$

$$[G] = \begin{bmatrix} .328767 & -.328767 \\ -.328767 & .328767 \end{bmatrix}$$

$$N = 11$$

$$[G] = \begin{bmatrix} .328515 & -.328515 \\ -.328526 & .328526 \end{bmatrix}$$

where

N is the order of polynomial used on each side.

Comparison of the solution for N = 11 and the mean of the upper and lower bounds obtained by the Variational method shows that they differ by about .035%.

Some computations performed on the IBM 7090 computer (with a word length of 36 bits) showed that the accuracy of the results decreases markedly for $N \geq 5$ because of rounding errors. However, when Chebychev polynomial trial functions were used instead of power polynomials, the error in the solutions due to rounding errors were less than $\pm$ 1 in the sixth significant figure for $N \leq 9$. These results demonstrate that the system of linear equation is well conditioned when Chebychev polynomial trial functions are used; as discussed previously it is recommended that numerical integration be used to obtain the matrix elements, otherwise the numerical accuracy is likely to be poor.

We now present some solutions of Laplace's equation where the boundary includes circular arcs as well as linear segments.

Example 4

The conductance matrix of a distributed resistance network consisting of a pair of concentric circular conductors was computed

with the normal derivative of the potential on the conductors approximated by a Fourier series. Since the normal derivative is a constant independent of the angular position, and the integration can be done analytically, without the need for numerical integration, the results obtained for this problem are exact except for rounding errors.

This problem was also solved by using polynomials to approximate the normal derivative of the potential on each of the conductors. Since the normal derivatives can be represented exactly by a polynomial for this problem, the errors in the solution are due to the approximate evaluation of the integrals, and to rounding errors. For a pair of concentric conductors with a diameter ratio of 1.5, and polynomials of order 6 on each side, it was found that the error in the approximate conductance matrix was less than ± 1 in the sixth significant figure; these errors are consistent with those which would be expected as a result of using the approximations (10.41), (10.42) and (10.45), (10.46).

In addition to the above examples, the computer program was also used to calculate the conductance matrices for the network shown in Fig. 10.8 with the subtended angle $\theta = \pi/2$ and $\theta = 3\pi/2$, and several diameter ratios between 1.5 and 3. For this problem a further source of error is introduced by having to approximate the potential on each of the radial lines by a polynomial. For each of the problems solved, polynomials of order six were used on each boundary segment. The resulting error in the solutions was less than ± 1 in the sixth significant figure.

Example 5

The conductance matrices of the two networks shown in

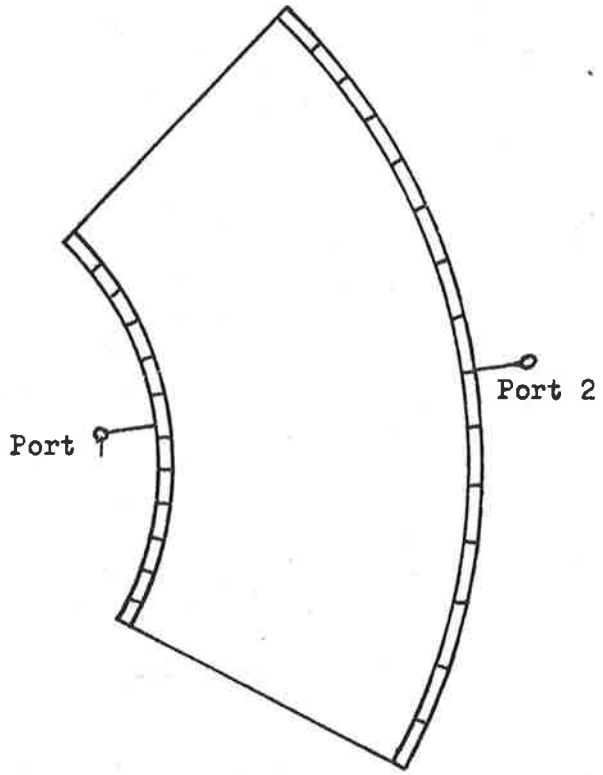

Figure 10.8. Two port resistance network - Example 4.

Fig. 10.9 were computed with the potential or its normal derivative on each boundary segment approximated by polynomials of order 4 and 6. The results obtained for the two networks (a) and (b) are shown below

(a) $N = 4$

$$[G] = \begin{bmatrix} 1.440007 & -1.440007 \\ -1.440016 & 1.440016 \end{bmatrix}$$

(b) $N = 4$

$$[G] = \begin{bmatrix} 1.285372 & -1.285372 \\ -1.285378 & 1.285378 \end{bmatrix}$$

(a) $N = 6$

$$[G] = \begin{bmatrix} 1.440032 & -1.440032 \\ -1.440032 & 1.440032 \end{bmatrix}$$

(b) $N = 6$

$$[G] = \begin{bmatrix} 1.285385 & -1.285385 \\ -1.285387 & 1.285387 \end{bmatrix}$$

This problem was also considered by Sinnott (67) who obtained the following results:

For network (a) in Fig. 10.9

$$|g_{ij}| = 1.4399 \pm .1\%$$

and for network (b) in Fig. 10.9

$$|g_{ij}| = 1.2854 \pm .1\%$$

Note that these results differ from those obtained by the integral equation method by less than .0001, so that the error limits are probably somewhat less than .1%.

The solution of problems of the type given in Fig. 10.9 is important for the design of comb-line and interdigital band-pass filters, and other transmission line components such as directional couplers (31), (68).

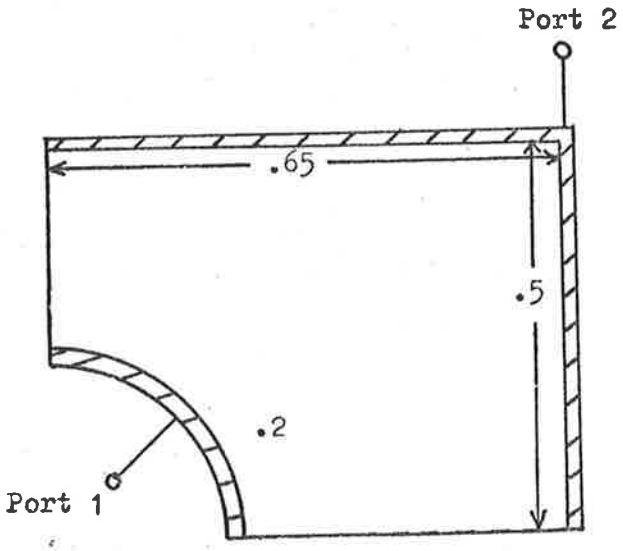

(a)

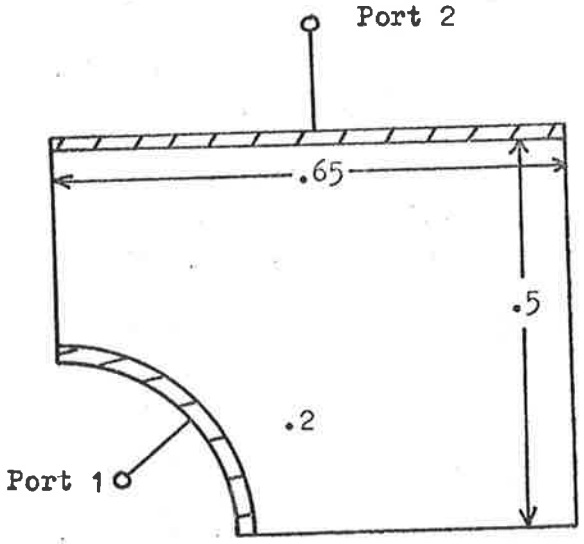

(b)

Figure 10.9. Two port resistance network - Example 5.

10.4.2 Frequency domain analysis of distributed RC networks

We now present the results of some calculations to determine the admittance matrices of several different distributed RC network at frequencies on the imaginary axis of the complex frequency plane. In general it is difficult to determine the errors in the approximate solutions since exact solutions are known for only a few geometries.

Example 1

The admittance matrix of the uniform RC line shown in Fig. 10.10 was obtained at $\omega RC = 1$, with the potential on each insulating boundary segment approximated by a third or sixth order polynomial; the normal derivative of the potential on the conducting boundaries can be exactly represented by a constant for this problem.

With $N = 3$ we obtain,

$$[Y] = \begin{bmatrix} 1.022027 + j.3312422 & -.9807584 + j.1646413 \\ -.9807484 + j.1646413 & 1.022027 + j.3312422 \end{bmatrix}$$

With $N = 6$ we obtain,

$$[Y] = \begin{bmatrix} 1.022013 + j.3312381 & -.9807634 + j.1646375 \\ -.9807634 + j.1646375 & 1.022013 + j.1646375 \end{bmatrix}$$

which is equal to the exact solution to seven significant figures.

Example 2

The admittance matrix of the two-port network with an exponential taper, Fig. 10.11, was computed with the unknown potential or its normal derivative approximated by a polynomial of

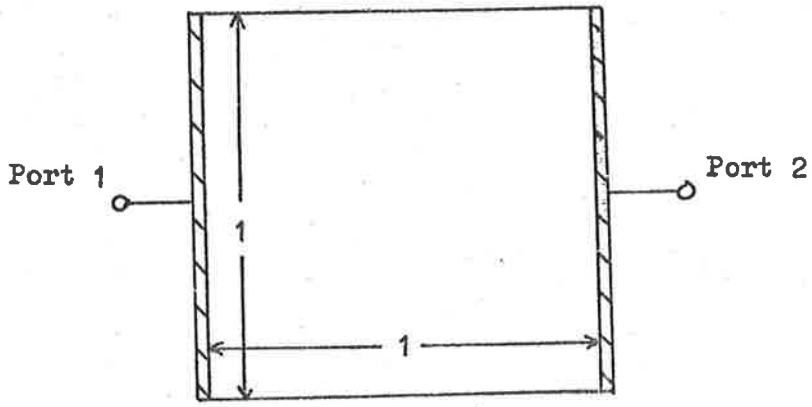

Figure 10.10. Uniform distributed RC line

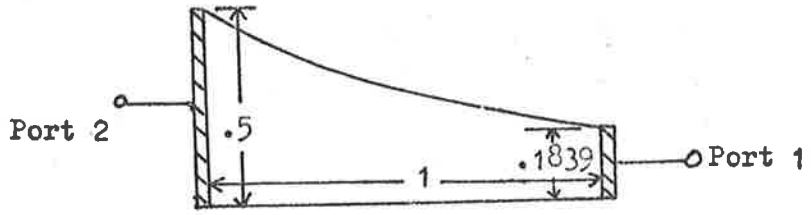

Figure 10.11. Distributed RC line with exponential taper.

order 6 on each side. At the two corners where the interior angle is not equal to 90°, special trial functions were used as previously discussed. The curved boundary segment was approximated by 9 linear segments.

With $\omega RC = 1$, the admittance matrix was found to be,

$$[Y] = \begin{bmatrix} .2951221 + j.1596134 & -.2791900 + j.04724454 \\ -.2791723 + j.04724306 & .2886483 + j.05986082 \end{bmatrix}$$

This may be compared with the approximate solution obtained by one-dimensional analysis,

$$[Y] = \begin{bmatrix} .301250137 + j.16035349 & -.28559058 + j.047152108 \\ -.28559058 + j.047152108 & .294763907 + j.058990751 \end{bmatrix}$$

The differences between the two solutions are about 2%, which suggests that the accuracy of the one-dimensional solution is adequate for this particular problem.

Example 3

The admittance matrices of the two networks in Fig. 10.12 where computed with the potential on each boundary segment approximated by fourth order polynomials. In addition, special trial functions were used at the singular corner (interior angle = 270°).

For the network of Fig. 10.12a, the admittance matrix was found to be,

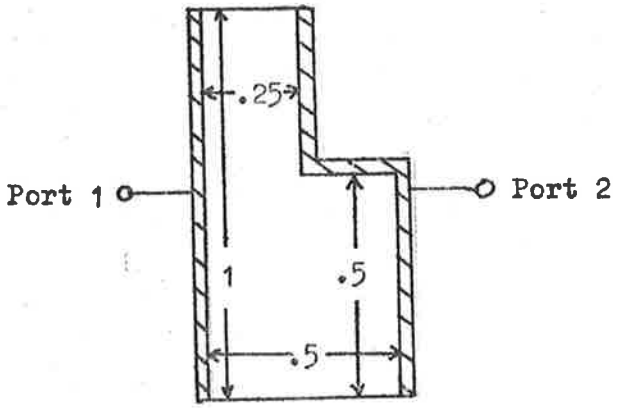

(a)

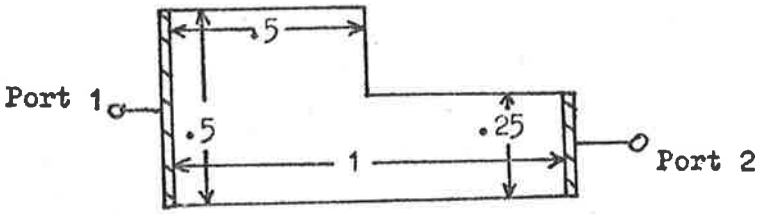

(b)

Figure 10.12. Two port distributed RC networks - Example 3.

$$[Y] = \begin{bmatrix} 3.250652 + j.1107953 & -3.248589 + j.05923675 \\ -3.248473 + j.05938409 & 3.250983 + j.1454948 \end{bmatrix}$$

where $\omega RC = 1$

For the network of Fig. 10.12b, the admittance matrix was found to be,

$$[Y] = \begin{bmatrix} .3221658 + j.1956044 & -.3015412 + j.05233333 \\ -.3015397 + j.05235143 & .3118521 + j.07161765 \end{bmatrix}$$

where $\omega RC = 1$

Since the off-diagonal elements y_{12}, y_{21} are very nearly equal for these two matrices, the errors in this solution are likely to be quite small.

10.4.3 Eigenvalue problems

We now present the results of some calculations to determine the poles and zeros of the admittance parameters of distributed RC networks. If the admittance parameters are evaluated at two or more frequencies in the complex frequency plane, a first approximation to the required pole or zero may then be found, by using an appropriate interpolation or extrapolation formula. If a pole of the admittance matrix is required, we may extrapolate or interpolate the value of the determinant of the coefficient matrix, or the reciprocal of any of the elements of the admittance matrix. Once an approximation to the required pole or zero has been obtained, successive approximations may then be found by interpolating with the previous solutions; usually only three or four iterations are required to give sufficiently accurate solutions.

Suppose that a zero of a function $f(s)$, $s = s_1$ say, has been found by the above method. A second zero may then be found by applying the method to the function $f(s)/(s-s_1)$, and so on until all of the required zeros have been found.

Example 1

The first pole of the admittance matrix of a uniform RC line of unit length was obtained by interpolating the values obtained for $1/y_{11}$ and $1/y_{12}$ at pRC = -9.8, -9.85, -9.90.

The potential on each of the insulating boundary segments was approximated by a sixth order polynomial; the normal derivative of the potential may be represented exactly by a constant on each of the conducting boundary segments.

The values obtained for the first pole are pRC = -9.8696103 and pRC = -9.8696097 respectively, depending on whether $1/y_{11}$ or $1/y_{12}$ is interpolated.

These values agree closely with the exact solution $\pi^2 = 9.8696044$.

Example 2

We now consider the linearly tapered RC network shown in Fig. 10.7 .

When polynomials of order 5 are used on each boundary segment, the interpolated value of the first pole of the admittance matrix is found to be

$$pRC = -7.86045$$

(the interpolation points were chosen to be pRC = -7.8, -7.9, -8.0).

When polynomials of order 7 are used we obtain

$$pRC = -7.8544$$

Finally, when polynomials of order 10 are used with the interpolation points, pRC = -7.84, -7.85, -7.86, we obtain the first pole at

$$pRC = -7.850065$$

These results may be compared with those obtained previously by the Variational method (Chapter 8). The most accurate result obtained previously was

$$pRC \geq -7.87061$$

which agrees closely with the results above.

The first zero of the matrix element y_{11} was obtained with polynomials of order 5 and 7 on each boundary segment, and interpolation points at pRC = -4.2, -4.25, -4.3. The approximate values of the zero were found to be

pRC = -4.2314 for 5th order polynomials

and pRC = -4.2319 for 7th order polynomials.

The most accurate result obtained previously (Chapter 8) was

$$pRC \geq -4.23205$$

which agrees closely with the above results.

The first zero of the matrix element y_{22} was obtained with polynomials of order 5 and 7 on each boundary segment, and with interpolation points at pRC = -.810, -8.30, -.850.

The approximate values of the zero were found to be

pRC = -.82125 for 5th order polynomials

and pRC = -.81981 for 7th order polynomials.

The most accurate result obtained previously, Chapter 8,

was $pRC \geq -.823089$ which agrees closely with the above results.

In addition to the above computations, the admittance matrix was computed at a number of different points in the range $pRC = -10$ to $pRC = -50$. The poles and zeros of the admittance parameters obtained by interpolating through the computed points were all found to agree closely with those obtained by the Variational method (Chapter 8).

10.5 Conclusion

In this Chapter we have considered the solution of the reduced wave equation (10.1) by transforming it to an integral equation.

When attempting a numerical solution of the integral equations it is necessary to take certain precautions to ensure that the accuracy of the results does not suffer unduly from the effects of rounding errors. If the unknown potential function along a boundary segment is approximated by a polynomial, it is preferable to use numerical integration instead of analytical solutions to evaluate the matrix elements. Secondly, if high order polynomial approximations are used, it is necessary to use a Chebychev polynomial approximation, or some other set of orthogonal polynomials, in order to avoid having to solve an ill-conditioned system of equations. In addition, it should be noted that it is possible to obtain accurate solutions with low order polynomials, provided that special trial functions are used at any singular corners of the network.

It is very difficult to make a quantitative comparison of the integral equation method with other methods such as the

finite-difference method and Variational methods. For the types of problems considered here it appears that the integral equation method gives more accurate solutions than the other methods for the same amount of computing time. The integral equation is considered to be superior to the finite-difference method since the iterative procedure used to solve the system of equations in the latter method often converges slowly; this is especially true for regions with complicated boundaries. A further disadvantage of the finite-difference method is that for a multi-terminal network the entire iterative procedure must be repeated for each set of specified conductor potentials. With the integral equation method it is only necessary to solve a set of equations with several different right hand side vectors, which takes little longer than one right hand side.

With the Variational methods of solution one has to integrate the products of the trial functions and/or the products of their derivatives over a two-dimensional region; this problem can usually be reduced to a one-dimensional integral. Similarly, with the integral equation method, the integrals are also one-dimensional, but it is necessary to use special techniques to evaluate these integrals because of the logarithmic singularity in the Green's function.

Finally, it is not considered that the integral equation method is suitable for obtaining the poles and zeros of the network parameters unless the approximate locations of these frequencies are known before hand. Otherwise, there is a possibility that some of the poles and zeros may not be located, or an excessive amount of computing time may be required. In this author's

opinion, the "direct" methods, such as the Variational methods, are most suitable for determining the eigenvalues, even though the integral equation method may be capable of greater accuracy. The integral equation method is probably most suitable for problems where the admittance matrix parameters are required at a relatively small number of frequencies. For problems where these parameters are required at a large number of frequencies it is probably preferable to first obtain the dominant poles and zeros; the admittance parameters are then obtained in the form of a product form expansion which is readily evaluated at any specified frequencies.

Chapter 11

RELATED PROBLEMS

11.1 Introduction

Many of the theoretical results and numerical techniques described in the previous chapters can be used to solve problems arising in the analysis of other distributed networks.

In addition, the results of some work concerned with the transient analysis of transmission lines, and the application of equivalent network theory will be discussed in this chapter.

11.2 Two Dimensional Field Problems - Cartesian Coordinates

The methods described in previous chapters were primarily concerned with computation of the dc admittance parameters (i.e. the conductance matrix), and the poles and zeros of the admittance matrix of multiport distributed RC networks.

The conductance matrix of a multiport distributed resistance network may be easily transformed to the capacitance matrix of a multiconductor lossless transmission line network with the same cross-section; the characteristic admittances or impedances of the lines are obtained from the capacitance per unit length between the lines as described in (31). For both of these problems the potential between the conductors satisfies Laplace's equation, and the boundary conditions are identical.

For the distributed resistance network the current per unit width entiring each conductor is

$$J = \frac{1}{R_s} \frac{\partial \phi}{\partial n} \qquad (11.1)$$

where

ϕ is the potential in the resistive layer

R_s is the sheet resistance (ohms/square)

$\hat{n}$ is the outward-pointing unit normal on the boundary

and

J is the current density (amperes/unit width).

For the lossless transmission line network the charge per unit on the conductors is given by

$$\rho_s = \epsilon \frac{\partial \phi}{\partial n} \tag{11.2}$$

where

ρ_s is the charge density/unit length

and

ϵ is the dielectric constant of the dielectric between conductors.

Then, provided that the boundary conditions on ϕ are suitably chosen, the required conductance or capacitance matrix elements are each equal to the total current entering a conductor or the total charge on a conductor, which is obtained by integrating (11.1) or (11.2).

The method for computing the poles of the admittance matrix of a thin film distributed RC network can also be used to obtain the cutoff wavenumber of TE or TM modes in homogeneous waveguides of arbitrary cross-section. This follows since the waveguide modes can be obtained from a scalar wave function which satisfies the same differential equation and boundary conditions as the potential function for distributed RC networks (14), Chapter 8, (6).

In addition, the electric field normal to the conductors of a TEM planar microwave network, (62), also satisfies the same differential equation and boundary conditions as the potential function for distributed RC networks. For this class of networks the current per unit width entering each port is given by

$$J = \frac{1}{jw\sqrt{u}} \frac{\partial E_z}{\partial n} \tag{11.3}$$

in place of (11.1). w is the frequency in radians per second, $\sqrt{u}$ is permeability of the medium between conductors, and E_z is the electric field normal to the upper and lower conductors.

11.3 Two Dimensional Field Problems - Cylindrical Coordinates

One important class of problems which has not been considered here is that of analyzing lossless transmission lines with circular conductors and a field distribution which does not vary with the azimuthal angle.

The solution of such problems is important for the calculation of discontinuities in coaxial lines. Another important problem in this class is the calculation of the resonant frequencies of a coaxial cavity with longitudinal discontinuities in the conductors.

For this class of problem, Laplace's equation is

$$\frac{\partial^2 \phi}{\partial r^2} + \frac{1}{r} \frac{\partial \phi}{\partial r} + \frac{\partial^2 \phi}{\partial z^2} = 0 \tag{11.4}$$

where

r and z are the radius and distance along the axis respectively in cylindrical coordinates. (11.4) is identical in form

with Laplace's equation in cartesian coordinates except for the term $\frac{1}{r}\frac{\partial \phi}{\partial r}$.

It can be shown that the differential equation (11.4) is a necessary condition for the functional

$$F(\phi) = 2\pi\epsilon \iint_R r|\nabla \phi|^2 \, dr \, dz \qquad (11.5)$$

to be stationary, where the integral is evaluated over the region between the conductors.

The stationary value of (11.5) can also be shown to be proportional to the static capacitance between conductors in the coaxial system, provided that ϕ satisfies appropriate boundary conditions. The Rayleigh-Ritz method may be used to solve the stationary problem in a manner similar to that discussed in previous chapters.

Similarly, for TM modes in a coaxial resonator, it can be shown that the azimuthal component H_ϕ of the magnetic field satisfies

$$-\frac{\partial^2 H_\phi}{\partial r^2} - \frac{1}{r}\frac{\partial H_\phi}{\partial r} + \frac{\partial H_\phi}{\partial r^2} - \frac{\partial^2 H_\phi}{\partial z^2} = w^2 \mu\epsilon H_\phi \qquad (11.6)$$

and the eigenvalues $w_i^2 \mu\epsilon$ corresponding to the resonant frequencies are proportional to the stationary values of a functional of the form

$$F(H_\phi) = \frac{\iint_R \left[\left| \nabla H_\phi \right|^2 + \frac{H_\phi^2}{r^2} \right] r\,dr\,dz + \oint_{C_2} H_\phi^2 \, dl}{\iint_R H_\phi^2 \, r\,dr\,dz} \qquad (11.7)$$

Application of the Rayleigh-Ritz method to this problem leads to a matrix eigenvalue problem of the form obtained in previous chapters.

11.4 Application of Equivalent Network Theory

In accord with the meaning of equivalence used in lumped network theory, distributed networks are considered to be equivalent when they are electrically indistinguishable at their terminals.

For a distributed RC network with a given resistance $r(x)$ and capacitance $c(x)$ per unit length it is possible to generate an infinite number of equivalent networks with different $r(x)$ and $c(x)$.

One reason for considering equivalent RC lines is to broaden the limited class of nonuniform transmission lines for which known solutions are available. A further reason for considering such lines is that it may be easier to fabricate and adjust an equivalent line obtained from a given line.

Some methods for generating equivalent transmission lines are given in (78) - (81). In general it is found that the equivalent lines do not have $r(x)\,c(x) = \text{constant}$. In practice this means that if the line is constructed with uniform resistive

and dielectric sheets, the width of the ground plane will not be equal to that of the resistive film (81).

In addition, it should be noted that exact equivalence between tapered RC lines will not be achieved in practice because the one-dimensional model is only approximate.

An alternative method of generating equivalent RC lines is to apply the equivalent network theory of lumped networks (82), to an RC ladder approximation to the RC line. The results of some work carried out in this area are given in Appendix E.

11.5 Transient Analysis of Lossy Transmission Lines

In the course of the work on distributed RC networks, a method for transient analysis of lossy transmission lines (85) was investigated. At first sight this appears to be a very attractive method for computer solution; an exact solution for the voltage and current along the transmission line at a point x and time (t + h) is given in terms of the voltages and currents at $x \pm \Delta x$ and time t.

Unfortunately it was discovered that there was an error in the derivation of the solution, and the results are only correct for a distortionless line, as discussed in Appendix F.

11.6 Conclusion

Methods for solving some problems related to those encountered in the analysis of distributed RC networks have been considered.

For several problems it was seen that the analysis techniques are either identical to those for distributed RC

networks, or require only minor changes.

Thus the basic techniques described in this thesis are applicable to a wide range of practical problems.

Chapter 12

DISCUSSION

In the previous chapters we have considered numerical techniques for obtaining the admittance matrix of a multiport DRC network.

Some DRC networks can be adequately represented by a one-dimensional model, but in general it is necessary to perform a two-dimensional analysis.

Three methods were studied in detail. These methods may be classified according to the type of equation that the potential function is required to satisfy, as follows:

(1) Second-order partial differential equation (Chapter 3 and 8)

(2) Coupled first-order partial differential equations (Chapter 4 and 9)

(3) Integral equation formulation in terms of Green's functions (Chapter 10).

In addition to satisfying these equations, the solutions are also required to satisfy certain boundary conditions as previously discussed.

The types of expansion functions which were used to obtain approximate solutions of the boundary value problem may be classified as follows:

(a) nth order polynomials defined over the entire two-dimensional region R.

(b) nth order polynomials defined separately over each of a number of subregions of R, with constraints to ensure that the resulting solution is continuous over R.

(c) Continuous piecewise linear approximations over triangular subregions, and "triangle" functions over rectangular subregions. (These are extreme cases of 2).

(d) nth order polynomials defined separately on segments of the boundary C of R.

The first three types of approximation are used in conjunction with methods (1) and (2) above. The fourth is used in conjunction with the integral equation method (3), where the unknown potential within R is obtained from the potential and its normal derivative on C. Nonpolynomials expansion functions can also be used with methods (1) and (2), but they are generally not as convenient to use as polynomials, and they do not appear to offer any significant advantages. However it is definitely advantageous to use nonpolynomial expansion functions with the integral equation method (3), since the accuracy can be greatly improved as discussed in Chapter 10.

One question which naturally arises in this discussion is which is the best method for solving a particular problem?

From the results obtained in Chapters 8-10 it appears that for a given number of expansion functions the integral equation method gives better accuracy than the other two methods. However, when we wish to determine the poles or zeros of an admittance matrix element by using the integral equation method, we find that the eigenvalue appears as a nonlinear parameter in the matrix equation. Thus the numerical solution is not automatic - some "judicious" searching is needed, and this can be very time consuming. In contrast, to this method, the methods (1) and (2) lead to matrix eigenvalue problems which can be solved via well established algorithms.

A further problem which arises with the integral equation method is that it is generally more difficult to evaluate the matrix elements. In general it is difficult to evaluate the required contour integrals because of the singularity in the Green's function, and in addition, complex arithmetic is required. In contrast, the integrals required for methods (1) and (2) involve only real arithmetic, and the two-dimensional integrals and contour integrals can usually be transformed to one-dimensional integrals where the integrand is a polynomial. These one-dimensional integrals are easily evaluated by using a quadrature formula.

A comparison of the results obtained with methods (1) and (2) indicates that when piecewise linear expansions and triangle functions as in (c) above are used to approximate the unknown functions, then the accuracy of (2) is significantly better than (1). However, if nth order polynomials as in (a) above are used, then the results obtained by methods (1) and (2) appear to be identical. One problem which has not been investigated is whether (2) is significantly better than (1) when approximations of the type (b) above are used; this is an area for further research. A disadvantage of method (2) compared with (1) is that more work is required to get the equations into the standard matrix-eigenvalue form. With both of these methods, we generally find that extraneous solutions occur, and these can only be isolated by inspection of the eigenfunctions.

An important consideration in the application of the above methods is the availability of the computer programs. Only two such programs appear to have been widely distributed. Both of these are based on (1) above. The program described by Bulley (53)

uses polynomial approximations of the type (a) above, and Silvester's program (55) uses approximations of type (b) above, where the region R is subdivided into triangular elements. As discussed in Chapter 8, both of these programs can be readily modified to obtain the poles and zeros of the admittance parameters. However, with both of these programs the polynomial approximations are required to satisfy the Dirichlet boundary conditions, which may sometimes be a restriction. These restrictions could be overcome by using the techniques described in Chapter 8, and in (33) and (56).

It appears that there are no readily available computer programs based on method (2). The results presented in Chapter 8 were obtained with a program which could solve only a restricted class of problems, and it was necessary to modify a part of the program for each problem considered.

A program based on the integral equation method was described in (29), but it is not known whether a listing is available. In any case, (29) contains sufficient detail for the interested user to prepare his own program.

In conclusion, it appears that at present, there is no "best" method for solving the problems of the type considered here, and the method to be chosen for a particular problem will depend to some extent on the availability of a suitable computer program, and the personal preference of the user.

We have demonstrated the usefulness of several numerical techniques for solving multiport DRC networks, and we have shown that appreciable errors may result from the assumption of a one-dimensional model.

Appendix A

NOTATION OF LINEAR SPACES AND OPERATORS

The general methods of solution will be presented in the notation of linear spaces and operators, which are defined as follows.

Given a deterministic problem of the form $L(f) = g$, we must identify the operator L, its domain (the functions on which it operates), and its range (the function g resulting from the operation). The operator L may be a matrix operator which operates on a vector f, to give another vector g, or it may be a differential or integral operator.

We usually need an inner product $\langle f,g \rangle$, which is a scalar defined to satisfy

$$\langle u,v \rangle = \overline{\langle v,u \rangle} \tag{A.1}$$

$$\langle a_1u_1 + a_2u_2,v \rangle = a_1 \langle u_1,v \rangle + a_2 \langle u_2,v \rangle \tag{A.2}$$

$$\langle u,u \rangle > 0 \quad \text{if } u \neq 0 \tag{A.3}$$

$$= 0 \quad \text{if } u \equiv 0 \tag{A.4}$$

where the bar in (A.1) indicates the complex conjugate.

We sometimes need the <u>adjoint operator</u> L^a and its domain, defined by

$$\langle Lu,v \rangle = \langle u,L^av \rangle \tag{A.5}$$

for all u in the domain of L. An operator is <u>self adjoint</u> if $L^a = L$, and the domain of L^a is that of L. i.e.

$$\langle Lu,v \rangle = \langle u,Lv \rangle \qquad (A.6)$$

Properties of the solution depend upon properties of the operator. An operator is <u>real</u> if

$$\overline{Lu} = L\bar{u} \qquad (A.7)$$

In addition, a self adjoint operator is <u>positive definite</u> if

$$\langle Lu,u \rangle > 0 \qquad (A.8)$$

where u is not identically zero, and vanishes only when $u \equiv 0$.

An example of a scalar product for two-dimensional problems involving a differential or integral operator is

$$\langle u,v \rangle = \iint_R u.v \, da \qquad (A.9)$$

where

u and v are real functions, and R is the surface of integration.

The procedure for obtaining the adjoint of a differential operator is presented in (42), pp 148 - 149, together with some examples.

To find the adjoint of a differential operator in a space S, consider the scalar product $\langle v,Lu \rangle$. With the help of integration by parts, consider it as the scalar product of u with some vector w which depends on v. The transformation from v to w defines the adjoint operator L^a. The boundary conditions on v are determined by the requirement that the boundary terms resulting from the integration by parts vanish.

Appendix B

STATIONARY CONDITIONS FOR THE FUNCTIONAL $F_1(u,v)$ WITH u AND v CONSTRAINED TO SATISFY DIRICHLET BOUNDARY CONDITIONS

Consider the functional

$$F_1(u,v) = \frac{\iint_R \nabla u \cdot \nabla v \; da}{\iint_R u \cdot v \; da} \tag{B.1}$$

where

u and v satisfy the following boundary conditions

$$\begin{aligned} u &= 0 \qquad \text{on } C_2 + C_k \\ u &= U_j = \text{constant on } C_j \end{aligned} \tag{B.2}$$

$$\begin{aligned} v &= 0 \qquad \text{on } C_2 + C_j \\ v &= V_k = \text{constant on } C_k \end{aligned} \tag{B.3}$$

In addition, u and v are one differentiable in R, but are otherwise arbitrary.

Let

$$u = u_0 + \alpha \eta(x,y) \tag{B.4}$$

and

$$v = v_0 + \beta \mu(x,y) \tag{B.5}$$

where

α and β are arbitrary parameters, and $\eta(x,y)$ and $\mu(x,y)$ are arbitrary in R, but

$$\eta(x,y) = 0 \quad \text{on } C_2 + C_k$$
$$= \eta_j = \text{constant on } C_j \tag{B.6}$$

$$\mu(x,y) = 0 \quad \text{on } C_2 + C_j$$
$$= \mu_k = \text{constant on } C_k \tag{B.7}$$

In addition, suppose that u_0 and v_0 are such that $F_1(u,v)$ is stationary, and

$$\lambda_0 = F_1(u_0,v_0) \tag{B.8}$$

The conditions for $F_1(u,v)$ to be stationary are

$$\left.\frac{dF_1(u,v)}{d\alpha}\right|_{\alpha=0} = 0 \tag{B.9}$$

and

$$\left.\frac{dF_1(u,v)}{d\beta}\right|_{\beta=0} = 0 \tag{B.10}$$

If u and v in (B.1) are replaced by the expressions on the right of (B.4) and (B.5), and the stationary condition (B.10) is applied with $\alpha = 0$, we obtain

$$\iint_R \nabla u_0 \cdot \nabla \delta u \, da - \lambda_0 \iint_R u_0 \cdot \delta u \, da = 0 \qquad (B.11)$$

Then by using Green's formula

$$\oint_C v \frac{\partial u}{\partial n} \, dl = \iint_R \nabla u \cdot \nabla v \, da + \iint_R v \cdot \nabla^2 u \, da \qquad (B.12)$$

we obtain

$$- \iint_R \delta u (\nabla^2 u_0 + \lambda_0 u_0) \, da + \oint_{C_1 + C_k} \delta u \frac{\partial u_0}{\partial n} \, dl = 0 \qquad (B.13)$$

The contour integral in (B.13) is evaluated only over $C_1 + C_k$ because of the boundary condition (B.7), and

$$C = C_1 + C_2 + C_j + C_k \qquad (B.14)$$

Now choose $\delta u = 0$ on $C_1 + C_k$, but let δu be arbitrary in R. Then it follows from (B.13) that

$$\nabla^2 u_0 + \lambda_0 u_0 = 0 \qquad \text{in R} \qquad (B.15)$$

Next choose $\delta u = 0$ on C_k, but let δu be arbitrary on C_1 and in R.

Then it follows from (B.13) and (B.15) that

$$\frac{\partial u_0}{\partial n} = 0 \qquad \text{on } C_1 \qquad (B.16)$$

Then, since μ = constant on C_k, it follows that

$$\oint_{C_k} \frac{\partial u_0}{\partial n} dl = 0 \qquad \text{(B.17)}$$

Similarly, if the stationary condition (B.9) is applied to (B.1), with $\beta = 0$, we obtain

$$\nabla^2 v_0 + \lambda_0 v_0 = 0 \qquad \text{in R} \qquad \text{(B.18)}$$

$$\frac{\partial v_0}{\partial n} = 0 \qquad \text{on } C_1 \qquad \text{(B.19)}$$

$$\oint_{C_j} \frac{\partial v_0}{\partial n} dl = 0 \qquad \text{(B.20)}$$

Appendix C

STATIONARY CONDITIONS FOR THE EXTENDED FUNCTIONAL F(u,v) WITH NO BOUNDARY CONSTRAINTS ON u OR v

Consider the functional

$$F(u,v) = \frac{\iint_R \nabla u \cdot \nabla v \, da - \oint_{C_2+C_j+C_k} \left[(u-g_u) \frac{\partial v}{\partial n} + (v-g_v) \frac{\partial u}{\partial n} \right] dl}{\iint_R u \cdot v \, da} \tag{C.1}$$

where

$$\begin{aligned} g_u &= 0 && \text{on } C_2 + C_k \\ &= U_j = && \text{constant on } C_j \end{aligned} \tag{C.2}$$

$$\begin{aligned} g_v &= 0 && \text{on } C_2 + C_j \\ &= V_k = && \text{constant on } C_k \end{aligned} \tag{C.3}$$

u and v are once differentiable in R, but are otherwise arbitrary.

Let

$$u = u_0 + \alpha \eta(x,y) \tag{C.4}$$

$$v = v_0 + \beta \mu(x,y) \tag{C.5}$$

where α and β are arbitrary parameters, and $\eta(x,y)$ and $\mu(x,y)$ are arbitrary in R.

In addition, suppose that u_0 and v_0 are such that $F(u,v)$ is stationary, and

$$\lambda_0 = F(u_0,v_0) \tag{C.6}$$

The conditions for $F(u,v)$ to be stationary are

$$\left.\frac{dF(u,v)}{d\alpha}\right|_{\alpha=0} = 0 \tag{C.7}$$

and

$$\left.\frac{dF(u,v)}{d\beta}\right|_{\beta=0} = 0 \tag{C.8}$$

If u and v in (C.1) are replaced by the expressions on the right of (C.4) and (C.5), and the stationary condition (C.8) is applied with $\alpha = 0$, we obtain

$$\iint_R (\nabla u_0 \cdot \nabla \mu - \lambda_0 u_0 \cdot \mu)\, da - \oint_{C_2+C_j+C_k} \left[(u_0 - g_u)\frac{\partial \mu}{\partial n} + \mu \frac{\partial u_0}{\partial n}\right] dl \tag{C.9}$$

Then by using the Green's formula

$$\oint_C v \frac{\partial u}{\partial n}\, dl = \iint_R \nabla u \cdot \nabla v\, da + \iint_R v \cdot \nabla^2 u\, da \tag{C.10}$$

we obtain

$$-\iint_R \mu(\nabla^2 u_0 + \lambda_0 u_0)\ da - \oint_{C_2+C_j+C_k} (u_0 - g_u)\frac{\partial \mu}{\partial n}\ dl + \oint_{C_1} \mu \frac{\partial u_0}{\partial n}\ dl = 0 \tag{C.11}$$

Now choose $\frac{\partial \mu}{\partial n} = 0$ on $C_2 + C_j + C_k$ and $\mu = 0$ on C_1, but let μ be arbitrary in R. Then it follows from (C.11) that

$$\nabla^2 u_0 + \lambda_0 u_0 = 0 \qquad \text{in R} \tag{C.12}$$

Next choose $\mu = 0$ on C_1, but let μ be arbitrary in R and on $C_2 + C_j + C_k$. Then it follows from (C.11) and (C.12) that

$$u_0 = g_u \qquad \text{on } C_2 + C_j + C_k \tag{C.13}$$

Finally, if we allow μ to be arbitrary on C_1 it follows from (C.11), (C.12) and (C.13) that

$$\frac{\partial u_0}{\partial n} = 0 \qquad \text{on } C_1 \tag{C.14}$$

Similarly, if the stationary condition (C.7) is applied to (C.1) with $\beta = 0$, we obtain

$$\nabla^2 v_0 + \lambda_0 v_0 = 0 \qquad \text{in R} \tag{C.15}$$

$$v_0 = g_v \qquad \text{on } C_2 + C_j + C_k \tag{C.16}$$

$$\frac{\partial v_0}{\partial n} = 0 \qquad \text{on } C_1 \tag{C.17}$$

From (C.6), (C.12) - (C.14), (C.16) and the Green's formula (C.10) it also follows that

$$\oint_{C_k} \frac{\partial u_0}{\partial n}\, dl = 0 \tag{C.18}$$

is a necessary condition for F (u,v) to be stationary.

Similarly

$$\oint_{C_j} \frac{\partial v_0}{\partial n}\, dl = 0 \tag{C.19}$$

is a necessary condition for F (u,v) to be stationary.

Appendix D

STATIONARY CONDITIONS FOR THE FUNCTION $J_5(f,f^a)$

The functional $J_5(f,f^a)$ is given by (9.43), where $\langle f^a,f\rangle$ and $\langle f^a,L^e f\rangle$ are defined by (9.36) and (9.37) respectively.

By using Gauss' Integral Theorem (38), p. 9, i.e.

$$\iint_R \left[\frac{\partial}{\partial x}(\phi.u) + \frac{\partial}{\partial y}(\phi.v)\right] da = \oint_C \phi(n_x u + n_y v)\, dl \qquad (D.1)$$

and the rule for differentiating a product, we obtain

$$J_5(f^a,f) = \frac{\left[\begin{array}{l} \displaystyle\iint_R \left[\phi^a\left(\frac{\partial u}{\partial x} + \frac{\partial v}{\partial y}\right) + \phi\left(\frac{\partial u^a}{\partial x} + \frac{\partial v^a}{\partial y}\right)\right] da \\ \\ \displaystyle -\oint_{C_1} \left[(\phi^a - G_v)(n_x u + n_y v) + (\phi - G_u)(n_x u^a + n_y v^a)\right] dl \\ \\ \displaystyle -\oint_{C_2+C_j+C_k} \left[G_u(n_x u^a + n_y v^a) + G_v(n_x u + n_y v)\right] dl \end{array}\right]}{\displaystyle\iint_R (\phi^a\phi + u^a u + v^a v)\, da} \qquad (D.2)$$

$$J_5(f^a,f) = \frac{\left[-\iint_R \left(u\frac{\partial \phi^a}{\partial x} + v\frac{\partial \phi^a}{\partial y} + u^a\frac{\partial \phi}{\partial x} + v^a\frac{\partial \phi}{\partial y} \right) da + \oint_{C_2+C_j+C_k} \left[(\phi - G_u)(n_x u^a + n_y v^a) + (\phi^a - G_v)(n_x u + n_y v) \right] dl \right]}{\iint_R (\phi^a \phi + u^a u + v^a v)\ da} \qquad (D.3)$$

Let

$$f_0 = \begin{bmatrix} \phi_0 \\ u_0 \\ v_0 \end{bmatrix} \quad \text{and} \quad f_0^a = \begin{bmatrix} \phi_0^a \\ u_0^a \\ v_0^a \end{bmatrix} \quad \text{be functions such}$$

that $J_5(f^a,f)$ is stationary.

Now if $\phi^a = \phi_0^a + \alpha\eta(x,y)$ where $\eta(x,y)$ is an arbitrary function, and α is an arbitrary parameter, then the condition for $J_5(f^a,f)$ to be stationary is

$$\left.\frac{dJ_5}{d\alpha}\right|_{\alpha=0} = 0 \qquad (D.4)$$

From (D.2) and (D.4) it follows that

$$\iint_R \eta\left(\frac{\partial u_0}{\partial x} + \frac{\partial v_0}{\partial y}\right) da - \oint_{C_1} \eta(n_x u_0 + n_y v_0)\ dl - J_5^0 \iint_R \eta\phi_0\, da = 0 \qquad (D.5)$$

which must be true for arbitrary $\eta(x,y)$.

J_5^0 is the stationary value of $J_5(f^a,f)$.

First choose $\eta(x,y) = 0$ on C_1, but arbitrary inside R. Then from (D.5) we obtain

$$\frac{\partial u_0}{\partial x} + \frac{\partial v_0}{\partial y} = J_5^0 \phi_0 \qquad \text{in R} \tag{D.6}$$

Next choose $\eta(x,y)$ arbitrary on C_1 and in R. Then from (D.5) and (D.6) we obtain

$$n_x u_0 + n_y v_0 = 0 \qquad \text{on } C_1 \tag{D.7}$$

Now choose $u^a = u_0^a + \alpha.\eta(x,y)$. Then from the stationary condition (D.4) and (D.3) we obtain

$$\iint_R \eta \frac{\partial \phi_0}{\partial x}\, da + \oint_{C_2+C_j+C_k} (\phi_0 - G_u)\, n_x \eta\, dl - J_5^0 \iint_R \eta u_0\, da = 0 \tag{D.8}$$

Choose $\eta(x,y)$ arbitrary inside R, but $\eta(x,y) = 0$ on $C_2 + C_j + C_k$. Then from (D.8) we obtain

$$-\frac{\partial \phi_0}{\partial x} = J_5^0 \cdot u_0 \qquad \text{in R} \tag{D.9}$$

Next choose $\eta(x,y)$ arbitrary on $C_2 + C_j + C_k$ and in R. Then from (D.8) and (D.9) we obtain

$$\phi_0 = G_u \qquad \text{on } C_2 + C_j + C_k \tag{D.10}$$

Similarly, if we choose $v^a = v_0^a + \alpha.\eta(x,y)$, from the stationary condition (D.4), and (D.3) we obtain

$$-\frac{\partial \phi_0}{\partial y} = J_5^0 . v_0 \qquad \text{in R} \tag{D.11}$$

and

$$\phi_0 = G_u \qquad \text{on } C_2 + C_j + C_k \tag{D.12}$$

The corresponding relations for ϕ_0^a, u_0^a, and v_0^a are obtained by choosing $\phi = \phi_0 + \alpha.\eta(x,y)$, $u = u_0 + \alpha.\eta(x,y)$, and $v = v_0 + \alpha.\eta(x,y)$, and then applying the stationary condition (D.4).

From (D.6), (D.9) and (D.10) it follows that

$$\left\langle L^a f_o^a, f_o \right\rangle = J_5^0 \left\langle f_o^a, f_o \right\rangle \tag{D.13}$$

and, in addition we have

$$\left\langle L^{ae} f_o^a, f_o \right\rangle = J_5^0 \left\langle f_o^a, f_o \right\rangle \tag{D.14}$$

where L^{ae} is defined by (9.37).

It therefore follows by equating the expressions on the left of (D.13) and (D.14), and by using the boundary conditions (D.7) and (D.10), and the corresponding boundary conditions on ϕ_0^a, u_0^a, v_0^a that

$$\oint_{C_2 + C_j + C_k} G_u (n_x u^a + n_y v^a)\, dl = 0 \tag{D.15}$$

is a necessary condition for J_5^0 to be stationary.

Similarly it can also be shown that

$$\oint_{C_2 + C_j + C_k} G_v \, (n_x u + n_y v) \; dl \; = \; 0$$

is a necessary condition for J_5^0 to be stationary.

Haack, G. (1970). On the noncompleteness of continuously equivalent networks. *IEEE Transactions on Circuit Theory, 17*(4), 619-620.

Haack, G.R. & Branin, F.H. (1971). Comment on "Transient analysis of lossy transmission lines". *Proceedings of the IEEE, 59*(6), 1022-1023.

REFERENCES

(1) M.S. Ghausi and J.J. Kelly, "Introduction to Distributed-Parameter Networks with Application to Integrated Circuits". Holt, Rinehart and Winston, Inc., U.S.A. 1968.

(2) P.M. Morse and H. Feshbach, "Methods of Theoretical Physics". McGraw-Hill, U.S.A. 1953.

(3) Z. Kopal, "Numerical Analysis". Chapman and Hall, G.B., 1955.

(4) J.W. Dettman, "Mathematical Methods in Physics and Engineering". McGraw-Hill, U.S.A., 1962.

(5) W.M. Kaufman and S.J. Garrett, "Tapered Distributed Filters". IRE Transactions on Circuit Theory, Vol. CT-9, No. 4, pp 329-336, December 1962.

(6) N. Marcuvitz, "Waveguide Handbook". McGraw-Hill, U.S.A., 1951.

(7) J. Well, T.S. Murty and D.B. Rao, "Zeros of $J_n(\lambda)Y_n(\eta\lambda) - J_n(\eta\lambda)Y_n(\lambda)$ and $J_n'(\lambda)Y_n'(\eta\lambda) - J_n'(\eta\lambda)Y_n'(\lambda)$." Mathematics of Computation, Vol. 22, No. 101, p. 230, January 1968.

(8) M. Abramowitz and I.A. Stegun, "Handbook of Mathematical Functions." Dover Publications, U.S.A., 1968.

(9) J.J. Kelly and M.S. Ghausi, "Tapered Distributed RC Networks with Similar Immittances." IEEE Transactions on Circuit Theory, Vol. CT-12, No. 4, pp 554-558, December 1965.

(10) R.M. Bulley and J.B. Davies, "Computation of Approximate Polynomial Solutions to TE Modes in an Arbitrary Shaped Waveguide." IEEE Transactions on Microwave Theory and Techniques, Vol. MTT-17, No. 8, pp 440-446, August 1969.

(11) J.H. Wilkinson, "The Algebraic Eigenvalue Problem". New York, Oxford 1965.

(12) G.E. Forsythe, "Generation and Use of Orthogonal Polynomials for Data-Fitting with a Digital Computer." J. Soc. Indust. Appl. Math. Vol. 5, No. 2, pp 74-88, June 1957.

(13) C. Lancoz, "Applied Analysis." Pitman and Sons Ltd., London, p. 374, 1957.

(14) R.F. Harrington, "Field Computation by Moment Methods." New York, MacMillan, 1968.

(15) T. Havie, "On a Modification of Romberg's Algorithm." B.I.T. Nordisk Tidskrift for Informations Behandling, Vol. 6, pp 24-30, 1966.

(16) M. Abramowitz and I.A. Stegun, "Handbook of Mathematical Functions." Dover Publications, U.S.A., 1968, p. 18.

(17) B.B. Woo and J.M. Bartlemay, "Characteristics and Applications of a Thin Film Distributed Parameter Structure" IEEE International Convention Record, Vol. 11, No. 1, pp 56-75, 1963.

(18) K.L. Ochler, "Analysis and Synthesis of Distributed Parameter Circuits." Ph.D. Dissertation, University of Texas, 1964.

(19) H.F. Moulton, "Current Flow in Rectangular Conductors." Proc. Math. Soc. (London), SER. 2, Vol. VIII, pp 104-110, 1905.

(20) G.J. Herskowitz, "Computer-Aided Integrated Circuit Design." New York: McGraw-Hill, Ch. 10, 1968.

(21) G.M. Anderson, "The Calculation of the Capacitance of Coaxial Cylinders of Rectangular Cross-Section." AIEE Transactions, Vol. 69, pp 728-731, 1950.

(22) R.M. Hall, "Resistance Calculations for Thin Film Patterns." Thin Solid Films, Vol. 1, pp 277-295, 1967/68.

(23) H.E. Green, "The Numerical Solution of Some Important Transmission Line Problems." IEEE Trans. Microwave Theory Tech. Vol. MTT-13, pp 676-692, September 1965.

(24) A. Wexler, "Computation of Electromagnetic Fields." IEEE Trans. Microwave Theory Tech. Vol. MTT-17, No. 8, pp 416-419, August 1969.

(25) D.H. Sinnott, G.K. Cambrell, C.T. Carson and H.E. Green, "The Finite Difference Solution of Microwave Circuit Problems." IEEE Trans. Microwave Theory Tech. Vol. MTT-17, No. 8, pp 464-478, August 1969.

(26) E.G. Cristal, "A Comparison of Two Computer Methods for Solving TEM Problems." Presented at the 1969 International Microwave Symposium, Dallas, Texas, May 7, 1969.

(27) R. Courant and D. Hilbert, "Methods of Mathematical Physics". New York: Interscience, 1962. Vol. II, pp 252-256.

(28) J.A. Stratton, "Electromagnetic Theory." McGraw-Hill Book Co. Inc., New York, pp 166-170, and Problem 8, p. 219, 1941.

(29) J.L. Blue, "On Finding the Admittance Matrix of a Thin Film Network by Solving the Reduced Wave Equation in Two Dimensions." Journal of Computational Physics, Vol. 7, pp 327-345, 1971.

(30) P.C. Chestnut, "On Determining the Capacitances of Shielded Multiconductor Transmission Lines." IEEE Trans. Microwave Theory Tech., Vol. MTT-17, No. 10, pp 734-745, October 1969.

(31) E.G. Cristal, "Coupled Circular Cylindrical Rods Between Parallel Ground Planes." IEEE Trans. Microwave Theory Tech., pp 428-439, July 1964.

(32) B.R. Chawla and H.K. Gummel, "A Boundary Technique for Calculation of Distributed Resistance." IEEE Trans. Electron Devices, Vol. 17, No. 10, pp 915-925, October 1970.

(33) T.G. Hazel and A. Wexler, "Variational Formulation of the Dirichlet Boundary Condition." IEEE Trans. Microwave Theory Tech., Vol. MTT -20, No. 6, pp 385-389, June 1972.

(34) J.J. Blech, "A Theorem on Field Problems with Free Boundary Conditions." Journal of the Franklin Institute, Vol. 293, No. 5, pp 361-363, May 1972.

(35) C.T. Carson and G.K. Cambrell, "Upper and Lower Bounds on the Characteristic Impedance of TEM Mode Transmission Lines." IEEE Trans. Microwave Theory Tech., Vol MTT-14, pp 497-498, October 1966.

(36) E.L. Kulikov and N.N. Levina, "Variational Method of Computation of a Multiconductor Line." Radio Engineering and Electron Physics, Vol. 15, No. 5, pp 796-799, 1970.

(37) J.B. Diaz and A. Weinstein, "Schwartz' Inequality and the Methods of Rayleigh-Ritz and Trefftz." Journal of Mathematics and Physics, Vol 26, pp 133-136, 1947.

(38) S.G. Mikhlin, "Variational Methods in Mathematical Physics." Permagon Press, 1964.

(39) J.L. Synge, "Triangulation in the Hypercircle Method for Plane Problems." Proceedings of the Royal Irish Academy, Vol. 54, pp 341-367, 1951.

(40) J. McMahon, "Lower Bounds for the Dirichlet Integral in Euclidian n-Space." Proceedings of the Royal Irish Academy, Vol 58, pp 1-12, 1956.

(41) J.B. Davies, "Review of Methods for Numerical Solution of the Hollow Waveguide Problem." Proc. IEE, Vol. 119, No. 1 pp 37- , January 1972.

(42) B. Friedman, "Principles and Techniques of Applied Mathematics." John Wiley and Sons Inc., New York, 1956.

(43) T.R. Bashkow, "The A-Matrix, New Network Description." IRE Trans. on Circuit Theory, Vol. CT-4, pp 117 - 120, September 1957.

(44) P.R. Bryant, "The Explicit Form of Bashkow's A-Matrix." IRE Trans. on Circuit Theory, Vol. CT-9, September 1962, pp 303 - 306.

(45) P.R. Bryant, "The Order of Complexity of Electrical Networks." Proc. IEE, Vol. 106C, pp 174 - 188, June 1959.

(46) A. Dervisolgu, "Bashkow's A-Matrix for Active RLC Networks." IEEE Trans. on Circuit Theory, Vol. CT-11, pp 404 - 406, September 1964.

(47) F.H. Branin, "D-C and Transient Analysis of Networks Using a Digital Computer." IRE International Convention Record, Part 2, pp 236 - 256, March 1962.

(48) F.H. Branin, "A New Method for Steady State A-C Analysis of RLC Networks." IEEE International Convention Record, Part 7, pp 218 - 223, 1966.

(49) E.S. Kuh and R.A. Rohrer, "The State Variable Approach to Network Analysis." Proc. IEEE, Vol 53, pp 672 - 686, July 1965.

(50) C. Pottle, "State-Space Techniques for General Active Network Analysis." Chapter 7 in "System Analysis by Digital Computer." Editors: F.F. Kuo and J.F. Kaiser, Wiley, 1966.

(51) C. Pottle, "Comprehensive Active Network Analysis by Digital Computer - A State-Space Approach." Proc. 3rd Allerton Conf. on Circuit and System Theory, pp 659 - 668, October 1965.

(52) I.W. Sandberg and H.C.So, "A Two-Sets of Eigenvalues Approach to the Computer Analysis of Linear Systems." IEEE Trans. on Circuit Theory, Vol. CT-16, No. 4, pp 509-517, November 1969.

(53) R.M. Bulley, "Analysis of Arbitrarily Shaped Waveguide by Polynomial Approximation." IEEE Trans. Microwave Theory Tech., Vol. MTT - 17, No. 12, pp 1022 - 1028, December 1970.

(54) P. Silvester, "High-order Polynomial Triangular Finite Elements for Potential Problems." International J. Eng. Sci., Vol. 7, pp 849 - 861, 1969.

(55) P. Silvester, "A General High-Order Finite-Element Waveguide Analysis Program." IEEE Trans. Microwave Theory Tech., Vol. MTT-17, No. 4, pp 204 - 210, April 1969.

(56) D.J. Richards and A. Wexler, "Finite-Element Solutions within Curved Boundaries." IEEE Trans. Microwave Theory Tech., Vol., MTT-20, No. 10, pp 650-657, October 1972.

(57) D.T. Thomas, "Functional Approximations for Solving Boundary Value Problems by Computer." IEEE Microwave Theory Tech., Vol. MTT-17, No. 8, pp 447-454, August 1969.

(58) D. Tanaka and Y. Hatori, "Two Dimensional Analysis of Bessel RC Lines." IEEE Trans. Circuit Theory Vol, CT-18, pp 572-573, September 1971.

(59) P.C. Dunne, "Complete Polynomial Displacement Fields for Finite Element Method." J. Roy. Soc., Vol. 72, pp 245-246, 1965.

(60) T.E. Walsh, B.S. Perlman, and R.E. Enstrom, "Stabilized Supercritical Transferred Electron Amplifiers." IEEE J. Solid State Circuits, Vol. SC-4, pp 374-376, December 1969.

(61) P. Silvester, "Higher-Order Finite Element Waveguide Analysis," IEEE Trans. Microwave Theory Tech., Vol. MTT-17, No. 8, p 651, August 1969.

(62) P. Silvester, "Finite-Element Analysis of Planar Microwave Networks." IEEE Trans. Microwave Theory Tech., Vol. MTT-21, No. 2, pp 104-108, February 1973.

(63) I. Kaufman, "On Poles and Zeros of Linear Systems." IEEE Trans. on Circuit Theory, Vol. CT-20, No. 2, pp 93-101, March 1973.

(64) G. Peters and J.H. Wilkinson, "$Ax=\lambda Bx$ and the Generalized Eigenvalue Problem." SIAM J. Numer. Anal., Vol. 7, pp 479-492, December 1970.

(65) R.F. Harrington, K. Pontoppidan, P. Abrahamsen and N.C. Albertsen, "Computation of Laplacian Potentials by an Equivalent Source Method." Proc. IEE, Vol. 116, No. 10, pp 1717-1720, October 1969.

(66) A.H. Stroud and D. Secrest, "Gaussian Quadrature Formulas." Prentice Hall Inc., Edgewood Cliffs, N.J., 1966.

(67) D.H. Sinnott, "Upper and Lower Bounds on the Characteristic Impedance of TEM-Mode Transmission Lines with Curved Boundaries." IEEE Trans. Microwave Theory Tech., Vol. MTT-16, pp 971-1972, November 1968.

(68) G.L. Matthaei, L. Young and E.M.T. Jones, "Microwave Filters, Impedance Matching Networks, and Coupling Structures." McGraw-Hill Book Co., New York, 1964.

(69) B. Bianco and S. Ridella, "Transition from Two-Dimensional Line Analysis to One-Dimensional Model." Electronics Letters, Vol. 8, No. 13, pp 336-337, 29th June 1972.

(70) L.P. Huelsman, "The Distributed-Lumped-Active Network - Its Application to Filtering Problems." IEEE Spectrum, pp 51-58, August 1969.

(71) B. Bianco and S. Ridella, "Nonconventional Transmission Zeros in Distributed Rectangular Structures." IEEE Trans. Microwave Theory Tech., Vol. MTT-20, No. 5, pp 297-303, May 1972.

(72) G. Peters and J.H. Wilkinson, "Eigenvalues of $Ax=\lambda Bx$ with Band Symmetric A and B." Computer Journal, Vol. 12, No. 4, pp 398-404, November 1969.

(73) L. Fox, "The Numerical Solution of Two-Point Boundary Value Problems in Ordinary Differential Equations." Oxford Univ. Press, New York, p. 245, 1957.

(74) T.R. Goodman, "The Numerical Solution of Eigenvalue Problems." Mathematics of Computation, Vol. 19, pp 462-466, 1965.

(75) S. Ramo and J.R. Whinnery, "Fields and Waves in Modern Radio." John Wiley and Sons Inc., New York, Second Edition, July 1962.

(76) T. Moreno, "Microwave Transmission Design Data." McGraw-Hill, p. 231, 1948.

(77) M.J. Hellstrom, "Equivalent Distributed RC Networks on Transmission Lines." IRE Trans. on Circuit Theory, Vol. CT-9, September 1962, pp 247-251.

(78) S.B. Park and B.A. Shenoi, "Continuous Equivalence of General RLCG Nonuniform Transmission Lines." IEEE Trans. on Circuit Theory, Vol. CT-17, pp 139-141, February 1970.

(79) H. Berger, "Generalized Nonuniform Transmission Lines". IEEE Trans. on Circuit Theory, Vol. CT-13, No. 1, p. 92, March 1966.

(80) T. Chen, "A New Class of Nonuniform Distributed RC Filters." IEEE Trans. on Circuit Theory, Vol. CT-16, pp 530-532, November 1969.

(81) S.B. Park, "Comment on 'A New Class of Nonuniform Distributed RC Filters'." IEEE Trans. on Circuit Theory, Vol. CT-17, No. 4, pp 654-657, November 1970.

(82) R.W. Newcomb, "Linear Multiport Synthesis." New York, McGraw-Hill, 1966.

(83) J.D. Schoeffler, "The Synthesis of Minimum Sensitivity Networks." IEEE Trans. on Circuit Theory, Vol. CT-11, pp 271-276, June 1964.

(84) G.R. Haack, "On the Noncompleteness of Continuously Equivalent Networks." IEEE Trans. on Circuit Theory, Vol. CT-17, pp 619-620, November 1970.

(85) F.H. Branin Jr., "Transient Analysis of Lossy Transmission Lines." Proc. 6th Annual Allerton Conf. on Circuit and System Theory, pp 276-285, 1968.

(86) G.R. Haack, "Comment on 'Transient Analysis of Lossy Transmission Lines'." Proc. IEEE (Letters), Vol. 59, No. 6, pp 1022-1023, June 1971.

(87) B. Wendroff, "Bounds for Eigenvalues of Some Differential Operators by the Rayleigh-Ritz Method." Mathematics of Computation, Vol. 19, pp 218-224, 1965.

(88) M. Goddard, "An Iterative Method for the Solution of Eigenvalue Problems." Mathematics of Computation, Vol. 20 pp 399-406, 1965.

(89) K. Singhal and J. Vlach, "Approximation of Nonuniform RC-Distributed Networks for Frequency and Time Domain Computations." IEEE Trans. on Circuit Theory, Vol. CT-19, No. 4, pp 347-354, July 1972.

(90) B.E. Spielman, "Waveguides of Arbitrary Cross-section by solution of a Nonlinear Integral Eigenvalue Equation". Ph.D. Thesis, Syracuse University, Electrical Engineering Department, Tech. Report TR-71-1, January 1971.